ROLES OF INOSITOL DIPHOSPHATES IN DNA REPAIR

AND

EFFECTS OF ASPIRIN ANALOGUES ON OESOPHAGEAL CANCER

RAJAGOPAL SHARADA KILARI MSc

A thesis submitted in partial fulfilment of the

requirements of the University of Wolverhampton

for the degree of Doctor of Philosophy

December 2014

This work or any part thereof has not previously been presented in any form to the University or to any other body whether for the purposes of assessment, publication or for any other purpose (unless otherwise indicated). Save for any express acknowledgments, references and/or bibliographies cited in the work, I confirm that the intellectual content of the work is the result of my own efforts and of no other person.

Signature

Date

Abstract

Inositol phosphates (IPs) are important signalling molecules with various biological roles in a cell. One such role it is often associated with is DNA repair. The DNA repair process following DNA insult is considered crucial for the genomic integrity and stability. Failure to perform this task will result in mutations and possibly disease. Thus, it is important that we expand our knowledge on how these repair processes occur and identify the key factors involved in its regulation.

The aim of this project was to investigate whether DNA repair was mediated by inositol diphosphates (IDPs). Using a family of yeast knockout mutants with modulated levels of IPs, it was found that IDPs are crucial in repair of DNA following insult with bleomycin and 5-fluorouracil. The observed sensitivity of the mutants was thought to be due to lack of functional repair protein, UDG-like or APE-like, in the absence of essential cofactor such as IDPs. Experiments conducted revealed that the hypersensitive *kcs1Δ* contain both the repair proteins required to process the DNA lesions. However, extreme extraction methods were required to access these proteins, suggesting that the proteins are mislocalised and unavailable to access the damage site and perform DNA repair. GFP-tagging the proteins Ung1, Apn1 and Rad52 in *kcs1Δ* proved to be of little use as it failed to show exact localisation, movement and functionality status of these proteins following bleomycin insult.

The enzymes accountable for the dephosphorylation of the IDPs *in vivo* are the diphosphoinositol polyphosphate phosphohydrolases (DIPPs). Little is known regarding the Michaelis-Menten kinetics parameters for Ddp1p/DIPPs. In this study, using improved methods for the enzymatic synthesis and electrophoretic purification of 1-$InsP_7$, 5-$InsP_7$ and $InsP_8$, the DIPP family has been kinetically characterised. Each DIPP was found to

display similar K_m values for every substrate tested (range: 35-148 nM). The rank order of K_{cat} values (1-$InsP_7$ > 5-$InsP_7$ = $InsP_8$) was identical for each enzyme, although DIPP-1 activity was observed to be 10- to 60-fold more than DIPP-2α/β and DIPP-3α/β, irrespective of the substrate. This study reveals that Ddp1, the yeast DIPP, is capable of hydrolysing not only 5-$InsP_7$ but also 1-$InsP_7$ and $InsP_8$ to a single product, $InsP_6$. The HPLC data found $InsP_7$ accumulation to be relatively little during $InsP_8$ breakdown by DIPPs. Such low build-up was found to be due to rapid conversion of $InsP_7$ to $InsP_6$. Through this study it is also clear that $InsP_8$ prefers to dephosphorylate through 1-$InsP_7$. In contrary, metabolically and functionally significant steady-state route of $InsP_8$ synthesis was observed to be via 5-$InsP_7$.

Oesophageal cancer is considered as one of the deadliest cancers worldwide because of its aggressive nature and low survival rate. Epidemiologic studies have shown that low-dose daily intake of aspirin can decrease the incidence of oesophageal cancer. The data presented in this study show the effects of a number of in-house synthesized novel aspirin analogues on oesophageal cancer cell lines, squamous cell carcinoma (SSC) and adenocarcinoma (ADC). The aspirin analogues, fumaryldiaspirin (PN517) and benzoylsalicylates (PN524, PN528 and PN529), were observed to be more potent against the oesophageal cell lines than aspirin itself. Both, quantitative and qualitative apoptosis experiments conducted revealed that these compounds largely induced apoptosis, although some necrosis was evident with PN528 and PN529. Failure to recover following the treatment with these analogues emphasized that these drugs are largely cytotoxic in nature. The SSC cells (oe21) displayed increased sensitivity to the aspirin analogues compared to the ADC cell lines (flo-1 and oe33). The anticancer properties of these novel aspirin compounds appear to not involve the COX-enzymes at the tested concentrations. These initial findings support further studies into the potential of these aspirin analogues as chemotherapeutic agents against oesophageal cancer.

Table of Contents

Acknowledgements

Firstly, I would like to express my sincere gratitude to my supervisors Dr Steve Safrany and Dr Iain Nicholl for all their support and encouragement throughout my study. Without their expert guidance I would not have learnt or achieved as much as I have and for that I am truly grateful.

I would like to thank Dr Steve Shears for gifting us with Radiolabeled and non-radiolabeled InsP substrates and Professor McLennan for his kind gift of Ddp1p. I would also like to thank Mr Tim Underwood from University of Southampton for his generous gift of oesophageal cancer cell lines and Dr Stephen Dove, University of Birmingham for his gift of plasmid used in this study.

I would like to thank Dr Andrew Devitt from Aston University for his assistance with the flow cytometry studies, Professor Roslyn Bill and Ms Charlie Bland from Aston University for their help with the confocal microscopy.

Special thanks to all my friends and work colleagues at the University who have been there to help me when in need and cheer me up on those dull days.

I would never have made it this far without the unconditional support and encouragement of my parents, uncle and his family. I cannot thank enough my dear husband, who coped with my moods while writing up this thesis.

Finally, I would like to thank the Research Institute of Healthcare Sciences for funding my PhD and giving me this opportunity.

Abbreviations

$(PP)_2$-$InsP_3$ - Bis-diphosphoinositol trisphosphate

$(PP)_2$-$InsP_4$/$InsP_8$ - Bis-diphosphoinositol tetrakisphosphate

15R-HETE – 15R-hydroxyeicosapentaenoic acid

3′-PG – 3′-phosphoglycolate

^3H – Tritium or Hydrogen-3

5FU – 5-fluorouracil

5-LO – 5-lipoxygenase

AA - Arachidonic acid

ADC – Adenocarcinoma

AMPK - Adenosine monophosphate-activated protein kinase

Ap_5A - Diadenosine pentaphosphate

ApA - Diadenosine polyphosphate

APC - adenomatous polyposis coli

APE/Apn - Apurinic/apyrimidinic endonuclease

AP-site - Apurinic/apyrimidinic site or abasic site

ATP - Adenosine triphosphate

ATR - Ataxia telangiectasia and Rad3-related protein

Bax - Bcl-2-associated X protein

Bcl-2 – B-cell lymphoma 2

BER - Base excision repair

BO - Barrett's oesophagus

BSA - Bovine serum albumin

CDK - Cyclin-dependent kinases

CHAPS - 3-[(3-Cholamidopropyl)dimethylammonio]-1-propanesulfonate

CHFR - Forkhead-associated and ring finger domains

COX - Cyclooxygenase

CRC - Colorectal cancer

D. discoideum - *Dictyostelium discoideum*

D.P.M - Disintegration per minute

ddH_2O – double-distilled water

DIPP (mammals) or Ddp1p (yeast) - Diphosphoinositol polyphosphate phosphohydrolases

DMEM - Dulbecco's Modified Eagle's medium

DMSO - Dimethyl sulfoxide

DNA - Deoxyribonucleic acid

DNA-PK_{CS} - DNA-dependent protein kinase catalytic subunit

DO-His - Yeast synthetic drop-out media supplement without histidine

ds – Double-strand

DSDB - Double strand DNA break

dTMP - Deoxythymidine monophosphate

dTTP - Deoxythymidine triphosphate

dUMP - Deoxyuridine monophosphate

dUTP - Deoxyuridine triphosphate

E. coli - *Escherichia coli*

EDTA - Ethylenediaminetetraacetic acid

EGFR - Epidermal growth factor receptor

ERK - Extracellular signal-regulated kinases pathway

ESR - Environmental stress response

FACS - Fluorescence activated cell sorting

FAP - familial adenomatous polyposis

FASN - Fatty acid synthase gene

FBS - Foetal bovine serum

F-DiA - Fumaryldiaspirin

FdUMP - Fluorodeoxyuridine monophosphate

FdUTP - Fluorodeoxyuridine triphosphate

FGFR - Fibroblast growth factor receptor

FUTP - Fluorouridine triphosphate

G418 – Geneticin

GFP - Green fluorescent protein

GI - Gastrointestinal

GOJ - Gastro-oesophageal junction

GORD - gastro-oesophageal reflux disease

HBSS - Hank's Balanced Salt Solution

HDAC - Histone deacetylases

HEPES - 4-(2-hydroxyethyl)-1-piperazineethanesulfonic acid

HGF - Hepatocyte growth factor

HPLC - High-performance liquid chromatography

HR - Homologous recombination

IDP - Inositol diphosphate

IC_{50} – Half maximal inhibitory concentration

Ids1p (yeast) - Inositol diphosphoryl synthase

IL - Interleukin

$Ins(1,4,5)P_3$/$InsP_3$ - Inositol 1,4,5-trisphosphate

$InsP_4$ - Inositol tetrakisphosphate

$InsP_5$ - Inositol pentakisphosphate

$InsP_6$ - Inositol hexakisphosphate

$InsS_6$ - Inositol hexakissulphate

IP - Inositol phosphate

IP6K (mammals) or Kcs1p (yeast) - $InsP_6$ kinase

Ipk - Inositol polyphosphate kinase

IPMK - Inositol polyphosphate multikinases

IR - Ionising radiation

IRI - Irinotecan

K_m - Michaelis constant

LB - Luria Bertani

LOH - Loss of heterozygosity

mAbs - Monoclonal antibodies

MAPK - Mitogen activated protein kinase

MIPP - Multiple inositol polyphosphate phosphatase

miR - microRNA

MMP - Matrix metalloproteinase

MMS - Methyl methane sulfonate

mRNA - messenger RNA

mTOR - mechanistic target of rapamycin

MTT – 3-(4,5-Dimethyl-2-thiazolyl)-2,5-diphenyl-2H-tetrazolium bromide

NF-κB - Nuclear factor kappa-light-chain-enhancer of activated B cells

NHEJ - Non-homologous DNA end-joining

NSAID – Non-steroidal anti-inflammatory drug

NUDT/NudT - Nudix-type

OD – Optical density

OGG1 - 8-oxoG DNA glycosylases

PAGE - Polyacrylamide gel electrophoresis

PARP - poly (adenosine diphosphate-ribose) polymerase

PBS - Phosphate buffered saline

PCR - Polymerase chain reaction

PDK-1 – 3-Phosphoinositide-dependent-kinase-1

PGE_2 - Prostaglandin E_2

PGG_2 - Hydroperoxy endoperoxide

PGI_2 – Prostacyclin

PI - Propidium iodide

PI3K - Phosphoinositide 3-kinase

Plc - Phospholipase C

PP-$InsP_4$ - Diphosphoinositol tetrakisphosphate

PP-$InsP_5$/$InsP_7$ - Diphosphoinositol pentakisphosphate

PPIP5K/ IP7K (mammals) or Vip1p (yeast) - PP-IP_5 kinases

PtdIns(4,5)P_2/PIP_2 - Phosphatidylinositol 4,5-bisphosphate

RCT - Randomized controlled trial

RNA - Ribonucleic acid

RPMI - Roswell Park Memorial Institute medium

S. cerevisiae - *Saccharomyces cerevisiae*

S1P - Sphingosine-l-phosphate

SA - Salicylic acid

SDS - Sodium dodecyl sulphate

SEM - Standard error of the mean

SMUG1 - Single-strand-specific monofunctional uracil DNA glycosylases-1

SNP - Single nucleotide polymorphism

SP – side population

Sp - Specific protein

ss – Single-strand

SSC - Squamous cell carcinoma

TCF - T-cell factor

TDG - Thymine DNA glycosylase

Tdp1 - Tyrosyl-DNA phosphodiesterase

TEMED – Tetramethylethylenediamine

TGF-β - Transforming growth factor beta

TKI - Tyrosine kinase inhibitor

TMPD - N,N,N',N'-tetramethyl-p-phenylenediamine

TS - Thymidylate synthase

TXA_2 - Thromboxane A_2

UDG/Ung - Uracil-DNA glycosylase

UTR - Untranslated region

UV – ultraviolet

VEGF - Vascular endothelial growth factor

V_{max} - maximum velocity of the enzyme

XPC - Xeroderma pigmentosum, complementation group C

XRCC - X-ray repair cross-complementing protein

YPD - Yeast Extract Peptone

Aspirin analogues

PN508 – Bis(2-carboxyphenyl) succinate or Diaspirin

PN510 – Adipoyldiaspirin

PN511 – Sebacoyldiaspirin

PN512 – Terephthaloyldiaspirin

PN517 – Fumaryldiaspirin

PN514 – Benzoylaspirin (Benzoylsalicylate)

PN524 – m-bromobenzoylsalicylate

PN528 – Methyl benzoylsalicylate

PN529 – Isopropyl-(m-bromobenzoylsalicylate)

PN525 – p-methyl benzoylsalicylate

PN526 – Methyl(2-carboxyphenyl)carbonate

PN527 – Ethyl(2-carboxyphenyl)carbonate

List of Figures

List of Tables

1. INTRODUCTION

1.1 Role of inositol diphosphates in DNA repair

1.1.1 History of inositol signalling

Diphosphoinositide, the first inositide, was isolated from brain by Jordi Folch in 1949 (Folch, 1949). Later in 1950s, in response to agonist such as acetylcholine, the phosphoinositides were observed to exhibit rapid turnover by cells (Hokin and Hokin, 1953). Following these findings, many phosphoinositides and inositol phosphates (IPs) were identified. Subsequent studies involved exploration of the functions and contributions of these identified molecules to cell signalling pathways. A study by Lapetina and Michell (1973) demonstrated an association of phosphoinositides turnover rate to membrane related receptors that induce intracellular calcium transport. Cleavage of Phosphatidylinositol 4,5-bisphosphate [PtdIns(4,5)P_2 or PIP_2] to yield inositol 1,4,5-trisphosphate [Ins(1,4,5)P_3 or $InsP_3$] and diacylglycerol, which are involved in the release of calcium and activation of protein kinase C, respectively, remains to be the most well characterised inositide signalling pathway (Berridge, 1983; Streb *et al.*, 1983; Toker, 2012). Since the discovery of phospholipase C (Plc) mediated breakdown of PIP_2, inositol lipids are considered as the precursor for the inositol polyphosphate that are involved in cellular signalling. Once detached from the diacylglycerol tail, the soluble $InsP_3$ can be further phosphorylated to form higher IPs and inositol diphosphates (IDPs), or hydrolysed to yield myo-inositol (Wilson *et al.*, 2013). However, in *Dictyostelium discoideum*, synthesis of higher IP forms can bypass Plc, as they have developed an independent phosphorylation route from myo-inositol to inositol hexakisphosphate ($InsP_6$) (Stephens and Irvine, 1990). This finding of distinct phosphorylation and dephosphorylation properties of inositol lipids and IPs led to the concept of IP signalling pathway

.

1.1.2 Structure and nomenclature of inositol

The simple myo-inositol, a hexahydroxycyclohexane in nature, forms the basis of the diverse family of IPs. This six-carbon sugar molecule is likely to exist in the more thermodynamically stable chair configuration *in vivo*. In this confirmation, one group is axial at D-2 with the rest being equatorial. Visualizing this confirmation three dimensionally has been made easier by relating it to a turtle with the axial D-2 hydroxyl indicating the turtle's head and the other five hydroxyl groups, turtle's limbs and tail, numbered in a counterclockwise fashion with the tail indicating the D-5. Replacing the hydroxyl groups of the inositol molecule with phosphates, thus results in a variety of inositol polyphosphates. Phosphatidylinositol on the other hand is formed by connecting a diacylglycerol to the D-1 of the inositol ring through a phosphodiester bond [Irvine and Schell (2001)]. The three commonly used structural representations of inositol are shown in **Fig. 1.1.1**

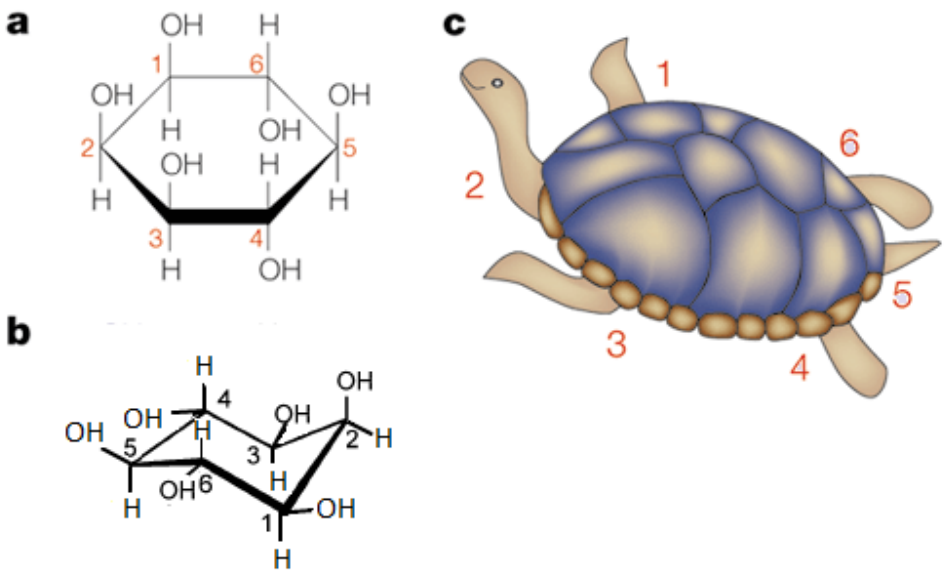

Figure 1.1.1 Structure of myo-inositol: (a) Haworth projection, (b) stable chair conformation and (c) Agranoff's turtle, a mnemonic. Adapted from Irvine and Schell (2001).

1.1.3 Higher inositol polyphosphates

The focus of this thesis is the higher IDPs that are derived from inositol pentakisphosphate ($InsP_5$) and $InsP_6$. $InsP_5$, which serves as a metabolic centre in higher IP metabolism are found primarily in the mammalian cells in the form Ins(1,3,4,5,6)P_5, although studies report that they exist in Ins(1,2,4,5,6) P_5 and Ins(2,3,4,5,6) P_5 forms in Jurkat T cells and T5-1B cells (Irvine and Schell, 2001). Further phosphorylation of the phosphate groups in $InsP_5$ generates the IDPs such as diphosphoinositol tetrakisphosphate (PP-$InsP_4$) and bis-diphosphoinositol trisphosphate [$(PP)_2$-$InsP_3$] (Wilson *et al.*, 2013) **(Fig. 1.1.2)**. On the other hand, phosphorylation of $InsP_6$ results in IDPs such as diphosphoinositol pentakisphosphate (PP-$InsP_5$ or $InsP_7$) and bis-diphosphoinositol tetrakisphosphate [$(PP)_2$-$InsP_4$ or $InsP_8$] (Stephens *et al.*, 1993). $InsP_7$ in yeast has been found to have pyrophosphate at position-5 or 1 or 3 (Ye *et al.*, 2013) whereas in mammalian cells it is found at position-5 (Irvine and Schell, 2001). Isomeric forms of $InsP_8$ present in mammalian cells and yeast have pyrophosphates at position-1 or 5 (Lin *et al.*, 2009; Wilson *et al.*, 2013). Despite similar enzymology, $InsP_8$ in *D. discoideum* has been found to contain pyrophosphates at positions-5 or 6 and in *Polysphondylium*, it has been found to be at 1,5 and/or 3,5 isomer (Laussmann *et al.*, 1998). The structure of higher inositol polyphosphates are shown in the **Fig. 1.1.2**.

1.1.3a Properties and regulation of higher inositol polyphosphates

Unlike inositol lipids, which are hydrophobic in nature and confined to cellular membranes, IPs are water soluble and free to move in a cell. $InsP_5$ and $InsP_6$ are the most abundantly found IPs in almost all eukaryotic cells (Safrany, Caffrey, *et al.*, 1999). $InsP_5$ concentration in the cells has been found to vary between 1-5 µM, whilst $InsP_6$ levels are between 15-100 µM (Jones and Divecha, 2004; Shears, 2004). However, their free concentration could be much lower as they may be firmly bound to proteins or be isolated

in the subcellular compartments. At physiologically relevant ionic concentrations, $InsP_6$ has been proposed to form '$InsP_6$-cation-phospholipid sandwich' at the intracellular membrane surface (Poyner *et al.*, 1993; Shears, 2001). $InsP_5$ and $InsP_6$ levels have been reported to vary during the key stages of cell cycle and cellular differentiation (Shears, 1998, 2001). In *Schizosaccharomyces pombe*, hyperosmotic stress induces overexpression of $InsP_6$ (Ongusaha *et al.*, 1998). Studies have also reported increase in $InsP_8$ levels in DDT1-MF2 and human embryonic kidney mammalian cell lines in response to hyperosmotic stress (Pesesse *et al.*, 2004; Safrany, 2004). The highly phosphorylated IDPs are found at much lower concentrations, $InsP_7$ having the highest concentration of 1-5μM (Shears, 2004).

Although the cellular concentration of IDPs remains mostly constant in most cells, in mammalian cells, the inter-conversion of $InsP_7$ and $InsP_8$ marks the most rapid turnovers (Glennon and Shears, 1993). Inhibition of dephosphorylation by fluoride exposure has been found to result in increased concentration of the IDPs in mammalian cells. This experiment revealed that in an hour about 50% of the $InsP_6$ pool, as well as 20% of the $InsP_5$ pool, were converted into IDPs (Menniti *et al.*, 1993). Although these observations have led to the idea that IDPs have a dynamic role with a potential molecular switch regulating activity (Safrany, Caffrey, *et al.*, 1999), the physiological significance of these molecules remains largely unknown, mainly because fluoride exhibits multiple effects on cell signalling. Moreover, fluoride was found to be specific to mammalian cells and was observed to not affect IDP concentration in yeast or *D. discoideum* (Wilson *et al*., 2013).

IDPs, being highly negative charged molecules generated by high degree phosphorylation of $InsP_6$, could influence the electrostatics of the molecules leading to weak and non-specific protein-protein interactions. Several methodological criteria has been put forth to overcome issues of various interactions and influence of other IPs when exploring the

exact role of $InsP_6$. Few of those conditions include: a) controls using other IPs and inositol hexakissulphate ($InsS_6$) , a non-physiological $InsP_6$ analogue, that exhibits specificity for $InsP_6$, and b) presence of divalent cations (Ca^{2+} and Mg^{2+}) to simulate the intracellular ionic environment (Shears, 2001).

1.1.3b Metabolism of the higher inositol phosphates

Pathway for the synthesis of IPs **(Fig. 1.1.2)** has been well characterized in yeast at a molecular level. Although some information is available on the mammalian pathways, it still remains less well defined. Mammalian pathway of synthesis slightly differs from the yeast pathway. This difference might only be seen in humans due to evolutionary advancement or due to tissue specificity of certain enzymes.

In general, breakdown of PIP_2 to $InsP_3$ in the presence of Plc is believed to be the first step towards the synthesis of higher IPs. However, in plants and *Dictyostelium*, Plc-independent pathway involving production of $InsP_3$ from $InsP_5$ was observed (Van Dijken *et al.*, 1995). Investigations of biochemical fate of $InsP_3$ inside the cell have revealed the presence of a family of IP kinases, known as inositol polyphosphate multikinases (IPMK) in mammals, that phosphorylates the hydroxyl groups on the inositol ring to generate inositol tetrakisphosphate ($InsP_4$), $InsP_5$ and $InsP_6$. IPMK was cloned primarily as ARGRIII/Arg82, a transcriptional regulatory protein of arginine metabolism, and is now known as inositol polyphosphate kinase 2 (Ipk2) (Lee *et al.*, 2012; Saiardi *et al.*, 2000). Kcs1 was thought to be the only kinase involved in the phosphorylation of monophosphate to pyrophosphate groups in $InsP_7$ and PP-$InsP_4$ in yeast up until recently. Presence of second kinase, inositol diphosphoryl synthase (Ids1), in yeast that mimics the activity of $InsP_6$ kinase (IP6K, in mammals) has been observed in *kcs1Δddp1Δ* double knockouts. Ids1 has been reported to be more actively involved in the synthesis of $InsP_7$ than PP-$InsP_4$, although a small amount

of the latter was observed with *ipk1Δkcs1Δddp1Δ* mutant cells (York *et al.*, 2005). However, there is a possibility that Ids1 protein does not exist at all and the effect seen are as a result of Arg82 activity. Arg82 have been reported to act as $InsP_6$ kinase under extreme conditions to generate $InsP_7$ (Zhang *et al.*, 2001). The kinase responsible for the conversion of $InsP_7$ to $InsP_8$ has been identified to be PPIP5K (PP-IP_5 kinases), IP7K and Vip1 respectively in mammals and yeast (Mulugu *et al.*, 2007). Vip1 has also been reported to aid in the addition of pyrophosphates to the 1/3-hydroxyl group of $InsP_6$, to yield 1/3-$InsP_7$ (Wilson *et al.*, 2013) **(Fig. 1.2.1)**.

The catabolism of the IDPs *in vitro* can be achieved by dephosphorylation or by reversing reaction of the kinases through the action of multiple inositol polyphosphate phosphatase (MIPP). $InsP_5$ and $InsP_6$ are the preferred substrates *in vivo* for MIPP (Craxton *et al.*, 1997). A direct non-enzymatical phosphorylation action on proteins in the presence of Mg^{2+} has been proposed for high energetic pyrophosphates such as $InsP_7$. Nsr1p, a protein that has a role in ribosomal assembly and export, and Srp40p, that acts as a ribosomal chaperone are the two proteins identified to be phosphorylated in an acidic serine rich region (Saiardi *et al.*, 2004). The enzymes accountable for the dephosphorylation of the IDPs *in vivo* are the diphosphoinositol polyphosphate phosphohydrolases (DIPPs). These enzymes which exhibit a high affinity for $InsP_7$ and $InsP_8$, possess a nudix motif and are capable of metabolising nucleoside polyphosphates (Leslie *et al.*, 2002; Safrany, Caffrey, *et al.*, 1999). The DIPPs will be described in more detail later in this chapter (*Section* 1.2).

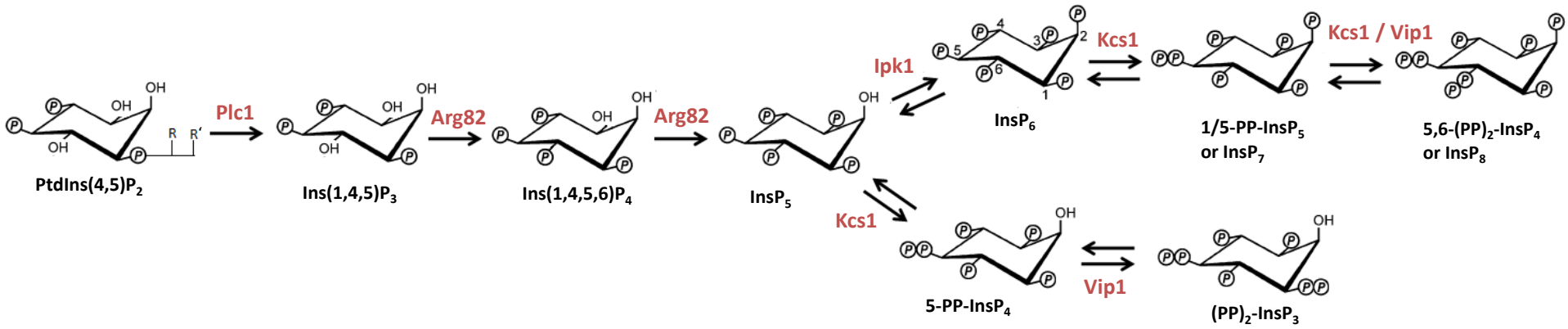

Figure 1.1.2 Pathways for production of inositol polyphosphates and IDPs in yeast. The route of IDPs synthesis is through sequential phosphorylation of PtdIns(4,5)P_2. Enzymes catalysing each step are indicated in red. P represents a single phosphate group (PO_3^{2-}); R and R′ indicates fatty acid chains. Adapted from Wilson *et al*., (2013).

1.1.4 Biological significance of IDPs

IPs are implicated in a range of cellular processes but their specific roles in such processes are not clearly defined. The uncertainty of specific roles of IPs could be due to their highly polar nature and their structural similarity. The rapid turnover of the IDPs and the presence of highly energetic pyrophosphate bonds in their structure suggest that they must have defined dynamic cellular function with potential molecular switch activity (Wilson *et al.*, 2013). With a portion of research being carried out in this area, it is now evident that all the IDPs have a specific role to play in the biological system. Use of yeast mutants lacking specific enzymes necessary for the formation of relevant IDPs and following reverse metabolism reactions of such IPs has contributed to understanding the fate of these molecules in the system.

1.1.4a IDPs in endocytosis

The complications in identifying the clear role of IPs are evident with its proposed role in endocytic membrane trafficking. $InsP_6$ was primarily shown to bind to clathrin-associated proteins such as AP3 and AP180 to regulate endocytic trafficking (Norris *et al.*, 1995). Later, $InsP_7$ (0.58 nM) and PP-$InsP_4$ (1.1 nM) were shown to compete with high affinity and specificity to bind to these assembly proteins than $InsP_6$ (1.7 nM) (Saiardi *et al.*, 2002). Further investigation reported a role for PIP_2 in membrane trafficking (Itoh *et al.*, 2001). Epsin N-terminal homology domain containing proteins involved in endocytic machinery was proposed to efficiently bind to PIP_2 than $InsP_7$ and $InsP_8$. However, phenotypic studies revealed accumulation of membranous structures in yeast mutants *arg82Δ, ipk1Δ, kcs1Δ and ipk1Δ/kcs1Δ* double knockouts. Dye-labelling and electron microscopic studies identified these structures to be endocytic vesicles and reported that endocytosis was inhibited in the mutants. Abnormal vesicular morphology observed particularly in double

knockout mutants lacking IDPs ($InsP_7$ and $InsP_8$) in their study is noteworthy. Although both $InsP_7$ and $InsP_8$ mutants had the same phenotype, the levels of PIP_2 was found considerably increased in the *arg82Δ* and decreased in *kcs1Δ*, thereby confirming the proposed role of $InsP_7$ and/or $InsP_8$ and not PIP_2 in endocytosis (Saiardi *et al.*, 2002).

1.1.4b IDPs role in Akt signalling, insulin regulation and weight gain

Akt signalling regulates glucose homeostasis and protein translation through the GSK3β and mTOR signalling pathways, respectively (Chakraborty *et al.*, 2010). These signalling pathways are not only implicated in several cancers but also in diet-induced obesity (Wang *et al.*, 2009). $InsP_7$, by binding to Pleckstrin Homology domains of Akt, prevents its phosphorylation and expression of 3-phosphoinositide-dependent kinase-1 (PDK-1) both *in vitro* and *in vivo*, and thus results in inhibition of Akt signalling. The knockout mice lacking the enzyme that synthesizes $InsP_7$ was reported to show insulin sensitivity and resistance to obesity caused by high fat diet or aging (Chakraborty *et al.*, 2010). Mouse knock-out models (male) lacking IP6K1 form showed infertility, defects in spermiogenesis and reduced serum insulin levels, whereas IP6K2 (human homologue of yeast Kcs1) form showed no fertility issues and displayed normal insulin levels (Bhandari *et al.*, 2008; Morrison *et al.*, 2001).

1.1.4c IDPs role in cell growth, environmental stress response and implications in cancer

1-$InsP_7$, a pyrophosphorylated product of $InsP_6$ by Vip1, synthesized in yeast during phosphate starvation conditions, is found bound to Pho80-Pho85 (Cyclin-dependent kinases, CDKs) leading to activation of phosphate-scavenging genes (Lee *et al.*, 2007). Both 1 and 5 forms of $InsP_7$ are reported to act together to regulate class I Histone deacetylases (HDAC) and therefore several stress-related gene expressions (Worley *et al.*,

2013). In yeast, this means activation of phosphate starvation pathway and the environmental stress response (ESR) by 1-InsP_7, and downregulation of glycolysis while activating the ESR by 5-InsP_7. This study also concluded that the IDPs act in parallel with the known coregulator of transcription in eukaryotes, transducer of regulated CREB activity 1(TORC1), to control Rpd3L HDAC complex (Worley *et al.*, 2013).

Findings of Worley *et al.* (2013) study have important implication for cancer research. Studies on human cells report that IP6K2 (Kcs1 in yeast), is crucial for the initiation of apoptosis during stress conditions and is found missing in few squamous cell cancers (Morrison *et al.*, 2001; Morrison *et al.*, 2009; Nagata *et al.*, 2005). According to another study, cells that lacked IDPs failed to activate apoptosis or pro-apoptotic genes and rather faultily induced a number of cell cycle arrest genes during stress (Koldobskiy *et al.*, 2010). The finding that IDPs are required for activation of HDAC explains why cells suffer cell-cycle-arrest before they undergo apoptosis. HDAC1 (homologue of Rpd3L) needs to work with p53 to downregulate the cell-cycle-arrest genes during stress (Lagger *et al.*, 2003). Thus it is possible that activation of HDAC1 by IDPs may push cancer cells to undergo apoptosis and not cell cycle arrest during an external stress such as chemotherapy. However, HDAC inhibition is stated to be necessary for the upregulation of p21, which induces cell cycle arrest or apoptosis (Ocker and Schneider-Stock, 2007).

IP6K2 is found situated in the 3p21 chromosomal region that is prone to allelic lose and are spotted in various human cancers. Also, *IP6K2* is found situated close to tumour suppressor genes such as *NPRL2*, *FUS1*, *RASSF1A*, *SEMA3B* and *SEMA3F* (Shames and Minna, 2008; Zabarovsky *et al.*, 2002). It is possible that a copy of the gene is lost along with the other suppressor genes in human cancers. Although IP6K2 might eventually turn out to be a tumour suppressor, there is no direct evidence to prove this.

1.1.4d Chromatin remodelling

Gene expression in eukaryotes is regulated by chromatin-remodeling. The effect of $InsP_6$ on adenosine triphosphate (ATP)-dependent chromatin-remodeling has been examined *in vitro*. In this investigation $InsP_6$ was shown to inhibit nucleosome mobilization by NURF, ISW2 and INO80 remodelling protein complexes. The inhibition appeared to happen via modulation of ATPase activity of the complexes. Controls used in the experiments such as $InsS_6$, $InsP_3$, $InsP_4$, EDTA and EGTA failed to show such an effect. However, a slight inhibition was noted with $InsP_5$. Nucleosome mobilization by the yeast complex SWI/SNF was shown to be stimulated by Ins(1,4,5,6)P_4 and $InsP_5$ but not by Ins(1,3,4,5)P_4 and $InsP_6$. These events did not appear to be due to ATPase activity of the protein complex. These complexes control the expression of *ino1* which is involved in the production of inositol-1-phosphate synthase protein. Northern analysis of mRNA for *ino1* in yeast showed absence of *ino1* mRNA in *plcΔ* and *arg82Δ* but showed decreased levels (41% reduction) in the *ipk1Δ* strains. This suggests a role for $InsP_4$, $InsP_5$, $InsP_6$ and IDPs (particularly $InsP_7$ and $InsP_8$, with some rescue from PP-$InsP_4$) for the reduced mRNA levels in *ipk1Δ* in transcription *in vivo* (Shen *et al.,* 2003). This data was in accordance with investigation on the induction of *pho5*, a gene that is induced by phosphate starvation, in yeast knockouts lacking *arg82*, hence $InsP_4$-$InsP_8$. The study showed the inability of *arg82Δ* strains to recruit SWI/SNF and INO80 complexes to *pho5* promoter region for chromatin remodelling and related gene transcription (Steger *et al.,* 2003). Both the reports mentioned here support the role of IPs in chromatin remodelling and the importance of relative levels/ratios of $InsP_4$, $InsP_5$ and $InsP_6$ in these processes.

1.1.5 Roles of IDPs in DNA repair

DNA damage can trigger variety of responses, of which DNA repair is a crucial one. Careful repair of the damaged DNA is essential for the upkeep of genomic stability and integrity. Errors in the repair process may result in genetic alterations and subsequent induction of cancer and other genetic diseases. Although there are numerous DNA repair pathways, this study will focus on the following three well-characterized pathways: non-homologous DNA end-joining (NHEJ), homologous recombination (HR) and base excision repair (BER). HR has been reported to accurately repair double-strand DNA breaks (DSDBs) without loss of genetic information, whereas NHEJ can be potentially mutagenic (Lieber *et al.*, 2003).

1.1.5a NHEJ

In mammals, DSDBs are mended through NHEJ, a process that involves recognition of damage and binding of Ku70/80 protein to the broken ends. This binding is followed by recruitment of DNA-PK_{CS} (DNA-dependent protein kinase catalytic subunit), a serine/threonine kinase whose precise substrate is unknown. The binding of Ku and DNA-PK_{CS} to DNA results in DNA-PK holoenzyme which helps in protecting DNA ends from nuclease attacks. This large complex also recruits DNA ligase IV heterodimer and prepares the damaged DNA ends for repair. Besides the above mentioned factors, a 'stimulatory factor' such as $InsP_6$ was reported to be necessary for the formation of the complex and efficient end-joining (Hanakahi *et al.*, 2000). This action was not restricted to $InsP_6$ as it was found that $InsP_4$ and $InsP_5$ were also capable of stimulating end-joining, though to a less extent and $InsS_6$ was found inactive. However, the possibility that the DNA repair may actually have been due to $InsP_7$ or $InsP_8$ was not completely ignored as the reactions could have been contaminated with IP6K (Kcs1) (Hanakahi *et al.*, 2000). $InsP_6$ was subsequently shown to directly bind Ku70 and this apparently increased the recruitment of DNA-PK_{CS}

(Hanakahi and West, 2002; Ma and Lieber, 2002). However, this was not the case with *S. cerevisiae* homologue yKu70 (Hanakahi and West, 2002). The recombinant Ku70 used for this experiment is unlikely to have $InsP_6$ kinase activity associated with it, but it is equally possible that the commercial $InsP_6$ has $InsP_7$ or $InsP_8$ in it.

1.1.5b HR

In the eukaryote yeast, DSDBs are thought to be predominantly repaired through high-fidelity HR mediated by the Rad52 epistasis group (Ozenberger and Roeder, 1991). The key DNA intermediates or stages in the HR process include (a) resection, where the 5′-ends of the break are chopped off, (b) strand invasion, where the overhanging 3′ single-stranded (ss) tail makes contact with an identical DNA by pairing complimentarily with the unbroken strand, and (c) Holliday junctions, where the ligation of broken strands forms a loop which further is cleaved and annealed to result in non-crossover products. Rad52 is a prerequisite for the efficient HR in yeast (Bai and Symington, 1996) and is often considered a genetic marker to define this process (Lisby *et al.*, 2001). Though its structure and properties are conserved from yeast to humans (Sung *et al.*, 2000), studies suggest a possibility of an alternative Rad52-independent repair pathway in higher eukaryotes (Yamaguchi-Iwai *et al.*, 1998). The importance of Rad52 in HR process has been attributed to its ability to look for and facilitate annealing of homologous DNA strands. Also, efficient strand exchange process *in vitro* was observed only when Rad52 offered a bridge between ss-DNA binding replication protein complex and the Rad51 recombinase (Lisby *et al.*, 2001).

In yeast, green fluorescent protein (GFP) –tagged Rad52, followed by DSDBs, showed relocalization from a diffused nuclear distribution state to formation of distinct foci at the region of genomic insult. These foci represent the sites of active DNA repair *in vivo*. Interestingly, the Rad52 were found forming DNA repair and recombination centres solely

during S phase of mitotic cells (Lisby *et al.*, 2001). Such coupling of repair process to S phase can be beneficial to cells as the DSDBs formed can be automatically spotted during the replication process and repaired through checkpoints before moving to G2/M phase.

Reports suggest that IDPs such as $InsP_7$ and $InsP_8$ are required for hyper-recombination events in yeast lacking protein kinase C (Huang and Symington, 1995; Luo *et al.*, 2002). A recent study regarded IDPs to be novel regulators of HR signalling in mammals (Jadav *et al.*, 2013). In this study, cells lacking IP6K1 showed decreased viability and reduced recovery following treatment with hydroxyurea, a replication stress inducer, or neocarzinostatin, a radiomimetic antibiotic. Although HR-mediated repair was initiated in these cells, an efficient repair of damaged DNA failed to occur. As a result, IP6K1 mutant cells underwent death while some survived with build-up of chromosomal aberrations.

Reports also suggest that DSDB recognition in yeast is mainly performed by Mec1 and Tel1 [*S. cerevisiae* homologue of mammalian ataxia telangiectasia and Rad3-related protein (ATR) and Ataxia telangiectasia mutated (ATM), respectively] (Craven *et al.*, 2002). Once stimulated, these sensors allegedly initiate a phosphorylation cascade that in turn activates Rad53. IDPs are reported to downregulate Tel1, which apart from playing a role in DSDBs response, also regulate telomere length in yeast (York *et al.*, 2005). IDP such as PP-$InsP_4$, but not $InsP_7$ or $InsP_8$, has been identified to regulate telomere length in yeast. Also, loss or gain of function of *kcs1* was found to result in either shortened or elongated telomeres. These examples suggest that IDPs play a crucial role in telomere length (York *et al.*, 2005) and thus, serve a protective role against DNA damage and/or involvement in cellular senescence.

1.1.6 Examples for DNA damage induced repair

Many of the commonly used chemotherapeutic cytotoxic compounds or ionising radiations (IR) cause high levels of DNA damage, that activate cell cycle checkpoints, leading to cell cycle arrest and/or cell death (Swift and Golsteyn, 2014). DSDBs, which are considered as the most fatal form of DNA damage, can be caused by agents such as radiomimetic chemicals (bleomycin and neocarzinostatin), antimetabolites 5-fluorouracil (5FU), IR, topoisomerase inhibitors (camptothecin), and chemicals that generate reactive oxygen species (Mahaney *et al.*, 2009; Swift and Golsteyn, 2014). However, innate or acquired resistance of tumours to some of these chemotherapeutics, e.g. 5FU (Jette *et al.*, 2008) and bleomycin (Ramotar and Wang, 2003), have caused therapeutic failures. DNA repair following chemotherapy insult is often associated with such tumour resistance. The understanding of how the cells respond to the DNA damage causing agents and/or manage to repair the lethal lesions becomes the key to increasing the efficacy of the anticancer agents. In this study, the focus will be on understanding of mechanism of action of two anticancer treatments: 5FU **(Fig. 1.1.3)** and bleomycin **(Fig. 1.1.4)**. The contribution of the activated repair pathways to these agents' resistance are also discussed herein.

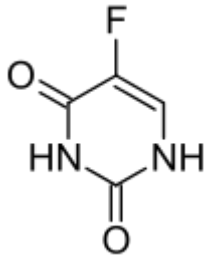

Figure 1.1.3 Structure of antimetabolite 5FU

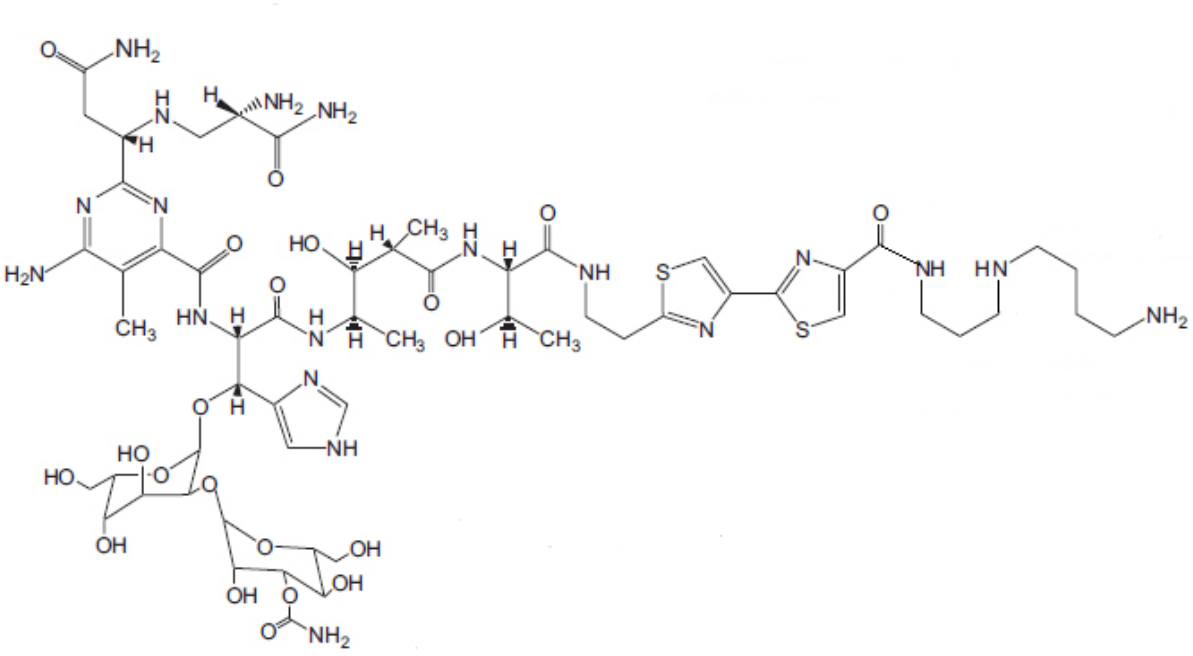

Figure 1.1.4 Structure of anticancer drug bleomycin. Adapted from (Ramotar and Wang, 2003)

1.1.6a 5FU-induced DNA damage

5FU is one of the widely used antimetabolite drug for treating malignancies including colorectal, breast, stomach, pancreatic, oesophageal and head and neck cancers. 5FU has been reported to work both by inhibiting vital biosynthesis processes and by integrating themselves into DNA and RNA, and preventing normal function. Evidence suggests a more complex mechanism for 5FU involving pyrimidine nucleotide balances, DNA repair processes and disruption in RNA metabolism (Longley *et al.*, 2003; Seiple *et al.*, 2006).

Intracellular enzymatic conversion of 5FU results in active metabolites: fluorodeoxyuridine monophosphate (FdUMP), fluorodeoxyuridine triphosphate (FdUTP) and fluorouridine triphosphate (FUTP). The mechanism of 5FU involves inhibition of thymidylate synthase (TS) covalently by the active metabolite FdUMP. TS is a vital enzyme needed for the catalysis of deoxythymidine monophosphate (dTMP) from

deoxyuridine monophosphate (dUMP) **(Fig. 1.1.5)** (Santi *et al.*, 1987). The binding of FdUMP to TS, blocks the access of dUMP to nucleotide binding site and inhibits synthesis of dTMP and subsequent deoxythymidine triphosphate (dTTP). Depletion of dTTP through various feedback mechanisms is reported to influence and disrupt the normal levels of dATP, dGTP and dCTP (Longley *et al.*, 2003). The imbalances particularly dATP/dTTP ratio is believed to interrupt DNA synthesis and repair and, result in fatal DNA damage (Houghton *et al.*, 1995). Additionally, TS inhibition and depletion of dTMP levels results in the accumulation of dUMP and subsequent deoxyuridine triphosphate (dUTP), which can be misincorporated into DNA. In *S. cerevisiae* the processing of such DNA requires base excision repair (BER) pathway to step in and remove the uracil from the DNA.

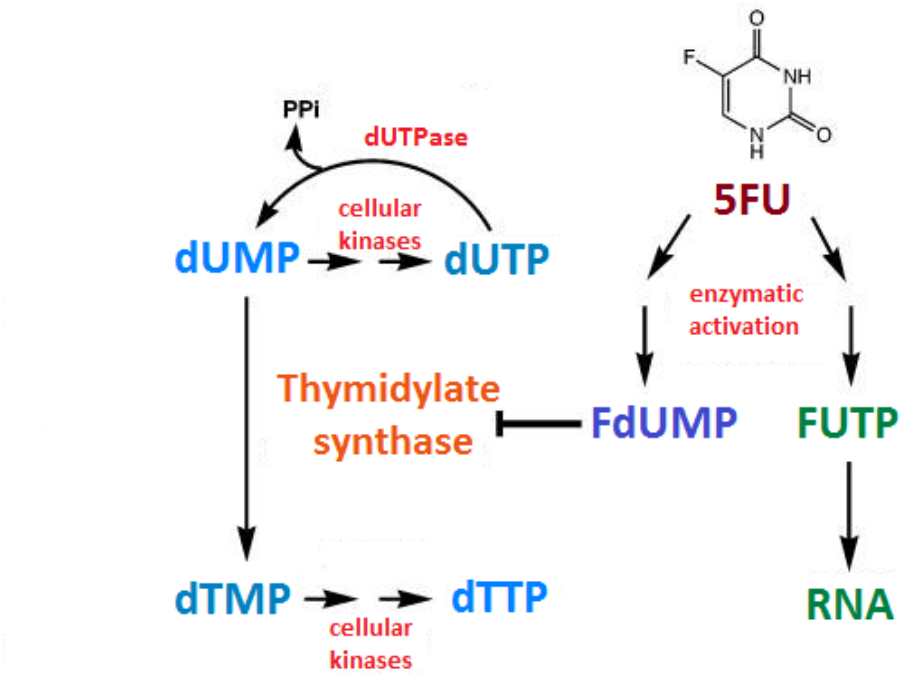

Figure 1.1.5 5FU toxicity and damage to RNA and DNA. 5FU is believed to interfere with nucleic acid structure and function by directly incorporating fluoronucleotides into DNA and RNA, and through inhibition of thymidylate synthase by the active metabolite generated by 5FU, which leads to imbalance in the nucleotide pool. Adapted from Seiple *et al.* (2006).

BER pathway begins with the excision of the uracil base from the DNA by the enzyme uracil-DNA glycosylase (UDG) (Ung1 in yeast) and creating an abasic site or apurinic/apyrimidinic (AP)-site. This is followed by cleavage of the DNA backbone at the abasic site by AP endonuclease enzyme (APE) (Apn1 or Apn2 in yeast). Further, Flap endonuclease, a DNA polymerase and DNA ligase (RAD27p, Polβ and cdc9p, respectively in yeast) insert the correct base in the nicked DNA and complete the repair process **(Fig. 1.1.6)**. However, increase in the levels of dUTP by 5FU could elevate the probability of deoxyuridine being incorporated into DNA again **(Fig. 1.1.6)**. Studies suggest that such

repeated cycles of uracil BER and incorporation of deoxyuridine results in permanent damage to DNA, replication fork failure and cell cycle arrest (Hoskins and Scott Butler, 2007; Ladner, 2001; Seiple *et al.*, 2006).

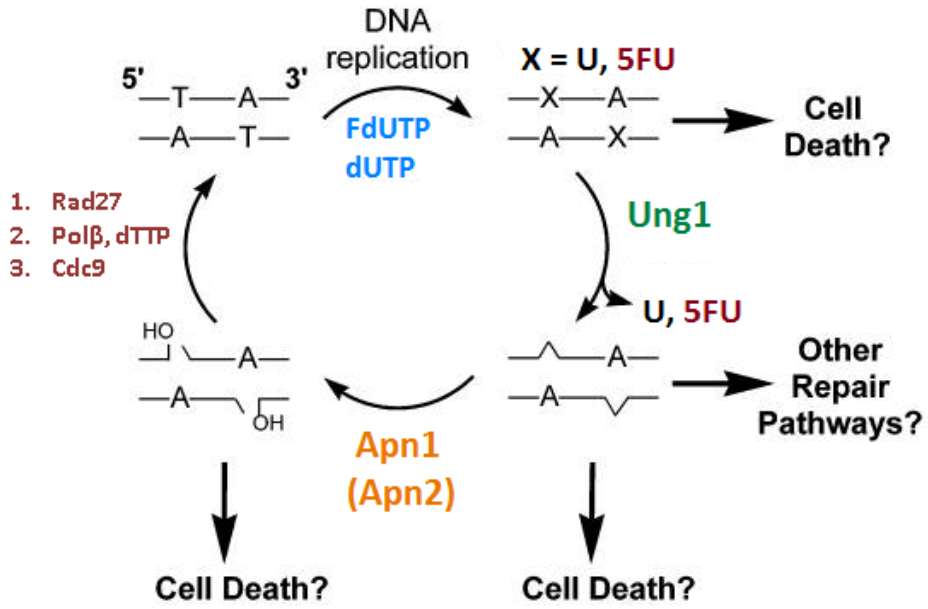

Figure 1.1.6 Uracil BER mediated 5FU toxicity. Attempts to remove misincorporated uracil by BER may result in lethal intermediates along this pathway. Possible intermediates in this process (clockwise) are the mutagenic 5FU base itself, AP-site containing strand (abasic DNA) generated as a result of Ung1 activity. Adapted from Seiple *et al.* (2006)

The importance of the mechanism involving 5FU induced-cytotoxicity was highlighted in experiments using yeast. According to this study, *ung1Δ* showed significant protection against 5FU whereas deletion of the major gene, *apn1*, encoding for AP endonuclease increased the sensitivity of the yeast cells to 5FU (Seiple *et al.*, 2006). Such results suggest that the intact-abasic intermediate created during the repair pathway, if not processed by a BER mechanism, can lead to inherent toxicity. Several backup pathways have been proposed to repair the abasic and 5′dRP groups in the absence of Apn1. Pathways involving Apn2 and other BER enzymes such as AP lyase are reported to account for efficient removal of abasic sites and successful repair in Apn1 mutant strains of yeast (Seiple *et al.*, 2006).

The reaction pathway involving production of dTMP from dUMP provides the single *de novo* source of thymidine precursors which is necessary for DNA synthesis and repair. Both of these processes are severely disrupted due to thymidine starvation (raise of dUTP that overwhelms dUTPase) and misincorporation of uracil in DNA (raise in nucleotide pool imbalance) following 5FU insult and therefore result in what is commonly referred to as ‘thymine-less death’ (Ladner, 2001; Longley *et al.*, 2003).

5FU induced disruption of RNA synthesis by FUTP is a less understood mechanism **(Fig. 1.1.5)**. Unlike thymidine-based 5FU toxicity in DNA, toxicity in RNA has been found to be induced by uridine. Cytotoxicity due to misincorporated 5FU into RNA has also been reported. The proposed effects of 5FU on RNA include mRNA splicing blockage, polyadenylation, base modification in ribosomal-RNA, small nuclear-RNA, and transfer-RNA, ribosomal-RNA processing and, self-splicing of group I introns. However, contribution of these effects to the cytotoxicity of 5FU remain unclear (Hoskins and Scott Butler, 2007).

1.1.6b Bleomycin-induced DNA damage

Radiomimetic drugs and IR are two of the anticancer treatments that induces tumour killing via DNA strand breaks. Bleomycin, a radiomimetic glycopeptide antibiotic, is used in the treatment of Hodgkin's lymphoma, non-Hodgkin's lymphoma, testicular cancer and cancers of head and neck. Bleomycin is less heavily used, and often causes impaired lung functions as a result of lipid peroxidation (Ramotar and Wang, 2003). Bleomycin is believed to induce DNA damage similar to that of IR but different to 5FU. IR generates numerous types of damaged bases, abasic sites and other fragmentary products in addition to ss-breaks with 3′-phosphoglycolate (3′-PG) esters (Fung and Demple, 2011). However, bleomycin causes much more restricted lesions such as 4′-oxidised abasic sites and direct strand breaks resulting in 3′-PG adducts and, 5′-abasic ends **(Fig. 1.1.7)**. The ss- breaks produced initially may further affect the opposite strands leading to DSDBs directly or through incision by DNA repair enzymes (Fung and Demple, 2011).

Bleomycin is reported to generate DNA base loss and cause ss- and ds- DNA damage in the presence of Fe(II) and oxygen (Chen and Stubbe, 2005). Extraction of a hydrogen molecule from the deoxyribose and formation of a free radical is believed to enable Bleomycin-Fe(II)-O_2 complex to break the DNA molecule (Lim *et al.*, 1995). This complex is also reported to cleave yeast $tRNA^{Phe}$, signifying that bleomycin oxidises RNA and as well as DNA (Huttenhofer *et al.*, 1992). Furthermore, the redox status of a given cell type is stated to influence the kind of lesions that bleomycin generates. Under low oxygen levels, bleomycin forms primarily AP-sites while in the presence of oxygen, it produces largely DNA strand breaks **(Fig. 1.1.7)** (Ramotar and Wang, 2003).

Removal of the 3′-PG adduct requires APE1 enzyme in mammals whereas it requires Apn1, Apn2, Mdt1 or tyrosyl-DNA phosphodiesterase (Tdp1) in yeast. *Mdt1* mutants are reported to be sensitive to bleomycin, while single *apn1*, *apn2* and *tdp1* mutants are not

sensitive requiring the triple *apn1apn2tdp1* knockout to confer sensitivity (Liu *et al.*, 2004). Whether it is the repair of the oxidised abasic site or the removal of unsaturated abasic residues generated by AP lyase activity, it requires APE1. Moreover, APE1 is also involved in the conversion of the 3′-PG (at oxidative breaks) to 3′-OH prior to gap filling/ligation process of DNA repair (Fung and Demple, 2011).

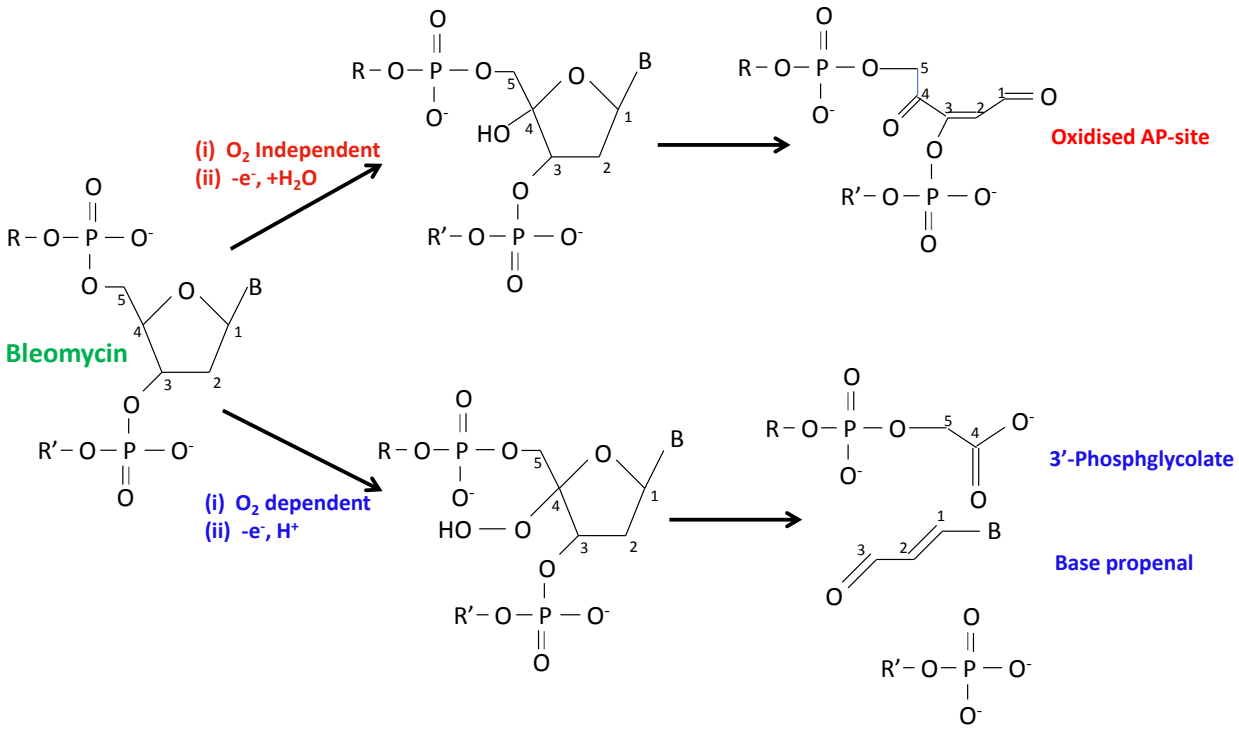

Figure 1.1.7 Bleomycin-induced DNA damage. The types of lesions induced by bleomycin are dependent on the oxygenation conditions. In the presence of oxygen, bleomycin produces primarily DSDB, such as 3′-PG, whereas in the absence of oxygen, bleomycin generates largely an oxidised AP-site. Adapted from Ramotar and Wang (2003).

Reports suggest that APE1 deficient cells are more sensitive to bleomycin than to IR. APE1 knockdown in TK6 lymphoblastoid cells and HCT116 colorectal cancer cells was found to make them sensitive, more greatly towards bleomycin than to IR (Fung and Demple, 2011). An explanation for this could be that: APE1 exhibits opposing effects in IR-induced cytotoxicity, one involving increased tumour killing through *de novo* DSDB formation (dual cutting of closely opposed AP-sites) and the other a protective role involving removal of 3′-PG containing AP-site. Removal of 3′-PG by bleomycin is thought to be a rate limiting step in the repair process. The 3′-PG diesterase activity of APE1 is proposed to be 100-fold slower than it's nicking of AP-site or C4′-oxidised residues in mammals (Xu *et al.*, 1998). Such narrower role of APE1 in repair of bleomycin-induced damage explains the high sensitivity of the cells and build-up of unrepaired DSDBs in APE1 deficient cells. In the absence of APE1, other enzymes that are capable of cleaving 3′-PG at DSDB lesions include polynucleotide kinase (removes 3′-P using ATP as a cofactor) (Xu *et al.*, 1998), Tdp1 (Zhou *et al.*, 2009) and Artemis (Povirk *et al.*, 2007).

In yeast, the repair of DNA lesions is not just restricted to enzymes that cleave AP-sites or 3′-PG groups but also involves Rad52 and Rad6 proteins, which represent the recombination and post-replication DNA-repair pathways, respectively (Ramotar and Wang, 2003). Ku, an important member of NHEJ pathway, has been reported to participate in the repair of bleomycin-induced damage mostly via telomere-specific functions/"chromosome healing" rather than NHEJ-dependent functions in yeast (Tam *et al.*, 2007). Furthermore, phleomycin (selective antibiotic of the bleomycin family) has been shown to activate Mec1-induced direct phosphorylation of Ser129 of histone H2A similar to methyl methane sulfonate (MMS). Failure to phosphorylate H2A has been found to attribute to hypersensitivity of cells to both phleomycin and MMS (Downs *et al.*, 2000). A more recent study suggested that increased translocation of HR proteins, Rad51 and Rad52, to short telomeres and not to single cut sites elicits a Mec1-dependent

hypersensitivity to bleomycin in telomerase deficient cells. This presents a potential mechanistic basis for the reduced DSDB processing in organisms with defective telomeres (Lin *et al.*, 2009).

1.1.7 BER pathway

Most of the complex ds-DNA damages are repaired by NHEJ and HR mechanisms (Lieber, 2010), whereas the majority of small lesions such as deamination of cytosine residues to uracil, single oxidised base, AP-sites and ss- breaks are repaired primarily by BER pathways (Fung and Demple, 2011). BER pathway, comprising of multiple repair enzymes, is an evolutionarily conserved pathway (Kim and Wilson, 2012). Regardless of any differences in the BER theme, the core pathway shares a set of common components and usually initiates five distinct enzymatic steps: (i) recognition and excision of incorrect/damaged base by DNA glycosylases to generate an abasic or AP-site intermediate, (ii) AP-site incision by an APE enzyme or AP-lyase, (iii) removal of fragmented sugar residues by a lyase or phosphodiesterase, (iv) correct base incorporation by a DNA polymerase and, (v) sealing the repaired ends by a DNA ligase. Defects in any of these BER components leads to increased mutations, reduced cell viability, and hypersensitivity to DNA-damaging agents (Kim and Wilson, 2012). Moreover, the pathway is stated to play a vital role in identifying cellular responses to relevant anticancer agents, such as nucleoside analogues (e.g. 5FU), alkylating agents (e.g. temozolomide) and IR (Kim and Wilson, 2012). In this study I will deal with only the initial two key enzymes of BER pathway i.e., DNA glycosylases (UDG specifically) and APE that are involved in the repair of 5FU- and bleomycin-induced damage.

1.1.7a UDG

A search for the mechanism underlying the repair of uracil in *E. coli* DNA led to the discovery of UDG and thereby the discovery of the BER pathway (Lindahl, 1974). The first step in BER is typically UDG catalysing the cleavage of the *N*-glycosidic bond between the 2′-deoxyribose and the substrate base to generate an AP-site (Kim and Wilson, 2012). Ung1 (coded by *ung1* gene) which is part of the UDG family is found to be highly conserved in herpes viruses, bacteria, yeast and human (Olsen *et al.*, 1989). An amino-acid sequence similarity of 40.3% was observed for UDG/Ung1 in humans and yeast (Krokan *et al.*, 1997). However, mammalian cells have been found to contain several additional glycosylases, such as thymine DNA glycosylase (TDG), single-strand-specific monofunctional uracil DNA glycosylases-1 (SMUG1), 8-oxoG DNA glycosylases (OGG1), methyl-CpG binding domain, 3-methyl-purine glycosylase and endonuclease VIII-like (Nei-like or NEIL), which are capable of excising the damaged DNA (Jacobs and Schar, 2012). In eukaryotes, Xeroderma pigmentosum, complementation group C **(**XPC) homologue in yeast, RAD4, has been reported to play UDG-like role in cells i.e., recognising structurally diverse DNA lesions (Sugasawa and Hanaoka, 2007).

In yeast, the Ung1 protein-coding gene (approximately 40 kDa) is found located on chromosome 13 (SGDatabase). The gene encodes for notably two isoforms; mitochondrial Ung1 and nuclear Ung2 in both human and yeast. Although the two isoforms have a common catalytic domain, they differ in their N-terminal sequences (Krokan *et al.*, 2002) and hence the difference in their locations. Ung1 are highly selective to uracil and their removal from U:G mismatches are considered to be faster than removal from U:A, although the preference is dependent on the DNA sequence around the particular mismatch (Slupphaug *et al.*, 1995). Ung2, besides repairing U:G mismatch in nucleoplasm of the cell, are also reported to interact with proliferation cell nuclear antigen and trimeric

replication factor A to induce long patch BER as well as replication (Otterlei *et al.*, 1999). In the absence of Ung, back-up repair mechanisms are reported to be activated among which SMUG1 may have a leading role (Nilsen *et al.*, 2000).

AP-site

AP-sites are the intermediates formed during the course of BER and can also be generated spontaneously as a result of hydrolytic cleavage of *N*-glycosidic bonds (Khodyreva *et al.*, 2010). Following excision and release of substrate base, DNA glycosylases were reported to bind to AP-site with high affinity (Waters *et al.*, 1999). Thus, separation of these two units is considered to be rate limiting step in the BER process. Since AP-site is an unstable intermediate, the binding of the glycosylases is thought to help protect cells from their toxic and mutagenic effects (Jacobs and Schar, 2012). Further, release of glycosylases is coordinated with the entry of downstream acting BER enzyme such as APE1. APE1 has been reported to stimulate the turnover rate of Ung2, TDG and OGG1, and similar effect was also seen with the XPC protein on TDG and SMUG1 (Jacobs and Schar, 2012; Shimizu *et al.*, 2010).

Dissociation of glycosylases from AP-site can also be regulated by means of posttranslational modification including conformational changes to the enzyme bound to the DNA. Increased ability to dissociate from AP-site and associate with replicating chromatin was observed when Ung2 were cell cycle specifically phosphorylated at serine-23. Such modifications apparently enables efficient repair of the misplaced uracil during ongoing DNA replication (Hagen *et al.*, 2008).

1.1.7b APE

The resulting AP-site from the DNA glycosylase activity is incised by a highly conserved repair enzyme, APE (Wang *et al.*, 2014). The Exo III family of APE comprises of two isoforms APE1 and APE2, which have homologues in several organisms including *S. cerevesiae* (Daley et al., 2010). APE1, an essential enzyme, performs key functions such as DNA/RNA repair and transcriptional regulation activities. APE2 has been recently reported to play a role in ATR-Chk1 checkpoint activation caused by oxidative stress (Wang *et al.*, 2014; Willis *et al.*, 2013).

The yeast Apn1 protein-coding gene (41.4kDa), a homologue of APE1, is found located at chromosome 11 followed by *rad27* gene (Dyakonova *et al.*, 2012). Apn1, unlike APE1, does not regulate any essential function under normal growth settings (Popoff *et al.*, 1990). In DNA repair, APE1 cleaves the phosphodiester bond between 5′-phosphate of the AP-site and the preceding nucleotide, leaving a 5′-deoxyribose phosphate (5′dRP) moiety and a free 3′-hydroxyl group at the end. Polymerase β (polβ) hydrolyses 5′-dRP and fills in the single nucleotide gap, which is followed by subsequent sealing of the nick using DNA ligase III-XRCC1 (X-ray repair cross-complementing protein 1) complex.

In addition to the above, APE1 possess three distinct functions: (a) 3′-phosphodiesterase activity, to clean-up the DNA lesions with 3′ blocked termini such as 3′-phosphoglycolate (3′-PG) and 3′-phosphate, (b) non-specific 3′-5′ exonuclease activity, which may serve as an autonomous proof-reading function during synthesis step of BER to prevent misincorporation of damaged/mismatched nucleotides by DNA polymerases, and (c) nucleotide incision repair activity that removes the oxidised DNA bases by creating a nick containing 3′-OH group and 5′-base residue (Wang *et al.*, 2014). Thus, APE1 is capable of repairing diverse DNA lesions.

APE1 is believed to exploit a common active site mechanism involving amino-acid residues Glu96, Asp210 and His309 to coordinate Mg^{2+} binding and catalyse breakdown of the phosphodiester bond (Mol *et al.*, 2000; Wang *et al.*, 2014). Glu96 and Asp210 are also considered to be crucial for APE1 reactions. Double mutation of these residues is reported to slow down the dissociation of APE1 from AP-site, while eliminating AP-site incision activity (McNeill and Wilson, 2007). Furthermore, the mutants were observed to exhibit increased sensitivity and accumulation of fatal AP-site damage with MMS treatment, whereas they failed to show sensitivity to bleomycin. In contrast, downregulation of APE1 level has been shown to increase cellular sensitivity to MMS and bleomycin (Fung and Demple, 2011). APE1 depleted cells have also shown to accumulate high levels of AP-sites, which when left unrepaired can threaten to be mutagenic and can induce apoptosis (Fung and Demple, 2005). He *et al.* (2001) reported A549 lung epithelial cells expressing Apn1 to exhibit significantly reduced DNA damage even in the presence 100 µg/ml of bleomycin.

1.2 Diphosphoinositol polyphosphate phosphohydrolases (DIPPs)

1.2.1 Introduction to DIPPs

The implication of IDPs (1-$InsP_7$, 5-$InsP_7$ and $InsP_8$) in crucial processes such as cell signalling and metabolic homeostasis has drawn particular attention to these high-energy signalling molecules lately. Understanding metabolic regulation of IDPs turnover appears essential to unveil how this signalling cascade is controlled. In fact, no metabolic pathway can claim to be complete or meaningful without the knowledge of the kinetic parameters of the participating enzymes (Rohwer, 2012). However, modelling of IDPs metabolism is complicated by there being two parallel kinase pathways from $InsP_6$ to $InsP_8$ (named I and II in (Padmanabhan *et al.*, 2009); **Fig. 1.2.1**), and by diphosphoinositol polyphosphate phosphohydrolases (DIPPs). A further confounding factor is that humans express five DIPP isoforms: type 1 (DIPP-1), types 2α/2β (DIPP-2α/DIPP-2β) and types 3α/3β (DIPP-3α/DIPP-3β) (Caffrey *et al.*, 2000; Hidaka *et al.*, 2002; Leslie *et al.*, 2002; Safrany *et al.*, 1998). However, *Saccharomyces cerevisiae* expresses only one: the diadenosine and diphosphoinositol phosphohydrolase (Ddp1).

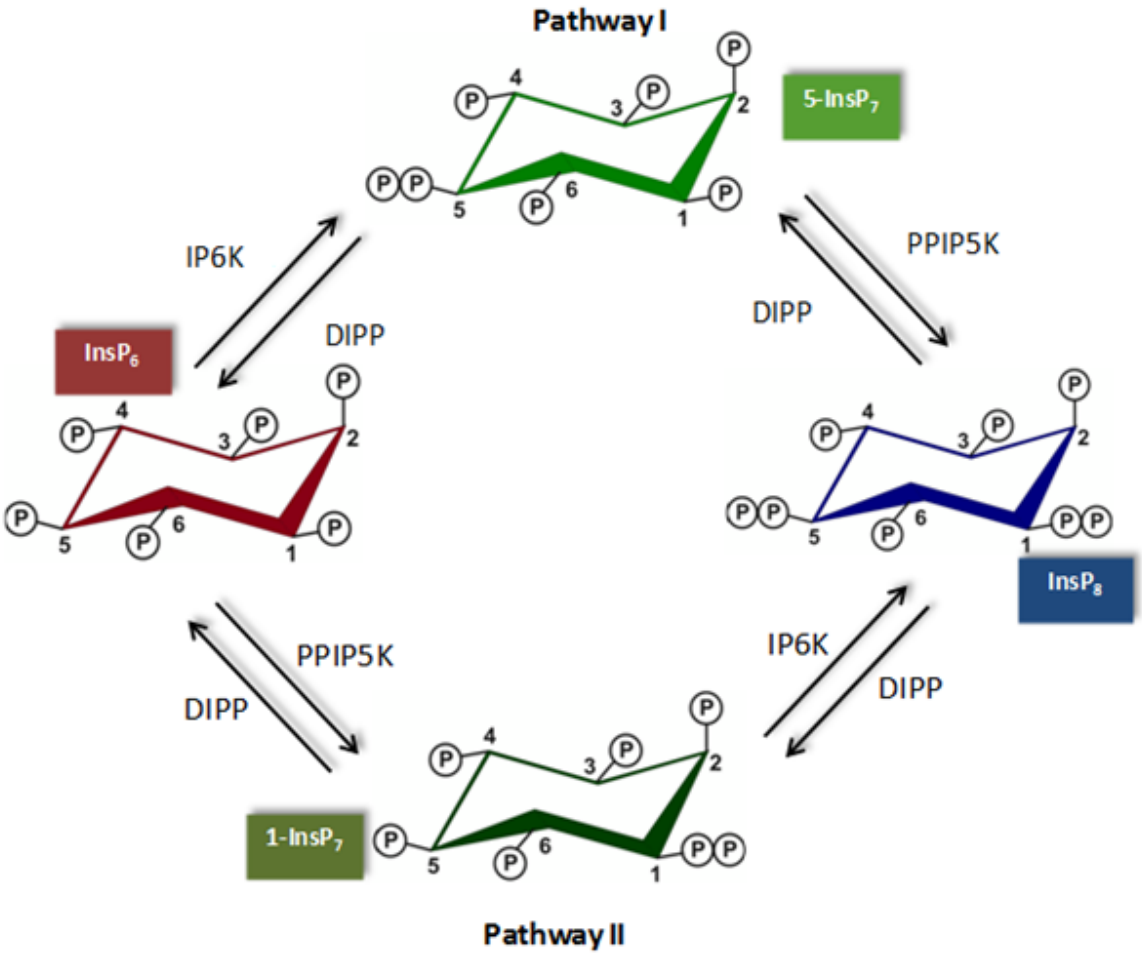

Figure 1.2.1 Metabolic interconversions of $InsP_6$, $InsP_7$ and $InsP_8$. Diphosphoinositol polyphosphate phosphohydrolases represented as DIPP (Ddp1 in yeast); Inositol hexakisphosphate kinase represented as IP6K (Kcs1 in yeast); Diphosphoinositol pentakisphosphate kinase represented as PPIP5K (Vip1 in yeast). Pathways I and II are named as in Padmanabhan *et al.* (2009).

The DIPP that dephosphorylate IDPs are as important as kinases to cell functions (Shears *et al.*, 2013). DIPPs are held responsible for rapid turnover of IDPs inside cells and are also the reason why mammalian cells mostly show low steady-state concentration of these molecules (Menniti *et al.*, 1993). Overall, the levels of $InsP_7$ range between 1-5 µM

(Shears, 2004), of which mammalian cells are reported to have mostly 5-isomer form (Albert *et al.*, 1997). In yeast and mammalian cells, the levels of PP-$InsP_4$ and $InsP_8$ are each recorded to be about 10-20% of those of $InsP_7$ (Safrany, 2004; Safrany *et al.*, 1998; Shears *et al.*, 2013).

1.2.2 DIPP isoforms

1.2.2a DIPP-1

The first DIPP form, DIPP-1 [also known as Nudix-type 3 (NUDT3)], that metabolises both $InsP_7$ and $InsP_8$ was purified, characterised and sequenced from rat liver by (Safrany *et al.*, 1998). $InsP_6$ is not a substrate of DIPP, but it is found to inhibit dephosphorylation of both $InsP_7$ and $InsP_8$. DIPP sequences of rat and human are reported to show considerable conservation. The human DIPP cDNA sequence greatly matched the regions of chromosome 6 and within the region is minimum four exons identified for the candidate gene. The DIPP-1 form is found expressed largely in brain, heart, pancreas and liver, with some degree of expression in all the tissue type tested (Safrany *et al.*, 1998). This study also found that physiologically relevant conditions such near neutral pH and Mg^{2+} concentration of 1-2 mM, can add to optimal hydrolysis of IDPs by DIPP. Also, fluoride was found to potently inhibit of DIPP-1 activity on both $InsP_7$ and $InsP_8$.

A site-directed mutagenisis study revealed the importance of several catalytically crucial residues in human DIPP-1 (Yang *et al.*, 1999), namely (i) Glu66 and Glu70 within Nudix-type (NudT) domain, (ii) the glycine repeat regions, GR1 and GR2, where GR1 consists of tripeptide (G50, G51 and G52) at the N-terminus of NudT catalytic motif, and glycine residues (G72, G75 and G82) within a consensus sequence, GX_2GX_6G at the C-terminus of the motif and (iii) His^{91} and Phe^{84} that are vital largely for $InsP_8$ than $InsP_7$ hydrolysis.

1.2.2b DIPP-2

A 21 kDa human isoforms, DIPP-2α and DIPP-2β, with a 76% identity to DIPP-1 was characterized by Caffrey *et al.* (2000). The catalytically essential residues seen in DIPP-1 along with the predicted secondary structure are conserved in DIPP-2α. DIPP-2 (also known as NUDT4) form is most highly expressed in heart compared to other tissues and the gene coding for it is located on chromosome 12 (Caffrey and Shears, 2001). The two isoforms of DIPP-2 differ from each other merely by DIPP-2β containing of an extra amino acid (Gln^{86}) (Caffrey *et al.*, 2000). Possible reasons that may contribute to the coexistence of the two isoforms are: nucleotide polymorphism in the gene or product of two different genes or variants produced as a result of alternative splice sites. DIPP-2β is considered less active than DIPP-2α against $InsP_7$. Moreover, DIPP-2α is reported to hold high activity on $InsP_7$, although it is considered less active than DIPP-1. Report by Caffrey *et al.* (2000) also suggests involvement of an array of alternative (canonical and non-canonical) polyadenylation signals in the synthesis of multiple mRNAs for DIPP-2α. These messenger molecules have identical α and/or β open reading frames but differ in the length of the 3′-UTR region (Caffrey *et al.*, 2000). The 5′-UTR region has high GC content (84%) and accommodates six CAG repeats. This feature of human DIPP-2 is considered unusual, as most of the eukaryotic transcription process involves only a single polyadenylation signal (Edwalds-Gilbert *et al.*, 1997). Such feature also suggests that expression of these proteins is regulated by several molecular processes.

1.2.2c DIPP-3

The two 19 kDa DIPP isoforms, namely DIPP-3α and DIPP-3β, which exhibits 90% identity to DIPP-2 (residues 2-165) and 74% identity to DIPP-1 (residues 2-164) were characterised by (Hidaka *et al.*, 2002). DIPP-3 has been shown to express in high levels in pancreas and heart (Leslie *et al.*, 2002). The genes *NudT10* encoding DIPP-3α and *NudT11*

encoding DIPP-3β are found just 152 kbp apart on chromosome X. Besides the resemblance in coding regions, the two DIPP-3 forms show high similarity in predicted intron/exon structure, aligned introns sequences and 5'-non-translated sequence, suggesting that the two genes encoding the isoforms might have arose as a result of gene duplication event. Such duplication event in human genome often emphasizes that the expressed protein serves some function and are not entirely redundant (Otto and Yong, 2002). A 33-residue active site region, Nudix-type catalytic motif, found in DIPP-3α showed strong conservation with DIPP-1 and -2. The motif was found flanked on either side (N-terminal GGG tripeptide and C-terminal GX_2GX_6G sequence) by short Glycine-rich sequences (Hidaka *et al.*, 2002).

The two isoforms of DIPP-3 was observed to differ from each other solely by DIPP-3β containing Arg-89 in the place of Pro-89 amino-acid, which is seen in the DIPP-3α form (Hidaka *et al.*, 2002). This Arg residue, which is also conserved in DIPP-1 and -2 forms, serves a catalytic role (Yang *et al.*, 1999) and thus makes DIPP-3β ~2-fold more active *in vitro* (Hidaka et al., 2002). The specificity constants (K_{cat}/K_m) for hydrolysis of $InsP_7$ by DIPP-3 was similar to that with DIPP-2β, however, it was 9-25-fold lower than the value for DIPP-1 (Safrany, Ingram, *et al.*, 1999) and -2α (Caffrey *et al.*, 2000). Previous work has shown the ability of DIPP family to metabolise diadenosine hexaphosphate (Ap_6A), another Nudix substrate (Leslie *et al.*, 2002; Safrany, Ingram, *et al.*, 1999). However, kinetic study of DIPP-3 has found IDPs to be the more physiologically relevant substrate compared to less efficiently metabolised substrate, Ap_6A (Hua *et al.*, 2003). A decline of 35% to 45% in the steady-state levels of $InsP_7$ and $InsP_8$ was observed with overexpression of either of the DIPP-3 forms (Hidaka *et al.*, 2002). This was the first report to show altered expression of DIPP in intact cells to affect the IDP concentrations *in vivo*. Both DIPP-3 forms require an optimum alkaline pH *in vitro* and also demand for the presence of divalent cations such as Mn^{2+} over Mg^{2+} for their activity (Leslie *et al.*, 2002). Although

role of these cations in these reactions is not clear, it is possible that they are required to neutralise the negative charges carried by substrate's phosphate groups or they may be directly involved in the catalytic act (Thomas and Potter, 2014).

1.2.2d Ddp1

The *Ddp1* of *S. cerevisiae*, located on chromosome 15, encodes for a 21 kDa protein that hydrolyses IDPs and diadenosine polyphosphates (ApAs) (Cartwright and McLennan, 1999; Safrany, Ingram, *et al.*, 1999). Ddp1 is a member of MutT family of hydrolases which is conserved from yeast to humans (Cartwright and McLennan, 1999). Ddp1, as an IDP phosphatase hydrolyses $InsP_7$ and $InsP_8$ to $InsP_6$ whereas, as an ApA phosphatase, it much readily dephosphorylates Ap_6A and is also capable of dephosphorylating diadenosine pentaphosphate (Ap_5A), adenosine pentaphosphate (p_5A) and adenosine tetraphosphate (p_4A). Ddp1p, which is considered as the yeast homologue of NUDT3 or DIPP-1 isoform of humans, has been found to have control over the evolutionarily conserved activity of mRNA decapping *in vitro* (Song *et al.*, 2013). Similar to DIPP-1 (Safrany *et al.*, 1998), Ddp1 activity was also found to be severely affected in the presence of fluoride (Lonetti *et al.*, 2011).

A recent report demonstrated Ddp1 to hydrolyse pyrophosphate group in the 1-position of 1-$InsP_7$ completely, but, failed to do the same with 5-isomer of 5-$InsP_7$ under the same conditions (Lonetti *et al.*, 2011). This was proposed to be due to 5-$InsP_7$ acting as a competitive inhibitor for Ddp1, especially when used in combination with Ap_5A substrate (Wu *et al.*, 2013).

1.2.3 Structure of a DIPP

All the mammalian DIPP isoforms are fairly small proteins with a molecular weight just about 20 kDa (Hua *et al.*, 2003; Leslie *et al.*, 2002; Safrany *et al.*, 1998). The binding site of each protein is usually dependent on the Nudix domain, which often has characteristic amino acid sequence Gx_5Ex_5[UA]xREx_2EExGU (where U signifies an aliphatic, hydrophobic residue) . This domain is more often found conserved in proteins with functions restricted to hydrolysis of substrates such as nucleoside di- and triphosphates, dinucleoside polyphosphates and nucleotide sugars [McLennan (2007) in Shears *et al.* (2013)]. A site-directed mutagenesis study by Yang *et al.* (1999) revealed that the residues, His(91) and Phe(84), found outside the Nudix domain to greatly influence the catalytic activity of human DIPP-1 towards IDPs. So far only one DIPP structure, human DIPP-1, has been presented (Thorsell *et al.*, 2009).

The human DIPP-1 structure has been reported to contain a canonical nudix fold comprising of two β-sheets flanked by short helices. The nudix domain, unlike the usual loop-helix-loop fold, exhibits a strand-loop-helix configuration in DIPP-1. This variation is due to insertion of six residues in the place of five between the N-terminal Gly and the first Glu in the domain (Thorsell *et al.*, 2009). Also, the first three residues of the nudix domain are found tightly associated with the neighbouring β-strand.

$InsP_8$ was not fully characterised when the DIPP-1 structure was published. However, Thorsell *et al.* (2009) managed to model both 1,5 and 3,5 alternative isomers of $InsP_8$ into the active site of DIPP-1 structure. This in turn led them to speculate that 3,5-$InsP_8$ form was most preferred of the two to form strong interactions with the active site residues of DIPP-1. However, it was later found out to be the 1,5-$InsP_8$ isomer by Wang *et al.* (2012). Structure of DIPP-1 is shown in **Fig. 1.2.2.**

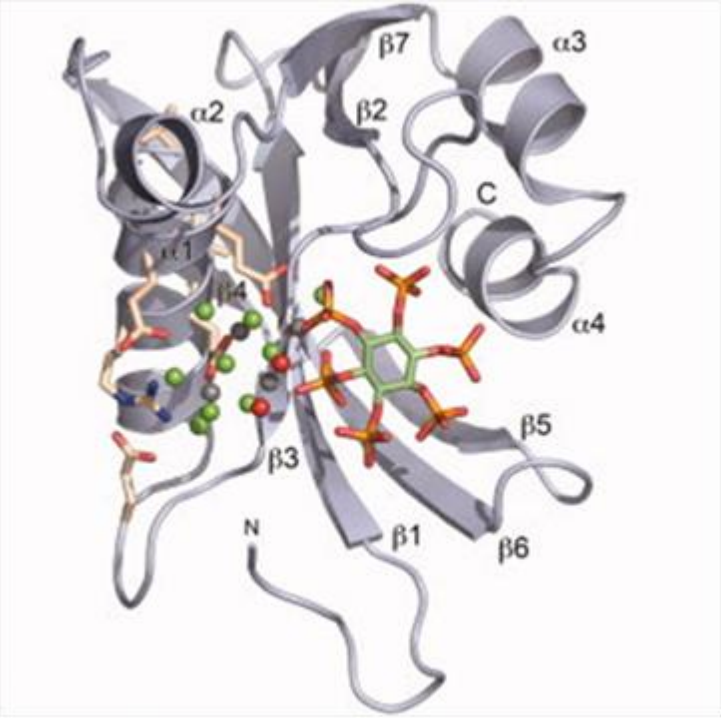

Figure 1.2.2 Structure of Homo sapiens-DIPP-1. Residues of nudix domain are represented as sticks and coloured beige. Magnesium ions are in grey, fluoride ions in green and water molecules in red. Adapted from Thorsell *et al.* (2009).

1.3 Effects of aspirin analogues on oesophageal cancer

1.3.1 Oesophageal cancer

Oesophageal cancer is considered as one of the deadliest cancers worldwide because of its aggressive nature and low survival rate. It is the 8th most common cancer seen worldwide and is the 6th most common cause of death from cancer [CRUK(b)]. According to incidence and mortality statistics by CRUK(b), oesophageal cancer is the 13th most common cancer and is the 6th most common cause of death in the UK. Cancer of the oesophagus usually occurs in one of two forms, squamous cell carcinoma (SCC) arising from the stratified squamous epithelial lining of oesophagus and adenocarcinomas (ADC) from the columnar glandular cells lining the oesophagus (Conteduca *et al.*, 2012). These two cancer types vary in occurrence, geographical distribution, ethnic difference, aetiology and nutritional intake/deficiencies (Kamangar *et al.*, 2009). The factors that differentiate oesophageal SSC from ADC, including the genetic alterations and potential tumour targets/markers are described in **Table 1.3.1**. Other rare variants of oesophageal cancer include sarcomas (~2%) and small cell carcinoma (0.05- 4%) (Yun *et al.*, 2007; Zhang, 2013). Additionally, a tumour occurring at less than 5 cm above or below the oesophagus-stomach juncture is classed as gastro-oesophageal junction (GOJ) cancer. Though GOJ act different to cancers of stomach and oesophagus, doctors' stage and treat GOJ tumours as oesophageal cancer [CRUK(a)].

Factors	oesophageal squamous cell carcinoma (SCC)	oesophageal adenocarcinoma (ADC)
Origin	Stratified squamous epithelial lining of oesophagus.	Columnar glandular cells lining the oesophagus.
Region of occurrence	Evenly distributed between the middle and lower third of the oesophagus (Enzinger and Mayer, 2003).	Three quarters occur in the distal oesophagus (type I ADC) (Enzinger and Mayer, 2003). Other types include type II (true carcinoma of the cardia/cardiac carcinoma) and type III (subcardial gastric cancer infiltrating the distal oesophagus) (Rudiger Siewert *et al*., 2000).
Risk factors	Tobacco and alcohol abuse lead to 20-fold increased risk of developing SCC (Lee *et al*., 2005).	-Precancerous and asymptomatic Barrett's oesophagus (BO, or Barrett's metaplasia) (Conteduca *et al*., 2012). -BO related dysplasia, oesophagitis and gastro-oesophageal reflux disease (GORD). -Distal oesophageal irritation due to achalasia, hiatus hernia, scleroderma or chemical injuries [CRUK(a)].
Family history and associated risk	Molecular alterations at phospholipase C epsilon 1 and C20orf53 (Wang *et al*., 2010), down-regulation of TGF-*β* signalling (SMAD1) (Chattopadhyay *et al*., 2009) , loss of heterozygosity (LOH) of chromosome 13 regions in Chinese patients (Hu *et al*., 2003), aberrant methylation on the promoter *p16* (Abbaszadegan *et al*., 2005).	Family history of BO, oesophagogastric junctional adenocarcinoma and ADC (Chak *et al*., 2002), hiatal hernia and prostate cancer (Jiang *et al*., 2014).
Geographical distribution	Developing countries, spreads out from northeast China to Middle East (Melhado *et al*., 2010).	Developed countries, increased occurrence in US and western Europe (Conteduca *et al*., 2012).
Racial group/gender	In the US, it affects four times more blacks than whites (Cook *et al*., 2009) and more in men than women (Melhado *et al*., 2010).	Occurs most often in whites. In the US, it affects five times more whites than blacks and eight times more men than women (El-Serag *et al*., 2002).
Survival rate	5-year survival rates with 37.1% for primary cancer, 18.5% for regionally spread cancers, and 3.1% for metastatic cancer (Wong *et al*., 2011). 5-year survival rates were 46% after tumour resection (Mariette *et al*., 2005).	5-year survival rates were 45% after tumour resection (Mariette *et al*., 2005).
Prognostic biomarkers and genetic alterations	-Expression of Metastasis suppressor-1 (Xie *et al*., 2011). -Down-regulation of gene deleted in oesophageal cancer 1 (*DEC1*) (Leung *et al*., 2008). -Up-regulation of COX-2 (Zimmermann *et al*., 1999), ß-catenin levels (Kimura *et al*., 1999), NFκB (Yang *et al*., 2005). -Altered expression of apoptosis related genes including B-cell lymphoma 2, caspase 3, TNF-related apoptosis-inducing ligand, EGFR, Fas-L and Fas (Chang *et al*., 2005). -Frequent LOH on human chromosome 1p, 3p, 4, 5q, 9, 11q, 13q, 17q and 18. These chromosome changes lead to a loss of putative tumour suppressor function (Stoner *et al*., 2007). -Single nucleotide polymorphism (SNP) in alcohol dehydrogenase 1B, acetaldehyde dehydrogenase 2 (Cui *et al*., 2009) and cytochrome p450 1A1 (Zhuo *et al*., 2009). -Mutations of *p53* (Gao *et al*., 1994; Dulak *et al*., 2013), *NOTCH1* (Forde and Kelly, 2013). Epigenetic silencing of RAS association domain family 1A and fragile histidine triad genes (Kuroki *et al*., 2003). -Low expression of miR-223 is associated with poor prognosis (Mathe *et al*., 2009). -Elevated miR-21 and reduced miR-375 expression levels (Mathe *et al*., 2009).	-GORD, oesophagitis, BO are important biomarkers. BO develops in 10% of patients with GORD (Gorecki, 2001). -11-fold increase in risk for ADC in BO patients compared to people without the condition (Hvid-Jensen *et al*., 2011). -Overexpression of cyclin-D1 in BO cells (Arber *et al*., 1996; Barrett *et al*., 1996). -Hypermethylation and mutation of CDKN2/p16 (Barrett *et al*., 1996; Klump *et al*., 1998; Dulak *et al*., 2013). -Increase in aneuploidy or tertraploid cell fraction and inactivation of *p53* in BO (Galipeau *et al*., 1996). -LOH on chromosomes 17p, 18q, 5q (Wu *et al*., 1998) and 9p21 (Barrett *et al*., 1996). -Polymorphisms in glutathione S-transferase M1, T1 and P1 (Kala *et al*., 2007). -Low levels of serum-selenium correlates with increased risk of high-grade dysplasia, tertraploid fractions and *TP53LOH* in persons with BO (Rudolph *et al*., 2003). -Low expression of miR375, miR233 is associated with poor prognosis (Mathe *et al*., 2009). -Elevated level miR-21, miR-223, miR-192, and miR-194 but reduced miR-203 expression (Mathe *et al*., 2009) and miR-196a (Luthra *et al*., 2008).

Table 1.3.1 Factors that differentiate oesophageal SSC from ADC

1.3.2 Treatment

With the increasing incidences of oesophageal cancer worldwide, arises the urgent need for effective treatments and new approaches to combat this disease. Chemotherapy has been a moderately effective treatment option for locally advanced and metastatic oesophageal cancer (Forde and Kelly, 2013). Recent focuses on the potential oncogenic targets in oesophageal cancer have resulted in the emergence of number of promising and efficient targeted therapies. Brief notes on the current therapies and future strategies are listed below.

1.3.2a Targeted therapy

Besides the advancements with combination therapies for oesophageal cancer, survival and/or cure rates have been low (17.5% surviving 5 years, SEER statistics as of 2004-2010). Targeted therapy which has been successful with cancers such as colon could prove useful for oesophageal cancer (Forde and Kelly, 2013). Molecular level knowledge on cancer signalling pathways have shed light on the potential targets in oesophageal cancer including nuclear factor-κB (NF-κB), CDKs, cyclooxygenase (COX)-2 inhibition, matrix metalloproteinases (MMPs), epidermal growth factor receptor (EGFR) and vascular endothelial growth factor (VEGF) (Campbell and Villaflor, 2010). A brief description on the most promising targets at present are stated below and some of the clinical trials carried out based on these targets are mentioned in the **Table 1.3.2**.

1.3.2a(i) EGFR

EGFR is at least of four types: EGFR (EGFR-1, HER-1), HER-2, HER-3 and HER-4. EGFR, a proto-oncogene, plays an important role in regulating cell proliferation, invasion, metastasis and apoptosis (Tabernero *et al.*, 2005). EGFR proteins are reported to be overexpressed in 30-70% of oesophageal SCC and ADC and their overexpression are often

correlated with poor prognosis (Itakura *et al.*, 1994; Wang *et al.*, 2007). In an effort to target EGFR in oesophageal or GOJ cancer, numerous clinical trials have been initiated with key agents like monoclonal antibodies (mAbs) and tyrosine kinase inhibitors (TKIs). The most common mAbs used currently for treatments and in clinical trials include cetuximab (IgG1), panitumumab (IgG2) **(Table 1.3.2)**. Trastuzumab (Herceptin) and T-DM1 are HER-2 receptor-targeted mAbs that are involved in current clinical trials. T-DM1 with its promising outcome as moved on to phase III trial whereas multimodality neoadjuvant treatment with trastuzumab is unclear because of its suspected cardiotoxicity in patients (**Table 1.3.2**). Studies of EGFR TKIs to date has been unsatisfactory, with comparatively high toxicity rates and limited signs of activity due to low incidence of activating mutations of EGFR in oesophageal cancer (Forde and Kelly, 2013).

1.3.2a(ii) VEGF

VEGF, an angiogenesis regulator is also considered a potential target to tackle oesophageal cancer. Similar to EGFR, overexpression of VEGF has also been reported in 28%-64% of oesophageal cancer and is likewise associated with poor prognosis (Forde and Kelly, 2013). In addition, evidences of increased expression of VEGF during chemotherapy and radiotherapy have made it an attractive target for multimodality neoadjuvant therapy (Campbell and Villaflor, 2010; Kulke *et al.*, 2004). Despite the hype, VEGF-targeted therapy is yet to yield a satisfactory response in case of oesophageal cancer. Although trials showed signs of efficiency with VEGF-targeted therapy in unselected populations, the efficacy failed to stand out in phase III randomised trials. However, a recent phase III trial (REGARD) with ramucirumab appears to be promising with a 1.4 month survival advantage (Forde and Kelly, 2013) (**Table 1.3.2**).

1.3.2a(iii) MET/hepatocyte growth factor (HGF) and Fibroblast growth factor receptor (FGFR)

Gene amplification of MET proto-oncogene has been reported in 2%-10% of oesophageal ADC but only 1% in SSC (Forde and Kelly, 2013; Kato *et al.*, 2013; Lennerz *et al.*, 2011). MET induced cancers are of higher grade and are usually diagnosed at an advanced stage. Phase III MET inhibitors trials including Onartuzumab and Rilotumumab are ongoing at the moment **(Table 1.3.3)**. Promising results from phase II trial with Rilotumumab combined with chemotherapy in patients with overexpressed MET has given hope that these agents may exhibit efficacy and give an added optional treatment for patients (Forde and Kelly, 2013).

Increased expression of FGFR-2, observed in 4% of oesophageal cancer, has been again associated with poor prognosis (Matsumoto *et al.*, 2012). Preclinical study by Yashiro *et al*., (2010) suggests that FGFR-2 inhibitors may yield synergistic anticancer effect with chemotherapy in gastric cancers (Yashiro *et al.*, 2010). Cediranib, an FGFR-2 oral inhibitor, despite of good tolerability outcome in phase I study in GOJ and ADC is yet to undergo further clinical investigation. A selective oral potent inhibitor of FGFR-1, FGFR-2, and FGFR-3 called AZD4547 is undergoing phase II trial for FGFR-advanced oesophageal GOJ. Amongst the various pathway-specific anticancer agents known, FGFR-tyrosine kinase inhibitors appears to be a more wise strategy that is likely to show clinically relevant benefits (Forde and Kelly, 2013).

1.3.2b Novel targets

Several other carcinogenic cellular pathways, molecular strategies and tumour targets are currently under clinical investigation for oesophagus related cancers (**Table 1.3.3**). Efficacy of everolimus which targets mTOR and inhibits downstream signalling is

currently being investigated. Synergistic effects of poly (adenosine diphosphate-ribose) polymerase (PARP) family of inhibitory proteins in combination with radiation are being tried in a phase I trial for locally advanced oesophageal and GOJ tumours (Forde and Kelly, 2013). Novel immune-based treatments are also being launched in clinical trials, including ipilimumab, an anti-cytotoxic T-lymphocyte antigen 4 antibody and adjuvant tumour vaccine following tumour resection. Next-generation immunomodulatory antibodies such as anti-programmed death-1 and anti-programmed death ligand-1 are also under clinical investigation for oesophageal and solid tumours. Chemotherapeutic treatments based on the methylation status of forkhead-associated and ring finger domains (CHFR) are also being experimented in clinical trials (Forde and Kelly, 2013).

Table 1.3.2 Some of the oesophageal cancer targeted therapies in clinical trials. Adapted from (Forde and Kelly, 2013). Abbreviations: BSC, best supportive care; CRT, chemoradiation; GOJ, gastro-oesophageal junction; NCT, clinicaltrials.gov identifier; ORR, overall response rate; OS, overall survival; pCR, pathologic complete response; PFS, progression-free survival; SWOG, Southwest Oncology Group; T-DM1, trastuzumab emtansine; TKI, tyrosine kinase inhibitor.

Targeted therapies	NCT identifier	Patient population	Treatment(s)	Results/status
Cetuximab (mAb targeting EGFR)	NCT00445861	Stage IIB-IIIC resectable esophageal/GOJ tumour	Preoperative cisplatin/docetaxel/cetuximab	Phase(IB/II) completed; promising with pCR and near pCR rates of 68%
	NCT00509561	Stage IA-IIIC oesophageal/GOJ (type I) tumours not candidates for surgery	Cisplatin/capecitabine/radiation ± cetuximab	Phase II/III completed; increased toxicity and poor survival
	NCT00109850 (SWOG 0414)	Stage III oesophagus/GOJ tumours not candidates for surgery	Cisplatin/Irinotecan (IR)/cetuvimab/radiation	Phase II closed early because of poor accrual; among 21 patients treated, 2 died
Panitumumab (mAb targeting EGFR)	NCT00757172 (ACOSOG Z4051)	Stage IIB-IV (M1a) oesophageal/GOJ adenocarcinoma	Preoperative cisplatin/docetaxel/radiation/panitumumab	Phase II completed; promising with pCR and near pCR rate of 55.2%. Trial closed for lack of efficacy
Trastuzumab (mAb targeting HER-2	NCT01041404	First-line HER-2-positive stage IV GOJ/gastric adenocarcinoma	Cisplatin/fluorouracil or cisplatin/capecitabine ± trastuzumab	Phase III results show 2.7 month OS advantage with addition of: trastuzumab/chemotherapy, 13.8 month; chemotherapy alone, 11.1 month (p=0.0046). No increase in significant toxicity
Lapatinib (TKI targeting HER-2 and EGFR)	NCT00680901	First-line stage IV HER-2-positive oesophageal/GOJ/gastric adenocarcinoma	Capecitabine and oxaliplatin ± lapatinib	Phase II trial completed accrual; awaiting results
T-DM1 (mAb-drug conjugate targeting HER-2)	NCT01641939	Second-line stage HER-2-positive GOJ and gastric cancer	T-DM1 versus taxane	Remarkably well tolerated in studies to date. Currently accruing for Phase III trial
Bevacizumab (mAb targeting VEGF-A)	NCT00354679	Stage IIA-IIC resectable oesophageal/GOJ adenocarcinoma	Preoperative irinotecan/cisplatin/radiation plus bevacizumab	Phase II trial showed prolonged survival compared to historical standards (pCR: 15%); median time to tumour progression:8.3 months; no increase in PFS or OS
	NCT00450203 (ST03,MAGIC-B trial)	Stage II-IV (M1a) resectable oesophageal/GOJ or gastric adenocarcinoma	Preoperative epirubicin/cisplatin/capecitabine ± bevacizumab for 3 cycles followed by postoperative epirubicin/cisplatin/capecitabine ± bevacizumab for 3 cycles	Currently accruing for Phase II/III trial
Ramucirumab (mAb targeting VEGF-R2)	NCT01246960	First-line oesophageal/GOJ or gastric adenocarcinoma	5FU /leucovorin/oxaliplatin ± ramucirumab	Completed accrual for phase III trial
	NCT00917384 (REGARD)	Second-line GOJ or gastric adenocarcinoma	BSC ± ramucirumab	Phase III results showing median OS: ramucirumab + BSC, 5.2 month; BSC, 3.8 month (p= 0.04753)

Targeted therapies	NCT identifier	Patient population	Treatment(s)
MET/HGF targeted therapy	NCT01611857 (phase I/II) NCT01662869 (phase III) NCT01697072 (phase III)	First-line stage IV molecularly unselected oesophageal/GOJ/gastric adenocarcinoma First-line stage IV HER-2-negative, MET-positive GOJ tumours First-line stage IV MET-positive GOJ or gastric tumours	5FU/leucovorin/oxaliplatin plus tivantinib (c-MET inhibitor) Modified 5FU/leucovorin/oxaliplatin 6 ± onaruzumab Epirubicin, cisplatin, and Capecitabine + placebo or rilotumumab
mTOR targeted therapy	NCT01490749 (phase I/IIB	Locally advanced oesophageal tumours	Capecitabine plus oxaliplatin/carboplatin/radiation ± everolimus (inhibitor of mTOR)
Immune-directed therapies	NCT01258868 (phase I) NCT01284231 (phase I) NCT01375842 (phase I) NCT01585987 (phase II)	Following resection of oesophagus tumours Advanced gastrointestinal adenocarcinoma, including GOJ tumours Solid tumours, including oesophageal cancer Following first-line chemotherapy for stage IV GOJ gastric tumours	Adjuvant ISCOMATRIX autologous tumour vaccine and celecoxib MEDI-565 (CEA/CD3 bispecific antibody T-cell activator) MPDL3280A (PD-L1 antibody) Ipilimumab
PARP	NCT01460888 (phase I)	Locally advanced oesophagus /GOJ tumours	Radiation with concurrent olaparib
Hedgehog signalling targeted therapy	NCT00982592 (phase II)	First-line unresectable or metastatic GOJ/gastric adenocarcinoma	5FU/leucovorin/oxaliplatin ± vismodegib
Akt	NCT01260701 (phase II)	Second-line stage IV GOJ/gastric adenocarcinoma)	MK2206 (Akt inhibitor)
FGFR	NCT01457846 (phase II)	Second-line stage FGFR-amplified oesophageal /GOJ/gastric adenocarcinoma	AZD4547 (FGFR inhibitor) versus paclitaxel
CHFR methylation	NCT01372202	Locally advanced oesophageal/GOJ tumours	Chemotherapy chosen based on CHFR methylation status
Claudin-18	NCT01671774	CLDN18.2 expression-positive stage IV oesophageal/GOJ or gastric cancer	iMAB362 (antibody targeting CLDN18.2 cell surface antigen) + zoledronic acid

Table 1.3.3 Novel targeted therapies for oesophageal cancer in clinical trials. Adapted from (Forde and Kelly, 2013). Abbreviations: CHFR, checkpoint with forkhead-associated and RING finger domains; PD-L1, programmed death-ligand 1.

1.3.2c Non-steroidal anti-inflammatory drugs (NSAIDs) and their role in cancer

NSAIDs are a class of drugs commonly used for treatment of fever, pain-related and inflammatory conditions such as headaches, menstrual cramps, mild-to-moderate pain from inflammation of tissue or injury and arthritis. The most prominent members of this group of drugs include aspirin, ibuprofen, naproxen, indomethacin, sulindac and piroxicam (Gurpinar *et al.*, 2013).

Epidemiological, clinical and preclinical studies provide substantial evidence that NSAIDs (including COX-2 selective inhibitors) possess potent antitumorigenic properties (Gurpinar *et al.*, 2013). The anticancer effect of NSAIDs against colorectal cancer (CRC) is particularly well-known. Several cohort studies have shown significantly reduced risk of colorectal adenomatous polyps and CRC in long-term users of NSAIDs than non-users (Chan, 2002; Giardiello *et al.*, 1995; Thun *et al.*, 2002). Reduction of precancerous colorectal polyps in patients with Garner's syndrome with the use of NSAID sulindac (Clinoril®) was the first clinical evidence to be reported in a case study (Waddell and Loughry, 1983). Furthermore, several randomized controlled trials (RCTs) reported that sulindac strongly inhibits the development of adenomatous polyps and causes regression of existing polyps in patients with familial adenomatous polyposis (FAP) (Giardiello *et al.*, 1993; Winde *et al.*, 1995). A study which compared the efficiency of several NSAIDs on UV-induced non-melanoma skin cancer in SKH-1 hairless mice reported sulindac to be the most potent NSAID in reducing skin cancer (Mikulec *et al.*, 2013). Suppression of adenoma formation in FAP patients was also reported with the use of the COX-2 selective inhibitor, celecoxib (Celebrex®) (Steinbach *et al.*, 2000). This led to the FDA approval of celecoxib treatment for FAP patients in 1999, but was later withdrawn due to drug related vascular and upper gastrointestinal (GI) side effects (Gurpinar *et al.*, 2013; Solomon *et al.*,

2005). Regular Ibuprofen intake was also found to reduce risk of breast cancer by about 50% in a cohort study (Harris *et al.*, 1999).

1.3.3 Aspirin

Acetylsalicylic acid, commercially known as aspirin, is one of the most widely used anti-inflammatory drug to date. The active metabolite of aspirin, salicylic acid, was first discovered by Greek physician Hippocrates more than 2000 years ago from the bark of the willow tree. However, aspirin was first synthesized in its stable form by Felix Hoffmann in 1897 at Bayer & Co laboratory (Gensini and Conti, 2009). Aspirin is a non-opioid analgesic with antipyretic and antiplatelet properties with a half-life of 15-20 min in the blood (Bruno *et al.*, 2012). Aspirin does not only act as an effective anti-inflammatory drug but also can prevent stroke and other cardiovascular diseases. A number of RCTs are still trying to address the issue of the safe use of prophylactic aspirin for the primary prevention of cardiovascular diseases (Sutcliffe *et al.*, 2013).

1.3.3a Aspirin as a chemopreventative drug

In the last few years the attention has been towards the potential role of aspirin in the prevention and possibly treatment of various cancers. Several studies have reported that continued use of aspirin can result in lesser incidence of cancers or deaths from cancers arising from various tissues. These include cancers such as breast (Harris *et al.*, 1999), lung (Muscat *et al.*, 2003), prostate (Jacobs *et al.*, 2005), ovarian (Cramer *et al.*, 1998), oesophagus, stomach, colon and rectum (Thun *et al.*, 1993). However, the possible chemoprotective benefit with the administration of aspirin was comparatively significant with digestive tract related cancers than others mentioned above (Thun *et al.*, 1993).

1.3.3b Aspirin and CRC

Of several chemotherapeutic strategies that are being pursued to combat CRC, use of aspirin is one of the most promising. In animal models, aspirin was found to reduce the initiation and progression of aberrant crypt foci in the colon (Liu *et al.*, 2008). Recent meta-analysis data with large number of patient studies indicates that daily use of aspirin at treatment dose for 5 years or more reduces the risk of developing multiple cancer types including CRC (Algra and Rothwell, 2012). In addition, the review indicated aspirin's ability to suppress the risk of cancer metastasis. Also, in a RCT of patients with Lynch syndrome (CAPP2 study), administering 600 mg dose of aspirin daily for ~2 years resulted in substantial decline of CRC incidence (Burn *et al.*, 2011). A recent study also reported significant decrease of CRC incidences in Scotland with only 75 mg daily-dose of aspirin for a period of 5 years (Din *et al.*, 2010). Regular use of aspirin post-diagnosis of non-metastatic CRC has also been reported to reduce CRC-specific mortality, an association that was strongest when the cyclooxygenase-2 (COX-2) was overexpressed in primary tumour (Chan *et al.*, 2009). Overexpression of COX-2 in majority of the oesophageal cancers has also been reported (Zimmermann *et al.*, 1999). Since inhibition of this enzyme is claimed by some to be the reason behind NSAIDs/aspirin's chemotherapeutic properties, it is possible that these drugs hold promising anticancer effects against oesophageal cancers.

1.3.3c Aspirin and oesophageal cancer

Multiple studies have suggested that aspirin and other NSAIDs protect against oesophageal cancer. According to a meta-analysis study based on exposure type, aspirin was found to have greater protective effect than non-aspirin NSAIDs (Corley *et al.*, 2003). Several epidemiological studies have reported that intake of aspirin and other NSAIDs could protect against oesophageal ADC by either preventing the development of precursor BO or

by reducing the possibility of BO advancing to ADC. A study reported 33% reduction in the risk of developing oesophageal ADC with the use of NSAIDs (Corley *et al.*, 2003). Furthermore, BO patients using NSAIDs exhibited significantly reduced risk of developing oesophageal ADC (6.6%) compared to non-users (14.3%) (Vaughan *et al.*, 2005). Reports suggest that such reduced cancer risk in BO patients using NSAIDs could be due to decreased rate of acquisition of somatic genomic abnormalities in individuals (Kostadinov *et al.*, 2013). In contrast, a cohort study found no substantial correlation between use of aspirin or non-aspirin NSAIDs and oesophageal ADC (Abnet *et al.*, 2009). Aspirin use was also associated with reduced risk (90%) of developing squamous cell carcinoma of head and neck (Ahmadi *et al.*, 2010). Liu *et al.* (2009) found that use of aspirin following an oesophagectomy for SSC patients improved the 5-year survival rate to about 49.8% compared to placebo (42.2%) and no tablet (41.2%) ($p = 0.26$).

1.3.3d Anti-metastatic property of aspirin

Aspirin not only reduces the risk of cancer death but also reduces the risk of metastasis in certain cancers. A review on daily aspirin against no aspirin for the prevention of cardiovascular diseases in five large UK trials showed that aspirin reduced (a) risk of distant metastasis by 30-40% and, (b) risk of metastatic adenocarcinoma by almost half (Rothwell, Wilson, *et al.*, 2012). Adenocarcinoma patients who did not have metastasis to start with but still continued to use daily aspirin up to or after diagnosis showed reduced risk of metastasis (by about 70%) on subsequent follow-up. Such effect was seen with a low-dose (75 mg), slow-releasing formulation of aspirin that had only little systemic bioavailability (Rothwell, Wilson, *et al.*, 2012). The mechanism behind the anti-metastatic effect of aspirin was shown to be inhibition of platelet formation or thrombocytosis (Gasic *et al.*, 1972; Langley *et al.*, 2011). However, aspirin's ability to decrease invasiveness in COX-2 negative colon cancer cells was attributed to up-regulation of *NM23* (a metastatic

suppressor gene) and down-regulation of carcinoembryonic antigen and CD44v6 (metastasis inducer) expression (Yu *et al.*, 2002).

1.3.3e Side effects of aspirin use

Besides the beneficial anticancer property of aspirin, there is the issue of serious side effects with its use. Long-term use of aspirin is reported to carry the risk of adverse gastrointestinal bleeding. Regular use of NSAIDs was found to cause ulcers in 15%-30% and annual incidence of upper GI clinical events in 2.5%-4.5% of patients (Laine, 2002). Dyspepsia, an upper GI symptom, was also found to occur in 15%-60% of NSAID users. Whether the risk of aspirin related side effects balances against its benefits is still debatable. However, the side effects profile of aspirin use is relatively small compared to adverse effects of most cancer treatments. Analysis by Rothwell, Price, *et al.* (2012) also showed that extended use of aspirin can reduce risk of major extracranial bleeds in patients. A meta-analysis study found aspirin use, at a low dose of 75-325 mg, to increase the risk of major bleeding by ~70%, but the absolute annual increase was limited at 0.13% for major bleeding, 0.12% for gastrointestinal bleeding and 0.03% for intracranial bleeding (McQuaid and Laine, 2006).

1.3.3f Adjuvant aspirin therapy

Several clinical and pre-clinical studies have been carried out to see whether aspirin in combination with an anti-acid reflux drug can reduce the side effects during the treatment. Examples of such studies are as follows:

1.3.3f(i) Aspirin with Proton-Pump Inhibitor esomeprazole

Aspirin along with an acid suppression drug called esomeprazole is being tried out in a randomised phase III AspECT trial in the UK (Das *et al.*, 2009). This study aims to find

the benefits of low or high dose of acid suppression drug with or without aspirin in decreasing the risk of BO and related ADC.

1.3.3f(ii) Ursodeoxycholic acid with aspirin

An *in vivo* study by Rizvi *et al.* (2010) reported that Urso in combination with aspirin reduces risk of oesophageal ADC in animals with reflux. The novel target of Urso-aspirin combination was proposed to be GLI1, a hedgehog-regulated transcription factor. The urso-aspirin combination was suggested to exert chemopreventative effect by downregulating pro-oncogenic gene GLI1 which in turn regulates activation of cell cycle regulator, CDK2 (Rizvi *et al*., 2010).

1.3.3f(iii) Statin with aspirin

A meta-analysis study stated that prolonged use of statin in combination with aspirin/NSAIDs could provide greater protective effect against oesophageal ADC (Singh and Singh, 2013). According to a recent study, endometrial cancer patients under statins and aspirin treatment had an 84% decreased threat of death compared to non-users and statin or aspirin users (Spoozak *et al.*, 2013). The toxicity profiles of statins by itself and its effect on aspirin induced gastropathy is unknown. Epidemiological data suggests that use of NSAIDs in combination with statins, 3-hydroxy-3-methylglutaryl-coenzyme A reductase inhibitors, appear to have an added protective effect in patients with BO (Kastelein *et al.*, 2011).

1.3.4 Molecular mechanisms involved in anticancer effects of aspirin

Increasing evidences in support of aspirin's anticancer role has raised the demand for an insight into the biological mechanism underlying it. Although many mechanisms of actions are postulated for aspirin so far, it still remains an area of much debate. Studies suggest

that aspirin mainly exerts its anticancer effects through COX-dependent or/and through COX-independent pathways.

1.3.4a COX-dependent mechanisms

Prostaglandin (PG) H-synthases or COX enzymes exists as two isoforms COX-1 and COX-2. COX is a bifunctional enzyme exhibiting both COX and peroxidase activity. The COX component of the enzyme coverts arachidonic acid (AA) to hydroperoxy endoperoxide prostaglandin G_2 (PGG_2), and the peroxidase part reduces the PGG_2 to corresponding alcohol (PGH_2) which acts as the precursor of prostanoids [i.e., prostaglandins, prostacyclin (PGI_2), and thromboxane A_2 (TXA_2)] (Hamberg and Samuelsson, 1973). Prostaglandins, regarded as vital messenger molecules, in their active state influences a number of pathophysiological processes such as cell growth, angiogenesis, invasion, apoptosis, immune response and thrombosis in an array of tissues (Langley *et al.*, 2011).

COX-1, which is expressed in most tissues, is thought to regulate a number of 'housekeeping' functions such as vascular homeostasis, renal blood flow and glomerular functions. COX-2, expressed in restricted tissues in physiological levels especially in endothelial cells, is thought to contribute to COX-2-dependent-PGI_2 effects such as anti-thrombosis and vasodilation **(Fig. 1.3.1)** (Hennan *et al.*, 2001). However, overexpression of COX-2 in tissues has been associated with pathological condition such as cancer (Seibert *et al.*, 1997; Williams *et al.*, 1999). Prostaglandin E_2 (PGE_2), a major prostanoid produced by COX-2 variant in the cancer cells, has been found to be the key agent promoting cell proliferation, metastasis, angiogenesis and resistance to apoptosis (Greenhough *et al.*, 2009). Studies have also reported a role for COX-1 in pathological process such as atherosclerosis and cancer (Daikoku *et al.*, 2005; McClelland *et al.*, 2009). An immunohistochemical study by Zimmermann *et al.* (1999) found COX-2 expression in

91% of oesophageal SCC and 78% of oesophageal ADC. This study also showed overexpression of COX-2 variant in cancerous tissue as opposed to normal oesophageal squamous epithelium. However, COX-1 expression in this study was found to be at physiological levels in both normal and cancerous tissues.

Cancer of SCC, BO and ADC are all associated with increased COX-2 expression (Shirvani *et al.*, 2000; Zimmermann *et al.*, 1999). Several studies have reported increased expression of COX-2 in oe33 (Abdalla *et al.*, 2005; Jimenez *et al.*, 2010), oe21 (Abdalla *et al.*, 2005) and flo-1 (Aggarwal *et al.*, 2000) cells. However, a latter study also found flo-1 to express only trace levels of either COX isoforms (Aggarwal *et al.*, 2000).

Most hypotheses have centred round aspirin's ability to modulate AA metabolism by COX inhibition. Unlike other NSAIDs, aspirin's capability to irreversibly inhibit COX enzymes is well known. Irreversible acetylation of serine molecule (i.e., Ser529 in human COX-1, and Ser516 in human COX-2) by aspirin results in blockade of the COX channel and thereby prevents access of AA to the active site of the enzyme (Chan and Detering, 2013). Preferential inhibition of COX-1 than COX-2 by aspirin is well established. Considering aspirin's short half-life in the blood and inclination to inhibit COX-1 variant >100-fold more than COX-2 (Dovizio *et al.*, 2012), it appears ideal for aspirin to act on COX-1 platelets and irreversibly block TXA_2-dependent platelet function **(Fig. 1.3.1)** (Clarke *et al.*, 1991). In contrast, a higher dose of aspirin in shorter intervals (because nucleated cells are quick to resynthesize the COX enzymes while platelets cannot) is required for inhibition of COX-2-dependent pathophysiological processes. *In vitro* studies show varying IC_{50} values for COX-1 and COX-2 inhibition by aspirin: in chondrocyte cells, COX-1 IC_{50}=3.57 µM and COX-2=29.3 µM (Blanco *et al.*, 1999); in intact cells, COX-1=4.3 µM and COX-2=714.3 µM (Botting, 2006; Mitchell *et al.*, 1993). However,

all the above studies reported aspirin to be highly selective for COX-1 compared to COX-2.

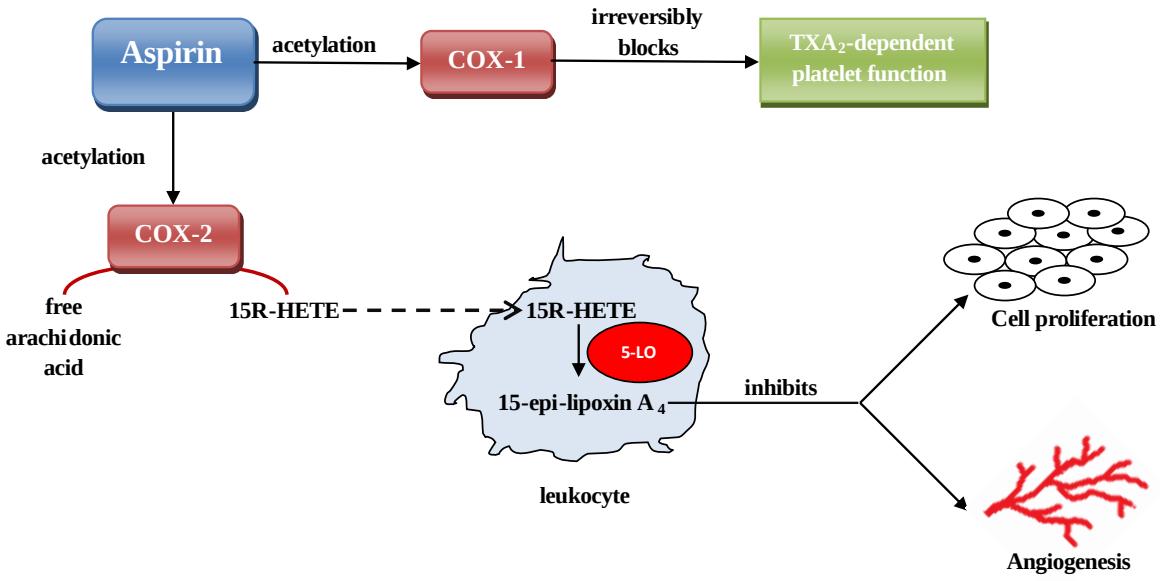

Figure 1.3.1 Anticancer effects of aspirin-triggered lipoxins. Aspirin acetylates COX-1 enzyme and irreversibly blocks TXA_2-dependent platelet functions to produce the beneficial cardiovascular effects. Contrarily, acetylated COX-2 participates in the transformation of free arachidonic acid to 15R-HETE, which is then metabolised by leukocytes (or monocytes) to 15-epilipoxinA_4 in the presence of the enzyme 5-lipoxygenase (5-LO). Adapted from Baker *et al.* (2009); Bruno *et al.* (2012).

The antiplatelet property of aspirin does not only reduce incidences of myocardial infarction but also is thought to partly contribute to aspirin's anticarcinogenic effect. Increased platelet activation or thrombocytosis is observed in 10-57% of cancer patients (Sierko and Wojtukiewicz, 2004). An increase in platelet count was associated with tumour progression and poor survival rate in oesophageal carcinoma patients (Shimada *et al.*,

2004). Oesophageal ADC patients were reported to show significantly higher platelet activation compared to SCC patients (Aminian *et al.*, 2011). Moreover, thrombocytosis has been reported to be involved in crucial stages of cancer development (Bambace and Holmes, 2011). Thrombocytosis promotes tumour driven platelet aggregation, release of cytokines (interleukin (IL)-1, IL-6), proteolytic enzymes (heparanase, MMPs), and platelet microparticles which can aid in cell proliferation, angiogenesis and metastasis. It is also proposed that aspirin-induced-thrombocytosis may promote COX-2 expression and metastasis development through the production of key factors such as IL-1β, platelet derived growth factor and transforming growth factor beta (TGF-*β*) in colorectal adenoma and CRC (Sciulli *et al.*, 2005).

Aspirin shows an incomplete allosteric inhibitory effect on COX-2 compared to COX-1 (Sharma *et al.*, 2010). Acetylation of COX-1 suppresses the enzyme activity, whereas acetylation of COX-2 alters the enzyme hampering its ability to form PGG_2 and thus produces an alternative product, 15R-hydroxyeicosapentaenoic acid (15R-HETE) from AA **(Fig. 1.3.1)**. Further, 15R-HETE are metabolized to the epi-lipoxins (also known as aspirin-triggered lipoxin) by the action of 5-LO in monocytes and leukocytes (Gilroy, 2005). Epi-lipoxins are shown to be potent inhibitors of cell proliferation and angiogenesis (Baker *et al.*, 2009). A recent study in a rat model with gastroesophageal reflux revealed low levels of PGE_2 and increased levels epi-lipoxin$_4$ at oesophageal tissue levels with aspirin treatment (50 mg/kg/day) compared to non-treated (Esquivias *et al.*, 2014). However, epi-lipoxin$_4$ was found ineffective in preventing the induction of oesophageal ADC in their study.

Yet another proposed mechanism of aspirin that helps protects against cancer is by the inhibition of sphingosine-l-phosphate (S1P) from human platelets, even in the presence of stimulated potent peptide agonist of the thrombin receptor PAR-1 (protease-activated

receptor-1) (Ulrych *et al.,* 2011). Expression of S1P from platelets, a regulatory molecule in cancer development (Kawamori *et al.,* 2009), is dependent on the activation of COX-1 dependent TXA_2.

1.3.4b COX-independent mechanism

Besides aspirin's ability to inhibit COXs, several other COX-independent mechanisms have been proposed to contribute to pharmacological effects of aspirin in CRC. NSAIDs and aspirin are reported to affect major cancer signalling pathways that are involved in cell proliferation and/or induce apoptosis.

1.3.4b(i) Induction of Apoptosis

Numerous reports suggest that the primary mechanism behind the anticancer effect of NSAIDs/aspirin is apoptosis. Sulindac sulphide was the first NSAID to be reported to exhibit a COX-independent antineoplastic effect on cancer cells (Shiff *et al.*, 1995). Administration of non-COX-inhibitory sulindac sulfone was found to result in induction of apoptosis selectively in rectal polyps of FAP patients but not in normal rectal mucosa (Stoner *et al.*, 1999). Such a feature of selective effect is not obvious even with the conventional chemotherapeutic drugs that are designed to act by inducing apoptosis (Gurpinar *et al.,* 2013). A study by Shureiqi *et al.* (2001) found that NSAIDs induce apoptosis in both oesophageal ADC and SCC cells by up-regulating expression of 15-lipoxygenase-1 (a tumour suppressor gene). Aspirin-induced apoptosis was also observed by Li *et al.* (2000) in oesophageal cancer cell lines. However, aspirin has been reported to induce cell cycle arrest and necrosis at higher concentrations *in vitro* in CRC (SW 620 and HT-29) cell lines (Subbegowda and Frommel, 1998).

Many mechanisms and targets have been associated with the NSAID's induction of apoptosis. Although a particular NSAID may have its own specific COX-independent target, it is possible that a combination of effects triggered by NSAIDs in different signalling pathways through direct or indirect target may contribute to induction of apoptosis. Major direct cellular targets that induce NSAID-mediated apoptosis are mentioned below.

1.3.4b(ii) IKKβ/NF-κB

Several studies have shown that NSAIDs may exert their apoptotic effect through direct modulation of NF-κB signalling pathway. NF-κB transcriptional factors such as p50 and p65 (Rel A) components remain in an inactive form in the cytoplasm when in association with IκB inhibitory regulatory protein (Gurpinar *et al.*, 2013). However, ubiquitination and proteasomal degradation events during phosphorylation of IκB by the cGMP-dependent protein kinase IKKβ results in release of free NF-κB. The free NF-κB then enters nucleus and binds to DNA, resulting in transcriptional activation **(Fig. 1.3.2)** (Brown *et al.*, 1995; Gurpinar *et al.*, 2013). Anti-apoptotic property of NF-κB is exhibited by activation of apoptosis inhibitors such as TRAF1/2 and c-IAP1/2, or c-myc (cell survival promoters). NF-κB mediated apoptosis has been evident in both *in vivo* and *in vitro* models of CRC i.e., HT29 xenograph model and $Apc^{Min+/-}$ mice. Aspirin (5 mM), sodium salicylate (5 mM), sulindac (1 mM), and its analogues sulindac sulphide (200 μM) and sulfone (1 mM) were all reported to directly bind and inhibit recombinant IKKβ and regulate NF-κB signalling in COS cells transfected with an NF-κB-responsive expression vector (Yamamoto *et al.*, 1999). Aspirin has been reported to inhibit cancer progression by induction of apoptosis in oesophageal SCC cells by inhibition of NF-κB signalling (Liu *et al.*, 2005). In this study, the induction of apoptosis was associated with down-regulation of COX-2 expression, prostaglandin synthesis and up-regulation of cytoplasmic IκB.

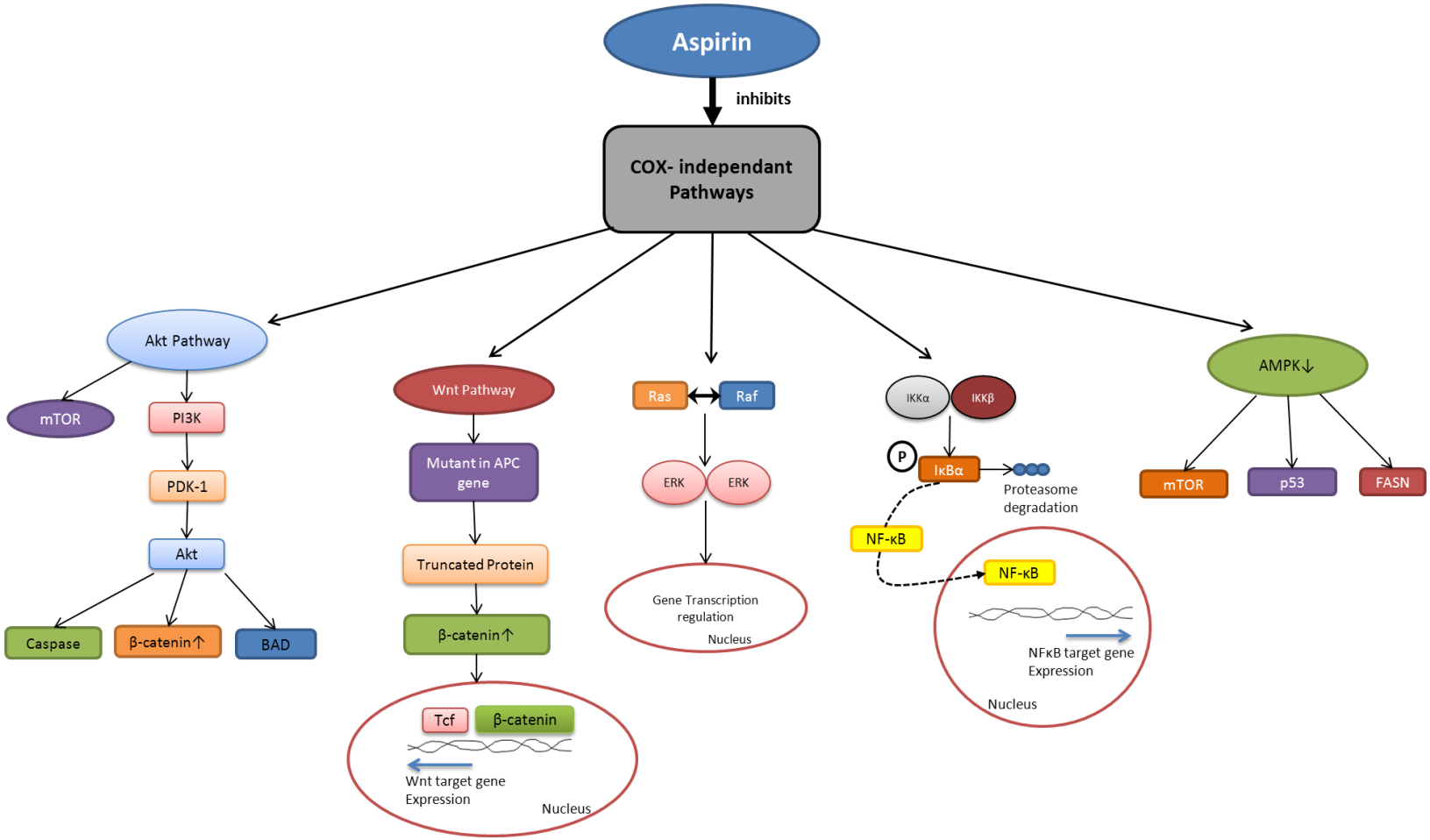

Figure 1.3.2 COX-independent mechanisms of aspirin. Aspirin has been associated with several off-target effects. Some, but not all, proposed pathways are shown above. Adapted from (Bruno *et al.*, 2012; Gurpinar *et al.*, 2013).

1.3.4b(iii) Wnt/β-Catenin pathway

An increase in the accumulation of cytoplasmic β-catenin and activation of Wnt/β-catenin pathway has been implicated in CRC cases (Munemitsu *et al.*, 1995). Activation of this pathway is a result of mutation in adenomatous polyposis coli (APC) gene **(Fig. 1.3.2)**. Mutated *apc* gene is reported to result in a truncated non-functional form of the protein which fails to form the complex that downregulates β-catenin (Munemitsu *et al.*, 1995). This translates into abnormally high level of cytoplasmic β-catenin which then translocate to the nucleus and binds to members of T-cell factor (TCF)/lymphoid enhancer factor family transcription factors and activates cyclin D and Myc transcription (Wnt targeted genes) (Shtutman *et al.*, 1999). A study by Bos *et al.* (2006) demonstrated that treating CRC cell lines with aspirin inhibits protein phosphatase 2A enzyme activity, a protein that influences phosphorylation of the β-catenin. Furthermore, increase in the level of phosphorylated β-catenin results in its degradation and thereby inactivation of the Wnt/β-catenin pathway.

1.3.4b(iv) ERK signalling

A higher concentration of aspirin *in vitro* has been reported to modulate COX-independent biological responses through differential regulation of kinases involved in the extracellular signal-regulated kinases pathway (ERK 1/2) [also known as, Ras-Raf-MEK-ERK pathway or mitogen activated protein kinase (MAPK) pathway] **(Fig. 1.3.2)** (Seger and Krebs, 1995). Activation of the ERK pathway by various extracellular stimuli in diverse tissue types result in phosphorylation of various downstream substrates that are involved in regulation of key processes such as cell cycle progression, cell migration, differentiation, proliferation, metabolism and transcription (Seger and Krebs, 1995). Mutations in the key kinases and/or aberrant activation of ERK pathway are reported in many types of cancer. A

study by Zheng *et al.* (2011) reported the expression and activation of ERK/MAPK cascade in an oesophageal SCC cell line (i.e., EC9706). The study also found ERK 2 to be more important than ERK 1 in the proliferation of SCC cells. It was recently shown that several NSAIDs including aspirin down-regulates ERK/MAPK cascade by inhibiting the binding of oncogene Ras to c-Raf which otherwise would activate ERK pathway leading to carcinogenesis (Pan *et al.*, 2008).

1.3.4b(v) AMPK/mTOR

Adenosine monophosphate-activated protein kinase (AMPK) is an energy-sensing enzyme capable of detecting and reacting to AMP:ATP variations during hypoxia, exercise, ischemia and glucose deprivation (Hardie, 2011). In order to live up to the energy demands, AMP inhibits ATP-consuming processes and in turn generates more ATP by initiating β-oxidation of fatty acids. Recent studies have reported that AMPK plays a pivotal role in regulating diverse oncogenes involved in cancer progression, such as p53, fatty acid synthase (FASN) and mechanistic target of rapamycin (mTOR) (Luo *et al.*, 2010). A study using CRC cells found that mM concentrations of aspirin was adequate to (a) down-regulate mTOR pathway by inhibiting mTOR effectors S6K1 and 4E-BP1 and (b) alter nucleotide ratio and activate AMPK pathway (Din *et al.*, 2012). In fact, AMPK activation and autophagy as a result of mTOR inhibition was greater when aspirin was given in combination with metformin (an AMP activator) treatment (Din *et al.*, 2012).

1.3.4b(vi) Acetylation of proteins by aspirin

Aspirin has been shown to acetylate several plasma constituents (hormones and enzymes), biomolecules (DNA and RNA) and proteins (haemoglobin and histones) *in vitro* (Alfonso *et al.*, 2009; Pinckard *et al.*, 1968). A study found aspirin (100 μM) to acetylate the key tumour suppressor protein p53 in human breast cancer cell line (Alfonso *et al.*, 2009). An

increase in acetylation of p53 by aspirin has been associated with increased p53 binding to DNA and expression of its two targeted genes, $p21^{CIP1}$ (protein involved in cell cycle arrest) and Bax (Bcl-2-associated X protein, a mitochondrial pro-apoptotic protein). According to a study, treating oesophageal cancer cell lines with aspirin reduced B-cell lymphoma 2 (Bcl-2) expression, whereas no changes were noted with expression of Bax and p21 (Li *et al.*, 2000).

1.3.4b(vii) Akt/PDK-1

3-phosphoinositide-dependent-kinase-1 (PDK-1), a kinase crucial in the activation of Akt pathway, is implicated in the progression of several cancers (Vivanco and Sawyers, 2002). Phosphoinositide 3-kinase (PI3K) indirectly regulates PDK-1 by phosphorylation of PtdIns(4,5)P_2, co-recruiting PDK-1 and its substrate Akt, leading to phosphorylation and activation of Akt, a critical regulator of cell growth, proliferation, motility and survival. Anti-apoptotic property of Akt is exerted by phosphorylated inactivation of pro-apoptotic protein BAD (Bcl-2 associated death promoter), direct phosphorylation of proteins that down-regulates β-catenin levels, phosphorylation of caspase 9 to prevent its cleavage to active form of caspase 9 **(Fig. 1.3.2)** (Hanada *et al.*, 2004). Several studies have reported that the apoptotic effect of celecoxib is through inhibition of PDK-1 and Akt (Gurpinar *et al.*, 2013). The ability/efficiency of the drug celecoxib to induce apoptosis in HT-29 colon cells was found to be dependent on mutational or expression status of PDK-1 and/or Akt (Arico *et al.*, 2002).

1.3.4b(viii) Specific protein (Sp) regulated anticancer effect of aspirin

Sp or zinc transcription factor are key proteins involved in various cellular processes such as cell differentiation, growth, apoptosis and immune responses. A study indicated that use of aspirin-like nitro-NSAID ie., GT-094 exerted anticancer effect on CRC through a

reactive oxygen species-dependent regulation of Sp transcription factors and Sp-regulated genes. Sp regulated genes include key apoptosis-control genes like Bcl-2, survivin, hepatocyte growth factor receptor (c-MET), VEGF and its receptors VEGFR1 (Pathi *et al.*, 2011). Moreover, anticancer effect of aspirin on CRC was found to be through induction of apoptosis and down-regulation of Sp-regulated genes involved in CRC carcinogenesis (Pathi *et al.*, 2012). In the same study, the anticancer effect of aspirin was found to be similar to that of salicylate and thus they proposed that the chemotherapeutic effect of aspirin may primarily be due to salicylate metabolite.

2. MATERIALS and METHODS

2.1 Materials

2.1.1 Reagents

Unless otherwise stated all chemicals were standard reagent grade or higher and purchased from Sigma-Aldrich Company Ltd, Gillingham, Dorset, UK. Tissue culture media and supplements were all purchased from Life Technologies Ltd (Gibco), Inchinnan Business Park, Paisley, UK.

Amersham Pharmacia Biotech, Buckinghamshire, UK
-pGEX6P-1
-Glutathione Sepharose-4 Fast-Flow column

Calbiochem (EMD Chemicals), San Diego, CA, USA
-Bleomycin sulphate, *Streptomyces verticillus* (Cdk1 inhibitor III)
-Protease inhibitor cocktail set I
-$InsP_6$

Cayman Chemical Company, Ann Arbor, Michigan, USA
-Colorimetric COX (ovine) inhibitor screening assay kit. Cat No. 760111

Calbiochem/Novagen (EMD Chemicals), San Diego, CA, USA
-KOD hot start DNA polymerase kit

Fisher Scientific Ltd, Bishop Meadow Road, Loughborough, UK
-Acrylamide 40% solution (Acrylamide : Bis-acrylamide, 29 : 1)

ForMedium™, Hunstanton, Norfolk, UK
-Yeast nitrogen base without amino acids
-Yeast synthetic drop-out media supplement without histidine

Geneflow Ltd, Lichfield, Staffordshire, UK
-50x TAE buffer

Invitrogen Ltd, Paisley, Scotland, UK (incorporating Gibco, Life Technologies)
-Geneticin G-418 sulphate

Meridian Biotechnologies Ltd, Chessington, Surrey, UK
-ProFlo+ scintillant (custom preparation for high phosphate)

New England Biolabs Ltd, Hitchin, Hertfordshire, UK
-Uracil-DNA Glycosylase (UDG)

-AP endonuclease (APE-1)

-T4 DNA ligase

Oxoid Ltd (Thermo Scientific), Basingstoke, Hampshire, UK
-Bacteriological peptone

Promega Corporation, Madison, WI, USA
-1kb DNA ladder

QIAGEN Ltd., Crawley, West Sussex, UK
-MinElute pcr purification kit

-QIAquick gel extraction kit

-Q solution

-MinElute gel extraction kit

-Miniprep kit

-pQE30

Roche Diagnostics Operations Inc., Indianapolis, IN, USA
-Annexin-V-Fluos staining kit (flowcytometer)

Thermo Fischer Scientific Inc., Rockford, IL, USA
-4',6-diamidino-2-phenylindole (DAPI)

VWR International Ltd, Lutterworth, Leicestershire, UK
-Tris-(hydroxymethyl) aminomethane

Dr Tim Underwood, University of Southampton, UK
Kindly provided oesophageal cancer cell lines- oe21, flo-1 and oe33

Dr. Stephen K Dove's lab, University of Birmingham, UK
Vector pFA6a-GFP(S65T)-HIS3MX6 (Longtine *et al.* 1998) ((Fig.2.2.2)

University of Wolverhampton, UK
Aspirin analogues: PN508, PN510, PN511, PN512, PN514, PPN517, PN524, PN525, PN526, PN527, PN528 and PN529 prepared by Dr Chris Perry.

Professor A.G. McLennan
Kindly gifted Ddp1p

Dr S.B. Shears (NIEHS, NIH, RTP, NC, USA)
Radiolabeled and non-radiolabeled 1-$InsP_7$, 5-$InsP_7$ and $InsP_8$

2.1.2 Strains, nucleotide and primer sequences

Sigma-Genosys, Sigma custom product, Suffolk, UK

-Fluorescein tagged DNA strands – JJC, JJU and 16PG. Untagged reverse complements JJG and a hairpin loop (HP). Complete sequences are listed in the **Table 2.1.1.**

-List of primers used in this study and their sequences are mentioned in the **Table 2.1.3.** Primers SSW6-15 were adapted from (Longtine *et al.*, 1998).

Euroscarf, Frankfurt, Germany

Wild-type *S. cerevisiae* strain was used for the experiments. All the other yeast strains used in the study are given in the **Table 2.1.2.**

2.1.3 Media composition and solutions

Ingredients used for the solutions are listed in the **Table 2.1.4**

Sequence name	Nucleotide sequence (5′--3′)
JJC	Fluorescein-CGGAATTCGTCTAGGTTTGAGGTCGACATCGGATCCATGGTACCTCGAGGGCAATGTCTA
JJU	Fluorescein-CGGAATTCGTCTAGGTTTGAGGTUGACATCGGATCCATGGTACCTCGAGGGCAATGTCTA
JJG	TAGACATTGCCCTCGAGGTACCATGGATCCGATGTCGACCTCAAACCTAGACGAATTCCG
16PG	Fluoroscein-CAATAGAGTAACACGG-PG
HP	pCGACCAGTCCCTGCCTTTTGGCAGGGACTGGTCGGCCGTGTTACTCTATTG

Table 2.1.1 List of nucleotide sequences used in this study

Strain name	Genotype	source
BY4741	*MAT*a*; his3*Δ*1; leu2*Δ*0; met15*Δ*0; ura3*Δ	Euroscarf
plc1Δ	BY4741; *plc1*::*kanMX4*	Euroscarf
arg82Δ	BY4741; *arg82*::*kanMX4*	Euroscarf
ipk1Δ	BY4741; *ipk1*::*kanMX4*	Euroscarf
kcs1Δ	BY4741; *kcs1*::*kanMX4*	Euroscarf
vip1Δ	BY4741; *vip1*::*kanMX4*	Euroscarf
rad51Δ	BY4741; *rad51*::*kanMX4*	Euroscarf
rad52Δ	BY4741; *rad52*::*kanMX4*	Euroscarf
ku70Δ	BY4741; *ku70*::*kanMX4*	Euroscarf
adk1Δ	BY4741; *adk1*::*kanMX4*	Euroscarf
pho80Δ	BY4741; *pho80*::*kanMX4*	Euroscarf
pho81Δ	BY4741; *pho81*::*kanMX4*	Euroscarf
pho85Δ	BY4741; *pho85*::*kanMX4*	Euroscarf
ipk1Δ/kcs1Δ	Prepared by Dr. Steve Safrany	-

Table 2.1.2 List of *S. cerevisiae* strains used in this study

ID no.	Primer name	Primer sequence (5′--3′)
SSW6	Ung1-GFP (forward)(no stop)	GGAGGCAAATGCTCGCTTAGAGTCAGAATCAAAGG ACCCT***CGGATCCCCGGGTTAATTAA***
SSW7	Ung1-GFP (reverse)	AGAGTTTGGAAATCGAGACCTGCATATGCAATAGTA ATAT***GAATTCGAGCTCGTTTAAAC***
SSW8	Apn1-GFP (forward)(no stop)	CTTGTCACAAATGACAAAGAAGAGGAAGACTAAGA AAGAA***CGGATCCCCGGGTTAATTAA***
SSW9	Apn1-GFP (reverse)	CAAAAATTGATTACGTATTTAAAATTCTTCTCGCTTC TCA ***GAATTCGAGCTCGTTTAAAC***
SSW10	Apn2-GFP (forward) (no stop)	AAATAATACAGAATCATCTTGTGGGTTTTTTCAGTGG GTT***CGGATCCCCGGGTTAATTAA***
SSW11	Apn2-GFP (reverse)	GTGTTTTATTCTCCCAAAATATCAGCTGACGTTTTCA TAT***GAATTCGAGCTCGTTTAAAC***
SSW12	Rad51-GFP (forward) (no stop)	CTATGAAGATGGTGTTGGTGACCCCAGAGAAGAAGA CGAG***CGGATCCCCGGGTTAATTAA***
SSW13	Rad51-GFP (reverse)	GTAAACCTGTGTAAATAAATAGAGACAAGAGACCA AATAC***GAATTCGAGCTCGTTTAAAC***
SSW14	Rad52 GFP (forward) (no stop)	AAGACCAAAGATCAATCCCCTGCATGCACGCAAGCC TACT***CGGATCCCCGGGTTAATTAA***
SSW15	Rad52-GFP (reverse)	AATGATGCAAATTTTTTATTTGTTTCGGCCAGGAAGC GTT***GAATTCGAGCTCGTTTAAAC***
SSW21	Ung1 (~50bp upstream of junction)	AACGATTGGCTATACAATACCCGCGGAGAG
SSW22	Apn1 (~50bp upstream of junction)	AAGTTTGAGGTTAAACAAAAGAAGCGAGCT
SSW23	Apn2 (~50bp upstream of junction)	GAATCCATGCTGAAAACATCGAAAACTTCG
SSW24	Rad51 (~50bp upstream of junction)	CAAAAAGGGTAAGGGATGTCAAAGATTATGC
SSW25	Rad52 (~50bp upstream of junction)	GCCGCCTTCTAAGGTAGTACATCCTAATGG
SSW26	GFP (reverse)	CCTTCACCCTCTCCACTGACAG
SSW27	Kcs1-upstream	GTACATCTTTCTGTCTTCTC
SSW28	Kcs1-downstream	CGGACTGAAATAAGCGCAGC
SSW29	Ipk1-upstream	CGTGATATGCTACCAGTCG
SSW30	Ipk1-downstream	GTATGTGCATCTGCCAGTAC
SSW31	Arg82-upstream	GATATGTGCATACGTGTGCC
SSW32	Arg82-downstream	CAAGGTAAACTTCACCTCTC

Table 2.1.3 List of primers used in this study

Media/solutions	Composition
Luria Bertani (LB) + antibiotics	Yeast Extract (0.5%, w/v), tryptone (1%, w/v), NaCl (1%, w/v) + ampicillin (100 μg/ml) or/and Geneticin (G418) (200 μg/ml)
LB agar + antibiotics	LB + Bacto agar (2%, w/v)
Yeast Extract Peptone Dextrose (YPD) + antibiotic	Yeast Extract (1%, w/v), Bacto peptone (2 %, w/v), glucose (2 %, w/v) + ampicillin (100 μg/ml) or/and G418 (200 μg/ml)
YPD agar + antibiotics	YPD + Bacto agar (2%, w/v)
Yeast synthetic drop-out media supplement without histidine (DO-His) agar (1L) + antibiotics	Yeast nitrogen base without amino acids (0.67%, w/v), yeast synthetic drop-out media supplement without histidine (0.192%, w/v), Bacto agar (2%, w/v). The media was autoclaved for 15 min at 121°C. Media was cooled down to 55-60 ºC before adding glucose (2%, w/v) (from a 40% w/v stock) and ampicillin (100 μg/ml) or/and G418 (200 μg/ml).
10X DNA gel electrophoresis sample loading buffer [for urea-polyacrylamide gel electrophoresis (urea-PAGE)]	Glycerol (100%, v/v), bromophenol blue (0.1%, w/v) For every 20μl of sample, 2μl of the above sample buffer was used.
5X DNA gel electrophoresis sample buffer	Glycerol (30%, v/v), xylene cyanol (0.25%, w/v), bromophenol blue (0.25%, w/v). For every 10μl of sample, 3μl of the above sample buffer was used.
1X PAGE running buffer	Tris (25 mM), glycine (192 mM)
Phosphate buffered saline (PBS)	Sterile PBS was prepared using PBS tablets and filter-sterilized via a 0.22 μm filter or autoclaved.

Table 2.1.4 Media composition and solutions

2.2 Methods

2.2.1 Yeast strains and culturing requirements

Haploid strains of *S. cerevisiae* (BY4741) and deletion strains were obtained from Euroscarf. All the strains except for *ipk1Δ/kcs1Δ* were BY4741 with a background of MATa; his3Δ1; leu2Δ0; met15Δ0; ura3Δ0, utilizing the kanMX4 deletion strategy, unless specified otherwise. KanMX4 plasmid contains the G418 cassette which makes the strains resistant to antibiotic Geneticin (G418) (Brachmann *et al.*, 1998). *ipk1Δ/kcs1Δ* double knockouts were prepared by mating a *kcs1Δ* BY4741 MATa with a *ipk1Δ* BY4742 MATα - causing sporulation, and pulling tetrads (by Dr Steve Safrany). *Sporulation was of particularly low efficiency*. Tetrads were only considered when four colonies grew from any particular tetrad. Once colonies were established, a polymerase chain reaction (PCR) based analysis was performed to determine whether *kcs1*, *ipk1* or *kanMX* genes were present. All the mutants were tested by PCR using primers encompassing the relevant genes individually **(Fig. 2.2.1)**.

S. cerevisiae strains were grown in standard Yeast extract–Peptone-Dextrose (YPD) or Synthetic dropout media supplemented with essential amino acids. All the strains were grown in the presence of an antibiotic i.e., ampicillin to avoid contamination. Strains were generally cultured at 30 ºC in a shaking incubator. *ipk1Δ/kcs1Δ* and *kcs1Δ* are temperature sensitive and thus required an ideal temperature of 30 ºC and not above. All the yeast strains used in this study are listed in **Table 2.1.2**.

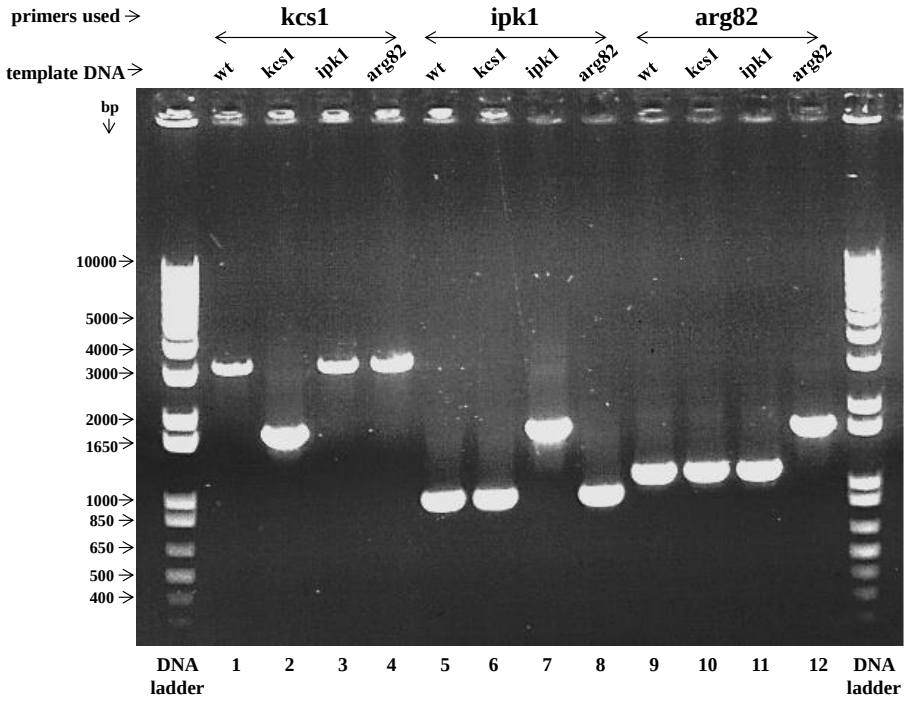

Figure 2.2.1 Verification of mutants using PCR. DNA was obtained from each of the strains e.g. wild-type, *kcs1Δ*, *ipk1Δ* and *arg82Δ* by following lyticase-sorbitol treatment as mentioned in *Section* 2.2.19. Following heat treatment, 1µl of this mixture was used as template DNA for each PCR reaction. Primers for specific genes were used; these flanked the gene of interest, beyond the region where the kanMX4 cassette should have been inserted. The example shows primers for Kcs1, Ipk1 and Arg82 testing wild-type, *kcs1Δ, ipk1Δ and arg82Δ* for the presence of the gene (varied sizes) or kanMX4 cassette (~2 kb). When genes were of a similar size to the kanMX4 cassette the PCR product was diagnosed using restriction enzyme mapping. DNA amplification was achieved using the following PCR setting: 95 ºC, 7 min, followed by 40 cycles of 95 ºC, 1 min; 45 ºC, 1 min; 72 ºC, 4 min. Finally the incubations were held at 72 ºC for 10 min.

Length of the G418 resistance marker product: ~2.0 kbp.

kcs1: length of the kcs1 product: 3274 bp.

ipk1: length of the ipk1 product: 953 bp.

arg82: Length of the arg82 product: 1135bp.

2.2.2 Polymerase chain reaction

All PCRs were performed with Labnet International's TC020A MultiGene II thermal cycler. KOD hot start DNA polymerase kit was used for PCR reactions. For all the standard PCR reaction setup in this study, following components were used: 10X buffer diluted to 1X final concentration, 1.5 mM magnesium sulphate ($MgSO_4$), 200 µM Deoxyribonucleotide triphosphate (dNTPs) (each) and 0.02 U/µl KOD polymerase were mixed in one "master mix" made up to 40 µl total volume with ddH_2O. To this master mix, appropriate upstream primer (300 nM) and downstream primer (300 nM) were added. Total reaction volume remained constant at 50 µl for all the reaction setup. In addition, a plasmid DNA template (pFA6a-GFP(S65T)-HIS3MX6) at a concentration of 10 ng was included for PCR reactions involving amplification of template DNA. The temperature cycling profile was as is shown in **Table 2.2.1**. A single step PCR program was used for all PCR reactions with varying annealing temperature. The annealing temperature was calculated by presuming that all the bases in the primer sequence were complimentary to those on the target DNA.

Polymerase activation	Denaturation	Annealing	Extension	Final extension	Soaking temperature
96 °C	96 °C	50 °C	70 °C	70 °C	10 °C
2 min	0.33 min	0.33 min	1.5 min	5 min/kb	12 h
1 cycle	30 cycles				1 cycle

Table 2.2.1 PCR cycling profile

2.2.3 Drug sensitivity assay of yeast mutants

Spot assay for yeast was employed to examine the sensitivity of anticancer drugs such as bleomycin and 5FU on wild-type and yeast mutants lacking IDPs or repair enzymes. Stock solution of 10 mg/ml of 5FU was prepared by dissolving in dimethyl sulfoxide (DMSO). Bleomycin was dissolved in water to give a stock concentration of 10 U/ml. YPD agar + ampicillin (to avoid bacterial contamination) plates were treated with bleomycin (10 mU/ml) and 5FU (2 µg/ml) respectively overnight prior to the addition of yeast strains. Yeast strains (wild-type, *kcs1*Δ, *arg82*Δ, *ipk1*Δ, *ku70*Δ, *rad52*Δ, *adk1*Δ, *vip1*Δ, *rad51*Δ, *mdt1*Δ, *ung1*Δ, *apn1*Δ, *apn2*Δ, *pho80*Δ, *pho81*Δ, *pho85*Δ *and imp2*Δ) were grown to exponential phase and serially diluted to achieve half-log dilutions from 10,000 to 3 cells/µl. Serially diluted strains (1 µl/spot) were then pin-frogged/spotted onto drug-free (control) and drug-treated YPD agar-ampicillin plates. After 48 h of incubation at 30 ºC, growth was assessed and plates photographed.

2.2.4 Preparation of DNA oligonucleotide working solution

Double stranded oligonucleotide sequences as previously described by Owen *et al.* (2007); Sartori *et al.* (2001) were used as substrates for the experiments. Oligonucleotide sequences JJU and JJC used in this study are both 60 bp long and contain a fluorescein molecule tagged at 5′-terminus. Oligonucleotide JJG is a 60 bp long untagged reverse complement sequence. The ds- sequence employed have a matching pair of oligonucleotides containing a C:G (JJC/JJG) or a specific U:G mismatch (JJU/JJG). The oligonucleotide sequences are given in **Table 2.1.1**. The oligonucleotide working solution was prepared in the presence of annealing buffer comprising of 10 mM tris at pH 7.8, 50 mM NaCl and ddH_2O. Two oligonucleotide working solutions: (a) fluorescein-labelled ss-DNA (JJU; JJC) (0.5 µM) and (b) ds-DNA made of labelled ss-DNA (0.5 µM) and

unlabelled reverse strand (1 µM) (JJU+JJG; JJC+JJG) were prepared by heating the oligonucleotides at 95 ºC for 5 min in the presence of annealing buffer and then cooling them slowly down to room temperature.

In a similar way, F-16PGmer plus hairpin (HP) was prepared by annealing fluorescein-tagged 16PGmer (3′-PG) to 5′ phosphate HP loop at 95 ºC for 5 min in the presence of annealing buffer (same as above). The solution was slowly cooled to room temperature.

2.2.5 Urea-PAGE for separation of DNA oligonucleotide substrates

Separation of substrate and the product was achieved using urea-PAGE. The assay protocols mentioned in the literature (Owen *et al.*, 2007) were found to be inadequate and resulted in poor product resolution. Hence, assay conditions such as: a) presence of SDS, b) urea concentration **(Table 2.2.2)**, c) presence of stacking gel d) temperature at which gel was run, e) loading buffer and f) running buffer were altered to optimise the assay to our research needs.

In general, resolving gel was prepared by using relevant concentration of urea and acrylamide **(Table 2.2.2)** along with 45 mM tris at pH 8.8, 0.02 mg/ml of ammonium persulphate and 0.1% TEMED. The resolving gel was casted first into the PAGE equipment and iso-propyl alcohol was pipetted on top to remove air bubbles and even-out the surface. After polymerisation of the gel, iso-propyl alcohol was removed by washing with ddH_2O. A stacking gel, where required, was prepared by using appropriate concentration of urea and acrylamide **(Table 2.2.2)** along with 125 mM tris at pH 6.8, 0.02 mg/ml of ammonium persulphate and 0.1% TEMED. The stacking gel was casted on top of the resolving gel holding the combs in place and was left to polymerize.

For all the experiments, fluorescein-tagged DNA strands (ss- or ds-) were used at a final concentration of 50 nM. Oligonucleotide substrate samples were prepared by heat treating

labelled ss- or/and ds-DNA for 5 min at 96 ^{o}C in the presence of 10X sample loading buffer (10% glycerol containing 0.01% bromophenol blue). Equal quantity of samples were then loaded onto the gel and subjected to electrophoresis at 100 V/gel for 2 h at room temperature or for 1 h at 60 ^{o}C in the presence of tris-glycine buffer.

Reaction products were visualised using a Storm 840 phosphorimager using ImageQuant software. A blue-excited fluorescence (520-nm long-pass) filter was chosen to scan the gels at 800 V (photomultiplier tube voltage) with a pixel size of 100 microns.

Urea gel concentration	**Acrylamide final concentration**	
	Resolving gel	**Stacking gel**
0 M	38%	4%
0.5 M	36%	4%
1 M	36%	4%
3 M	32%	4%
5 M	30%	4%
7 M	25%	4%

Table 2.2.2 Table outlining the acrylamide concentrations used in correspondence to urea concentrations in urea-PAGE gels. Acrylamide concentration for stacking gel remains constant at 4% regardless of urea concentration whereas acrylamide concentration for resolving gel differs with concentration of urea as outlined above.

2.2.6 Denaturants for separation of DNA oligonucleotide substrates

Fluorescein-labelled DNA strands, JJC (ss-DNA) and JJC+JJG (ds-DNA) were used as substrates for this experiment. APE1-buffer/NE-buffer-4 at a concentration of 1X (50 mM potassium acetate, 20 mM tris-acetate, 10 mM magnesium acetate, 1 mM dithiothreitol, pH

7.9 at 25 ºC) was added to all samples to avoid changes in the pH. Both, ss- and ds- DNA substrates were treated with denaturants – glycerol, formaldehyde, formamide and DMSO individually at varying concentrations and incubated for 30 min at 30 ºC. The final concentrations of the denaturants ranged from 20% - 80%. The samples were then heat treated in the presence of 10X sample loading buffer for 5 min at 96 ^{o}C before loading it onto urea-PAGE gel. A 7 M urea-PAGE gel was opted for this experiment. Gel was run at 100 V/gel for 2 h at room temperature or for 1 h at 60 ^{o}C. Substrate-product separation was visualised using a Storm 840 phosphorimager with the help of ImageQuant software. Scan settings were same as mentioned in *Section* 2.2.5.

2.2.7 Recombinant enzymes on single and double stranded DNA

Catalytic activity of recombinant enzymes, UDG and APE1, on ss- and ds- DNA substrates were tested using this experiment. Labelled DNA strands, JJU (ss-DNA) and JJU+JJG (ds-DNA) were used as substrates for this purpose. 1X NE-buffer-4 was added to all the samples. Initially, both ss- and ds-DNA (50 nM) were treated with 10 U/assay of human UDG enzyme (except for the control). Then, varying concentrations of human APE1 enzyme (half-log dilutions from 10 U/assay) was added to the samples and incubated for 30 min at 30 ^{o}C. A control, containing just the substrate and NE-buffer-4 was included in the experiment for comparison. The samples were heat treated for 5 min at 96 ^{o}C in the presence of 10X sample loading buffer before loading it onto 7 M urea-PAGE gel. The gel was run at 100 V/gel for 1 h at 60 °C. Substrate-product separation was visualised using a Storm 840 phosphorimager with the help of ImageQuant software (*Section* 2.2.5).

Similarly, to examine UDG activity on ss- and ds-DNA, fluorescein-tagged substrates were treated with varying concentrations of UDG enzyme (half-log dilutions from 10 U/assay) (except for control). The mixture was incubated for 30 min at 30 ^{o}C and then heat treated

in the presence of 10X sample loading buffer. Samples were loaded onto a 7 M urea gel and run at 100 V/gel for 1 h at 60 °C. Gels were scanned using phosphorimager.

2.2.8 Protein extraction from yeast

Yeast strains were grown overnight at 30 °C in sterile YPD medium supplemented with ampicillin to minimize the chances of bacterial infection. The yeast strains were sub-cultured next morning and allowed to grow (3-4 h) until cells attained log-phase. Number of cells in the culture was determined and equal number of cells for each of the yeast strains was obtained. Cells were spun down (3000 rpm, 3 min) and washed with ddH_2O to remove traces of medium. The cell pellet was treated with 0.5 ml of the lysis buffer containing 1X protease inhibitor cocktail I (500 µM serine proteases, 150 nM serine proteases and esterases, 1 µM cysteine proteases, 0.5 mM metalloproteases, 1 µM cysteine proteases and trypsin-like proteases). The lysis buffer consists of 400 mM tris at pH 7.6, 2 M NaCl, 0 mM or 1 mM or 100 mM EDTA, and the presence or absence of 2% Tween-20. Cell lysates were prepared by sonicating the cells for 1 min; cycle-1×10%; power-65%; using tapered tip (KE76) probe (Bandelin electronic). Supernatant was collected and stored at -20 ^{o}C for further use. The concentration of the protein was estimated using Bradford assay as described in *Section* 2.2.13.

2.2.9 Identification of UDG-like enzyme in yeast extracts (Glycosylase assay)

Both wild-type and *kcs1Δ* yeast extracts were prepared as described in *Section* 2.2.8. These extracts were tested for the presence of UDG-like enzyme. For this experiment, fluorescein-tagged JJU+JJG ds-DNA was used as substrate. 1X NE-buffer-4 was added to all the samples to avoid pH changes. The substrate (50 nM) was individually treated with wild-type yeast extract and *kcs1Δ* extract and incubated for 30 min at 30 ºC. A negative control containing untreated substrate and a positive control for UDG activity containing

substrate treated with UDG enzyme (10 U/assay) was included in the experiment for comparison. Following incubation, the samples were heat treated at 96 ºC for 5 min in the presence of 10X sample loading buffer. Samples were loaded onto 7 M urea-PAGE gel and run at 60 ºC for 1 h with 100 V/gel. Gel was visualised using Storm 840 phosphorimager (*Section* 2.2.5).

2.2.10 Borohydride-trapping assay

Sodium borohydride ($NaBH_4$) has been previously shown to protect AP-sites in DNA from heat-treatment (Petronzelli *et al.*, 2000). Thus, $NaBH_4$ was used in this experiment to protect the AP-site, created by UDG enzyme, from heat treatment. Fluorescein-tagged JJU+JJG (50 nM) was used as substrate for this experiment. 1X NE-buffer-4 was included in all samples to avoid pH changes. To confirm the presence of UDG-like and APE1-like activity in both wild-type and *kcs1Δ* yeast extracts, the following conditions were included in the experiment.

To determine APE1 activity, the substrate was treated with relevant yeast extract in combination with (i) UDG, (ii) UDG+$NaBH_4$, and (iii) $NaBH_4$. To determine UDG activity, the substrate was treated with relevant yeast extract in combination with (i) APE1, and (ii) $NaBH_4$. A positive control for $NaBH_4$ containing substrate with UDG+ $NaBH_4$ was included for comparison. A negative control containing untreated substrate and positive controls for recombinant enzymes (i) UDG, (ii) APE1, (iii) UDG+APE1 (each enzyme at 10 U/assay) were also included for comparison.

The samples following addition of yeast extracts and/or recombinant enzymes were incubated for 30 min at 30 ºC. And then, where required, $NaBH_4$ was added to the samples at a final concentration of 100 mM and was further incubated at room temperature for 15 min. ($NaBH_4$ was freshly prepared in ddH_2O just before the start of the experiment). All

the samples were heat treated at 96 ºC for 5 min in the presence of 10X sample loading buffer. Samples were then loaded onto 7 M urea-PAGE gel and run at 60 ºC for 1 h with 100 V/gel. Gel was visualised using Storm 840 phosphorimager (*Section* 2.2.5).

2.2.11 EDTA inhibition assay

In this study, to ensure efficient extraction of protein from yeast, an extraction buffer containing high concentration of EDTA was employed. However, EDTA has been reported to inhibit DNA strand cleavage (Ason and Reznikoff, 2004). Thus, an experiment was conducted to check whether EDTA is involved in the catalysis of DNA substrate cleavage.

For this experiment, yeast extracts prepared in the absence of both Tween-20 and EDTA was used. The fluorescein-tagged JJU+JJG ds-DNA was first treated with the relevant yeast extracts and then with increasing concentration of EDTA i.e., 0, 12.5, 25, 50 and 100 mM final concentration. Samples were incubated for 30 min at 30 ºC and were heat treated for 5 min at 96 ºC in the presence of 10X sample loading buffer. Samples were loaded onto 7 M urea gel and electrophoresed at 100 V/gel for 1 h at 60 ºC. Gel was scanned using Storm 840 phosphorimager (*Section* 2.2.5).

2.2.12 Phosphoglycolate repair assay

Reports suggest that APE1 is not only involved in nicking of the DNA at AP-site, but is also involved in the removal of 3′-PG (Parsons *et al.*, 2004; Z. Wang *et al.*, 2014). In this study, an oligonucleotide substrate (16mer) blocked with a 3′-PG moiety and complimentary 5′-phosphate HP were used to check for the ability of yeast extracts (wild-type and *kcs1Δ*) to remove the blocking 3′-PG moiety and perform repair in the presence of T4 ligase.

In this experiment, F-16PGmer along with HP (250 fmol/reaction) was incubated with either APE1 enzyme or relevant yeast extract for 1 h at 37 ºC in the presence of 1X NE-buffer-4. To this mixture, 800 U/assay of T4 ligase along with T4 buffer was added and were further incubated for varying lengths of time (15, 30, 45 and 60 min) at 37 ºC. Following incubation, the samples were heat treated at 96 ºC for 5 min in the presence of 10X sample loading buffer. Samples were loaded onto 7 M urea-PAGE gel and run at 60 ºC for 1 h with 100 V/gel. Gel was visualised using Storm 840 phosphorimager using same settings as mentioned in *Section* 2.2.5.

2.2.13 Estimation of protein concentration

Protein concentrations were determined using an adaptation of methods previously described by Bradford (1976). Coomassie brilliant blue G-250 solution (Bio-Rad) was diluted 1:4 with ddH_2O. Assays were performed by adding 100 ul of this diluted reagent with 10 ul of known standard or unknown sample in a 96-well plate. The samples were left for at least 5 min at room temperature and the absorbance was determined at 595 nm. The standard curve was created using bovine serum albumin (BSA) each time. The protein concentration was calculated with reference to this standard curve of BSA.

2.2.14 Isolation of plasmid DNA from *Escherichia coli*

E. coli (strain DH5α) containing plasmid DNA pFA6a-GFP(S65T)-HIS3MX6 (Longtine *et al.*, 1998) **(Fig. 2.2.2)** were grown on LB agar plates supplemented with 100 µg/ml ampicillin. LB broth containing ampicillin antibiotic was inoculated with *E. coli* and was cultured overnight at 37 ºC. The bacteria were spun down and the plasmid was isolated by following Qiagen's Miniprep protocol. Steps followed in the plasmid isolation include sequential lysis, precipitation and elution using Miniprep kit.

Figure 2.2.2 Plasmid pFA6a-GFP(S65T)-His3MX6 map obtained from SnapGene resources webpage (SnapGene).

2.2.15 GFP-tagging yeast proteins

A modified version of green fluorescent protein (GFP) from the jellyfish *Aequorea victoria* is expressed in various organisms and it represents a good tool for determination of the subcellular localisation of proteins (Cubitt *et al.*, 1995). In contrast to other bioluminescent systems, GFP works without exogenously added proteins, substrates or co-factors, allowing expression to be monitored *in vivo* (Chalfie *et al.*, 1994). Tagging of chromosomal genes of budding yeast was done by HR via transforming corresponding PCR fragments into the desired strains.

For the chromosomal GFP tagging at 3′-terminal of target DNA repair genes, the knock-in fragment was amplified from the plasmid pFA6a-GFP(S65T)-HIS3MX6 (Longtine *et al.*, 1998) by PCR using primers that included the sequences for annealing to the template plasmid, flanked by sequences complementary to the 40 nucleotides immediately before and after the stop codon of the target gene. All primer sequences used for the above purpose are listed in **Table 2.1.3**. PCR reaction mixture preparation and the thermocycler settings used were same as described in *Section* 2.2.2 and Table 2.2.1. To check if the PCR was successful and whether it yielded correct size products, the PCR products were visualised using agarose gel electrophoresis (*Section* 2.2.16). **Fig. 2.2.3** represents the gel showing the PCR products. The products were then excised from the gel, extracted (*Section* 2.2.17) and used to transform wild-type and *kcs1Δ* yeast strains.

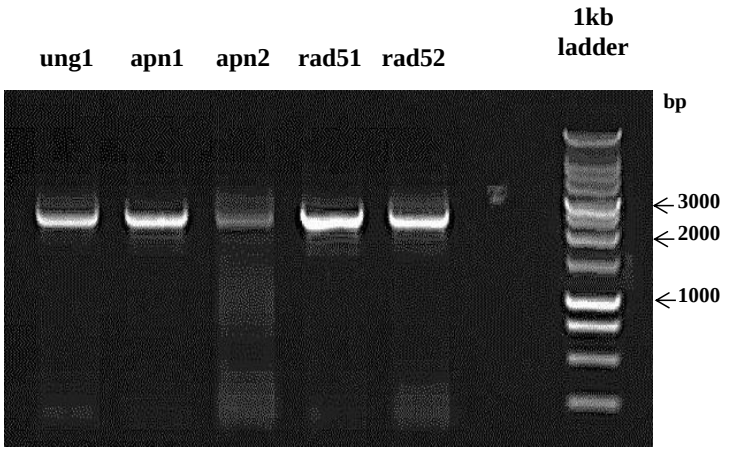

Figure 2.2.3 Gel showing PCR products. Primer pairs were used to insert GFP into the C-terminus of each protein using selected primer pairs (SSW6 and 7 for Ung1; SSW8 and 9 for Apn1; SSW10 and 11 for Apn2; SSW12 and 13 for Rad51; SSW14 and 15 for Rad52) and plasmid pFA6a-GFP(S65T)-His3MX6 as template. PCR products were purified on an agarose gel before transformation into either wild-type or *kcs1Δ* mutant yeast.

2.2.16 Agarose gel electrophoresis

1% w/v agarose gels were prepared by dissolving appropriate amount of ultra-pure electrophoresis grade agarose in 1X TAE buffer containing 0.5 µg/ml of ethidium bromide. The solution was heated to dissolve the agarose and was left to cool down to ~50 ^{o}C. The molten agar was poured into the casting tray with a plastic comb in place to form the loading wells. The gel was immersed in the gel tank containing 1X TAE buffer with 0.5 µg/ml of ethidium bromide.

Appropriate volume of 5X DNA loading buffer (3 µl for every 10 µl sample) was added to the samples before loading into the wells. The gel was run at 100 V for 45 min. The gel was removed and the fluorescing ethidium bromide with DNA was observed under ultraviolet (UV) light. The gel image was captured using GeneSnap software (Syngene) for further reference.

2.2.17 Extraction of DNA from agarose gel

The DNA bands were viewed using a UV trans-illuminator. Desired band was excised from the gel using a sterile scalpel with minimal exposure to the DNA. The excised slice of gel was transferred to a microfuge tube and the DNA was extracted using the Qiagen's MinElute Gel Extraction Kit following the manufacturer's protocol. Extracted DNA was eluted in ddH_2O.

2.2.18 Transformation of *S. cerevisiae* with plasmid DNA

Yeast strains (wild-type and *kcs1Δ*) were grown overnight at 30 °C in sterile YPD medium supplemented with 100 µg/ml ampicillin. The yeast strains were sub-cultured next morning and were allowed to grow (3-4 h) until cells attained log-phase. Yeast cells were spun down (3000 rpm, 3 min) and washed with ddH_2O to remove traces of medium. Cells were

spun down and the pellet was re-suspended in 1 ml of 100 mM LiAc for 5 min at room temperature. Cells were pelleted and the reagents – 32% PEG, 0.1 M LiAc, 0.27 mg/ml carrier DNA (salmon sperm DNA), approximately 10 µg of relevant PCR product (refer *Section* 2.2.15 and Fig. 2.2.3) were added in the same order mentioned as above. The contents were vortexed vigorously after each reagent was added. The suspension was then subjected to heat shock at 42 °C for 90 min. The cells were spun down (8000 rpm, 3 min) and the pellet was re-suspended in sterile YPD medium containing ampicillin. The yeast cells were allowed to recover at 30 °C for 3 h. Cells were pelleted (5000 rpm, 3 min) and washed with distilled water to remove traces of medium. Cells were pelleted (5000 rpm, 3 min) and re-suspended in sterile ddH_2O. The yeast cells were then plated on DO-His (plasmid pFA6a-GFP(S65T)-HIS3MX6 has a 'histidine' marker) agar plates containing 100 µg/ml ampicillin (Sambrook *et al.*, 1989). The plates were incubated for 3-4 days at 30 °C until clones appeared on the plate**.** Once colonies grew on the selective media, the plates were stored at 5 ºC

2.2.19 Extraction of genomic DNA from yeast

Single yeast colonies were picked from the DO-His agar plates (refer *Section* 2.2.18) and suspended in buffer (10 µl) containing lyticase (200 U/assay) and 1.2 M sorbitol (lyticase-sorbitol treatment). Samples were incubated at 37 ºC for 1 h and then heat treated at 94 ºC for 1 min. 1 µl of this sample/DNA was used for further amplification of the desired fragment using PCR.

For GFP-tagged proteins in yeast: A gene-specific upstream primer (SSW21-25) along with a GFP/common downstream primer (SSW26) was used **(Table 2.1.3)** for amplification of desired fragment. PCR was carried out with the same settings as described in *Section* 2.2.2 and Table 2.2.1. The resultant product was electrophoresed in agarose gel (*Section* 2.2.16) and visualised **(Fig. 2.2.4)**. A DNA marker was run alongside the samples.

The products/bands were checked for the right size and purity. Desired bands were excised, extracted (*Section* 2.2.17) and were sent for sequencing (Source BioScience LifeSciences sequencing service, Nottingham, UK).

The samples were screened for the presence of a GFP-tag downstream of the gene of interest and putative knock-in strains were to be confirmed by sequencing the appropriate locus of genomic DNA recovered from transformed cells.

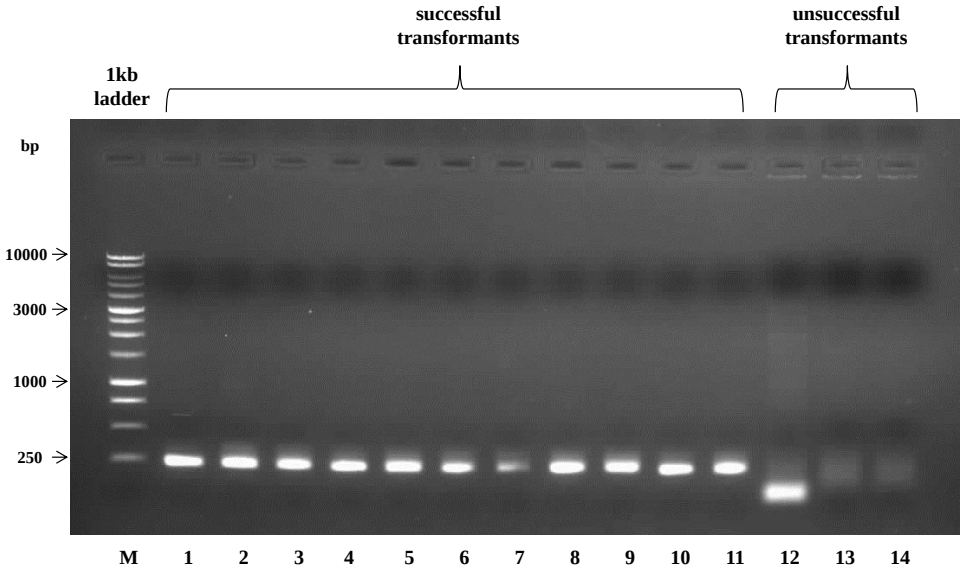

Figure 2.2.4 PCR amplification of genomic DNA of successful GFP-tagged yeast clones. Lanes 1-2: wild-type-GFP-Ung1, lane 3: wild-type-GFP-apn1, lanes 4-5: wild-type-GFP-apn2, lanes 6-7: wild-type-GFP-rad51, lanes 8-9: wild-type-GFP-rad52, lanes 10-11: *kcs1Δ*-GFP-apn2, lane 12: *kcs1Δ*-GFP-Ung1, lanes 13-14: *kcs1Δ*-GFP-apn1. Lanes 1-11 show successful incorporation of the GFP-kanMX4 cassette, whereas lanes 12-14 show unsuccessful colonies.

2.2.20 Subcellular localization of GFP-tagged protein

GFP-tagged (GFP-Ung1, GFP-Rad51, GFP-Rad52 and GFP-Apn1) successful wild-type and *kcs1Δ* yeast clones were grown to exponential phase in YPD medium supplemented with ampicillin. Using confocal microscopy, images of the live yeast cells constitutively expressing GFP-tagged protein were captured. Leica microsystems TCSSP5 system confocal microscope with an argon laser set at 488 nm and a 63x oil objective was used to capture live images of the yeast cells. At first, images of untreated live yeast cells (control) were captured by placing them on a glass slide covered with a glass coverslip. Next, the clones were individually treated with 5 mU/ml bleomycin (bleomycin was diluted in YPD medium) for 90 min at room temperature. Localisation of GFP-tagged protein in wild-type and *kcs1Δ* was visualised. Further, the medium containing the drug was removed by pelleting the yeast cells (5000 rpm, 3 min). The cells were re-suspended in drug-free YPD medium containing ampicillin and were allowed to recover for 1 h at room temperature. Localization of GFP-tagged proteins post recovery was examined.

2.2.21 Glutathione S-transferase (GST)-tagging of recombinant proteins

GST-tagging of DIPP-3α (hAps2) and DIPP-3β (hAps1) was performed exactly as described by Leslie *et al.* (2002). The GST-tagged DIPPs 1, 2α and 2β plasmids (Caffrey *et al.*, 2000; Safrany *et al.*, 1998) were prepared by subcloning the relevant DIPP from pQE30 into pGEX6P-1 using *BamHI* and *SalI*. All clone sequences were verified. Expression plasmids based on pGEX6P-1 were transformed into *E. coli* strain BL21, and induced at 26 ºC overnight with 100 μM isopropyl β-D-1-thiogalactopyranoside. Cells were then harvested and disrupted by sonication (3 × 15 s) in the presence of buffer A containing 20 mM Tris, 150 mM NaCl, 2 mM dithiothreitol, 0.1 mM EGTA, pH 7.5, supplemented with 5 μg/ml leupeptin and 1 μg/ml aprotinin. Floating particles were removed by centrifugation. The supernatant containing GST-DIPPs were subsequently

purified using a 5 mm × 5 cm Glutathione Sepharose-4 Fast-Flow column at a flow rate of 1 ml/min. Using buffer A, the column was washed for 5 min. Proteins bound to the column was eluted using a gradient generated by the mixing of buffer A and buffer B (buffer A plus 25 mM glutathione, pH 7.5) as follows: 0-10 min, 0-50% buffer B; 10-13 min, 100% buffer B. The eluted proteins were stored at -80 ºC in 10% v/v glycerol.

2.2.22 Enzymatic synthesis and purification of IDPs

Three IDPs, both radiolabeled and non-radiolabeled (1-$InsP_7$, 5-$InsP_7$ and $InsP_8$) were enzymatically-prepared, purified by PAGE-based technique as described (Loss *et al.*, 2011; Weaver *et al.*, 2013) and provided by Dr S. B. Shears. Samples from "blank" gels i.e., no IDPs, processed in parallel, provided vehicle controls. Purity of [^{3}H] 1-$InsP_7$, [^{3}H] 5-$InsP_7$ and [^{3}H] $InsP_8$ were assessed by HPLC and were found to be 95%, 86% and 94%, respectively. Such slight decomposition of the pyrophosphate groups have been reported to not affect assays of DIPP activity. All assays were corrected for the small proportions of products observed at "zero-time".

2.2.23 Enzyme Assay

Phosphatase activity was investigated at 30 ºC for Ddp1p or at 37 ºC for human DIPPs in a reaction buffer (20 µl) that simulates intracellular conditions. The ingredients of the reaction buffer include 50 mM KCl, 50 mM HEPES (pH 7.2 with KOH), 4 mM CHAPS, 0.05 mg/ml BSA, 1 mM Na_2EDTA, 2 mM $MgSO_4$. Appropriate [^{3}H]-radiolabeled (Tritium or Hydrogen-3) and non-radiolabeled $InsP_7$ or $InsP_8$ were added to the assays containing the relevant enzyme. After 2-25 min, corresponding to approximately 20% substrate metabolism, reactions were quenched with 20 µl of ice-cold 2 M perchloric acid, centrifuged, and the supernatant was neutralized with 26.5 µl of 2 M K_2CO_3, 5 mM Na_2EDTA. The potassium perchlorate precipitate was removed by centrifugation. Each

supernatant was further diluted in 100 µl Na_2EDTA (1 mM) and then loaded onto a HiChrom 4.6 × 125 mm Partisphere 5 µM SAX column. The bound inositol phosphates were eluted at 1 ml/min using one of the two protocols generated by mixing buffer A (1 mM Na_2EDTA) with buffer B [A + 1.3 M $(NH_4)_2HPO_4$, pH 3.85 with H_3PO_4]. Protocol 1, where 1 ml fractions were collected: 0-5 min, B = 0%; 5-10 min, B = 0-45%; 10-55 min, B = 45-100%. Collection started at 24 min. Protocol 2, where 0.5 ml fractions were collected: 0-5 min, B = 0%; 5-10 min, B = 0-50%; 10-55 min, B = 50-100%. Collections started at 24.4 min. Fractions were mixed 1:3 with ProFlo+ scintillant and the [^{3}H]-labelled IDPs were assayed by liquid scintillation spectrometry. K_m and k_{cat} values were obtained by non-linear regression analysis (GraphPad Prism 6).

2.2.24 Mammalian cell culture

All procedures and experiments requiring tissue culture were carried out aseptically in a laminar tissue culture hood using sterile reagents and equipment. Different cell lines were cultured separately to avoid cross contamination. An inverted phase contrast microscope (Nikon Eclipse TS100) was used to view the culture flask for cell morphology and confluency.

2.2.24a Culturing mammalian cells

All solutions used for tissue culture were warmed to room temperature before use. Cells in culture were regularly split to maintain and to provide sufficient amount of cells for experiments. To perform this, cells were washed gently with 0.25% Trypsin-EDTA to remove trace of foetal bovine serum (FBS). Cells were detached from the substratum by further incubation with 0.25% Trypsin-EDTA. After the cells had completely detached, fresh medium containing FBS was added to inactivate trypsin. Depending on the cell density and the rate at which the cells grow, splitting ratio was decided. Cells were seeded

accordingly in a tissue culture flask with fresh medium and then incubated at 37 ºC in a humidified 5% CO_2 atmosphere. The medium was changed every third day until cells reached confluency.

2.2.24b Oesophageal cancer cell lines and their requirements

All the oesophageal cancer cell lines were a kind gift from Mr Tim Underwood, (Clinical scientist, Cancer Sciences Division, University of Southampton). Details and properties of the cell lines are given in **Table 2.2.3** and morphology in the **Fig. 2.2.5**.

Oesophageal cancer cell lines, oe21 (oesophageal squamous cell carcinoma) and oe33 (oesophageal adenocarcinoma), were both cultured in vented culture flasks in the presence of RPMI-1640 medium supplemented with 10% (v/v) heat inactivated FBS, 200 mM L-glutamine and 1% antibiotic solution (10,000 U/ml penicillin/ 10 mg/ml streptomycin solution). The cells were incubated at 37 ºC with an atmosphere of 5% CO_2.

Flo-1 cell line (oesophageal adenocarcinoma) were cultured in vented culture flasks in the presence of Dulbecco's Modified Eagle Medium (DMEM) supplemented with 10% heat inactivated FBS, 200 mM L- glutamine and 1% antibiotic solution (10,000 U/ml penicillin/ 10 mg/ml streptomycin solution). The cells were incubated at 37 ºC with an atmosphere of 5% CO_2.

Cell line	Other names	Biological source	Tissue	Cell line origin	Growth mode	Morphology
oe21	JROECL21	Human	Oesophagus	Squamous carcinoma of mid oesophagus of a 74 year-old male patient.	Adherent	epithelial
oe33	JROECL33	Human	Oesophagus	adenocarcinoma of the lower oesophagus (Barrett′s metaplasia) of a 73 year old female patient	Adherent	epithelial
flo-1	-	Human	Oesophagus	primary distal oesophageal adenocarcinoma in a 68 year-old Caucasian male	Adherent	epithelial

Table 2.2.3 Details and properties of oesophageal cancer cell lines used in this study.

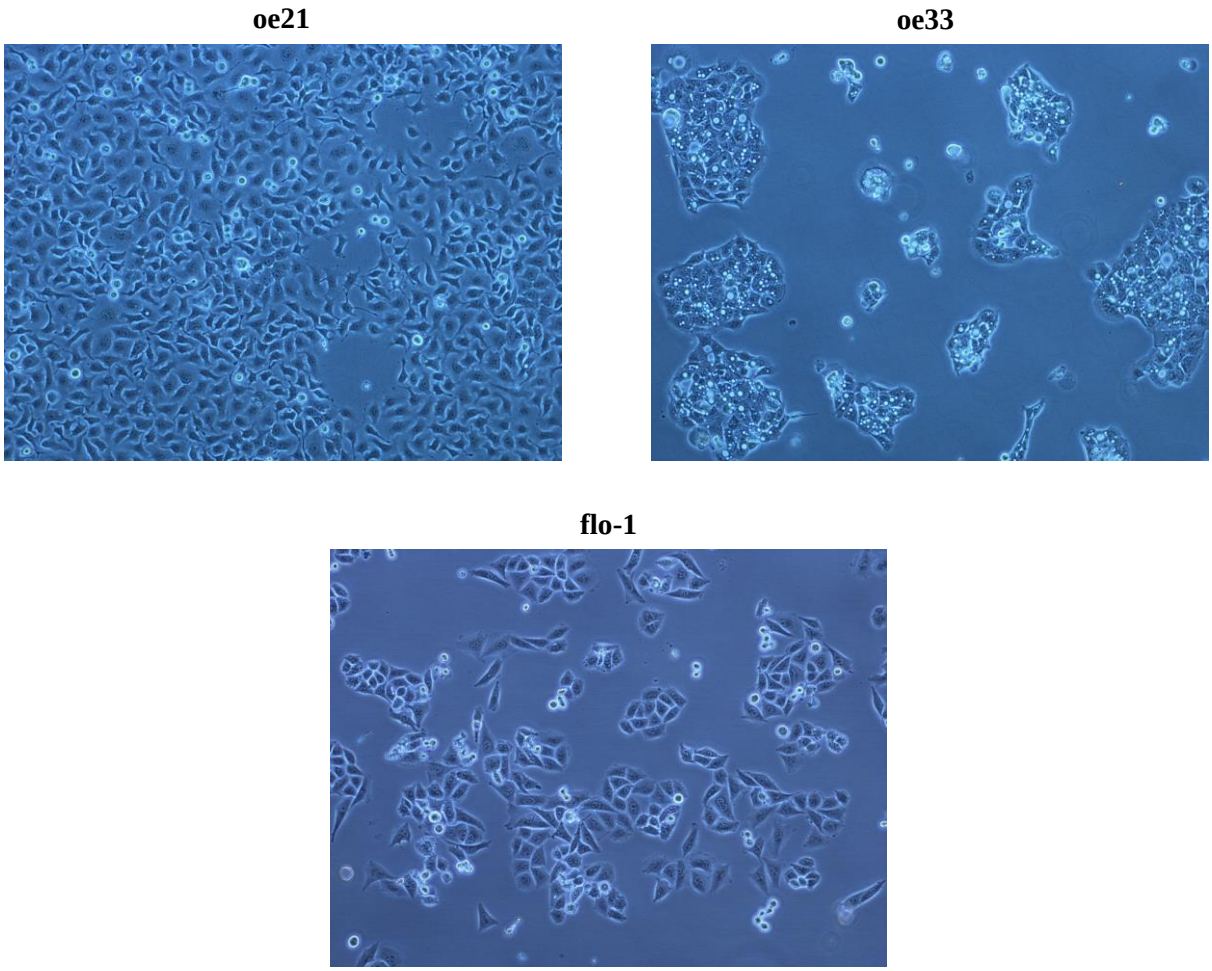

Figure 2.2.5 Morphology of oe21 (SCC), oe33 (ADC) and flo-1 (ADC) oesophageal cancer cell lines. Phase-contrast images showing characteristic phenotypic differences between the three oesophageal cancer cell lines. Images were captured at 100x magnification.

2.2.24c Cell counting

Followed by detachment of cells (*Section* 2.2.24a), a small aliquot of cell suspension was pipetted onto a haemocytometer to count. The number of cells in a 16-square grid of the haemocytometer was recorded and then the number was multiplied by 10,000 to get the number of cells present in 1 ml of the solution.

2.2.24d Cryopreservation of cell lines

Cell line to be cryopreserved was grown to a confluency of 90%. The cells were harvested and centrifuged at 5000 rpm for 5 min. The supernatant was removed and the cells were re-suspended in 2 or 3 ml of the freeze medium (90% (v/v) FBS and 10% (v/v) DMSO). The suspension was gently mixed and 1 ml aliquots of cell suspension were pipette into the labelled cryovials. The cryovials containing cells were frozen slowly in a -80 ºC freezer overnight and then were transferred to liquid nitrogen (-180 ºC) vessel for long term storage .

2.2.24e Resuscitation of frozen cell lines

Cryovial containing frozen cells from liquid nitrogen storage was quickly thawed by placing in a 37 ºC water bath. Cells were then transferred to 25 cm^2 flask containing pre-warmed medium and allowed to recover overnight in a 37 ºC incubator with 5% CO_2. After 24 h, media was replaced to minimise the toxic effects of the cryoprotectant DMSO. From then after, cells were periodically sub-cultured and maintained as per requirements of each cell line.

2.2.25 Preparation of aspirin and aspirin analogue stock solutions

Aspirin and aspirin analogues were prepared as fresh stock solutions in DMSO, usually at a concentration of 0.25 M, before each experiment. A higher stock solution of 0.5 M was

used for working concentrations over 1 mM in order to keep the DMSO levels within the tolerable limit (~10%). Working concentration of a drug was prepared by diluting calculated amount of stock solution in the culture medium. This medium containing the drug was used to treat the cells.

2.2.26 Cell viability assay

Cell viability was measured by 3-(4,5-Dimethyl-2-thiazolyl)-2,5-diphenyl-2H-tetrazolium bromide (MTT) reduction assay. Oesophageal cancer cells were seeded at a density of 2.5×10^3 or 1×10^4 cells/well in a 96-well plate and incubated overnight at 37 ºC with 5% CO_2. After 24 h of seeding, the culture medium was replaced with fresh medium containing the drug at required concentrations and was further incubated for 72 h or any required length of time. A negative control consisting of cells treated with medium only and a vehicle control consisting of cells treated with medium containing DMSO (to determine any effects of solvent on the cells) was also included in these experiments. On the completion of incubation time (72 h), supernatant was aspirated from each well and 300 µl of MTT substrate (0.5 mg/ml) prepared in the relevant medium was added to the cells. After 3 h incubation, the resultant formazan crystals were dissolved with 200 µl of DMSO. The quantity of formazan formed was measured by recording changes in the absorbance at 540 nm in a microplate reader (Microplate Reader Thermo Multiskan Ascent 96 & 384). A standard curve for formazan was constructed to examine the relation between formazan concentration and absorbance **(Fig. 2.2.6)**. All experiments were performed in triplicates and the viable cells were expressed as a percentage relative to the negative control cells (formula used is shown below).

$$\%\ \text{Cell viability} = \frac{\text{Absorbance}_{540}\ (\text{treated cells} - \text{blank})}{\text{Absorbance}_{540}\ (\text{control cells} - \text{blank})} \times 100$$

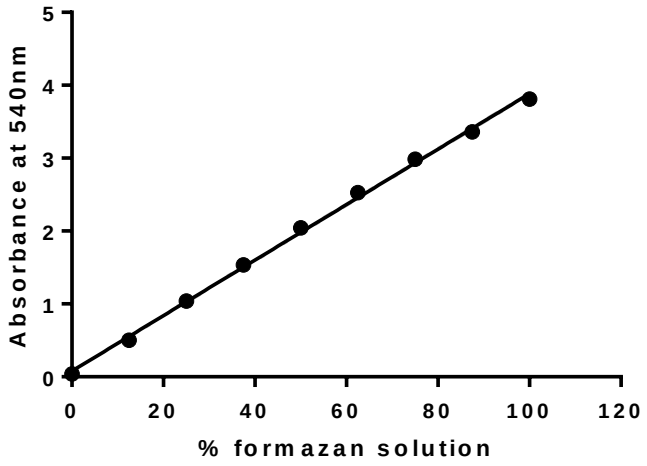

Figure 2.2.6 Standard curve for formazan. Formazan samples were diluted with increasing amounts of DMSO. This assay shows a remarkable linear range when comparing amount of formazan with absorbance [linear up to Absorbance (540 nm) of 4]. Linear regression analysis indicated R-squared value to be 0.99 and the data was shown to fit well with the model. This permitted absorbance to be linked directly to cell activity and number.

2.2.27 Apoptosis assays

Induction of apoptosis/necrosis in oesophageal cancer cells by aspirin and aspirin analogues were examined using flow cytometric analysis and fluorescence imaging.

In case of both the assays, three controls were included: (a) negative control consisting of cells treated with medium only, (b) positive control for apoptosis (irinotecan, 25 µM) and (c) positive control for necrosis (hydrogen peroxide or H_2O_2, 2 mM). Irinotecan, a topoisomerase I inhibitor used in the treatment of CRC, has been previously reported to demonstrate cytotoxic effect via induction of apoptosis (Deb *et al.*, 2011; Rudolf *et al.*, 2012). Hence, irinotecan was used as a positive control for apoptosis in the experiments. Irinotecan was prepared as stock solution in DMSO and further diluted to a final

concentration of 25 µM in culture medium. Induction of necrosis by H_2O_2 at higher concentrations (500 µM and above) has been previously reported (McKeague *et al.*, 2003). Hence, H_2O_2 was used as a positive control for necrosis at a final concentration of 2 mM in the experiments. Freshly prepared 0.25 M stock solutions of the aspirin compounds were used to prepare final drug concentration of 1 mM each. Since the drug exposure time is crucial for induction of apoptosis, different exposure time points (24, 48 and/or 72 h) were used in the experiment.

2.2.27a Flow cytometric analysis of apoptosis

Annexin-V-Fluos staining kit was used for the purpose of detection and quantification of apoptosis in drug-treated cells as opposed to control cells. The staining kit comprises of 2 dyes: (1) Annexin-V, a Ca^{2+} -dependent dye that binds to phosphotidylserine upon initiation of apoptosis (Vermes *et al.*, 1995), and (2) Propidium iodide (PI), a membrane-impermeant dye, stains the non-viable cells by intercalating into ds-DNA (Chou *et al.*, 1987).

Oesophageal cancer cells were cultured in 25 cm^2 vented flask until they reached 50% confluency. Cells were then incubated for 24, 48 and 72 h with aspirin and aspirin analogues at 1 mM concentration. Additionally, three controls: cell control, irinotecan (25 µM) and H_2O_2 (2 mM) were included in the experiment. After incubation, the cells were harvested and washed in Hank's balanced salt solution (HBSS) buffer. The cells were then incubated with labelling solution (100 µl incubation buffer with 2 µl Annexin-V-Fluos reagent and 2 µl of PI used for ~10^6 cells) for 10-15 min at room temperature as per the manufacturer's instructions. The cells were then diluted with 0.5 ml of HBSS buffer (per 10^6 cells) and analysed on a flow cytometer (BD Biosciences, Facscalibur).

Flow cytometer settings used are as follows. An excitation wavelength of 488 nm and bandpass filter of 530 nm was set for fluorescein (green) detection. For PI, a bandpass filter of 600 nm was employed. For detection of early apoptosis and late apoptosis/necrosis, cells were gated into four populations: $Annexin^{-}/PI^{-}$, $Annexin^{+}/PI^{-}$, $Annexin^{+}/PI^{+}$ and $Annexin^{-}/PI^{+}$ **(Fig. 2.2.7)**.

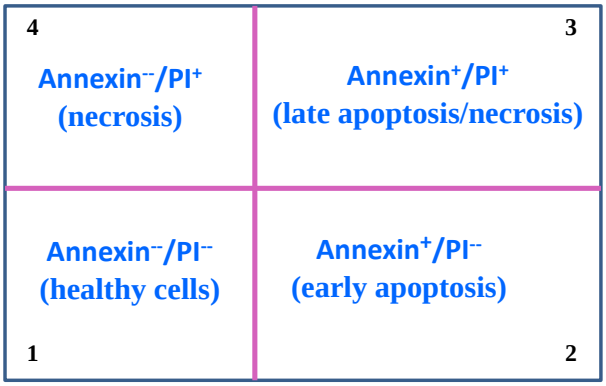

Figure 2.2.7 Gating live cells undergoing apoptosis and necrosis using flow cytometer. Figure represents the quadrants drawn on a cytogram to distinguish different cell populations that are stained $Annexin^{+/-}$ and $PI^{+/-}$. Population (healthy cells) that shows negative staining for both Annexin and PI fall in the 1st quadrant. Early apoptotic cells that take up only Annexin stain fall in the 2nd quadrant. Late apoptotic cells that take up both Annexin and PI fall in the 3rd quadrant. Cells or sometimes debris show positive staining for PI and move towards 4th quadrant.

2.2.27b Fluorescence imaging of apoptosis

Sigma's Apo-TRACE cell staining kit was used for fluorescence imaging. Apo-TRACE dye selectively marks the cells undergoing apoptosis (Damianovich *et al.*, 2006) and the PI stains the non-viable cells. Appropriate number of oesophageal cancer cells were seeded

on sterile cover slips placed in a 6-well plate and were incubated at 37^{o}C, 5% CO_2. Cells were grown until they reached 50-60% confluency and were then incubated with aspirin and aspirin analogues at 1 mM concentration for 24 and 48 h. After the treatment time, supernatant was aspirated carefully and the coverslip was gently washed with PBS. The staining medium (75 µg/ml Apo-TRACE and 75 µg/ml PI in assay medium), prepared according to manufacturer's instruction, was added on to the cover slip and incubated at room temperature for 15-20 min protected from light. The coverslip was gently washed with PBS and laid cell-side down on a drop of mounting medium dotted on to a glass slide. The cell staining was observed using a fluorescence microscope (BX61; Olympus optical, UK) with filter settings - DAPI (excitation:350 nm; emission:470 nm) for Apo-TRACE and Texas red (excitation 596nm; emission 615nm) for PI staining. The images were taken at 200x magnification.

2.2.28 Recovery of drug treated cells

To examine if aspirin analogues had the ability to induce cytostasis, recovery experiments were performed on drug-treated oesophageal cancer cells. Cells were seeded at a density of 5×10^3 or 2×10^4 cells/well and incubated overnight at 37 ºC, 5% CO_2. Cells were then treated with aspirin and aspirin analogues at a final concentration of 1 mM each for 72 h. At the end of incubation, the medium containing drug along with dead floating cells were removed and the adherent cells were harvested and washed with sterile PBS. Cells were then reseeded at a density of 5×10^3 or 2×10^4 cells/well in a fresh plate with drug-free medium and allowed to recover for 72 h in a 37^{o}C, 5% CO_2 incubator. At the end of the experiment, cells were collected by trypsinization and counted using a Beckman Coulter Z1 cell counter with an orifice of 100 µm and threshold size of 10 µm.

All the three controls: non-treated cell control, irinotecan and H_2O_2 treatments were included in this experiment. All experiments were performed in triplicates and the total number of viable cells was expressed as a percentage relative to the non-treated control cells.

2.2.29 COX inhibitor screening assay

Colorimetric COX (ovine) inhibitor screening assay kit from Cayman Chemical was used to determine whether or not the aspirin compounds inhibited COX enzymes. This assay measures the peroxidase activity of COX colorimetrically by monitoring the appearance of oxidized N,N,N',N'-tetramethyl-p-phenylenediamine (TMPD) at 590 nm.

The compounds to be tested were prepared as stock solutions on the day of the experiment by dissolving in DMSO. Stock concentrations were prepared such that a final volume of 10 µl was added to the assay.

Assay was performed as described in the user's manual in a 96 well plate. The final volume of the assay was fixed at 220 µl in all the wells. Wells were divided into 3 groups: (a) non-enzymatic/ background wells (in duplicate), (b) 100% enzyme activity wells (in duplicate) and (c) Inhibitory wells (each inhibitor assayed in duplicate). The background wells comprised of 160 µl of assay buffer (0.1 M Tris-HCl, pH 8) and 10 µl of the Heme provided. The 100% enzyme activity wells and inhibitory wells both comprised of 150 µl assay buffer, 10 µl Heme and 10 µl of enzyme (either COX-1 or COX-2). In addition to above, 10 µl of inhibitor (aspirin or aspirin analogues) was added to the inhibitory wells and 10 µl of solvent (DMSO) was added to the 100% enzyme activity wells and the background wells. The plate was carefully agitated for few seconds and incubated for 5 min at 25 ºC. To all the wells 20 µl of colorimetric substrate (TMPD) was added. Quickly, 20 µl of arachidonic acid (100 µM final concentration) was also added to all the wells. The

plate was carefully agitated for few seconds and incubated for ~2 min at 25 ºC. Absorbance of the samples was recorded at 590 nm using a plate reader.

For calculations, average absorbance of the each sample was determined. Absorbance of the background wells (no COX enzyme) was subtracted from 100% enzyme activity wells (positive control for COX enzyme) and the inhibitor wells (with aspirin and aspirin analogues). Percentage inhibition was calculated using non-linear regression (GraphPad Prism 6.0) using a log-linear sigmoidal dose response curve with 4 parameter analysis (max, min, log IC_{50} and slope).

2.2.30 Curve fitting and Statistical Analysis

All data analysis and curve fitting was performed using GraphPad Prism (version 6.02 for Windows). Characterization of enzyme profiles was performed using non-linear regression. Michaelis-Menten kinetics were determined using a rectangular hyperbolic fit of data to determine the maximum velocity of the enzyme (V_{max}) and Michaelis constant (K_m). V_{max} values were normally distributed and so mean ± SEM could be presented. K_m values are not normally distributed, so pK_m (-log K_m) values were calculated and statistically manipulated, allowing parametric analyses to be performed.

Growth inhibition values were determined using a log-linear sigmoidal plot with 4 variable parameters (Minimum, maximum, IC_{50} value and Hill slope were not fixed). pIC_{50} (-logIC_{50}), minimum, maximum and Hill slopes were treated as being normally distributed, allowing parametric analyses to be performed.

Column statistics were performed using unpaired analyses assuming equal sphericity and normal distribution. Data sets were compared using one-way ANOVA corrected for multiple comparisons. The mean of control data was compared to results from drug-treated cells using a Dunnett's post-hoc analysis.

3. RESULTS - ROLES OF INOSITOL DIPHOSPHATES IN DNA REPAIR

3.1 Introduction

DNA damage comes in many forms and can affect any aspect of the DNA molecule. The correct repair of these lesions is vital for the cell to prevent loss of genetic information, and genetic instability is one of the hallmarks for cancer and/or subsequent death (Zhivotovsky and Kroemer, 2004). The growing list of human genetic diseases due to defects in DNA metabolism makes it particularly important that we expand our knowledge on how these processes occur. Conversely, rapidly proliferating tumour cells can be targeted and destroyed using agents that cause DNA damage (Swift and Golsteyn, 2014). Tight control over DNA repair mechanisms following DNA insult appears more crucial than first thought, as overactive repair is a proposed mechanism for tumour resistance against several anticancer agents (Jette *et al.*, 2008; Ramotar and Wang, 2003).

5FU and bleomycin are the two oldest chemotherapeutics used today in the clinic. Although both the drug causes DSDB (Mahaney *et al.*, 2009; Swift and Golsteyn, 2014), 5FU does it by irreversibly inhibiting TS and causing imbalance in the deoxynucleotide pool whereas bleomycin causes oxidative DSDBs in the presence of free radicals and metal ions. Action of these two drugs on DNA results in intermediates such as AP-site or/and 3′-PG adducts which when left unrepaired can threaten to be cytotoxic and mutagenic to cells. Whether acquired or innate, tumour cells have found ways to exploit cellular repair mechanisms to correct the lesions and gain resistance against the damage causing agents.

NHEJ and HR are two of the well characterised primary pathways of DSDB repair. HR lead to accurate repair of DSDBs whereas NHEJ is potentially mutagenic (Lieber *et al.*, 2003). Higher eukaryotes employ both the repair mechanisms while HR-mediated repair is predominantly seen in yeast (Ozenberger and Roeder, 1991; Pfeiffer *et al.*, 2004). Irrespective of the origin, it is widely accepted that the AP-site or/and 3′-PG removal

requires a BER downstream enzyme, APE1. APE2 exhibits a weak endonuclease activity but possess strong exonuclease and 3′-phosphodiesterase activity (Burkovics *et al.*, 2006). Correspondingly APE1 appears to be the common enzyme that brings together the repair mechanisms of 5FU and bleomycin. However, recent studies report that there is "division of labour between NHEJ and BER" in repair of AP-sites based on the DNA sequence around the particular mismatch. Ku, an NHEJ complex, has been reported to nick AP-sites near broken DNA ends, if they were to obstruct the progression of ligation of DSDB during NHEJ (Strande *et al.*, 2012). Furthermore, Li *et al.* (2013), has proposed a role for free Ku70 and free Ku80 in the BER process. Ku70 in particular has been found to bind to the AP-sites and downregulate BER process by inhibiting APE1 activity (Choi *et al.*, 2014).

Of many cofactors that are necessary for efficient DNA repair, IPs are considered vital. $InsP_6$, a precursor of IDPs, was found to be an essential 'stimulating-factor' for DNA-PK dependent NHEJ *in vitro* in cell extracts (Hanakahi *et al.*, 2000). $InsP_6$ was subsequently shown to bind Ku70 (Hanakahi and West, 2002; Ma and Lieber, 2002). In this study, these results have been reassessed using live yeast to determine whether such events are important *in vivo*. This study also tries to address whether the DNA repairs observed are actually mediated by IDPs rather than their precursors. IDPs which possess highly energetic pyrophosphate bonds in their structure have been long suggested to own defined dynamic functions in vital cellular processes and it is possible that IDPs could contribute as cofactors to the repair mechanism.

A genetically tractable eukaryotic model: *S. cerevisiae* has been employed for experiments in this study. This unicellular eukaryotic organism was selected in particular because a) many processes seen in higher multicellular eukaryotes are also utilized in yeast, b) knockout and overexpression methodologies which are extremely time consuming and

difficult can be completed rapidly and easily in yeast and, c) gene function is highly conserved (Tugendreich *et al.*, 1994), phenotypes seen in yeast can alert us to functions in higher organisms that one may not study in mice due to gene redundancy, functional sterility or death *in utero*. In addition, homologues of many yeast genes in human DNA, especially those that are involved in cell cycle regulation, meiosis and DNA repair are well established (Game, 2002). Mutation of these key genes in yeast and phenotypic study on them could lead to new and greater understanding of human genes that are vital in cancer and other diseases.

In this study, a particular family of yeast knockout mutants with modulated levels of IPs **(Fig.1.1.2** in chapter 1**)** were used as a model to investigate the role of IDPs in DNA repair. All mutants used herein are from the same BY4741 background, utilizing the KanMX4 deletion strategy, unless specified otherwise. Family of *S. cerevisiae* strains, with deletion mutation in genes that controls the levels of IP, used in this study include *kcs1Δ*, *ipk1Δ*, *arg82Δ* and *vip1Δ* **(**refer **Fig. 1.1.2)**. Additionally, a family of yeast mutants with modulated levels of various DNA repair enzymes involved in repair processes including *rad51Δ*, *rad52Δ*, *ku70Δ*, *ung1Δ*, *apn1Δ*, *apn2Δ*, *mdt1Δ*, *imp2Δ*, *pho80Δ*, *pho81Δ* and *pho85Δ* were used for the experiments. In addition, *adk1Δ* was also tested as it appeared to have similar properties to IDP mutants. Two DNA damage-inducing anticancer agents, 5FU and bleomycin were exposed to this panel of mutants to see if knockdown of some of the key IPs or repair enzymes led to increased sensitivity of the yeast cells.

The sensitive mutants were chosen to study further the factors behind drug intolerance. Increased sensitivity of mutants to the drugs was speculated to be due to defects in DNA repair. The focus of this study was on the two key repair enzymes, Ung1/UDG and Apn/APE1, which brought together the 5FU and bleomycin repair pathways. We wished to know if these enzymes were responsible for the increased sensitization of mutants to the

drugs. More importantly, we were interested to know if IDPs or inorganic phosphates participated as cofactors in these repair reactions. To monitor repair enzyme activity, a fluorescein-tagged ds- oligonucleotide substrate containing a G:U mismatch was used for the experiments. Denaturing urea-PAGE method was developed to suit the experimental needs and to achieve efficient and, clear separation of strands. Extracts from wild-type and the sensitive yeast mutant were checked for the activity of UDG-like and APE1-like enzymes. Presence or absence of these enzymes was judged based on the separation of the product from the substrate in the urea-PAGE gels (refer **Table 3.1.1**). Ability of extracts to remove 3′-PG moiety and further perform the end-joining repair process in the presence of T4 ligase was also investigated in this study using fluorescien-tagged-16PGmer (F-16PG) and a oligonucleotide containg hairpin-loop (HP, a 51mer).

Our hypothesis is that the yeast mutants lack a functional enzyme due to the absence of essential IP cofactors. In circumstances where there is a functional enzyme and our initial hypothesis was wrong, then we planned to GFP-tag the candidate repair enzymes and track their movement and localization using confocal microscopy studies.

UDG	APE1	Action	Result
✗	✗	No AP-site formation and no nicking of substrate	No product formed
✓	✗	Removal of uracil and formation of AP-site	Partially formed product
✓	✓	Formation of AP-site and nicking of the substrate at AP-site	Completely formed product
✗	✓	No AP-site formation and therefore no nicking of the substrate	No product formed

Table 3.1.1 Activity of repair enzymes on mismatched DNA substrate

3.2 Strains lacking IDPs are sensitive to bleomycin and 5FU

$InsP_6$, a precursor of IDPs, was found to be an essential 'stimulating-factor' for DNA-PK dependent NHEJ *in vitro* in cell extracts (Hanakahi *et al.*, 2000). Following this report, we wanted to reassess these results using live yeast to determine whether such events are important *in vivo*. We also speculated that the observed DNA repair might actually be mediated by high energy IDP molecules rather than their precursor. In this regard, a spot assay was conducted to examine the sensitivity of yeast to agents causing DSDBs. The agent used to cause such insult was bleomycin. When bleomycin did, indeed, selectively kill mutants lacking IDPs a screen of other anticancer drugs was undertaken. Before my starting this project, the IDP mutants had been shown to have wild-type sensitivity to the following drugs: actinomycin-D, caffeine, camptothecin, carboplatin, Congo Red, copper sulphate, cyclophosphamide, cytosine-β-arabinofuranoside, deferoxamine, doxorubicin, EDTA, EGTA etoposide, ferric chloride, hydrogen peroxide, hydroxyurea, methotrexate, methyl methanesulphonate (MMS), mimosine, 4-nitroquinoline-1-oxide, paclitaxel, tamoxifen, valinomycin and UVA or UVC irradiation (data not shown). However, in addition to bleomycin, these mutants were found to be sensitive to 5FU.

The results of this assay clearly show that yeast mutants were over 1000-fold more sensitive to bleomycin and 100-fold more sensitive to 5FU than the wild-type **(Fig. 3.2.1)**. Both *kcs1Δ* and *arg82Δ* showed extreme sensitivity to bleomycin, whereas *ipk1Δ* showed resistance equal to that of wild-type yeast cells. *kcs1Δ* and *arg82Δ* also showed high sensitivity to 5FU. *rad52Δ* were found to show similar sensitivity to bleomycin and 5FU. Interestingly, *vip1Δ* showed sensitivity equal to that of wild-type to both bleomycin and 5FU **(Fig. 3.2.1)**. *adk1Δ* were found to be highly sensitive to bleomycin, however, were less sensitive to 5FU. *apn1Δ* were severely affected with 5FU treatment but were found unharmed with bleomycin treatment.

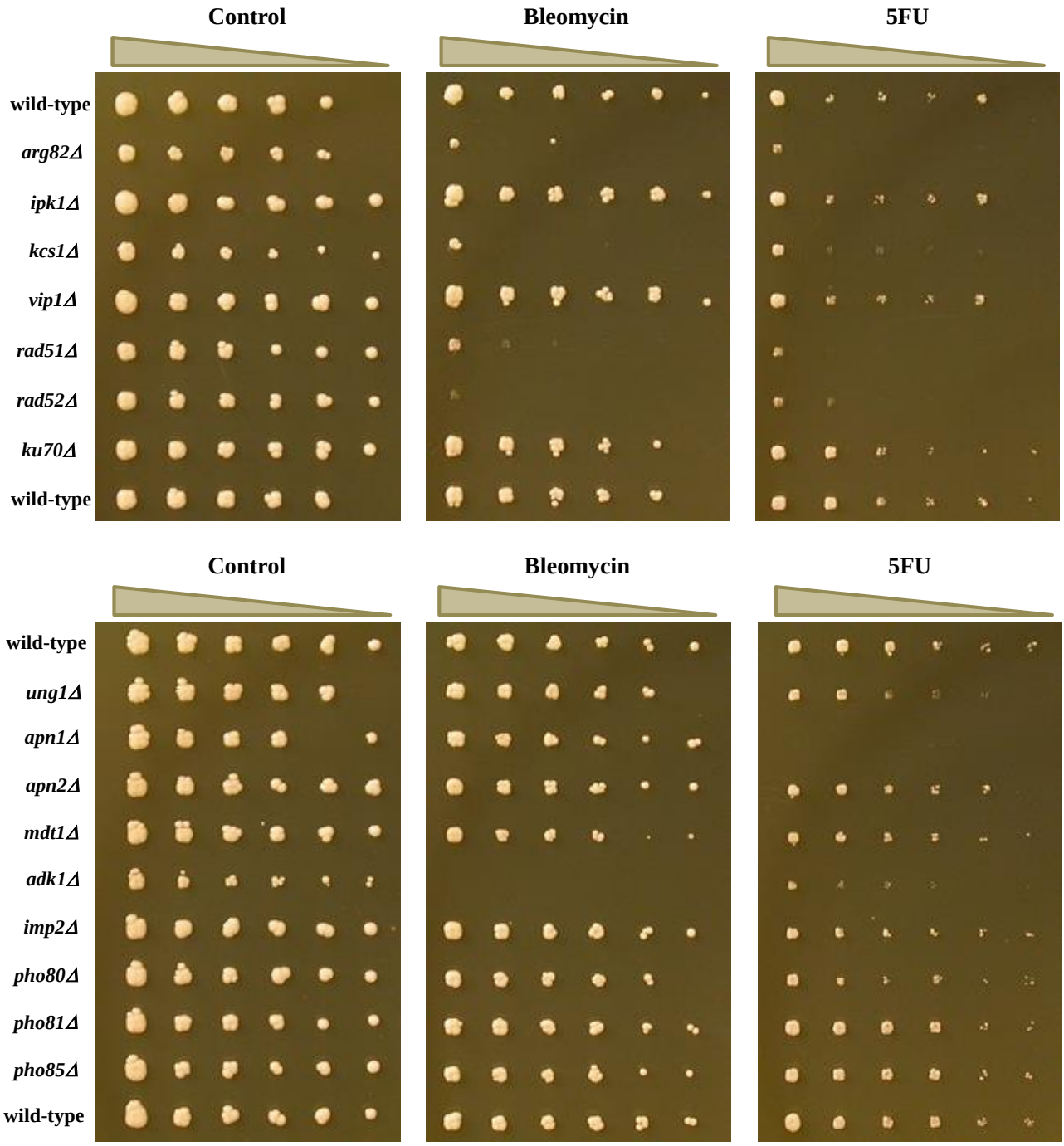

Figure 3.2.1 Effect of bleomycin and 5FU on mutant yeast strains lacking (a) IDPs and (b) repair enzymes. Yeast strains were grown to log-phase in YPD medium at 30 ºC. The strains were serially diluted at 1/3 with YPD medium and spotted onto YPD agar plates (left to right; starting at 10,000 cells/spot) containing bleomycin at 10 mU/ml and 5FU at 2 µg/ml concentrations (*Section* 2.2.3). A control, with yeast dilutions spotted onto a untreated YPD plate was also included. Plates were incubated at 30 ºC for 48 h and photographed.

3.3 Urea-PAGE for seperation of DNA

To understand, at a molecular level, why the IDP mutants were sensitive to bleomycin and 5FU, extracts were tested for their ability to repair damaged DNA *in vitro*. In order to monitor such repair mechanisms PAGE was used. Previously published methods were found unsatisfactory as they permitted re-annealing of ds-DNA (Owen *et al.*, 2007; Parsons *et al.*, 2004). Thus, polyacrylamide gels with varying concentrations of urea and acrylamide were employed (*Section* 2.2.5). Concentrations of urea used in this experiment include 0 , 0.5, 1, 3, 5 and 7 M **(Fig. 3.3.1)**. Corresponding acrylamide concentrations used for urea gels are outlined in the **Table 2.2.2**. A stacking gel containing urea was incorporated (unless specified otherwise) for all the experiments to maximise the resolution of DNA in the gel . SDS was omitted from all the gel and buffers as it reduced resolution (data not shown).

Fluoroscein-tagged DNA strands, i.e., JJC (Fluoroscein-tagged 60-mer) and untagged reverse complement (JJG) were used for this experiment. The ss- (JJC) and ds- (JJC+JJG) DNA sample mixtures were prepared as mentioned in *Section* 2.2.4 and run through different concentrations of polyacrylamide urea gels at room temperature (*Section* 2.2.5). As shown in **Fig. 3.3.1** the ds-DNA ran above the ss-DNA in all cases. The differences between the amount of seperation can be accounted for by the difference in acrylamide concentration. In terms of resolution of the substrate and product seperation, 7 M urea gel comprising of both resolving and stacking gel was considered the best **[Fig. 3.3.1(f)]**.

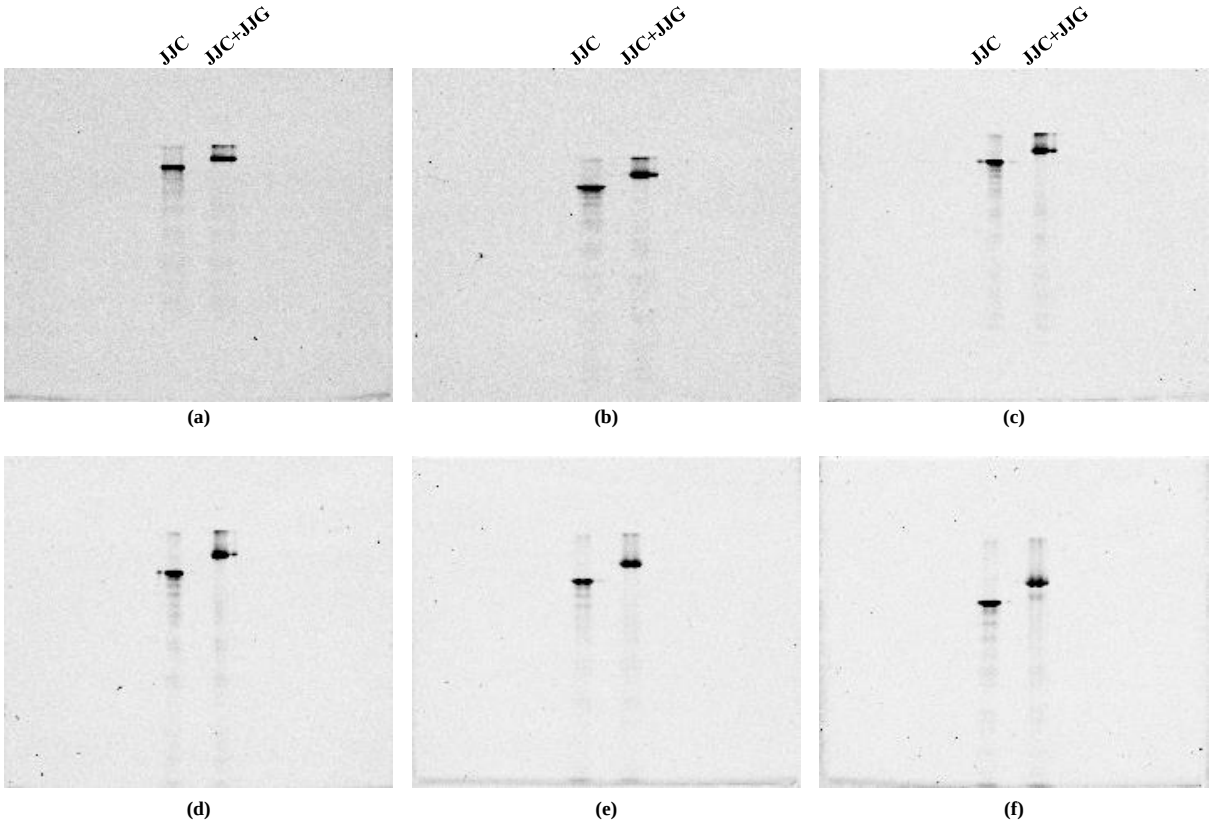

Figure 3.3.1 Urea-PAGE for separation of DNA. The ss (JJC) and ds (JJC+JJG) DNA substrates (50 nM each) were heat treated at 96 ºC for 5 min before loading it onto different concentrations of urea polyacrylamide gels: **(a)** 0 M urea; 38% acrylamide, **(b)** 0.5 M urea; 36% acrylamide, **(c)** 1 M urea; 36% acrylamide, **(d)** 3 M urea; 32% acrylamide, **(e)** 5 M urea; 30% acrylamide, and **(f)** 7 M urea; 25% acrylamide. The gels were run at room temperature for 2 h with 100 V/gel. Gels were scanned using phosphorimager (*Section* 2.2.5).

3.4 Denaturing of DNA using denaturants

In addition to urea, a denaturant was essential to dissociate ds- to ss-DNA. The denaturing agents assessed include glycerol, formamide, DMSO and formaldehyde. Denaturants were used at 20%, 40%, 60% and 80% concentrations, to determine the concentration at which there was clear dissociation of ds-DNA **(Fig. 3.4.1)**. Untreated controls were included for comparison. The results showed that the JJC+JJG complex failed to dissociate even in the presence of denaturants glycerol, DMSO and formamide **[Fig. 3.4.1(a), (c)** and **(e)]** at room temperature. Denaturing of the ds-DNA was possible only when the gel was run at 60 ºC **[Fig. 3.4.1(b), (d)** and **(f)]**.

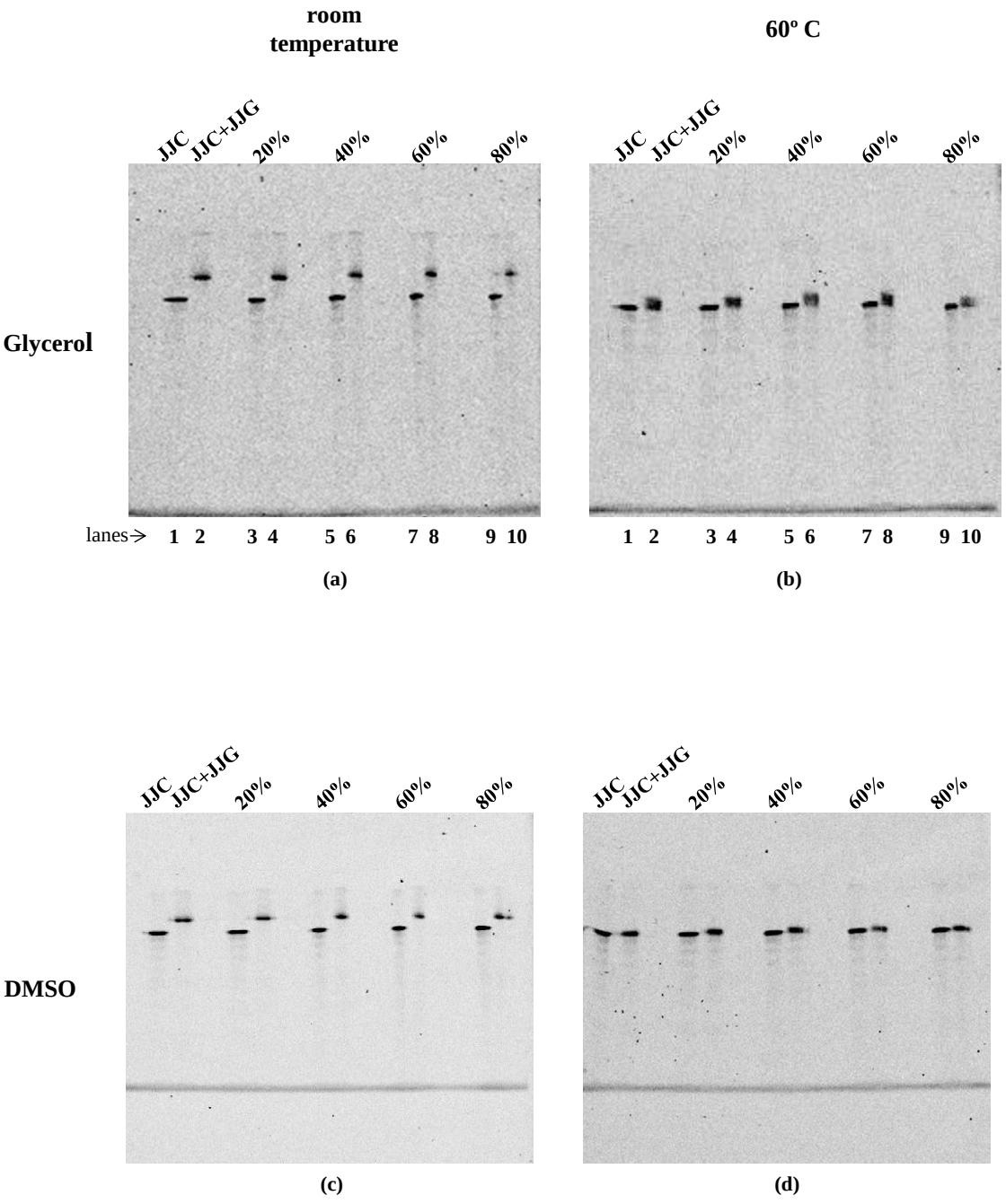
room temperature
60° C
Glycerol
DMSO
JJC
JJC+JJG
20%
40%
60%
80%
lanes→ 1 2 3 4 5 6 7 8 9 10
(a)
(b)
(c)
(d)

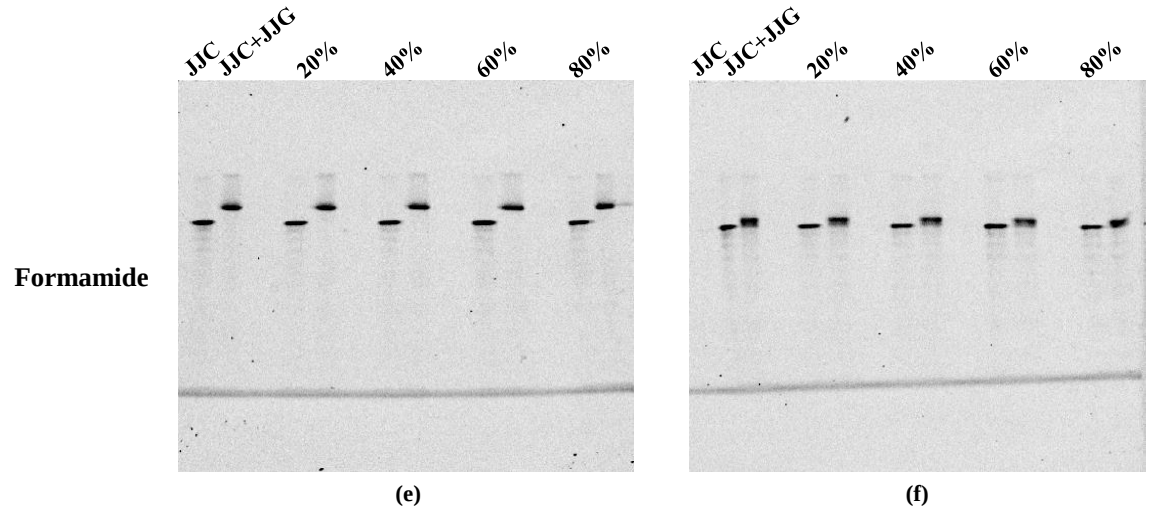

Figure 3.4.1 Denaturing of DNA using glycerol, DMSO and formamide. Substrates (50 nM) were incubated in the presence of varied concentrations of the denaturant for 30 min at 30 ºC. Samples were heat treated at 96 ºC for 5 min before loading it onto 7 M urea gel (*Section* 2.2.6). The gel was run either at room temperature **[(a), (c)** and **(e)]** for 2 h or at 60 ºC **[(b), (d)** and **(f)]** for 1 h with 100 V/gel. Gel was scanned using phosphorimager.

3.5 Denaturing of DNA using formaldehyde

Formaldehyde, a widely used denaturant, was also used to check for denaturation of ds-DNA. Samples were similarly incubated with different concentrations of formaldehyde and heat treated at 96 ºC for 5 min before loading onto the gel (*Section* 2.2.6). The gel was run at both room temperature and 60 ºC. All samples treated with formaldehyde resulted in unclear bands as observed in the **Fig. 3.5.1(c)** and **(d)**. Presuming that heating had an effect on the sample mixture, it was avoided and the samples were run without heat treatment. Although the resultant product was slightly better compared to previous result, the problem with clear differentiation between the bands still existed [**Fig. 3.5.1(a)** and **(b)]**.

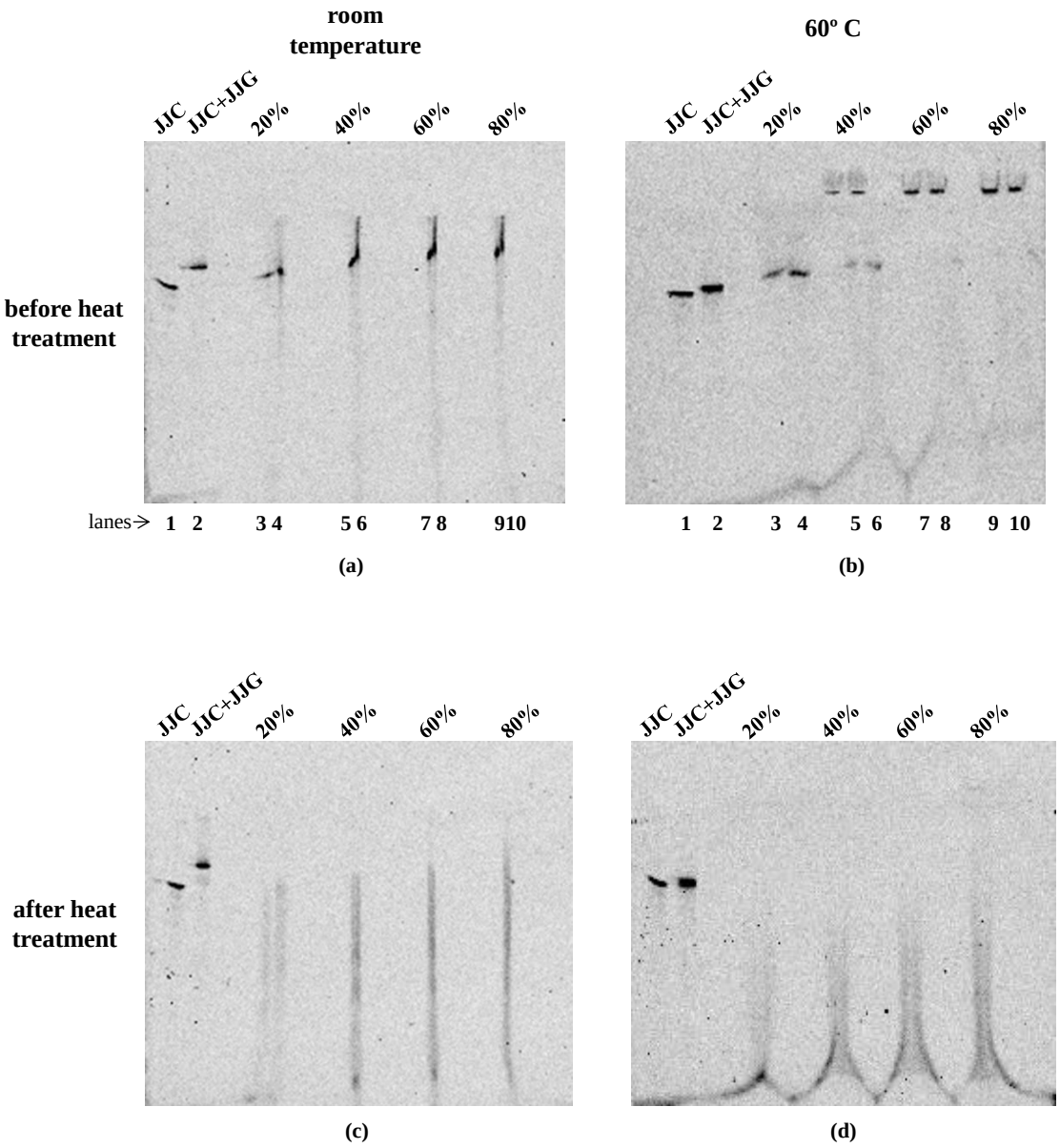

Figure 3.5.1 Denaturing of DNA using formaldehyde. Substrates (50 nM) were incubated in the presence of varied concentrations of formaldehyde for 30 min at 30 ºC. Samples were either heat treated at 96 ºC for 5 min **[(c)** and **(d)]** or not **[(a)** and **(b)]** before loading it onto 7 M urea gel. The gel was run either at room temperature for 2 h or at 60 ºC for 1 h with 100 V/gel. Gels were scanned using phosphorimager.

3.6 Urea as a denaturing agent and influence of stacking gel on the resolution of urea-PAGE gels

Though denaturants like glycerol, DMSO and formamide were useful in dissociating ds-DNA, it was crucial to have urea in the gel. Gels prepared free of urea and run at room temperature resulted in ds-DNA undissociated even in the presence of other denaturants **[Fig. 3.6.1(a)]**. However, partial dissociation was witnessed when run at 60 ºC **[Fig. 3.6.1(b)]**. Moreover, comparing **Fig. 3.6.1** with **Fig. 3.3.1(a)**, it is clear that the presence of stacking gel greatly aids in increasing the resolution of the bands. Gels prepared with 7 M urea and run at room temperature resulted in partial dissociation of ds-DNA even in the presence of denaturants **[Fig. 3.6.2(a)]**. However, complete dissociation of ds-DNA was observed when the gel was run at 60 ºC [**Fig. 3.6.2(b)]**. The resolution of bands in both the gels was again poor compared to previous result **[Fig. 3.3.1(f)]** due to the absence of stacking gel.

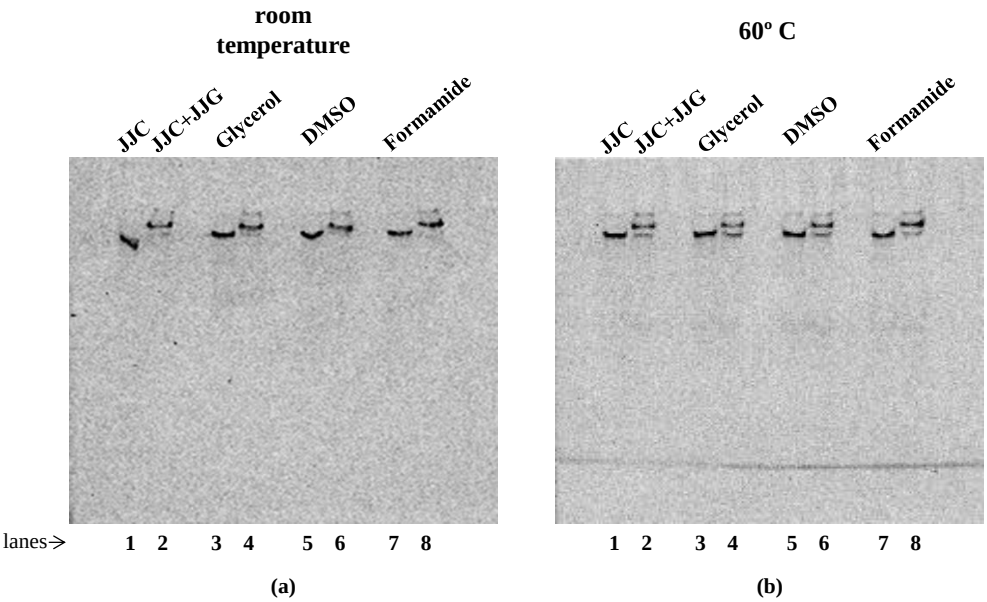

Figure 3.6.1 Denaturing of DNA using denaturants in urea free gel (without stacking gel). Substrates (50 nM) were incubated with appropriate denaturants at a final concentration of 20% each for 30 min at 30 ºC (*Section* 2.2.6). The mixture was heat treated at 96 ºC for 5 min before loading onto urea free gel (without stacking gel). The gel was electrophoresed **(a)** at room temperature for 2 h and **(b)** at 60 ºC for 1 h. Gels were scanned using phosphorimager.

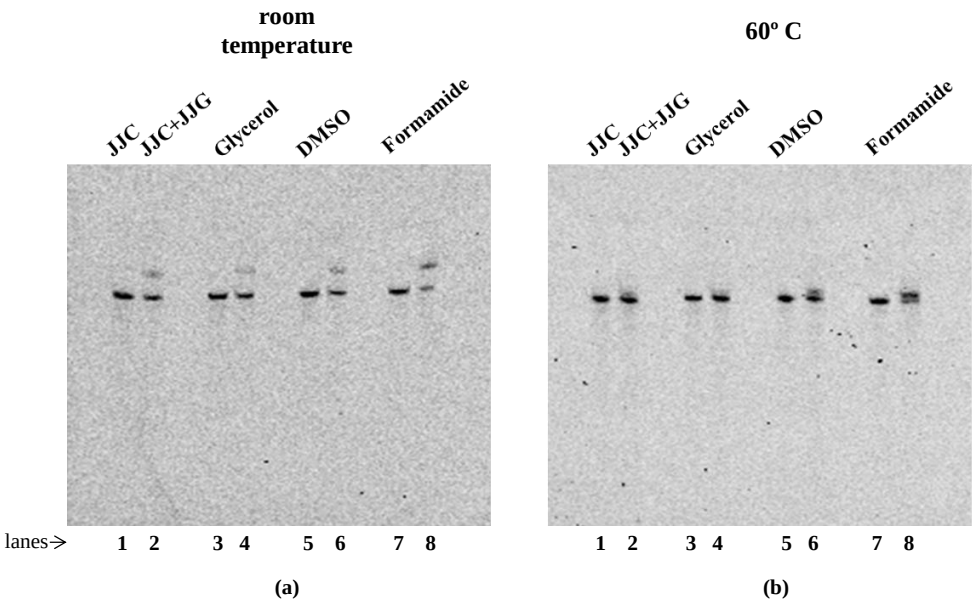

Figure 3.6.2 Denaturing of DNA using denaturants in 7 M urea gel (without stacking gel). Substrates (50 nM) were incubated with appropriate denaturants at a final concentration of 20% each for 30 min at 30 ºC (*Section* 2.2.6). The mixture was heat treated at 96 ºC for 5 min before loading onto 7 M urea gel (without stacking gel). The gel was electrophoresed (a) at room temperature for 2 h and (b) at 60 ºC for 1 h. Gels were scanned using phosphorimager.

3.7 Recombinant enzymes on single and double-stranded DNA

Recombinant enzymes involved in the DNA BER pathway are long thought to act on AP-site/abasic site of only ds-DNA. A study by Marenstein *et al.* (2004) disproved this theory by presenting evidence that APE1 can also act on AP-site of ss-DNA. To check and reconfirm these results in our hands, catalytic activity and efficiency of recombinant enzymes, APE1 and UDG, on ss- and ds-DNA were tested (*Section* 2.2.7). Activity of these enzymes on ds-DNA was included for comparison. Fluoroscein-tagged JJU and untagged reverse complement JJG was used for this experiment. Results showed that recombinant UDG and APE1 act well on both ss- and ds-DNA **[Fig. 3.7.2** and **Fig. 3.7.1]**.

The UDG enzyme added (10 U/assay) removes the uracil from the strand leaving an AP-site, which is further cleaved by APE1. Higher concentration of APE1 (10 U/assay) in the presence of UDG nicks the DNA completely resulting in a product/band at the bottom of the gel **[lanes 3,4** in **Fig. 3.7.1(a)]**. However, decreasing concentrations of APE1 (half-log dilutions from 10 U/assay) resulted in incomplete nicking of the substrate and therefore the bands are seen at the top of the gel **[lanes 5,6,7** in **Fig. 3.7.1(a)]**. Under conditions tested ds-DNA was 10-times more sensitive to APE1 than ss-DNA.

A high concentration of UDG enzyme (10 U/assay), in the absence APE1, was found to partially dissociate both ss- and ds-DNA **[Fig. 3.7.2 (a)** and **(b)]**. The dissociation of substrate to product decreased with decrease in UDG concentration (half-log dilutions from 10 U/assay) **[lanes 2-7** in **Fig. 3.7.2]**. Under conditions tested ds-DNA was 10-times more sensitive to UDG than ss-DNA.

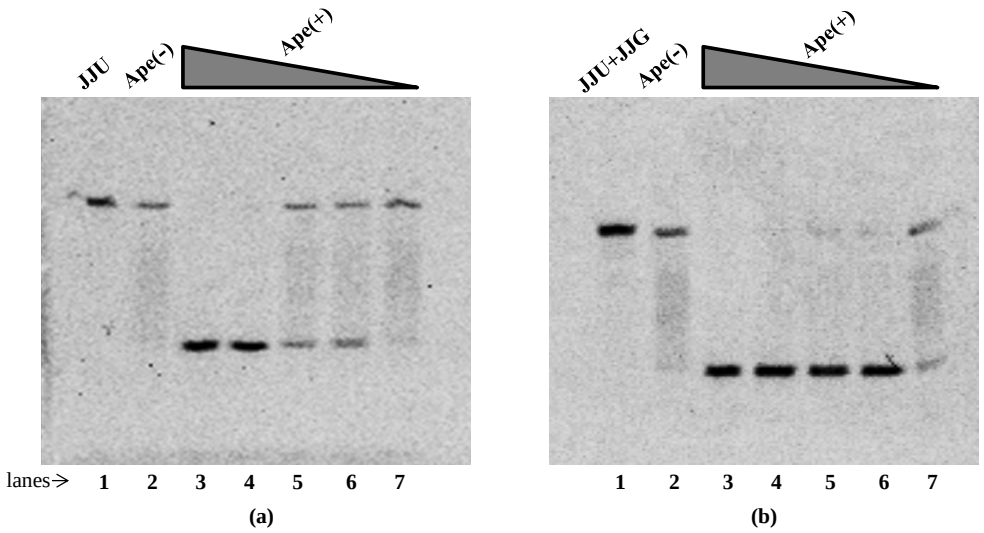

Figure 3.7.1 Effect of recombinant enzyme APE1 on (a) ss-DNA and (b) ds-DNA. Fluorescein-tagged ss- and ds-DNA (50 nM each) were first treated with 10 U/assay of UDG enzyme followed by addition of half-log dilutions of 10 U/assay of APE1 enzyme (*Section* 2.2.7). The mixture was incubated for 30 min at 30 ºC and heat treated at 96 ºC for 5 min with 10% loading buffer. Samples were loaded onto 7 M urea gel and run at 60 ºC for 1 h. In both the gels; lanes 2-7 contain substrates treated with UDG enzyme, lanes 3-7 contain decreasing concentrations of APE1 enzyme and lane 1 contain untreated substrates (control).

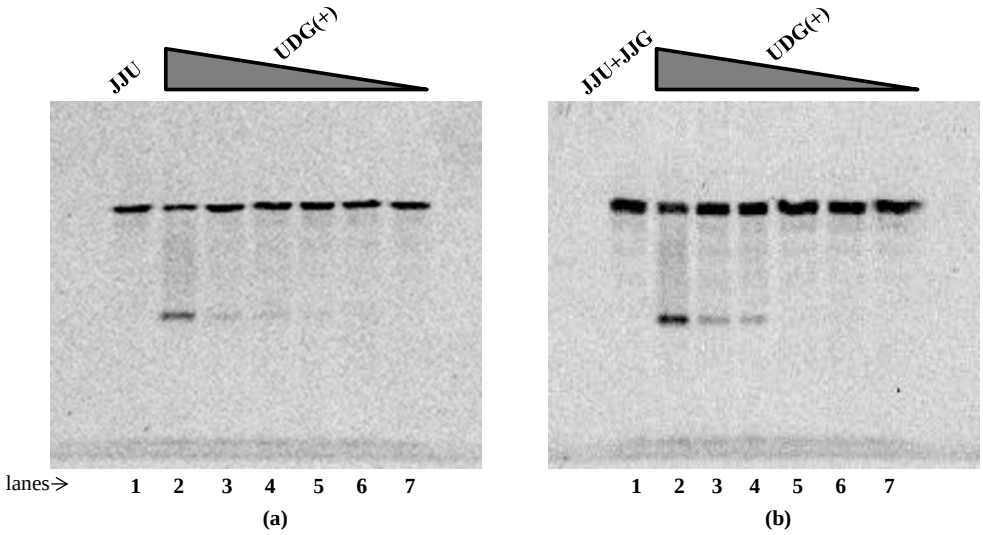

Figure 3.7.2 Effect of recombinant enzyme UDG on (a) ss-DNA and (b) ds-DNA. Fluorescein-tagged ss- and ds-DNA (50 nM each) were treated with half-log dilutions of 10 U/assay of UDG enzyme. The mixture was incubated for 30 min at 30 ºC and heat treated at 96 ºC for 5 min (*Section* 2.2.7). Samples were loaded onto 7 M urea gel and run at 60 ºC for 1 h. In both the gels; lanes 2-7 contain substrates treated with decreasing concentrations of UDG enzyme and lane 1 contain untreated substrate (control).

3.8 Yeast extracts and their resemblance to UDG-like enzymes

Both wild-type and *kcs1Δ* yeast extracts were prepared to check for the presence of DNA repair enzymes with properties similar to UDG. Yeast extracts were prepared in the presence or absence of detergent Tween-20 and with varying concentrations of EDTA (0, 1 and 100 mM) (*Section* 2.2.8). Fluorescein-tagged JJU+JJG substrate was used in this experiment. The wild-type yeast extracts, regardless of EDTA concentration and presence or absence of Tween-20, showed UDG-like activity (creating AP-site) **(lanes 2, 4, 6, 8, 10** and **12** in **Fig. 3.8.1)**. On the other hand, *kcs1Δ* extracts lacked UDG-like activity in the absence of Tween-20 and presence of 0 mM and 1 mM EDTA **(lanes 3, 7** in **Fig. 3.8.1)**. However, *kcs1Δ* extracts prepared in the absence of Tween-20 and presence of 100 mM

EDTA showed UDG-like activity **(lane 11** in **Fig. 3.8.1)**. Further, inclusion of Tween-20 into the yeast sonication buffer greatly increased UDG-like activity of the *kcs1Δ* extracts regardless of EDTA concentration **(lanes 5, 9, 13** in **Fig. 3.8.1)**. The cleaved product at the bottom of the gel, observed in extracts showing UDG-like activity, could be a resultant of either APE1-like activity (nicking of DNA at AP-site created by UDG) or heat-induced break.

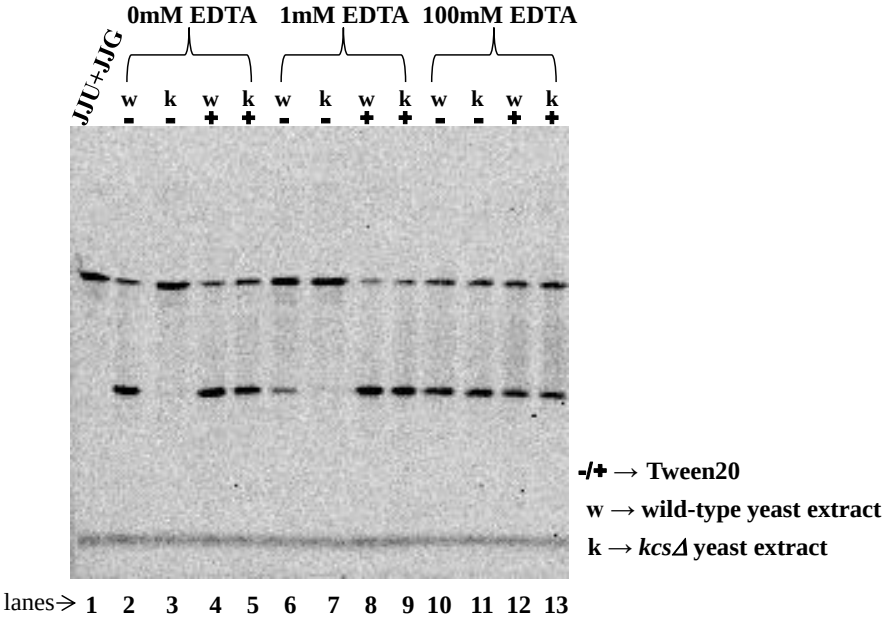

Figure 3.8.1 Yeast extracts and their resemblance to UDG-like enzyme. Extracts of wild-type and *kcs1Δ* were prepared (*Section* 2.2.8) in the presence or absence of Tween-20 and in the presence of 0, 1 and 100 mM EDTA. The ds-DNA (50 nM) was incubated with relevant yeast extracts for 30 min at 30 ºC and heat treated at 96 ºC for 5 min (*Section* 2.2.9). Samples were loaded onto 7 M urea gel and run at 60 ºC for 1 h. Gel was scanned using phosphorimager. Lane 1: untreated substrate (50 nM). Lane 2-5: substrates treated with wild-type and *kcs1Δ* extracts prepared in the presence or absence of Tween-20 (no EDTA). Lane 6-9: substrates treated with yeast extracts prepared in the presence or absence of Tween-20, with 1 mM EDTA. Lane 10-13: substrates treated with yeast extracts prepared in presence or absence of Tween-20, with 100 mM EDTA.

3.9 Yeast extracts and their resemblance to APE1-like enzymes

Following identification of UDG-like enzyme in yeast extracts, experiments were conducted to check if they also possess APE1-like activity. As heat-treatment of DNA containing AP-site can cause cleavage (Ma *et al.*, 2008), the presence or absence of APE1-like activity in these extracts was uncertain. To ensure that nicking of the AP-site was through APE1-like activity and not through heat treatment at high temperature, borohydride-trapping assay was performed (*Section* 2.2.10). **Fig. 3.9.1** shows the trapping assay performed with recombinant repair enzymes and yeast extracts prepared in the presence of Tween-20 and 1 mM EDTA (*Section* 2.2.8). From the **Fig. 3.9.1(a)** and **(b)**, following conclusions can be reached: (a) wild-type and *kcs1Δ* extracts show UDG-like activity i.e., creating an AP-site for APE1 to act on it (lane 2 and 4 show low molecular weight band as a result of AP-site being nicked after heat treatment), (b) wild-type and *kcs1Δ* extracts show APE1-like activity i.e., nicking the DNA at AP-site (lanes 2, 3, 8 and 10 show low molecular weight band following heat treatment, even in the presence of $NaBH_4$, which prevents thermal cleavage of AP-site) and (c) $NaBH_4$ protects the AP-site from being cleaved when exposed to high temperatures (lane 9). Most importantly, **lanes 8** and **10 in Fig. 3.9.1** confirms that the dissociation of substrate to low molecular weight product is due to nicking of AP-site by APE1-like enzyme and not heat treatment.

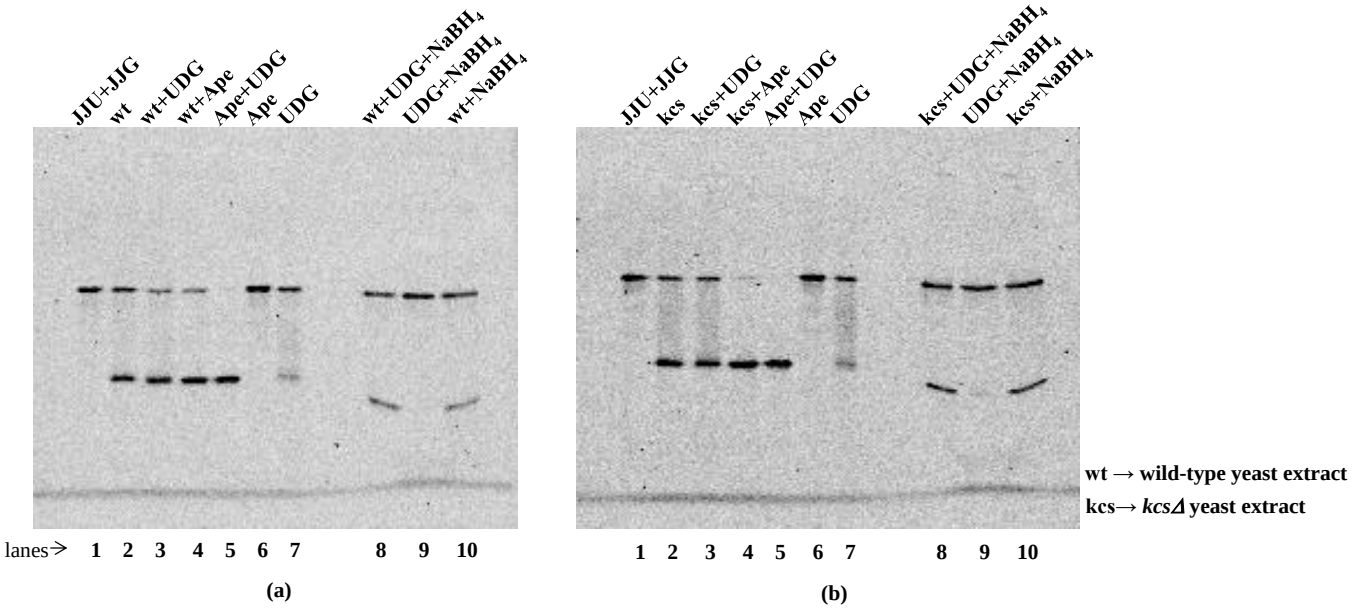

Figure 3.9.1 Borohydride-trapping assay to determine APE1-like activity in (a) wild-type yeast extracts and (b) *kcs1Δ* extract. Substrate JJU+JJG was incubated for 30 min at 30 ºC with: no enzyme or yeast extract (lane 1) (control); with yeast extract (lane 2) (shows UDG- and APE1-like activity); with yeast extract and UDG enzyme (lane 3) (APE1-like activity); with yeast extract and APE1 enzyme (lane 4) (UDG-like activity); with APE1 and UDG enzyme (lane 5) (positive control for APE1 and UDG activity); with APE1 enzyme only (lane 6) (positive control for UDG activity); with UDG enzyme only (lane 7) (positive control for APE1 activity); with yeast extract, UDG enzyme and 100 mM $NaBH_4$ (lane 8) (APE1-like activity); with UDG and $NaBH_4$ (lane 9) (positive control for $NaBH_4$); with yeast extract and $NaBH_4$ (lane 10) (UDG- and APE1-like activity). Then, samples were heat treated at 96 ºC for 5 min and loaded onto 7 M urea gel and run at 60 ºC for 1 h (*Section* 2.2.10). Gels were scanned using phosphorimager.

3.10 Effect of EDTA on repair enzymes

The clear effect of EDTA was unexpected (refer *Section* 3.8). Incorporation into the extraction procedure appeared to either release the sought activity or activate the enzymes once extracted. In order to distinguish between these two outcomes, both wild-type and *kcs1Δ* extracts prepared in the absence of Tween-20 and EDTA (*Section* 2.2.8) were chosen to examine the effect of EDTA on APE1-like and UDG-like activities. Substrate JJU+JJG was treated with yeast extracts as mentioned in *Section* 2.2.11 and was incubated with 0, 12.5, 25, 50 and 100 mM EDTA (final concentration) for 30 min at 30 ºC. The samples were heat treated and electrophoresed in a 7 M urea gel. Results showed that EDTA at a concentration of 50 mM partially inhibited DNA cleavage **(lane 8** in **Fig. 3.10.1)** and at 100 mM concentration completely abolished DNA cleavage **(lane 10** in **Fig. 3.10.1)**

.

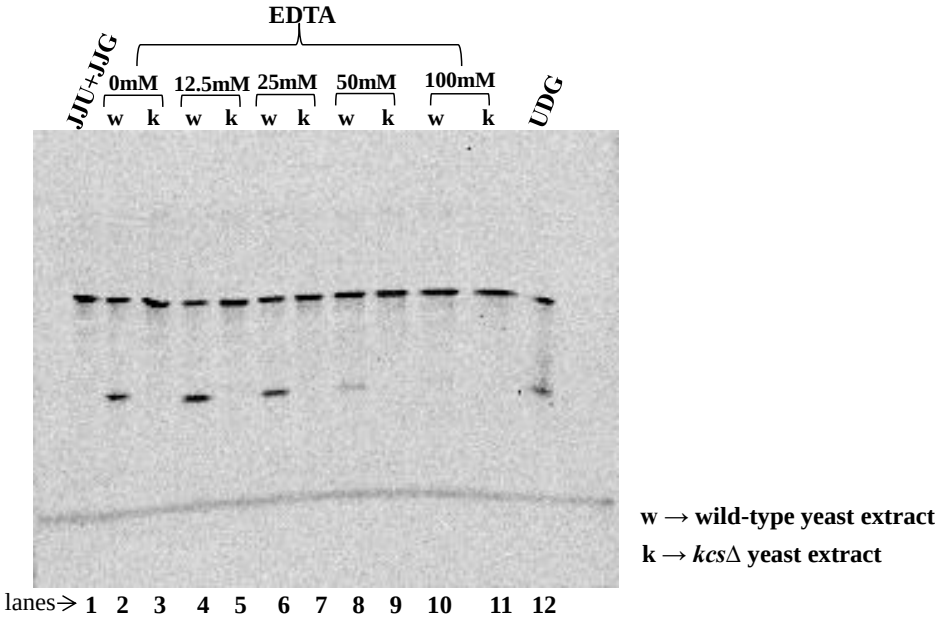

Figure 3.10.1 Inhibition of UDG-like activity by EDTA. Fluorescein-tagged JJU+JJG substrate was first treated with yeast extracts prepared in the absence of Tween-20 and EDTA. To this reaction mixture increasing concentrations of EDTA (0, 12.5, 25, 50 and 100 mM EDTA) were added and incubated for 30 min at 30 ºC (*Section* 2.2.11). Samples were heat treated at 96 ºC for 5 min and subjected to 7 M urea-PAGE. Lane 1: untreated substrate. Lane 2-12: substrate treated with relevant yeast extracts. Lane 2-3: no EDTA added. Lane 4-5: added 12.5 mM EDTA. Lane 6-7: 25 mM EDTA. Lane 8-9: 50 mM EDTA. Lane 10-11: 100 mM EDTA. Lane 12: substrate treated with UDG enzyme. The samples were heat treated at 96 ºC for 5 min and electrophoresed in a 7 M urea gel for 1 h at 60 ºC. Gel was scanned using phosphorimager.

3.11 Phosphoglycolate removal by APE1

It is often debated that APE1 is involved in PG removal in addition to nicking of AP-sites (Wang *et al.*, 2014). APE1 is not only involved in nicking of abasic DNA following the removal of an inappropriately incorporated base such as uracil, it is also key in the removal of PG moieties caused when bleomycin damages DNA (Fung and Demple, 2011). F-16PG plus HP were incubated in the presence of extracts from both wild-type and *kcs1Δ* yeast and T4 ligase (800 U/assay) (*Section* 2.2.12). The rationale for this approach was that APE1 removes the 3′-PG group, decreasing the size of F-16PGmer **(lane 2** in **Fig. 3.11.1)**. However, the resolution of this product from the starting material is poor. In order to determine the release of the PG moiety, HP was designed to covalently link to the F-16mer once the blocking PG group has been removed, producuing a high molecular weight product **(lane 4** in **Fig. 3.11.1)**. This is achieved by the T4 ligase present in most samples. There was no high molecular weight product with wild-type or *kcs1Δ* **(lanes 5, 6, 7** and **8** in **Fig. 3.11.1)** except for in the presence of T4 ligase **(lanes 9, 10, 11** and **12** in **Fig. 3.11.1)**. However, the intensity of this band was not time-related. It is therefore suspected that the appearance of this band is merely due to the presence of some unphosphoglycolated starting material.

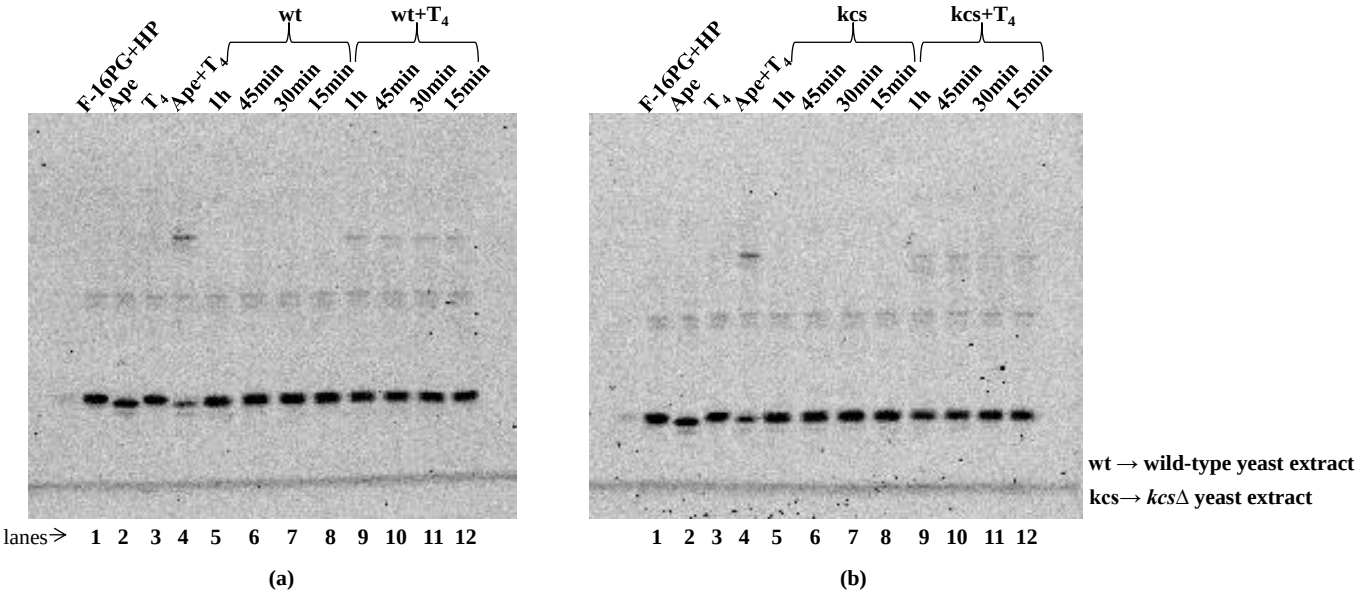

Figure 3.11.1 Removal of phosphoglycolate moiety by (a) wild-type yeast extract and (b) *kcs1Δ* extract. F-16PG plus HP was incubated with yeast extracts (lanes 5-12) for 30 min at 37 ºC (*Section* 2.2.12) and was further incubated for 15, 30, 45 and 60 min at 37 ºC in the presence of T4 ligase enzyme (lanes 9-12). A positive control for PG removal followed by end-joining by APE1 enzyme and T4 ligase (lane 4), respectively, was included for comparison. A positive control for APE1 (lane 2) and T4 enzyme (lane 3), and an untreated substrate control (lane 1) was also included in the experiment. The samples were heat treated at 96 ºC for 5 min and electrophoresed in a 7 M urea gel for 1 h at 60 ºC. Gel was scanned using phosphorimager.

3.12 Subcellular protein localisation studies using confocal microscopy

As it appears that the DNA repair enzymes with APE1- and UDG-like activities are present in *kcs1Δ* strain of yeast, but that extreme extraction methods are required to access these proteins, we decided to GFP-tag several proteins in order to see whether their cellular localisation was different in *kcs1Δ* when compared to wild-type yeast (*Section* 2.2.15). Rad52, Ung1 and Apn1 were successfully GFP-tagged in both wild-type and *kcs1Δ* backgrounds. However, tagging Rad51 in *kcs1Δ* and Apn2 **(Fig. 2.2.3)** in both the backgrounds were unsuccessful. Confocal microscopy images of cells that are (i) non-treated (control) (ii) bleomycin treated and (iii) recovery from bleomycin treatment (*Section* 2.2.20) showed no difference in the proteins studied. The GFP signal was too weak to image and to judge the exact localisation or movement of the tagged proteins. All the proteins roughly appeared to localise in the nucleus **(Fig. 3.12.1)**. Rad51 in wild-type background was the only strain to show bright GFP signal **[Fig. 3.12.1(c)]**. Although not very clear from the images, Rad51 (wild-type background) **[Fig. 3.12.1(c)]** and Rad52 (*kcs1Δ* background) **[Fig. 3.12.1(d)]** appeared to form foci after bleomycin treatment. Also from the images, it was noted that *kcs1Δ* contain large vacuole-like structures inside the cell **[Fig. 3.12.1(a)** and **(d)]**. The *kcs1Δ* has been previously reported to contain swollen and leaky vacuoles (Dubois *et al.*, 2002; Saiardi *et al.*, 2000).

(a) Ung1

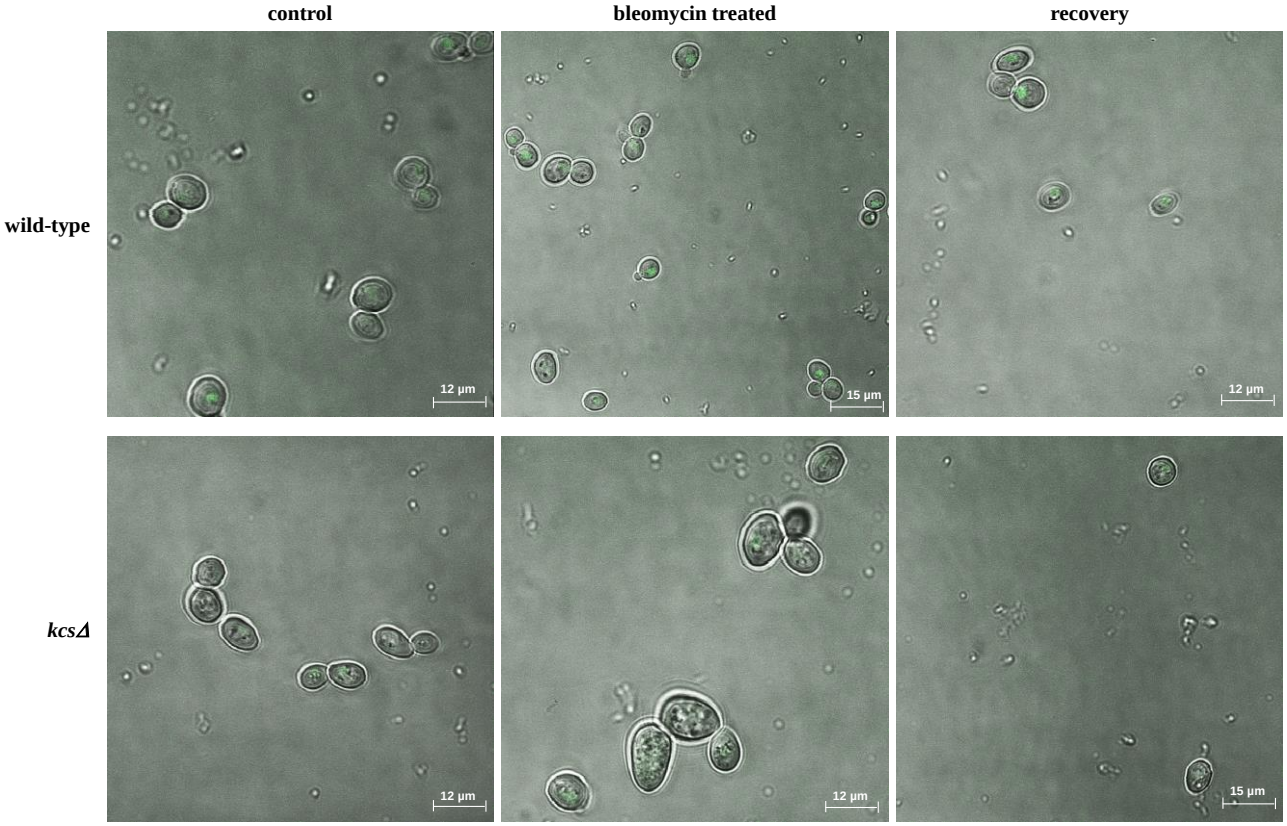
control
bleomycin treated
recovery
wild-type
kcsΔ
12 µm
15 µm
12 µm
12 µm
12 µm
15 µm

(b) Apn1

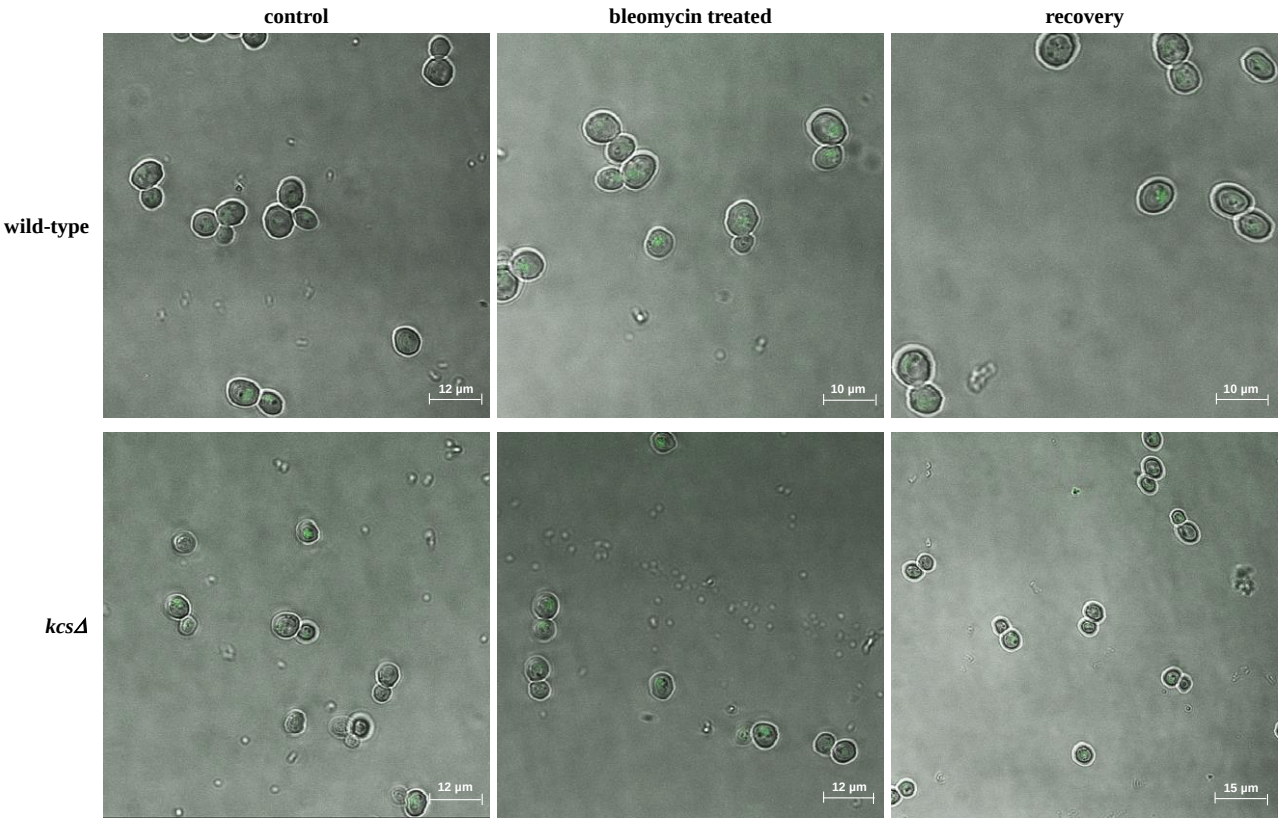
control
bleomycin treated
recovery
wild-type
kcsΔ
12 µm
10 µm
10 µm
12 µm
12 µm
15 µm

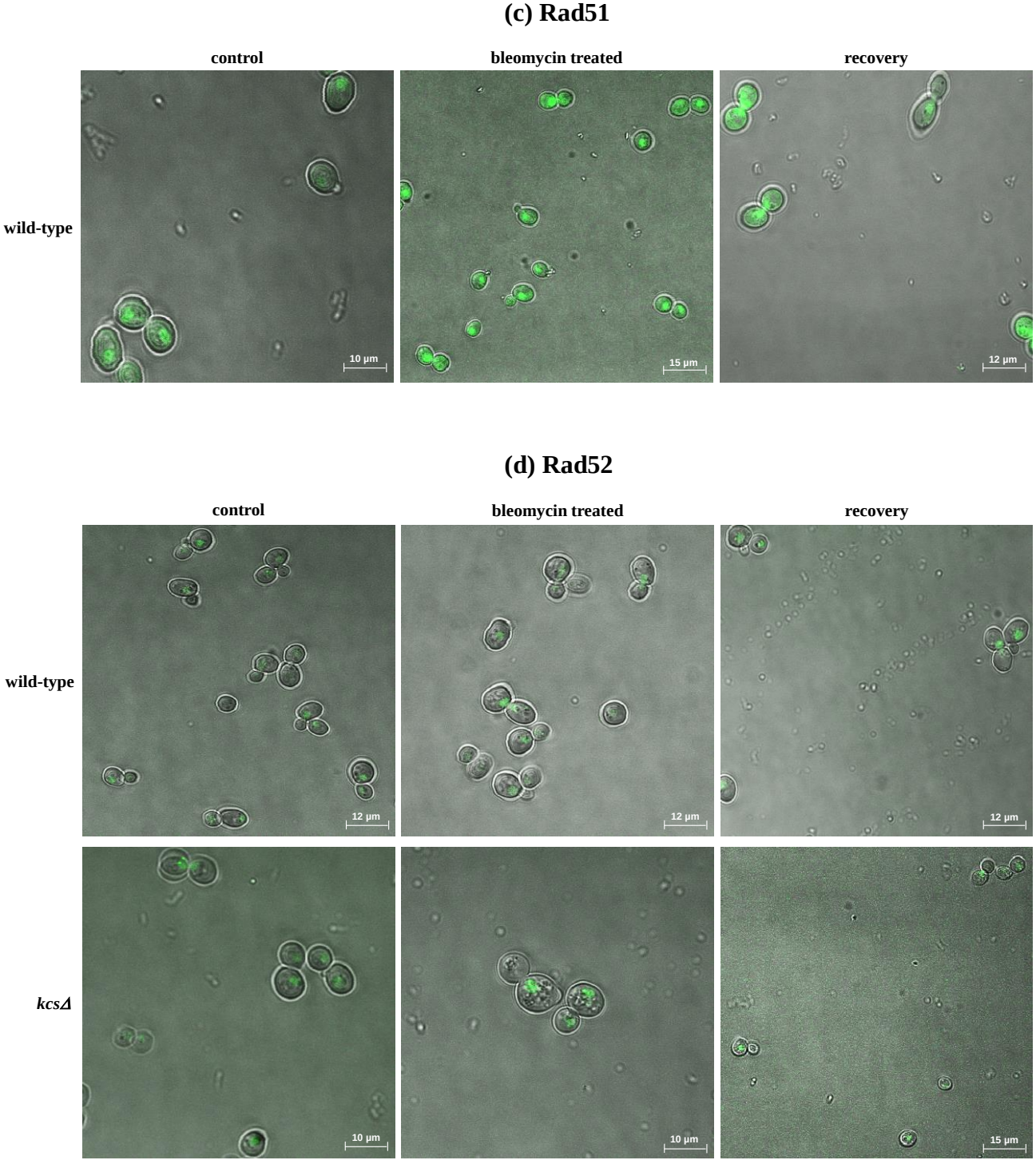

Figure 3.12.1 Subcellular localisation of GFP-tagged proteins (i) Ung1, (ii) Apn1, (iv) Rad52 in wild-type and *kcs1Δ* backgrounds, and (iii) Rad51 in wild-type background. Confocal microscopic images of live yeast cells expressing GFP-tagged proteins; the green GFP fluorescence was overlaid onto a phase-contrast image of the cells. The GFP-tagged clones were treated with 5 mU/ml of bleomycin for 90 min and were visualised (*Section*

2.2.20). Following removal of the drug, the yeast cells were allowed to recover for 1 h in YPD medium and were visualised. GFP-tagged proteins appear to localise in the nucleus of yeast cells. A 63x oil objective was used to capture images.

3.13 Discussion

Tumour resistance to anticancer agents like bleomycin and 5FU are often associated with the ability of cells to recover quickly through overactive cellular repair mechanisms. Moreover, drugs like bleomycin are less heavily used as it often causes impaired lung functions (Ramotar and Wang, 2003). Knowledge on the mechanisms and the factors that the tumour cells exploit to elicit resistance against chemotherapeutics would prove valuable to treat the disease much more effectively. We believe one such potential factor involved in the process of tumour resistance/DNA repair is IDPs.

IDPs are regarded as novel regulators of HR signalling in mammals (Jadav *et al.*, 2013). IDPs such as $InsP_7$ and $InsP_8$ are also reported to be crucial for hyper-recombination events in yeast lacking protein kinase C (Luo *et al.*, 2002). In fact, the initial observations which have led us to determine the great importance of IDPs in DNA repair were found on the observation that $InsP_6$ acts as a 'stimulatory factor' in NHEJ (Hanakahi *et al.*, 2000). NHEJ in mammalian cells relies on a holoenzyme containing Ku70, Ku80 and DNA-PK, a complex that is activated *in vitro* by $InsP_6$.

In this study, a family of genetically modified yeast with modulated levels of IPs and repair enzymes were used as a model to investigate the role of IDPs in DNA repair. The results from the study suggest that IDPs are crucial in repair of DNA following insult with bleomycin and 5FU, but not of a myriad of other chemotherapeutics. The tested mutants were over 1000-fold more sensitive to bleomycin and 100-fold more sensitive to 5FU than wild-type yeast **(Fig. 3.2.1)**. Three particular mutants- *plc1Δ* (data not shown), *arg82Δ* and *kcs1Δ*, all lacking IDPs and reportedly inorganic polyphosphates (Auesukaree *et al.*, 2005) were found to be hypersensitive to bleomycin and 5FU **(Fig. 3.2.1)** and not to other drugs like H_2O_2 (Onnebo and Saiardi, 2009). These findings clearly indicate that the enhanced sensitivity to bleomycin and 5FU cannot be due to the mutants being generally sick, or

having increased cell wall permeability. The increased sensitivity could be due to a range of toxic intermediates, such as complex DSDBs, or juxtaposed AP-sites and/or 3′ damage comprising ss- breaks, formed by bleomycin in particular (Chen and Stubbe, 2005).

In our experiments, *ipk1Δ* showed resistance equal to that of wild-type yeast cells. The *ipk1Δ* mutants lack the enzyme responsible for the synthesis of $InsP_6$ and $InsP_7$, however are capable of synthesizing PP-$InsP_4$ and $(PP)_2$-$InsP_3$ **(Fig. 1.1.2)** which supposedly can perform DNA repair alike $InsP_7$ or $InsP_8$ (Saiardi *et al.*, 2002). The *rad52Δ* were found to show high sensitivity to both drugs. However, *rad52Δ* were also sensitive to IR, camptothecin, doxorubicin, hydroxyurea, MMS and UV. These differences would suggest that the mechanism of action of the IDP mutants is not through the Rad52 epistasis group.

$InsP_7$ kinase has recently been identified as Vip1 (Choi *et al.*, 2007; Mulugu *et al.*, 2007), although mutants have not been shown to lack the product ($InsP_8$). The *vip1Δ* tested in the experiment was as sensitive as wild-type yeast, suggesting that the effects are not regulated by $InsP_8$. Results from the screening experiment identified that only mutants lacking all IDPs are sensitive to bleomycin and 5FU. IDPs comprise below 5% of total IP pools, and, as such, removal of these from the general pool does not significantly alter the total IP levels. Therefore, the bulk phosphate effect can be excluded. Further, several other proteins that are involved in DNA repair including Rad, yKu, Msh, Cln and Sir family of proteins were all found to be less sensitive to bleomycin than the IDP mutants, and, therefore, were excluded as candidate proteins for which IDPs or inorganic polyphosphates act as cofactors (S.T. Safrany, personal communication).

Pulsed-field gel electrophoresis studies performed previously in the group showed wild-type, *rad52Δ*, and *kcs1Δ* to have equal damage following treatment and therefore the increased sensitivity of the mutants have been correlated with a defect in DNA repair. The

rad52Δ were able, albeit slower than wild-type, to repair DSDB, whereas *kcs1Δ* failed to recover in these studies (U. Padmanabhan and S.T. Safrany, personal communication). Similarly, in comparing the wild-type, *arg82Δ, ipk1Δ* and *kcs1Δ*, only wild-type and *ipk1Δ* were found to recover from the damage. Of all the preliminary studies done in the group, the most interesting finding was that, unlike *rad52Δ, mre11Δ, xrs2Δ,* mutants lacking IDPs (*plc1Δ, arg82Δ, kcs1Δ* and *ipk1Δ/kcs1Δ*) showed no increased sensitivity to γ-irradiation. This is the first observation, to our knowledge, in which mutants sensitive to bleomycin are resistant to IR. Bleomycin is described as a γ-ray mimetic, yet frequent reports show that ligation of DNA following bleomycin-induced damage proceeds more slowly that following γ-irradiation (Moore, 1990). The possible explanation for this would be that the adducts formed *in vivo* are different between these two agents. Also, higher survival of irradiated cells than bleomycin-treated cells could be implicated to fewer DSDBs generated by γ-irradiation compared to bleomycin (Moore *et al.*, 2000).

Of all the mutants tested in this study, hypersensitivity of *kcs1Δ* was intriguing **(Fig. 3.2.1)**. Kcs1, a key enzyme involved in the synthesis of all IDPs ($InsP_7$, PP-$InsP_4$ and $[PP]_2$-$InsP_3$) excluding $InsP_8$, is a slow growing and temperature sensitive (best grown at 30 ºC) mutant which failed to survive after bleomycin and 5FU treatment. A similar outcome of decreased viability and reduced recovery has been observed in a recent study with *kcs1Δ*, in response to radiomimetic antibiotics and hydroxyurea (Jadav *et al.*, 2013). The study concluded that such sensitivity was due to failure of efficient DNA repair. This finding is in support of our hypothesis that IDPs are vital for DNA damage repair. Conversely, there are reports suggesting that human homologue of *kcs1*, IP6K2, and the associated IDPs are necessary to activate apoptosis during stress conditions (Morrison *et al.*, 2001; Morrison *et al.*, 2009; Nagata *et al.*, 2005). Experiments relating to this showed inability of IDP-deficient cells to induce apoptosis and instead induced untimely activation of various cell

cycle arrest genes during stress (Koldobskiy *et al.*, 2010). Although a possible role for *kcs1* in tumour suppression has been indicated in these studies, there is no strong direct evidence so far to prove this.

It was speculated earlier that bleomycin and 5FU converge through the APN family of repair proteins. To understand the role of Apn1 and its preceding protein Ung1 in the repair pathway of bleomycin- and 5FU-induced DNA damage, series of experiments were performed. The first approach was to come up with ways to nick the mismatched ds-DNA at AP-site which is the target for Apn1. Denaturing urea-PAGE technique was employed to determine whether the DNA was cleaved. Urea-free PAGE gels failed to show clear separation of ss- from ds-DNA and also resulted in poor resolution of gels **(Fig. 3.6.1)**. A number of variations were introduced to the prevailing urea-PAGE technique (Owen *et al.*, 2007) to develop a system that suits our experimental needs. It was found that running the fluorescein-tagged mismatched DNA (both ss- and ds-DNA) in a higher concentration urea (7 M) gel with an added stacking gel, vastly helped in the resolution of the gel and also in clear differentiation between the strands **[Fig. 3.3.1(f)]**. Although this setting failed to dissociate the ds-DNA, a partial degradation was evident in the absence of a stacking gel **[Fig. 3.6.2(a)]**.

Use of denaturants such as glycerol, DMSO and even formamide proved ineffective in separation of ds-DNA at room temperature **[Fig. 3.4.1(a), (c)** and **(e)]**. Formamide's ability to lower melting temperature and destabilize the helical state of DNA has been reported to be dependent on the G+C composition, helix conformation and state of hydration (Blake and Delcourt, 1996). Since the G+C composition is slightly high in the oligonucleotide substrate used in this experiment, it is possible that they serve as energetic barriers to further melting of the DNA. Use of formaldehyde as denaturant in this experiment appeared to damage the fluorescein molecule and thereby result in loss of fluorescence

signal. Such effect was obvious when formaldehyde was heated with the substrate containing fluorescein molecule **(Fig. 3.5.1)**.

It was found that irrespective of the presence or absence of denaturants, running the gel at 60 ºC in a 7 M urea gel greatly aids in dissociating the ds-DNA **[Fig. 3.4.1(b), (d)** and **(f)]**. These results are in agreement with a recently published report where the combination of urea and temperature of 45-55 ºC during the gel run was shown to dissociate unstructured DNA or RNA molecules (Summer *et al.*, 2009). However, unlike their technique, our method does not involve 'pre-running of the gel' step, yet it did not appear to affect our results.

Various DNA-*N*-glycosylases in BER have been shown to act on damaged bases of ss-DNA (Boorstein *et al.*, 2001; Dou *et al.*, 2003). However, APE1 is long thought to act on AP-sites of only ds-DNA, with a view to allow insertion of correct nucleotide during repair. Experiments in this study have shown that both APE1 [**Fig. 3.7.1(a)]** and UDG **[(Fig. 3.7.2(a**)] can act on AP-sites of ss-DNA. However, AP-site of ds-DNA was observed to be 10-times more sensitive to the enzymes than that of ss-DNA. A study by Marenstein *et al.* (2004) found the catalytic efficiency of AP-site in ss-DNA to be approximately 20-fold less than that of ds-DNA. Their study also found that unlike the activity of AP-sites in ds-DNA, APE1 demonstrates no product inhibition when acting on an AP-site in ss-DNA. Due to such lack of product inhibition, APE1 is let free to dissociate from the ss-break instead of participating in the coordinated transfer of ss-break to downstream repair enzymes, polβ. Further processing of this toxic intermediate is mandatory and repair proteins such as XRCC are thought to repair ss-DNA breaks in mammalian cells (Marenstein *et al.*, 2004).

Subsequently, extracts from wild-type and *kcs1Δ* yeast were checked for the activity of Ung1 and Apn1 enzymes. The ability of the yeast extracts to recognise and create AP-site

by removal of the mismatched 'uracil' from the oligonucleotide substrate was checked using the Glycosylase/UDG activity assays. Results of this experiment showed varied results depending on (a) presence or absence of Tween-20 and, (b) concentration of EDTA in the sonication/lysis buffer. Wild-type yeast, regardless of EDTA concentration and inclusion or exclusion of Tween-20, showed UDG-like activity **(Fig. 3.8.1)**. In contrary, *kcs1Δ* extract lacked UDG-like activity in the absence of Tween-20 and presence of lower concentration of EDTA. This would mean that *kcs1Δ* which lacked IDPs did not participate in DNA repair. However, a higher concentration of EDTA (100 mM) in the lysis buffer, irrespective of inclusion or exclusion of the detergent, was found to greatly increase UDG-like activity **(Fig. 3.8.1)**. From these experiments, it is clear that presence of either Tween-20 or a high concentration of EDTA is necessary to release the repair enzymes from the yeast strains.

A possible role of the detergent or EDTA in inhibiting or enhancing the activity of the repair enzymes cannot be completely disregarded. Increase in the activity of enzymes when prepared in the presence of a detergent has been previously shown in different experimental setups (Arthur *et al.*, 1984; Martin *et al.*, 2003). A recent study has found Tween-20, at a concentration of 0.2 %, to induce genotoxic effects and exhibit DNA cleavage properties in cancer and endothelial cell lines (Eskandani *et al.*, 2013). However, there appears to be no similar report published with yeast cells. Moreover, provided that the yeast cell wall is very tough to disrupt, lowering concentrations of detergent/Tween-20 and/or EDTA may not be sufficient to lyse cells and successfully release the proteins.

Furthermore, combination of (10 mM each) of EDTA and Mg^{2+} together has been implicated in loss of activity of enzymes such as nictotinamide adenine dinucleotide (NADH) dehydrogenase (Madden *et al.*, 2004). The endonuclease activity of APE1 on both ss- and ds-DNA is Mg^{2+}-dependent (Marenstein *et al.*, 2004). EDTA, being a

powerful chelator of divalent cations, could potentially seize the Mg^{2+} ions and stop the APE1 from functioning (stops the APE1 reaction on 3′-PG moieties). However, results from this study show UDG-like activity with extracts prepared only in the presence of higher concentration of EDTA. This result could mean that incorporation of EDTA into the extraction procedure may either help in release of the sought activity or activate the enzymes once extracted. Experiments to distinguish between these two outcomes resulted in the finding that EDTA at a higher concentration (100 mM) completely inhibits UDG-like activity **(Fig. 3.10.1)**. This result confirms that (a) EDTA in the lysis buffer helps in the release of enzyme activity and, (b) EDTA, added to yeast extract, is involved in inhibiting the enzyme activity and not activating it.

Heat-treatment of abasic DNA is reported to cause double-strand cleavage (Sugiyama *et al.*, 1994). In this study, the presence or absence of APE1-like activity in the yeast extracts appeared indecisive as the experimental protocol involved exposure of samples to high temperatures. Thus, $NaBH_4$ was used to reduce the heat-labile unstable abasic DNA to generate a heat-protected stable complex (Hill *et al.*, 2001; Petronzelli *et al.*, 2000). Outcome of this experiment confirmed the presence of APE1-like activity in both the wild-type and *kcs1Δ* extracts **(Fig. 3.9.1)**. However, the APE1-like activity found in the extracts was inefficient in removing 3′-PG group of 16-PGmer. This may have resulted in poor repair of the strands or linking of HP to 16-mer by T4 ligase and thus resulted in a faint high molecular weight product **(Fig. 3.11.1)**. Appearance of such band could also merely be due to the presence of some unphosphoglycolated starting material. Using human whole cell extracts, Parsons *et al.* (2004) demonstrated that repair of an oligonucleotide containing 3′-PG is much slower compared to repair of same length oligonucleotide without 3′-PG. However, with the yeast extracts in this study, there was no sign of efficient

repair of 3′-PG even after an hour of recovery time. It is possible that the yeast biology is different to human in this aspect.

Human APE1 and APE2 proteins, which shares extensive homology with yeast Apn2, accounts for only <10% of AP endonuclease activity in yeast. The majority of AP endonuclease activity in yeast is carried out by Apn1, which shares high homology with *E. coli* endonuclease IV (Guzder *et al.*, 2004). Thus, some of the repair process seen in yeast cannot be translated to humans (Guzder *et al.*, 2004). Kcs1 in yeast is a much larger protein (120 kDa) than its mammalian counterpart IP6K (50-60 kDa). Considering the large protein size, it is likely that Kcs1 is multifunctional and therefore its knockdown in yeast may affect other activities not yet ascribed to this protein (Dubois *et al.*, 2002). However, as this protein is present in *plc1Δ* and *arg82Δ* this explanation is not convincing.

In this study, confirmation of the presence of both UDG- and APE1-like activity in yeast lacking IDPs fails to support our initial hypothesis. However, the activity of these repair proteins was observed in *kcs1Δ* only when the extracts where prepared with either Tween-20 or high concentration of EDTA, suggesting that UDG- and APE-1 like proteins may be mislocalised and unavailable to access the damage site and repair DNA following bleomycin- or 5FU-insult. Hence, the fluorescent-tagging of proteins that often offers a rapid and effective route to their localisation and isolation was employed. GFP-tagging in the wild-type yeast yielded better success rate compared to *kcs1Δ*. In addition to exhibiting growth impaired phenotype (evident with temperature above 30 ºC), *kcs1Δ* were also observed to contain swollen **[Fig. 3.12.1(a)** and **(d)]** and leaky vacuoles with related compromise on stress responses and defects in cell wall integrity (Dubois *et al.*, 2002). Provided with such a fragile and morphologically abnormal yeast mutant, it was challenging to get a higher rate of successful transformants. Anecdotal evidence observed during this and previous studies in the lab showed that transfection and DNA manipulation

is particularly difficult in *kcs1Δ* with less than 1% the efficiency of wild-type yeast. However, we were able to obtain cells expressing GFP-tagged DNA repair enzymes being expressed under their native promoters.

Confocal microscopy studies of the successful clones, due to poor GFP signal/expression of tagged proteins, failed to show the clear localisation and movement of the tagged proteins before or after bleomycin insult. However, Rad51 in the wild-type background showed a clear and bright fluorescent GFP signal **[Fig. 3.12.1(c)]**. Monitoring of the protein following bleomycin treatment showed no clear foci formation required for DNA repair. Failure to transmit good signals by the fluorescent molecules could be because of the following reasons: (a) the GFP may have misfolded thereby losing on the native expression signals and resulting in a poor signal (b) protein tagging at the C-terminal may have made the GFP fusion protein unstable and/or non-functional (Honda and Selker, 2009) (c) the native expression of these proteins is inherently low. Problems encountered in (b) and (c) could have been resolved by N-terminal tagging of the proteins or using an overexpression vector with a strong promoter. An alternative approach would be to use antibodies against each protein. This was not attempted as the use of fluorescent tags was thought more cost-effective. However, it is clear that these studies may now need to be performed.

$InsP_7$ has been shown to participate in non-enzymatic pyrophosphorylation of both mammalian and yeast proteins (Saiardi *et al.*, 2004). Such pyrophosphorylation events suggest a role for $InsP_7$ in post-translational modification of proteins (Bhandari *et al.*, 2007; Onnebo and Saiardi, 2009). The differential sensitivity observed in wild-type and *kcs1Δ* yeast may be due to altered $InsP_7$-mediated phosphorylation and pyrophosphorylation of proteins/repair enzymes. Exogenous pyrophosphorylation of β subunit of adaptor protein–3 (a serine-rich acidic region) was found to be significantly

higher in *kcs1Δ* compare to wild-type (Azevedo *et al.*, 2009). Such pyrophosphorylation events have also been proposed to mediate and inhibit protein-protein interactions.

3.14 Conclusion

In this study a panel of genetically modified yeast with modulated levels of IPs were used to examine the role of IDPs in the DNA repair process. Two well-known anticancer drugs, bleomycin and 5FU, which causes DSDBs were used to induce DNA damage in yeast cells. Experiments revealed that mutants *kcs1Δ* and *arg82Δ* yeast, which lacks all the IDPs, were hypersensitive to both bleomycin and 5FU. However, *vip1Δ*, which lacks $InsP_8$ failed to show sensitivity. Although the two anticancer treatments act through different pathways, they appeared to converge through APN family of repair proteins. The effects seen with the mutants were suspected to be mediated by the inability of yeast to regulate the repair proteins in the absence of co-factors such as IDPs. Hence, the *kcs1Δ* were checked for the presence of functional repair proteins Ung1 and Apn1. Glycosylase and sodium borohydride assays confirmed the presence of both UDG-like and APE1-like repair proteins in the *kcs1Δ* yeast extract. However, the proteins appeared to be mislocalized in the cell, unable to reach the damage site to initiate repair process. Thus, the repair proteins were GFP-tagged to detect their subcellular localisation in the cell. However, confocal microscopy studies failed to show clear localisation or movement of these proteins following bleomycin insult. This raises the question of whether tagging of GFP to the protein rendered it non-functional.

4. RESULTS - KINETIC CHARACTERISATION OF THE DIPPs

4.1 Introduction

While little is known about the role(s) IDPs play in cell biology, the enzymes involved in their formation and breakdown have now been identified. IP6Ks are involved primarily in the formation of $InsP_7$ with PPIP5Ks being able to phosphorylate $InsP_6$ as well as $InsP_7$. The breakdown of all IDPs is governed by the DIPP family of proteins. However, little is known regarding the Michaelis-Menten kinetics parameters for Ddp1p/DIPPs. Although there are some kinetic data reported for 5-$InsP_7$, there is no information available for 1-$InsP_7$ isomer and $InsP_8$. Moreover, with the recent improvements in the enzymatic (Loss *et al.*, 2011) and chemical methods (Capolicchio *et al.*, 2013; Wu *et al.*, 2013) for generating IDPs, the quality of some of the previously published data on 5-$InsP_7$ is being questioned for its reliability. For instance, Michaelis constant (K_m) values for 5-$InsP_7$ vary from 4 nM for DIPP-1 (Safrany *et al.*, 1998) to 4 µM for DIPP-3β (Leslie *et al.*, 2002). Provided that the DIPP catalytic domain shares high similarity between these two isoforms, the variation in the substrate concentration seems unreliable.

In this study, using improved methods for the enzymatic synthesis and electrophoretic purification of 1-$InsP_7$, 5-$InsP_7$ and $InsP_8$ (Loss *et al.*, 2011), DIPP family has been kinetically characterised.

4.2 Ddp1 kinetics

The main aim of this study has been to perform the first side-by-side kinetic characterization of human and yeast DIPP forms for each of their substrates: 5-$InsP_7$, 1-$InsP_7$ and $InsP_8$. The recombinant Ddp1 from *S. cerevisiae* was assayed first **(Fig. 4.2.1)**. HPLC was used to analyse Ddp1-mediated dephosphorylation of 1-$InsP_7$ and 5-$InsP_7$ and it was found that they both were metabolised to single product, $InsP_6$ **[Fig. 4.2.1(a) and (b)]**. $InsP_8$ was also dephosphorylated to $InsP_6$, but with relatively little accumulation of $InsP_7$ **[Fig 4.2.1(c)]**. Substrate saturation plots **(Fig. 4.2.1)** showed that the K_m values for each substrate tested were very similar (93 nM, 105 nM, 148 nM in **Table 4.3.1**). Similar was the trend with the rates of hydrolysis of 5-$InsP_7$ and $InsP_8$, but 1-InsP7 was hydrolysed 5 to 6-fold faster **(Table 4.3.1)**.

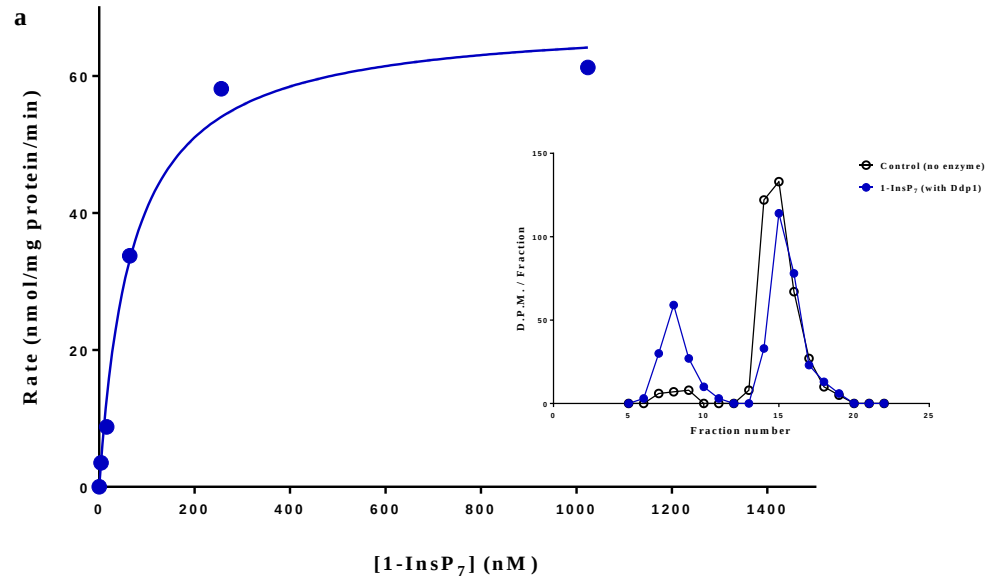
a
Rate (nmol/mg protein/min)
0
20
40
60
0
200
400
600
800
1000
1200
1400
[1-InsP7] (nM)
D.P.M. / Fraction
0
50
100
150
0
5
10
15
20
25
Fraction number
Control (no enzyme)
1-InsP7 (with Ddp1)

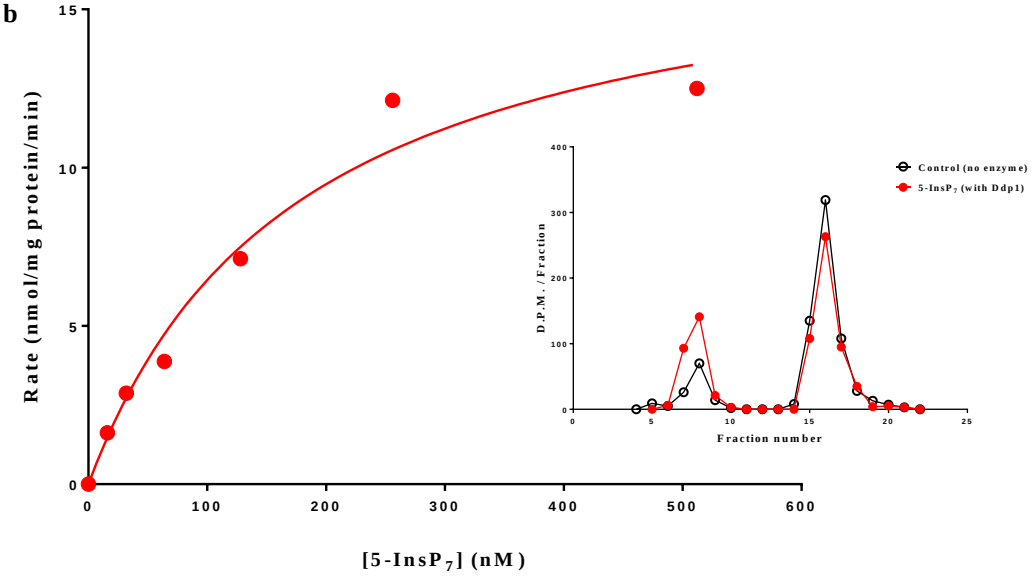
b
Rate (nmol/mg protein/min)
0
5
10
15
0
100
200
300
400
500
600
[5-InsP7] (nM)
D.P.M. / Fraction
0
100
200
300
400
0
5
10
15
20
25
Fraction number
Control (no enzyme)
5-InsP7 (with Ddp1)

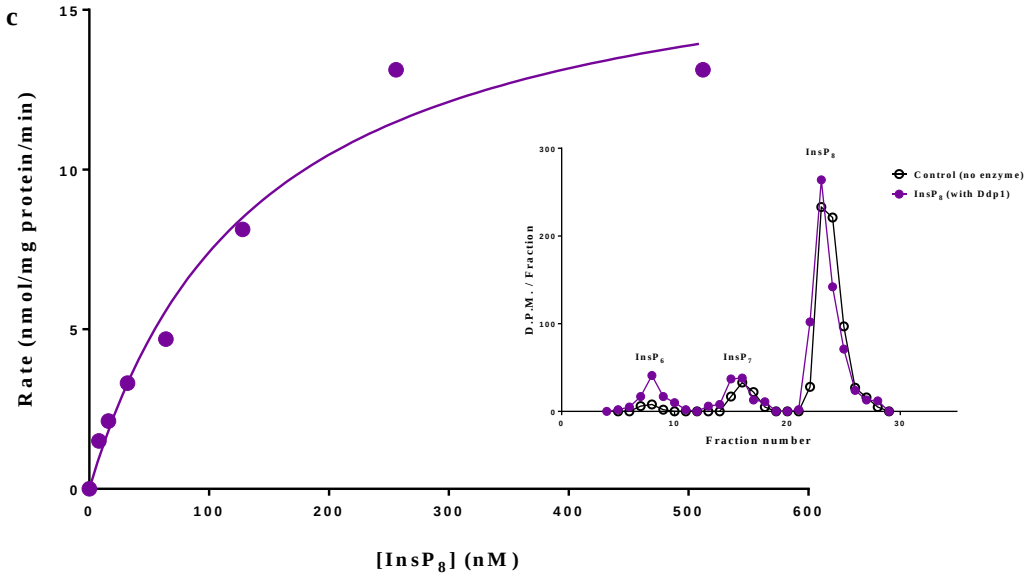

Figure 4.2.1 Analysis of the catalytic activities of Ddp1. Shown are substrate saturation curve for Ddp1. HPLC was used to obtain substrate saturation plots for Ddp1 against either **(a)** 1-$InsP_7$, (0-1024 nM incubated with 2 ng Ddp1 for 0-25 min); **(b)** 5-$InsP_7$, (0-512 nM incubated with 8 ng Ddp1 for 0-25 min); **(c)** $InsP_8$, (0-512 nM incubated with 8 ng Ddp1 for 0-25 min). Insets provide illustrative HPLC analysis using Protocol 1 (*Section* 2.2.23): **(a)** 10 nM 1-$InsP_7$, 20 ng Ddp1, 10 min (not used in the substrate saturation plot). **(b)** 10 nM 5-$InsP_7$, 10 ng Ddp1, 6 min (not used in the substrate saturation plot). **(c)** 16 nM $InsP_8$, 8 ng Ddp1, 4 min. In the insets, black open circles represent controls with no enzyme and coloured filled circles represent enzyme treated substrates.

4.3 Human DIPP kinetics

Next, substrate saturation plots (not shown) for all the five human DIPP-types-1, 2α, 2β, 3α and 3β were obtained, from which K_m and k_{cat} values for each were determined **(Table 4.3.1)**. The k_{cat} data indicated DIPP-1 to be the most active enzyme of this group of phosphatases, irrespective of the substrate.

Similar to the reaction rates seen with Ddp1, the K_{cat} values for 1-InsP$_7$ was noted to be 5-20 fold higher than those for 5-InsP$_7$ and InsP$_8$ **(Table 4.3.1)**. However, the K_m data only differ over a 4-fold range (35 to 148 nM), across every enzyme and every substrate. The results demonstrate that rates of InsP$_7$ dephosphorylation in general equal or exceed those of InsP$_8$ metabolism **(Table 4.3.1)**.

Substrates / enzyme	**1-InsP$_7$**		**5-InsP$_7$**		**InsP$_8$**	
	K_m (nM)	**10^2 x k_{cat} (s^{-1})**	**K_m(nM)**	**10^2 x k_{cat} (s^{-1})**	**K_m (nM)**	**10^2 x k_{cat} (s^{-1})**
Ddp1	105	2.4 ± 0.05	93	0.4 ± 0.1	148	0.5 ± 0.1
DIPP-1	42	110 ± 30	52	13 ± 3	85	10 ± 2
DIPP-2α	60	5 ± 2	35	0.7 ± 0.2	55	0.24 ± 0.08
DIPP-2β	70	1.7 ± 0.5	40	0.3 ± 0.09	42	0.16 ± 0.02
DIPP-3α	104	23 ± 2	146	4 ± 2	126	2.2 ± 0.4
DIPP-3β	73	8 ± 2	63	0.88 ± 0.07	78	0.37 ± 0.06

Table 4.3.1 Ddp1/DIPP kinetic data. Kinetic data were obtained as described in *Section* 2.2.23 and 2.2.30. Average (N = 3-5) substrate affinities were first compiled as –logK_m (SEMs were < 3% of the mean) and then transformed to K_m for the Table. k_{cat} are presented as mean ± SEM (N=3-5).

4.4 Understanding positional specificity of DIPPs towards $InsP_8$

A full understanding of physiological fluxes through the different pathways of IDPs turnover would be advanced if we knew the positional specificity of DIPPs towards the 1- and/or 5-diphosphate groups of $InsP_8$ **(Fig. 1.2.1** in chapter 1**)**. This question has not been addressed in previous experiments with recombinant DIPPs, mostly due to insufficient accumulation of $InsP_7$ during dephosphorylation of $InsP_8$ **(**e.g. **Fig. 4.4.1)**. Moreover, it is difficult to separate 1-$InsP_7$ from 5-$InsP_7$ by strong anion-exchange HPLC. In the current study, a consistent 1 min peak-to-peak separation of 1-$InsP_7$ from 5-$InsP_7$ was recorded **[Fig. 4.4.2(a)].** The columns used in these experiments yielded a partial separation, particularly when smaller fractions were collected from a shallower gradient **[Fig. 4.4.2(a)]**.

During the dephosphorylation of $InsP_8$ by Ddp1, DIPP-1, DIPP-2α and DIPP-3α, the accumulation of new $InsP_7$ product was 45-70% above the level of the (predominantly) 1-$InsP_7$ that was present in the zero time assays **(Fig. 4.4.2)**. During this metabolism, the increase in $InsP_7$ peak height and the larger peak spreading indicates some accumulation of both 1- $InsP_7$ and 5-$InsP_7$. However, the k_{cat} data **(Table 4.3.1)** obtained from these experiments conveys that, 1-$InsP_7$ formed as a result of dephosphorylation of $InsP_8$ is 10-fold faster to degrade than the 5-$InsP_7$ that is produced. In other words, the rate of 5-phosphate removal from $InsP_8$ (producing 1-$InsP_7$) is underestimated relative to the rate of 1-phosphate removal from $InsP_8$ (generating 5-$InsP_7$). Further, to confirm this result, equal quantities of 1-$InsP_7$ and 5-$InsP_7$ were incubated with DIPP-1 in the presence of either [^{3}H] 1-$InsP_7$ or [^{3}H] 5-$InsP_7$ to monitor rates of breakdown of each under these conditions. Yet again, 1-$InsP_7$ was found to undergo dephosphorylation at a faster rate than 5-$InsP_7$ **(Fig. 4.4.3)**.

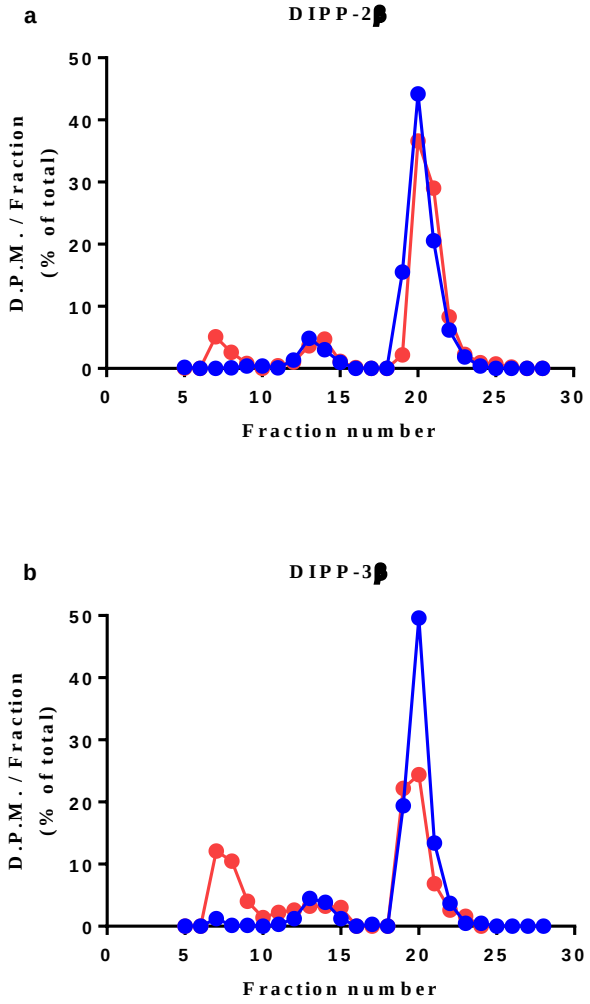

Figure 4.4.1 HPLC analysis of hydrolysis of $InsP_8$ by DIPP-2β and DIPP-3β. HPLC analysis (Protocol 1; *Section* 2.2.23) of the metabolism (red filled circles) of 16 nM $InsP_8$ at 37 ºC in the presence of **(a)** 10 ng DIPP-2β for 6 min, or **(b)** 22.5 ng DIPP-3β for 2 min. Blue filled circles represent zero-time controls.

a

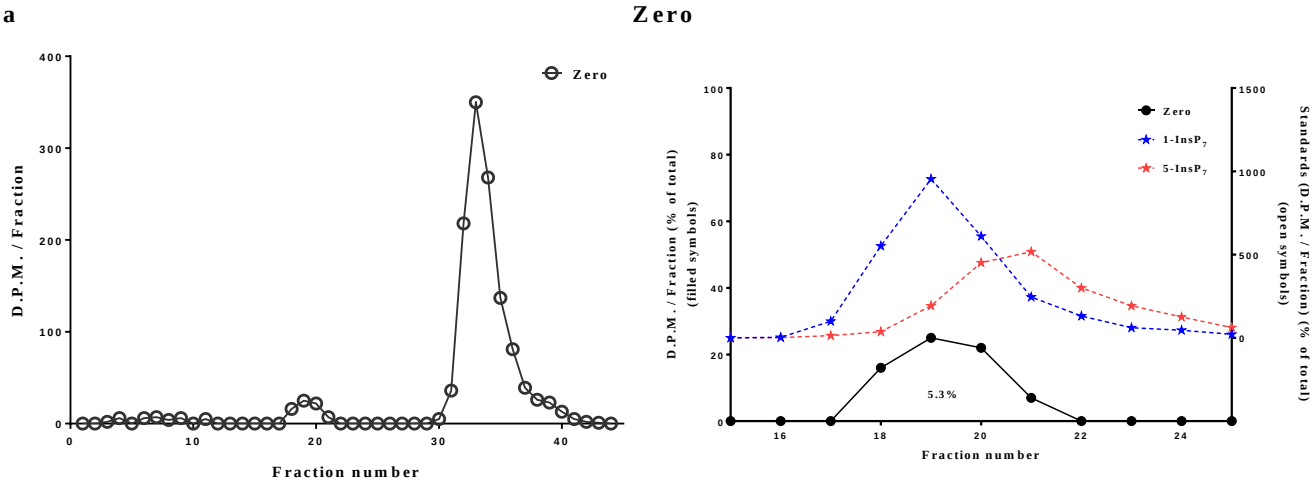
Zero
D.P.M. / Fraction
Fraction number
Zero
1-InsP7
5-InsP7
D.P.M. / Fraction (% of total) (filled symbols)
Standards (D.P.M. / Fraction) (% of total) (open symbols)
5.3%
Fraction number

b

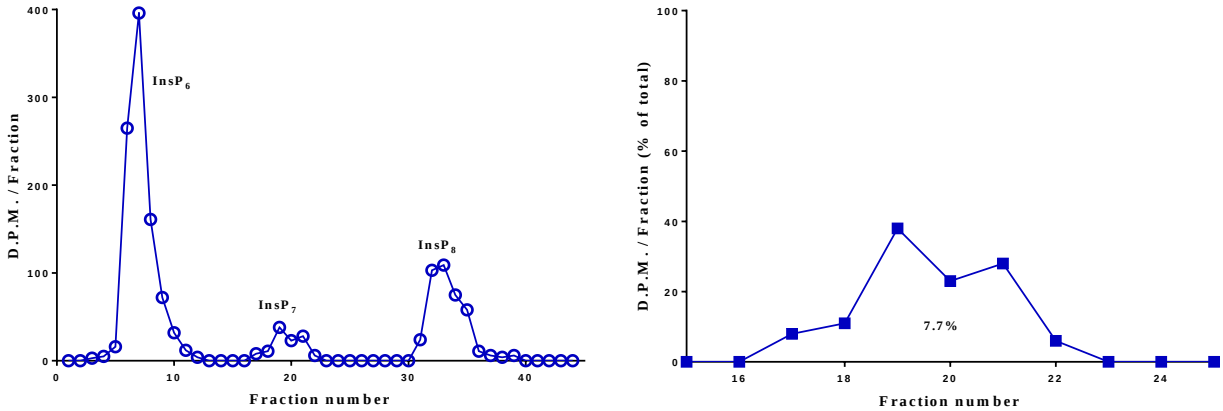
Ddp1
InsP6
InsP7
InsP8
D.P.M. / Fraction
Fraction number
D.P.M. / Fraction (% of total)
7.7%
Fraction number

c

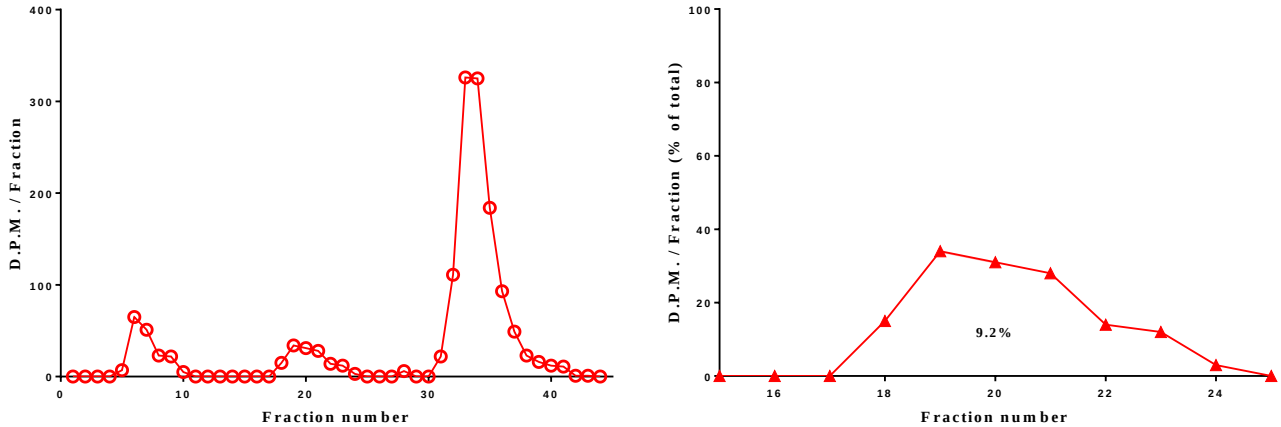
DIPP-1
D.P.M. / Fraction
Fraction number
D.P.M. / Fraction (% of total)
9.2%
Fraction number

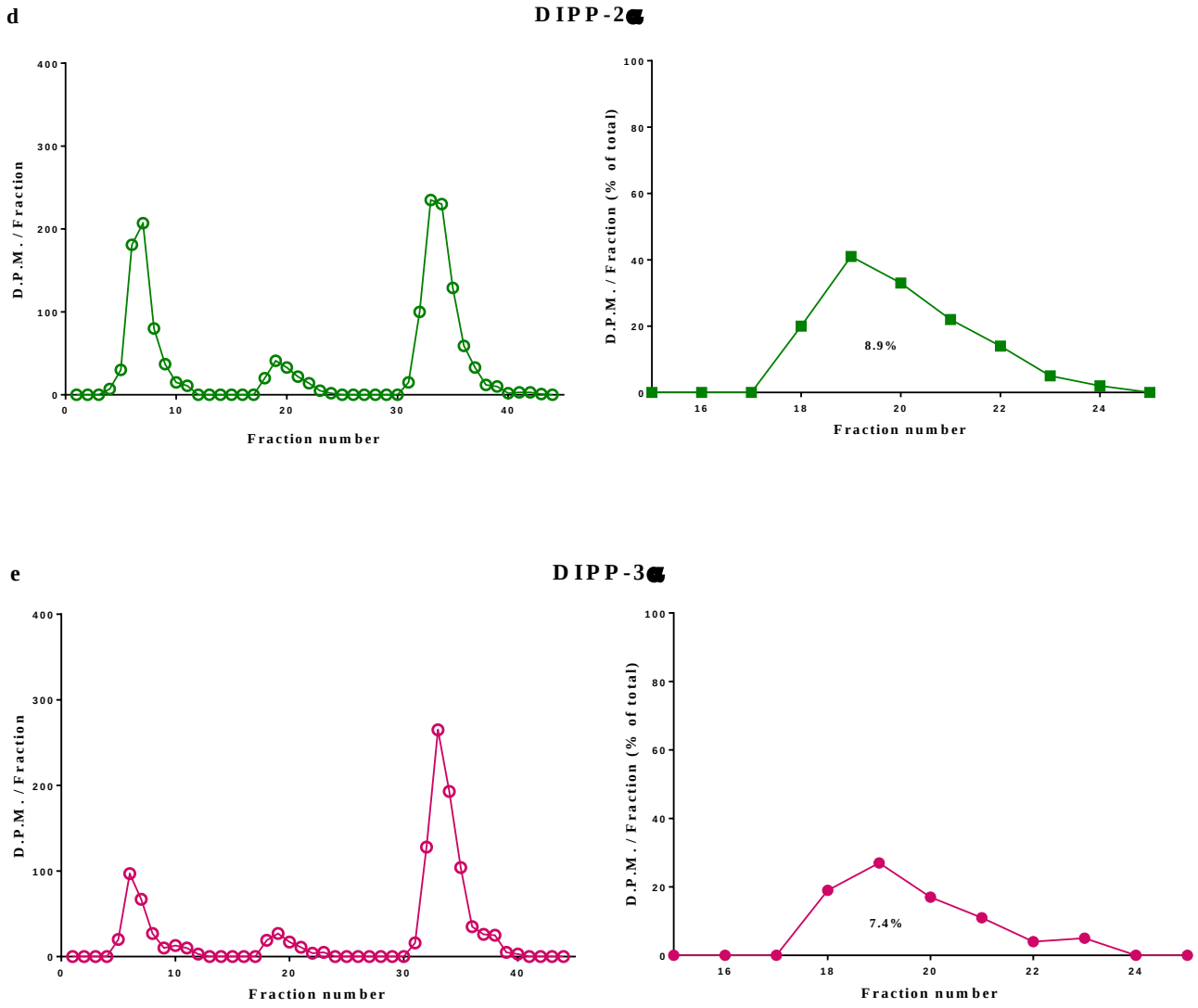

Figure 4.4.2 Analysis of $InsP_8$ dephosphorylation by Ddp1, DIPP-1, DIPP-2α and DIPP-3α.

Representative HPLC runs (Protocol 2; *Section* 2.2.23) are shown for reactions containing either no enzyme [**(a)**; "zero"], or **(b)** 16 ng Ddp1, **(c)** 2 ng DIPP-1, **(d)** 20 ng DIPP-2α and **(e)** 10 ng DIPP 3α, all incubated for 8 min with 16 nM $InsP_8$. The right hand panels in each pair amplify the $InsP_7$ region of the chromatography (all symbols excluding star; $InsP_7$ is quantified as percentage of total); star symbols show elution of 1-$InsP_7$ and 5-$InsP_7$ standards (determined individually).

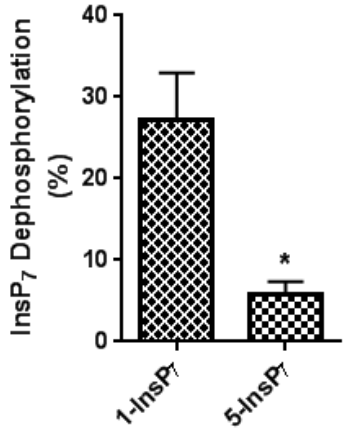

Figure 4.4.3 Dephosphorylation of $InsP_7$ isomers by DIPP-1. Metabolism of a 1:1 mixture of 1-$InsP_7$ and 5-$InsP_7$ by DIPP-1. Both the $InsP_7$ isomers, 10 nM each, were together incubated for 10 min with 0.3 ng DIPP-1 along with about 1000 D.P.M of either 1-[^{3}H]$InsP_7$ [left-hand bar; 27 ± 6 % metabolism, n = 3 (mean ± SEM)] or 5-[^{3}H]$InsP_7$ [right-hand bar; 5.7 ± 0.9 % metabolism, n = 3 (mean ± SEM)]. HPLC analysis was employed to determine the metabolism of each $InsP_7$. *p = 0.02 (t-test; N=3).

4.5 Discussion

In this study, the dephosphorylation of [^{3}H]-radiolabeled substrates [^{3}H] 1-InsP$_7$, [^{3}H] 5-InsP$_7$ or [^{3}H]-InsP$_8$ have been kinetically characterised. HPLC analysis indicated the purity of IDPs prepared to be less than 100% (*Section* 2.2.22) and a slight decomposition was apparent. Such decomposition of pyrophosphate groups appears inevitable during preparation and storage of high energy molecules such as IDPs, however, this does not significantly affect the DIPP activity in the assays performed (Wu *et al.*, 2013).

The first assay was designed to check the activity of Ddp1 on the IDP substrates. In agreement with the previous report (Safrany, Ingram, *et al.*, 1999), Ddp1 was found to hydrolyse 5-InsP$_7$ to a single product, InsP$_6$ **[Fig. 4.2.1(b)]**. Furthermore, Ddp1 was also shown to dephosphorylate 1-InsP$_7$ **[Fig. 4.2.1(a)]** and InsP$_8$ **[Fig. 4.2.1(c)]** to InsP$_6$. There was relatively little build-up of InsP$_7$ in the case of InsP$_8$ breakdown **[Fig. 4.2.1(c)]**. No previous studies have described Michaelis-Menten kinetic parameters for Ddp1 activity towards either 1-InsP$_7$ or InsP$_8$. There is one earlier study that incubated Ddp1 with 250 µM of either 1-InsP$_7$ or 5-InsP$_7$; in an electrophoresis analysis, and found only 1-InsP$_7$ to be dephosphorylated to yield a product (Lonetti *et al.*, 2011). The inability to detect 5-InsP$_7$ metabolism in their study may reflect lack of assay sensitivity when the concentration of substrate exceeds the K_m value by 3 orders of magnitude **(Table 4.3.1)**. Also, SDS-PAGE mass analysis is less sensitive than is HPLC analysis of [^{3}H]-labelled substrates. So although it is known that Ddp1 favours 1-InsP$_7$ over 5-InsP$_7$ (Lonetti *et al.*, 2011), the new kinetic data from the current study indicate that the relative rates of Ddp1-mediated dephosphorylation of the two InsP$_7$ isoforms **(Table 4.3.1)** are much closer than previously thought.

The next aim was to obtain substrate saturation plot for all the five human DIPPs. In accordance with previously concluded results (Leslie *et al.*, 2002; Safrany *et al.*, 1998), the k_{cat} data indicated DIPP-1 to be the most active enzyme amongst the five DIPPs, irrespective of the substrate **(Table 4.3.1)**. Thus, for example, the relative levels of cellular expression of DIPP-1, versus the 20- to 60-fold less active DIPP-2 isoforms, could dictate the rapidity of IDP turnover on a cell-to-cell basis. This is similar to how differential expression of cyclic adenosine monophosphate-phosphodiesterases isoforms regulate cell-to-cell differences in the sensitivity of agonist-mediated cyclic adenosine monophosphate signalling (Houslay, 1998).

The kinetic data from this study demonstrates the rates of $InsP_7$ dephosphorylation in general to be equal or exceed those of $InsP_8$ metabolism **(Table 4.3.1)**. In other words, the $InsP_7$ was found to rapidly convert to $InsP_6$. This explains why so little $InsP_7$ accumulates when $InsP_8$ was incubated with DIPPs **(Fig. 4.4.1)**. Further, the kinetic data from this study leads to some significant physiological conclusions. First, since cellular concentrations of 5-$InsP_7$ are about 1-2 µM (Ingram *et al.*, 2003; Leslie *et al.*, 2002), these can now be considered sufficient **(**refer **Table 4.3.1)** to be at a saturating concentration for all DIPPs. Second, k_{cat} values for 5-$InsP_7$ dephosphorylation are 5 to 9-fold lower than that of 1-$InsP_7$ **(Table 4.3.1)**. However, the affinity of the two isoforms of $InsP_7$ to DIPPs are similar, so it appears likely that the steady-state rates of dephosphorylation of 1-$InsP_7$ and 5-$InsP_7$ will be quite similar *in vivo*, so they will compete for the DIPP active sites in direct proportions to their cellular concentration ratios. Third, the steady-state levels of 1-$InsP_7$ in mammalian cells are 10 to 15-fold lower than that of 5-$InsP_7$ and therefore, it is unlikely that the steady-state rates of hydrolysis of the previous will be significantly greater than that for 5-$InsP_7$ *in vivo*.

Furthermore, the positional specificity analysis **(Fig. 4.4.2)** and metabolism results for 1-$InsP_7$ and 5-$InsP_7$ (1:1 mixture; with DIPP-1; **Fig. 4.4.3**) obtained from this study suggests that, 1-$InsP_7$ formed from $InsP_8$ is 10-fold faster to degrade than the 5-$InsP_7$ that is produced. Thus, it can be concluded that Ddp1 **(Table 4.3.1)**, and at least some of the DIPPs **(Fig. 4.4.2)**, preferentially, although not exclusively, hydrolyses the 5-phosphate from $InsP_8$. Positional specificity in case of DIPP-2β/3β was less clear. However, based on the similarity observed in terms of both sequence conservation and enzyme kinetics, it appears likely that even they will show positional specificity for the 5-phosphate of $InsP_8$.

Thus, the pathway that $InsP_8$ chose to degrade (via 1-$InsP_7$) is metabolically distinct from the main pathway for $InsP_8$ synthesis (via 5-$InsP_7$).

4.6 Conclusion

This study, by presenting the first kinetic characterization of Ddp1/DIPP-mediated hydrolysis of 1-$InsP_7$, 5-$InsP_7$ and $InsP_8$ has increased the insight into the turnover of IDPs. Each DIPP was found to display similar K_m values for every substrate tested (range: 35-148 nM). The rank order of K_{cat} values (1-$InsP_7$ > 5-$InsP_7$ = $InsP_8$) was identical for each enzyme, although DIPP-1 activity was observed to be 10- to 60-fold more than DIPP-2α/β and DIPP-3α/β. Through this study it is also clear that $InsP_8$ prefers to dephosphorylate through 1-$InsP_7$. In contrary, metabolically and functionally significant steady-state route of $InsP_8$ synthesis was observed to be via 5-$InsP_7$.

5. RESULTS - EFFECTS OF ASPIRIN ANALOGUES ON OESOPHAGEAL CANCER

5.1 Introduction to aspirin analogues

There is abundant evidence indicating that NSAIDs, including aspirin are anticarcinogenic and can prevent CRC in humans (See chapter 1). Recent studies have also shown aspirin's utility in treating oesophageal cancer (Ahmadi *et al.*, 2010; Corley *et al.*, 2003). However, universal use of aspirin as an anticancer drug is restrained because of its potential side effects (Laine, 2002). Thus there is an overwhelming rationale to identify aspirin-related compounds that retain the specific toxicity to cancer but are safer and more effective than aspirin itself.

In this regard several derivatives of salicylate/aspirin molecule have been tested for their anticancer property. For example, mesalazine (5-aminosalicylic acid), NCX-4040 (an NO releasing aspirin, 2-(acetyloxy)benzoic acid 4-[(nitrooxy)methyl] phenyl ester), NCX-4016 (an NO derivative of aspirin, 2-(acetyloxy)benzoic acid 3-[(nitrooxy)methyl] phenyl ester), MDC-43 (a para-positional isomer of phosphoaspirin, 4-[(diethoxyphosphoryloxy)methyl] phenyl 2-acetoxybenzoate) were all found to inhibit cell growth in several cancer types (Claudius *et al.*, 2014).

A panel of variants of salicylate were developed recently at the University of Wolverhampton [Dr Iain Nicholl and Dr Chris Perry] with an intention to identify molecules that show the anticancer effects of aspirin against CRC, but with increased anti-proliferative activity. The aspirin analogues developed include diaspirins, benzoylsalicylates and carbonates. Structures and purity of the compounds were verified using standard procedures such as nuclear magnetic resonance, IR, UV spectra and thin-layer chromatography analysis.

Previous investigations on these novel analogues revealed that diaspirins, in particular PN517 (fumaryldiaspirin, F-DiA, **Fig. 5.1.1**), to be the most potent agent exerting anti-

proliferative effect against SW480 colon cancer cells (Claudius *et al.*, 2014; Deb *et al.*, 2011). The study also revealed that analogues exerted their anticancer effects by causing repression of NFκB-driven transcription. Promising results, both *in vitro* and in *in vivo* mouse model with CRC, suggests potential role of F-DiA as an efficient chemotherapeutic agent (Claudius *et al.*, 2014).

Having witnessed the efficiency of aspirin analogues on CRC, we wanted to investigate if these analogues have any effect on oesophageal cancer cell lines. In this regard, the anticancer effects of a number of in-house synthesized novel aspirin analogues on three established oesophageal cancer cell lines was examined: Flo-1 (oesophageal adenocarcinoma), oe33 (oesophageal adenocarcinoma) and oe21 (squamous cell carcinoma). Representative morphology of the three oesophageal cancer cell lines under phase contrast microscope is shown in the **Fig. 2.2.5**. Aspirin analogues used in this study include: diaspirins (PN508, PN510, PN511, PN512 and PN517), benzoylsalicylates (PN514, PN524, PN525, PN528 and PN529) and carbonates (PN526 and PN527). Structure and molecular weight of the aspirin analogues used in this study are shown in the **Fig. 5.1.1**.

To start with, the panel of aspirin analogues mentioned above were all screened on the three oesophageal cancer cell lines, looking for the most potent agents. Cell viability assay (MTT) was employed for this purpose. COX inhibitor screening assay was performed simultaneously to determine whether the analogues inhibited any of the COX enzymes. Based on the cell killing ability data from initial screening, potent aspirin analogues were chosen for further pharmacodynamic analysis. More MTT assays were performed to construct dose-response curves and calculate IC_{50}s for aspirin and its analogues on the three oesophageal cancer cell lines. In order to validate that the killing by these novel analogues is through programmed cell death and not necrosis, both qualitative

(fluorescence imaging of apoptosis cells) and quantitative (flow-cytometric analysis of apoptosis) assays were performed. Further, ability of the drug-treated-cell-population to recover, following withdrawal of the drug was also checked to find out whether the analogues are cytotoxic or cytostatic in nature.

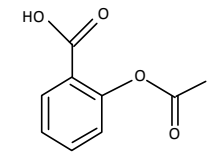

Aspirin (acetylsalicyclic acid)

MW=180

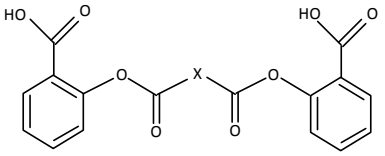

X = -CH_2CH_2-

Diaspirin

Bis(2-carboxyphenyl) succinate (PN508)

MW=358

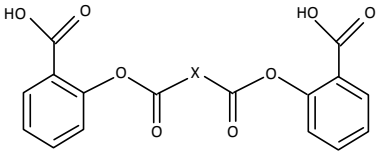

X = -$CH_2(CH_2)_2CH_2$-

Adipoyldiaspirin (PN510)

MW=386

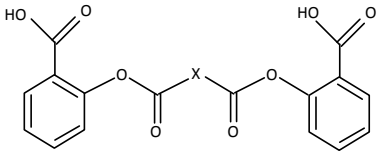

X = -$CH_2(CH_2)_6CH_2$-

Sebacoyldiaspirin (PN511)

MW=442

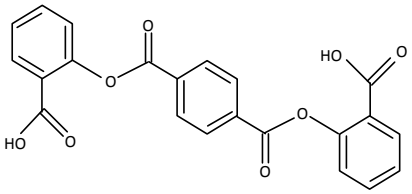

Terephthaloyldiaspirin (PN512)

MW=406

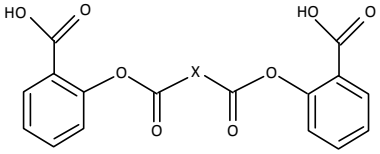

X = -CH=CH- (trans)

Fumaryldiaspirin (PN517)

MW=356

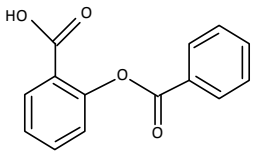

Benzoylaspirin

(Benzoylsalicylate) (PN514)

MW=242

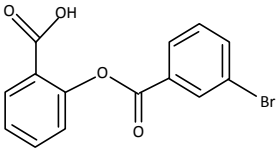

m-bromobenzoylsalicylate (PN524)

MW=321

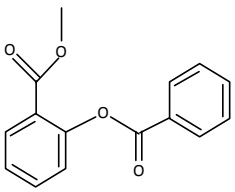

Methyl benzoylsalicylate (PN528)

MW=256

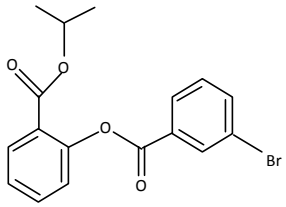

Isopropyl-(m-bromobenzoylsalicylate) (PN529)

MW=363

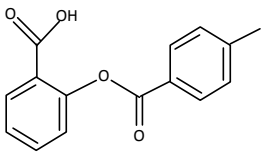

p-methyl benzoylsalicylate (PN525)

MW=256

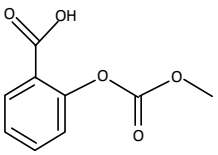

Methyl(2-carboxyphenyl)carbonate (PN526)

MW=196

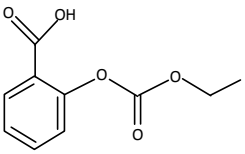

Ethyl(2-carboxyphenyl)carbonate (PN527)

MW=210

Figure 5.1.1 Structure and molecular weight of aspirin and aspirin analogues. Adapted from (Claudius *et al*., 2014).

5.2 Screening aspirin analogues for their potency on oesophageal cancer cell lines

Effect of aspirin compounds on the three oesophageal cancer cell lines were examined using cytotoxicity (MTT) assay. Oesophageal cancer cell lines: oe21, oe33 and flo-1 were exposed to aspirin, salicylic acid (SA) and aspirin analogues at a concentration of 1 mM for 72 h. The screened aspirin analogues include diaspirins: PN508, PN510, PN511, PN512 and PN517; benzoylsalicylates: PN514, PN524, PN525, PN528 and PN529; carbonates: PN526 and PN527. Aspirin and SA were included in the experiment as controls given that they are reported to be protective against cancer (Pathi *et al.*, 2012). Percentages of cells that are viable after drug treatment were determined. Screening results showed that several aspirin analogues had better killing ability than aspirin in all the three cell lines tested. In case of both oe21 and oe33 cell lines, benzoylsalicylates and in particular PN524, PN528 and PN529 compounds were significantly more potent than aspirin **[Fig. 5.2.1(a) and (b)]**. Although not as effective as benzoylsalicylates, the diaspirins- PN508 and especially PN517 showed robust killing ability. Other compounds such as PN512 and PN514 showed moderate effect on both oe21 and oe33 cell lines. Conversely, flo-1 cell line was resistant to almost all the compounds tested other than PN528 and PN529 **[Fig. 5.2.1(c)]**. SA showed similar toxicity to aspirin in the cancer cell lines tested. Compounds including PN510, PN511, PN525, PN526 and PN527 failed to show robust cancer killing ability in the all the three cell lines and thus were not used for further experiments.

Figure 5.2.1 Screening and assessment of the potency of aspirin analogues on oesophageal cancer cell lines *in vitro.* **(a)** oe21, **(b)** oe33 and **(c)** flo-1 cells were plated at a density of 10^4 cells/ml in 96-well microtitre plates (200 µl/well) in their respective basal medium. Twenty-four hours after seeding, the cells were treated with compound-containing culture medium for a further 72 h. The anti-proliferative effects were measured in an MTT assay (*Section* 2.2.26). All compounds were prepared as stock solutions in DMSO (0.5 M stocks) and further diluted to 1 mM final concentration in culture medium (*Section* 2.2.25). The MTT results were plotted as percentage of cell viability against drug concentration using GraphPad Prism 6. Data plotted as mean ± SEM (N=3). The effect of aspirin and SA is included for comparison.

a

oe21 (squamous cell carcinoma)

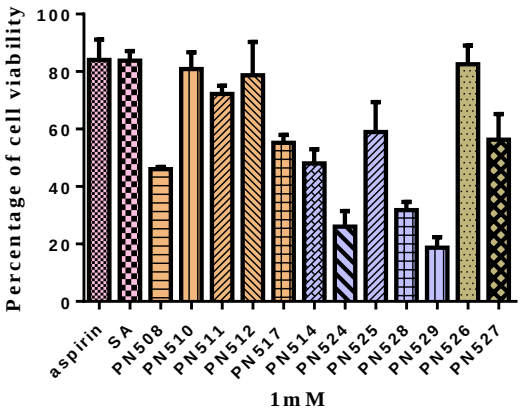

b

oe33 (oesophageal adenocarcinoma)

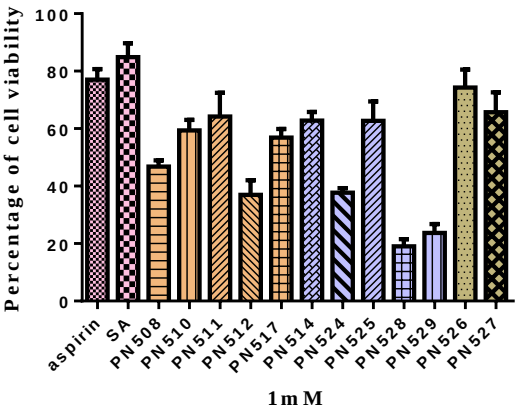

c

flo-1 (oesophageal adenocarcinoma)

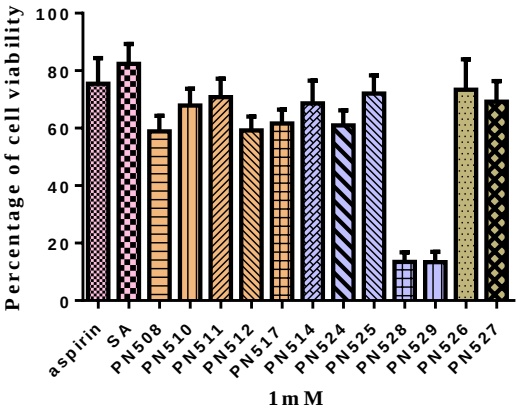

Carbonates Benzoylsalicylates Diaspirins

5.3 IC_{50} analysis of the potent aspirin analogues

Aspirin analogues that were found potent against oesophageal cancer cells compared to aspirin in the initial screening experiment were chosen for the IC_{50} analysis. Appropriate drug stock solutions were prepared fresh using DMSO for each experiment (DMSO content in the working solution was kept well within the tolerated dose by the cells i.e., ~10%). All the three cell lines were incubated for 72 h with the compounds (30 µM – 3 mM) individually and assayed using MTT. A dose response curve was plotted using the data obtained from MTT analysis and IC_{50} for each of the compound was calculated (*Section* 2.2.30). IC_{50} values for compounds tested on oe21, oe33 and flo-1 cell lines are listed in the **Table 5.3.1** and represented in **Fig. 5.3.1**.

Aspirin analogues were found to supress the proliferation of oesophageal cancer cell lines in a dose-dependent manner. From the results, it was clear that PN529 was the most cytotoxic compound with IC_{50} values as low as 100 µM and high as 400 µM in oe21 and oe33 cell lines respectively **(Table 5.3.1)**. This was followed by PN528 with IC_{50} values ranging between 0.2 – 1.6 mM. Statistical analysis of the MTT data highlighted PN517 to be an interesting and important analogue with a distinct Hill slope profile in all the three cell lines **(Table 5.3.1; Fig. 5.3.1)**. IC_{50} values for PN517 ranged between 0.4 – 1.1 mM. The other analogue with significant killing curve was PN524 with IC_{50} values: 0.24, 0.7 and 0.9 mM in oe21, oe33 and flo-1 cells respectively **(Table 5.3.1)**. PN512 and PN514 showed only moderate killing ability in these cell lines. In general, the low IC_{50} trend for compounds exposed to oe21 cells suggest that it is the most sensitive cell line out of the three tested. Although flo-1 cells were sensitive to some of the benzoylsalicylate compounds, resistance to most of the analogues was apparent with high IC_{50} values **(Table 5.3.1)**.

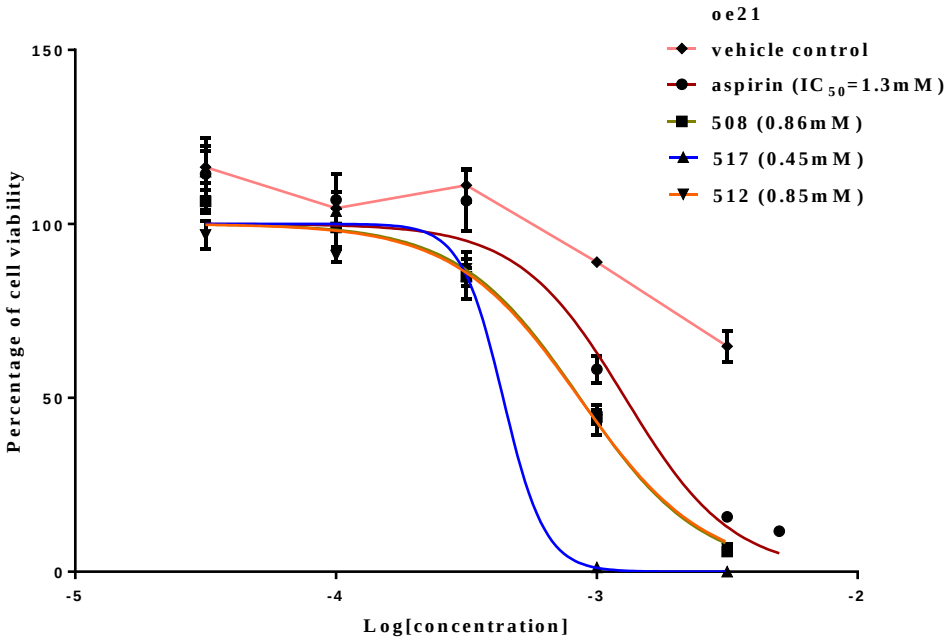

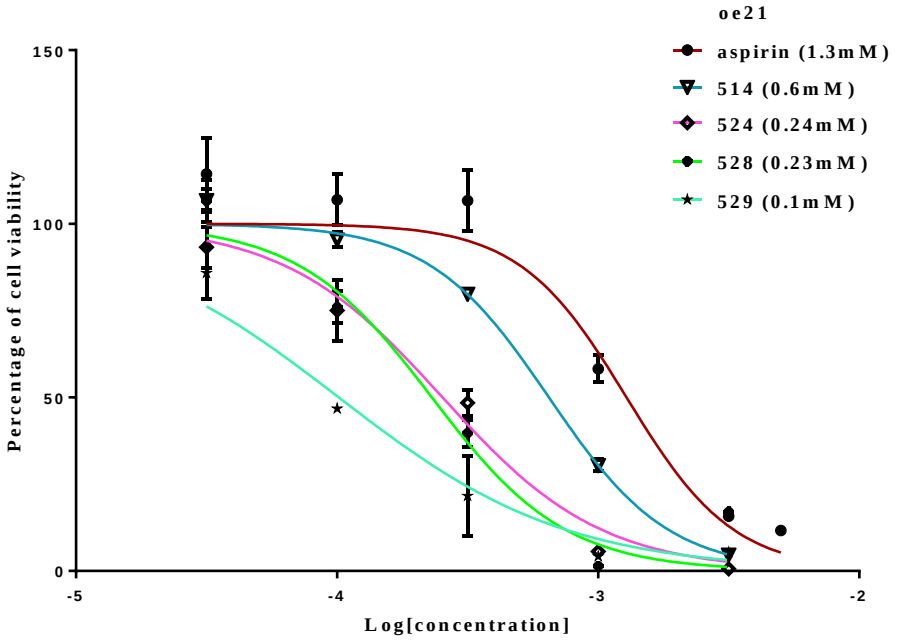

Figure 5.3.1 Dose response curves for oe21 cell line

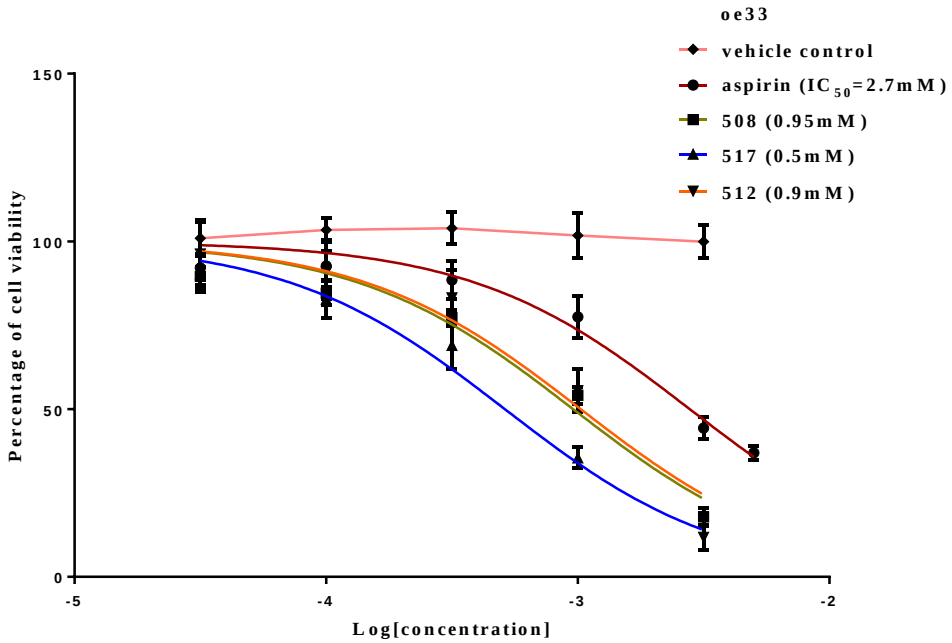

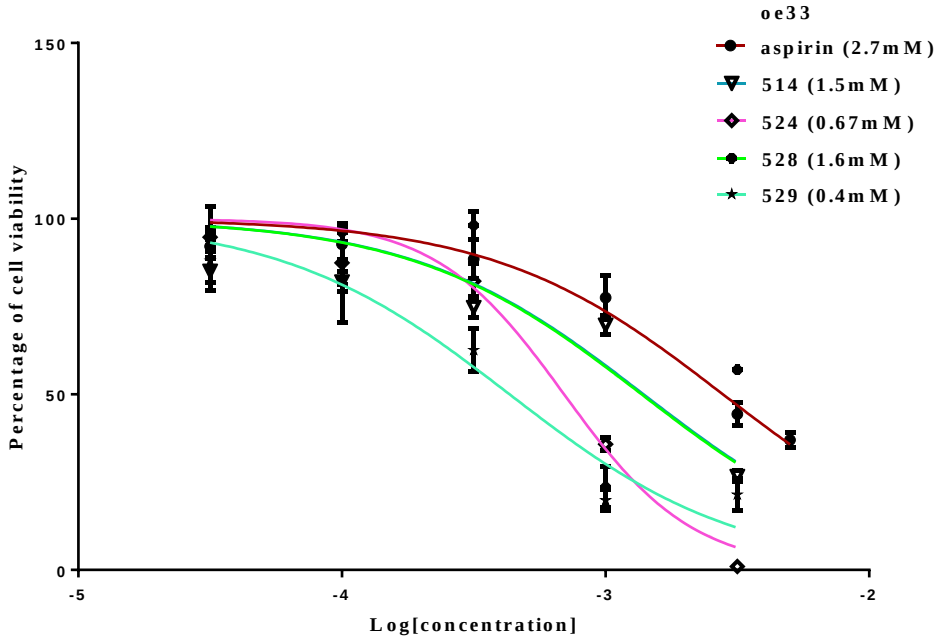

Figure 5.3.1 Dose response curves for oe33 cell line

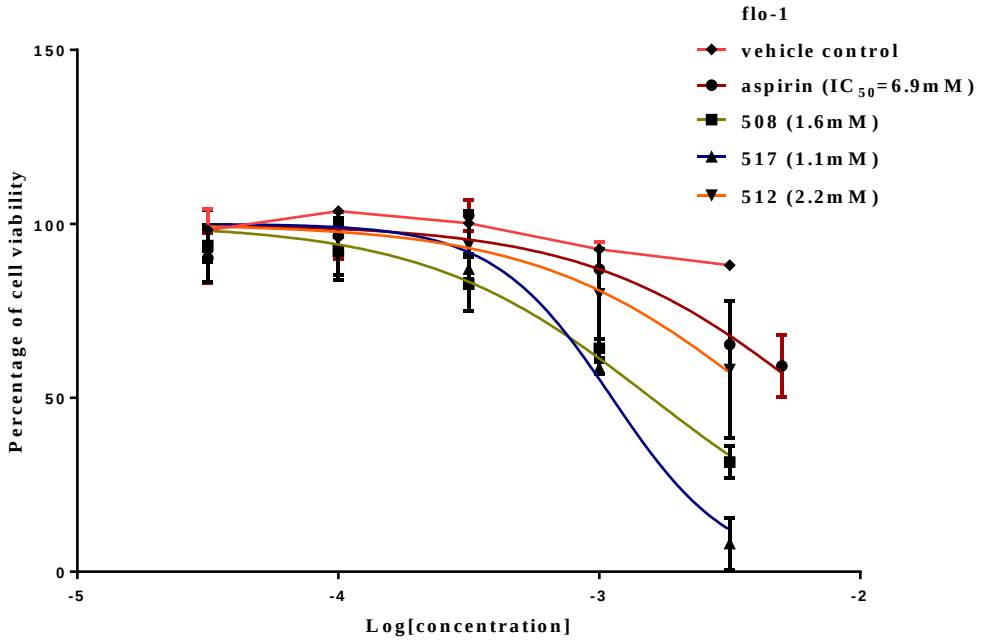

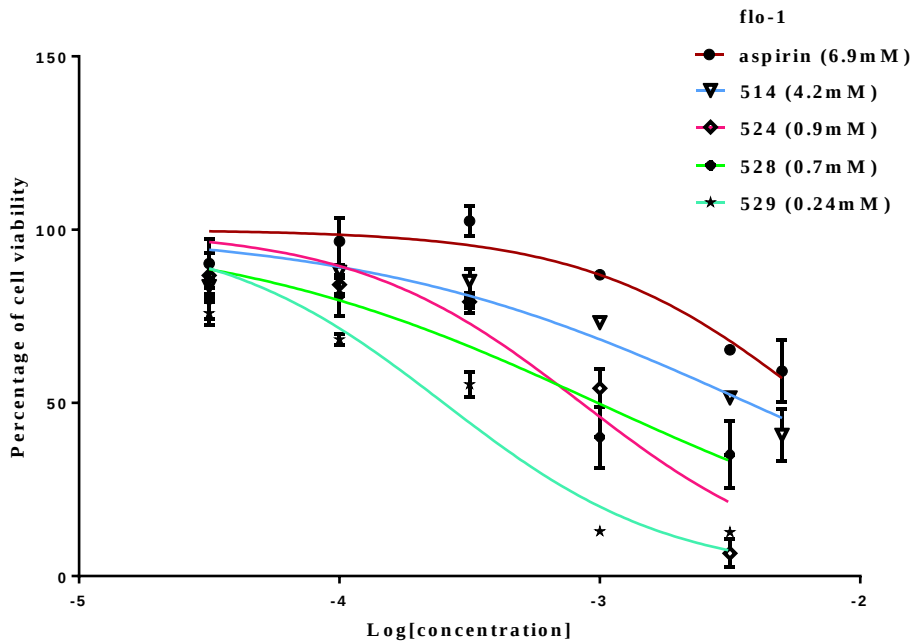

Figure 5.3.1 Dose response curves for flo-1 cell line

Figure 5.3.1 Dose response curves for cell lines oe21, oe33 and flo-1 treated with aspirin and aspirin analogues. Aspirin analogues used herein include PN508, PN512, PN517, PN514, PN524, PN528 and PN529. Oe21 cells at a density of 2.5×10^3 cells/ml and oe33, and flo-1 cells at a density of 10^4 cells/ml was plated in 96-well plates in their respective basal medium. Twenty-four hours after seeding, the cells were treated with compound-containing culture medium for a further 72 h. The anti-proliferative effects were measured in an MTT assay (*Section* 2.2.26). All compounds were prepared as stock solutions in DMSO and further diluted to a final concentration of 30 µM, 100 µM, 300 µM, 1 mM and 3 mM in culture medium (*Section* 2.2.25). Data plotted as mean ± SEM (N=3) (*Section* 2.2.30). The effect of aspirin and DMSO (vehicle control) is included for comparison.

	aspirin analogues	aspirin	PN508	PN512	PN517	PN514	PN524	PN528	PN529
oe21	**pIC50 ±SEM**	2.90± 0.04	3.07± 0.01	3.07± 0.04	3.34± 0.04	3.189± 0.007	3.62± 0.10	3.64± 0.05	3.99± 0.04
	IC_{50} (in mM)	**1.3**	**0.86**	**0.85**	**0.45**	**0.65**	**0.24**	**0.23**	**0.1**
	Hill slope ±SEM	2.0 ±0.3	1.9 ±0.1	1.8 ±0.1	5.6 ±0.7	1.9 ±0.1	1.5 ±0.3	1.7 ±0.1	1.7 ±0.6
oe33	**pIC50 ±SEM**	2.57 ±0.07	3.02 ±0.06	3.03 ±0.09	3.3 ±0.1	2.83 ±0.02	3.17 ±0.06	2.80 ±0.07	3.4 ±0.1
	IC_{50} (in mM)	**2.7**	**0.95**	**0.9**	**0.5**	**1.5**	**0.67**	**1.6**	**0.4**
	Hill slope ±SEM	1.0 ±0.3	0.97 ±0.04	1.5 ±0.6	1.3 ±0.3	0.7 ±0.2	1.8 ±0.4	0.79 ±0.05	1.0 ±0.2
flo-1	**pIC50 ±SEM**	2.16 ±0.02	2.80 ±0.03	2.65 ±0.09	2.95 ±0.05	2.4 ±0.1	3.05 ±0.07	3.15 ±0.05	3.62 ±0.03
	IC_{50} (in mM)	**6.9**	**1.6**	**2.2**	**1.1**	**4.2**	**0.9**	**0.71**	**0.24**
	Hill slope ±SEM	1.0 ±0.1	1.1 ±0.4	0.9 ±0.3	2.0 ±0.5	0.56 ±0.06	1.26 ±0.05	0.87 ±0.05	0.80 ±0.04

Table 5.3.1 IC_{50} values for aspirin and aspirin analogues on the three oesophageal cancer cell lines. IC_{50} values were obtained by non-linear regression (GraphPad Prism 6) with 4 variables. pIC_{50} and Hill slope are shown and are expressed as the mean ± SEM of the data from three independent experiments (*Section* 2.2.30).

5.4 Do aspirin analogues mediate cell death through apoptosis?

Differential cell killing ability of aspirin analogues was evident from the MTT data. The next step was to examine whether treatment with aspirin analogues resulted in cell death through apoptosis or necrosis. For this purpose, two assays: fluorescence activated cell sorting (FACS) or flow cytometric analysis of apoptosis (quantitative assay) and fluorescence imaging of apoptotic cells (qualitative assay) were performed.

Irinotecan hydrochloride (irinotecan or IRI or CPT-11), a potent anticancer drug, has been reported to exhibit its cytotoxicity in colon cancer cells *in vitro* by inducing apoptosis (Deb *et al.*, 2011; Rudolf *et al.*, 2012). On the other hand, hydrogen peroxide (H_2O_2) at a higher concentration has been reported to induce necrosis in human breast cancer cell lines (McKeague *et al.*, 2003). Hence, irinotecan and H_2O_2 were used as positive controls for apoptosis and necrosis respectively in the following experiments.

5.4.1 Flow cytometric analysis of apoptosis

For FACS analysis, Annexin-V-Fluos apoptosis staining kit which responds to phospholipid scrambling, a unique feature of the apoptotic pathway (Vermes *et al.*, 1995), was used. Use of a counter-stain such as propidium iodide (PI) along with the principal stain in apoptosis experiments enabled easy discrimination of viable cells from non-viable and apoptotic cells from necrotic cells (Vermes *et al.*, 1995). Viable cells do not take up either stain whereas non-viable cells take up only PI stain. Apoptotic cells take up the principle Annexin-V stain but not PI whereas necrotic/late apoptotic cells take up both Annexin-V and PI stain **(Fig. 2.2.7)**. Oesophageal cancer cell lines at 50% confluency (in culture flasks) were treated with aspirin and aspirin analogues at a final concentration of 1 mM for 24 h, 48 h and 72 h (*Section* 2.2.27a). Irinotecan (25 µM), H_2O_2 (2 mM) and a vehicle control for DMSO was included in the experiments for comparison. Representative

flow cytometry plots showing the oe21 cells undergoing apoptosis, late apoptosis and/or necrosis following treatment with irinotecan, H_2O_2 and aspirin analogue PN524 are illustrated in **Fig. 5.4.1a**.

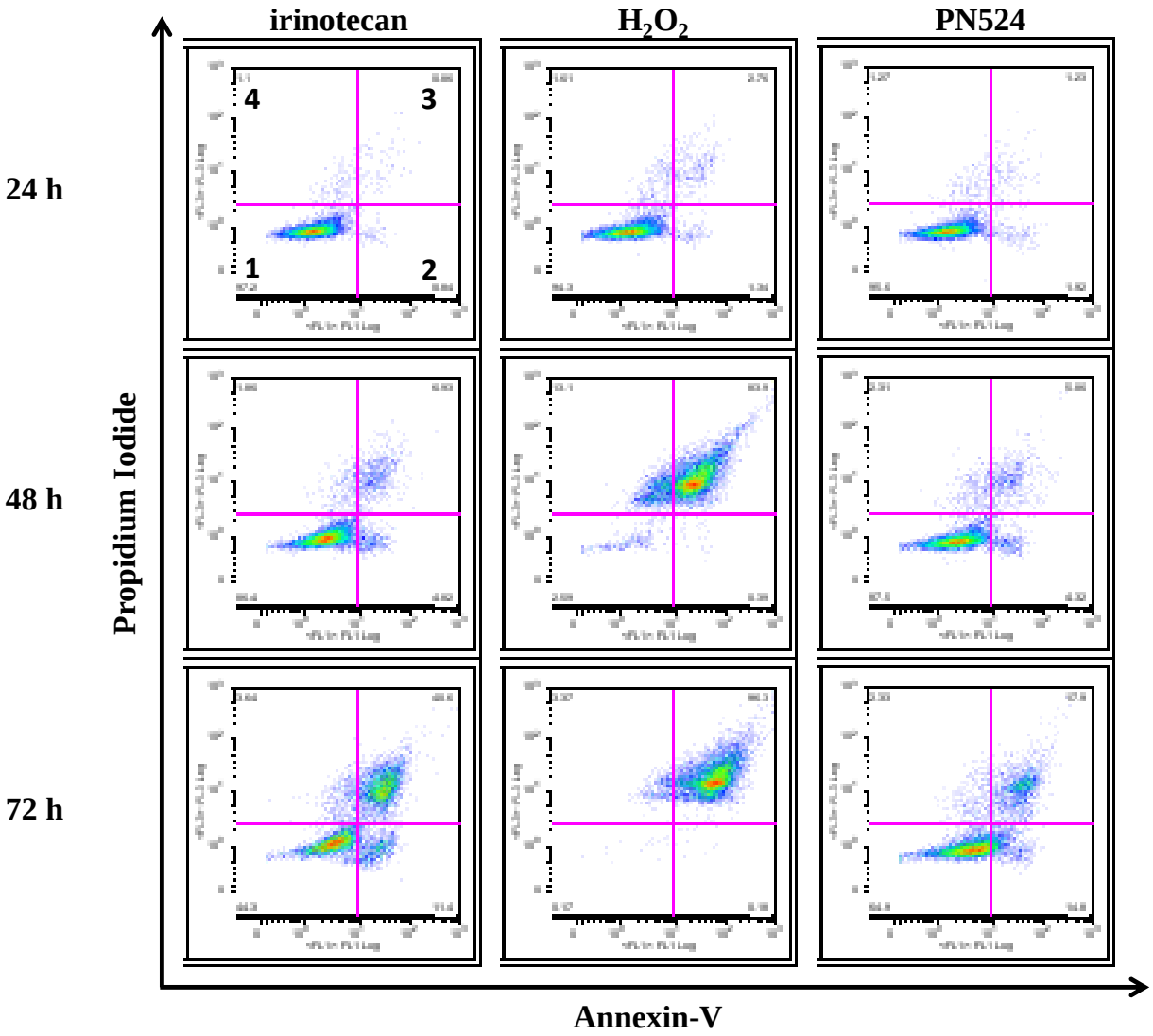

Figure 5.4.1a Flow cytometric analysis of apoptosis and necrosis. Induction of apoptosis/necrosis in oe21 cells following treatment with irinotecan, H_2O_2 and aspirin analogue PN524 for 24, 48 and 72 h were checked by labelling the cells with Annexin-V and PI stains. The above figure represents Annexin-V versus PI contour plots with quadrant gates showing four populations. Oe21 cells that were viable and non-apoptotic showed negative staining for both Annexin-V and PI and were observed to fall in quadrant

1 (see top left figure). Early apoptotic cells which showed positive staining for only Annexin-V were observed in quadrant 2. Late apoptotic cells which showed positive staining for both Annexin-V and PI were observed in quadrant 3. Cells or sometimes debris that shows positive staining for PI only were observed to move towards quadrant 4 (Refer Fig. 2.2.7 in *Section* 2.2.27a). Treatment with irinotecan or PN524 for 48 h showed a small proportion of oe21 cells undergoing apoptosis (positively stained Annexin-V cells in quadrant 2). With the increase in the treatment time (at 72 h), the cells appeared to be in their late apoptotic stage (positively stained cells for both Annexin-V and PI in quadrant 3). Treatment with H_2O_2 caused abrupt cell death apparent between 24 and 48 h. The profile of PN524 was similar to irinotecan, causing death by apoptosis.

All the compounds tested were able to drive apoptosis, which was observable by 24 h. Increased time of treatment increased the number of cells undergoing apoptosis **(Fig. 5.4.1b)**. This was the case with all three cell types, but more evident in oe21 cells **[Fig. 5.4.1b(i)]**. Oe33 cells appeared to induce more apoptosis than oe21 **[Fig. 5.4.1b(ii)]**, however, most of this population was suspected to be auto-fluorescent debris from the cells and not apoptotic cells. Flo-1 cells were resistant to most of the compounds and thus, in general, showed low percentage of apoptotic cells **[Fig. 5.4.1b(iii)]**. As expected, irinotecan treatment greatly induced apoptosis in all three cell types **(Fig. 5.4.1a** and **Fig. 5.4.1b)**. H_2O_2 treatment also presented some apoptosis at 24 h, however, this population decreased with increase in treatment time **(Fig. 5.4.1a)**. In oe21 cells, PN524 treatment exhibited highest percentage of apoptotic cells **(Fig. 5.4.1a)**, followed by PN517 treated cells. In oe33 cells, PN517 treatment induced highest percentage of apoptotic cells, followed by PN524 and PN528. In flo-1 cells, PN529 followed by PN528 showed increased apoptosis compared to other compounds.

(i)

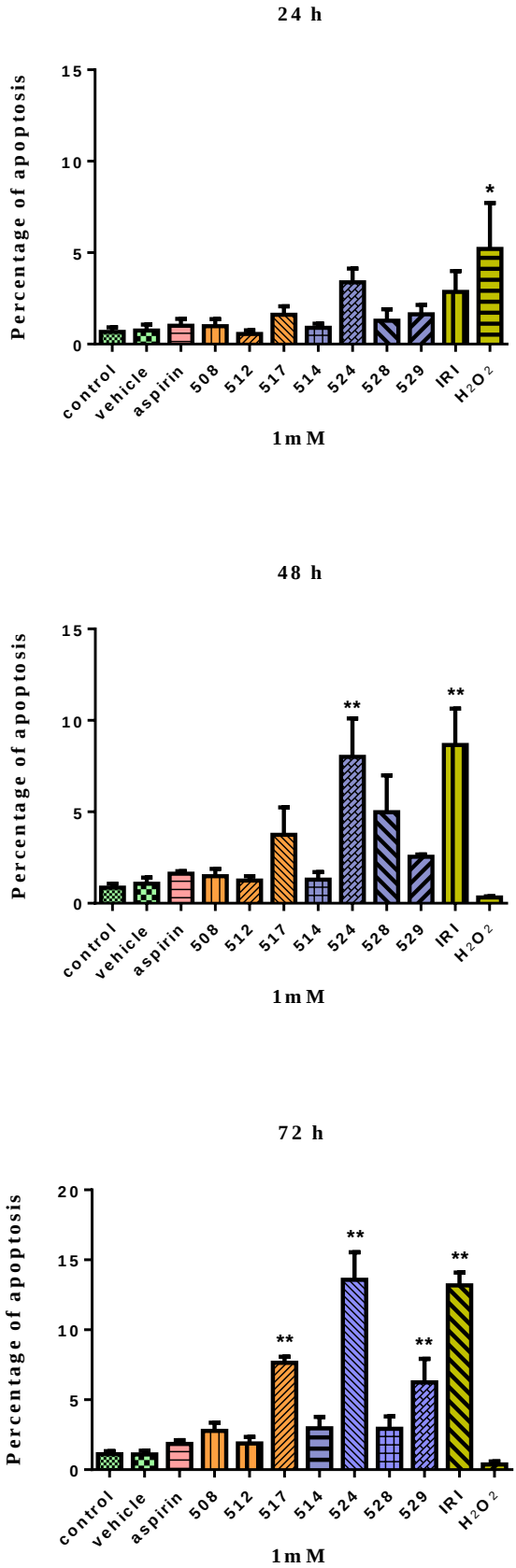

Figure 5.4.1b Flow cytometric analysis of aspirin analogues-induced-apoptosis in oe21

(ii)

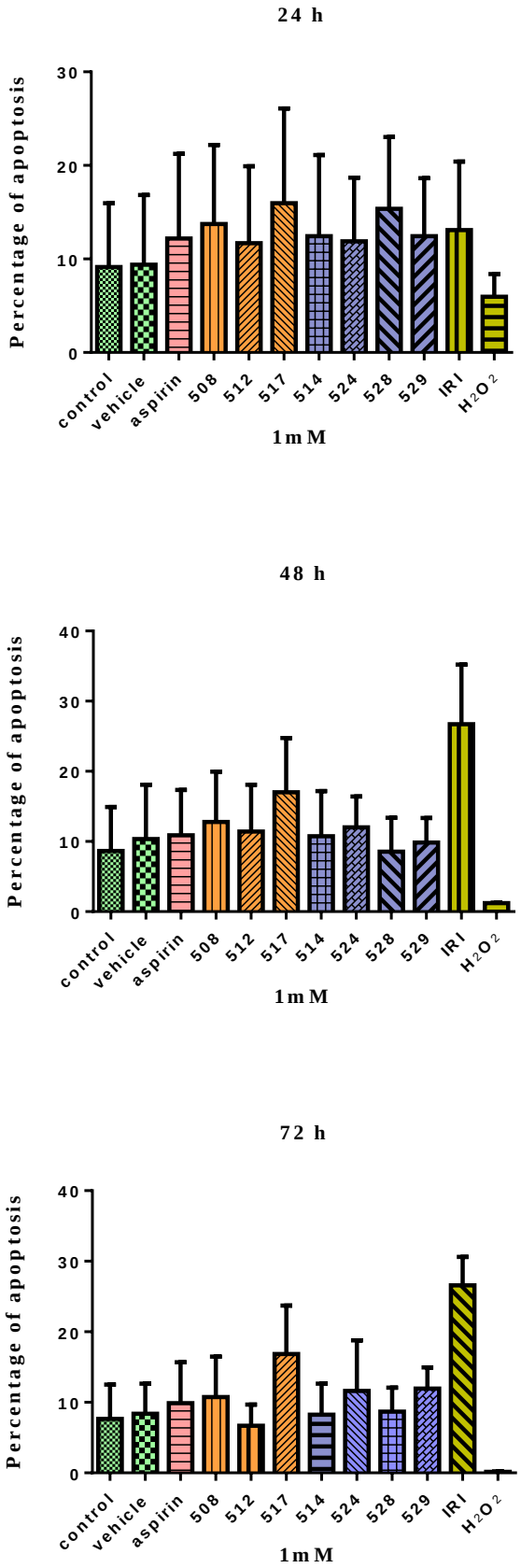

Figure 5.4.1b Flow cytometric analysis of aspirin analogues-induced-apoptosis in oe33

(iii)

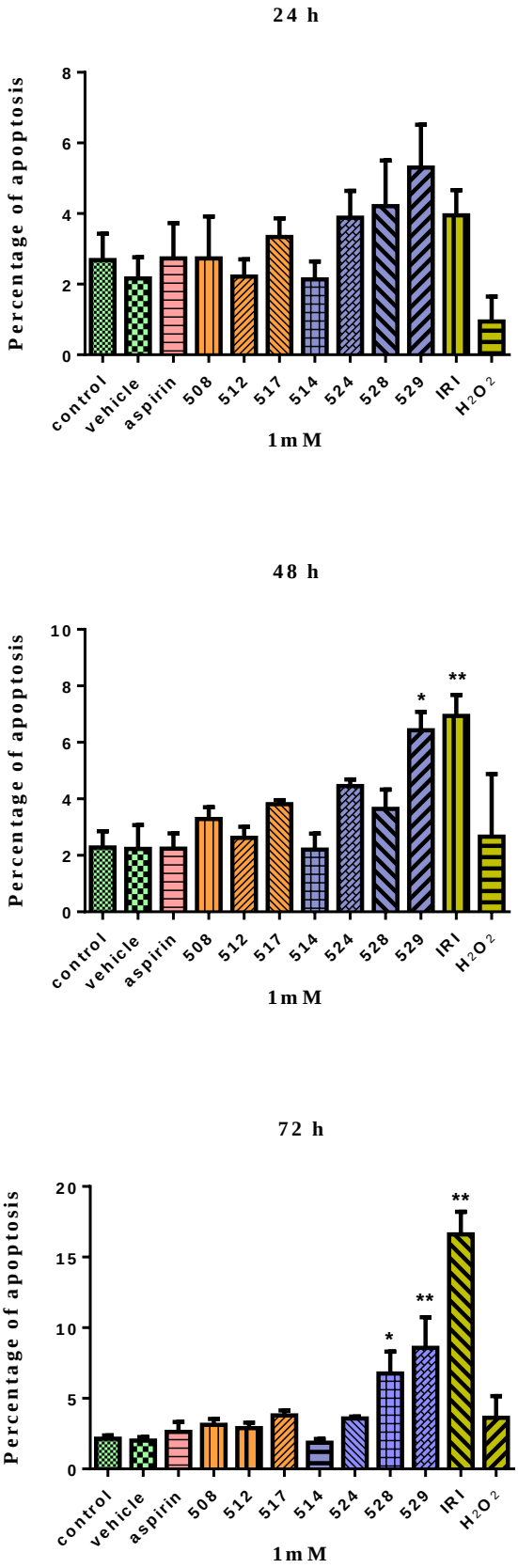

Figure 5.4.1b Flow cytometric analysis of aspirin analogues-induced-apoptosis in flo-1

Figure 5.4.1b Flow cytometric analysis of aspirin analogues-induced-apoptosis in (i) oe21, (ii) oe33 and (iii) flo-1 cell lines. Oesophageal cancer cells were cultured to 50% confluency and treated with compound-containing culture medium for a further 24 h, 48 h and 72 h. After treatment, cells were stained with Annexin-V-Fluos and counter-stained with PI (*Section* 2.2.27a). The population of cells undergoing apoptosis or necrosis were measured by FACS analysis using flow cytometer. All compounds were prepared as stock solutions in DMSO and further diluted to a final concentration of 1mM in culture medium (*Section* 2.2.25). Data plotted as mean ± SEM (N=3). Irinotecan (represented as IRI in the Fig.) and H_2O_2 were used as positive controls for apoptosis and necrosis, respectively. The effect of aspirin and DMSO (vehicle control) is included for comparison. * $p \leq 0.05$ and ** $p \leq 0.01$ (*Section* 2.2.30).

5.4.2 Flow cytometric analysis of necrosis

Although most of the aspirin analogues largely exerted cell killing via apoptosis, some of them appeared to induce more necrosis than apoptosis and some showed mixture of both populations. However, the percentage of apoptosis or necrosis population varied between the three cell lines. Drug-induced necrosis at 24 h in the three cell lines are shown in the **Fig. 5.4.2a** as an example. Necrosis after this time period was not taken into account, as it was difficult to differentiate actual necrosis from secondary necrosis (late apoptosis). As predicted, H_2O_2 efficiently induced necrosis within 24 h in all three cell types and in contrast, irinotecan initiated very little necrosis **(Fig. 5.4.2a)**. All the compounds, except for PN529, appeared to be poor inducers of necrosis in oe21 and flo-1 cell types **(Fig. 5.4.2a)**. Oe33 cells showed increased necrosis with almost all the compounds. This result is again suspected to be due to the noise created by the debris (auto-fluorescent) from the cells **(Fig. 5.4.2a)**.

24 h

oe21

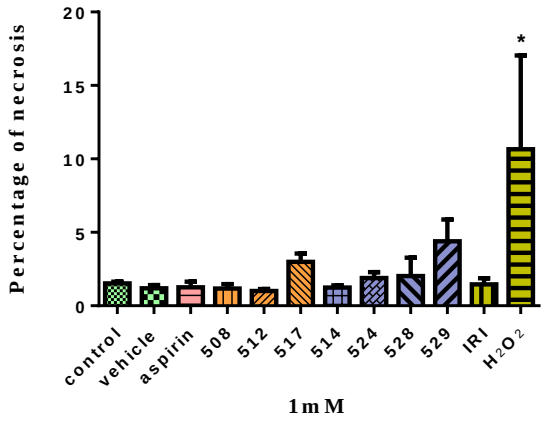

oe33

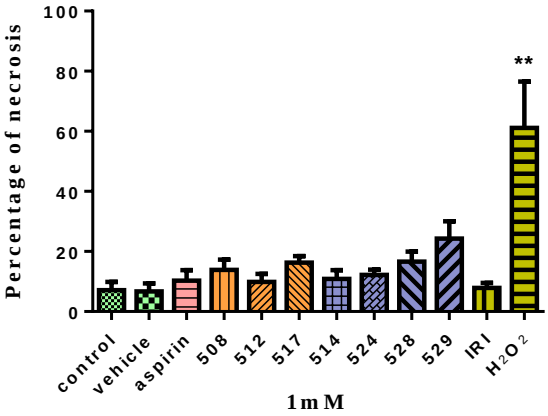

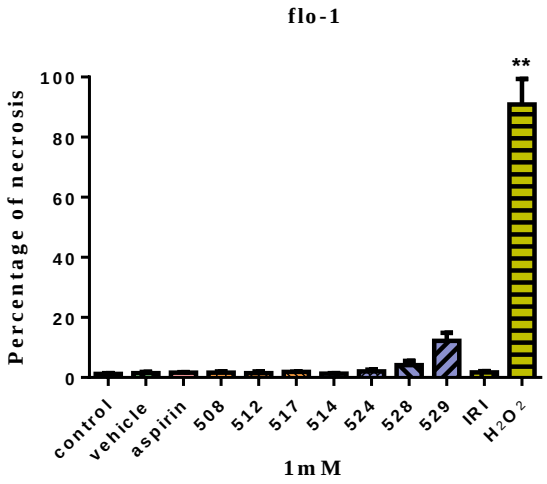

Figure 5.4.2a Flow cytometric analysis of aspirin analogues-induced necrosis in oesophageal cancer cell lines at 24 h. Experimental procedure (treatment and staining), flow cytometric and statistical analysis are the same as with apoptosis analysis **(Fig. 5.4.1b)**. * $p \leq 0.05$ and ** $p \leq 0.01$ (*Section* 2.2.30).

5.4.3 Fluorescence imaging of apoptotic cells

An Apo-TRACE cell staining kit that again responds to phospholipid scrambling was used for fluorescence imaging of apoptotic cells. The Apo-TRACE compound stains the cytoplasm of the apoptotic cells (Damianovich *et al.*, 2006). PI counter-stain, in contrary, stains only non-viable cells. Late stage of apoptosis and death are characterised by cells taking up both Apo-TRACE stain and PI counter-stain. In this experiment, oesophageal cancer cells grown to 50% confluency on glass-coverslips were treated with aspirin and aspirin analogues at a concentration of 1 mM for 24 h (data shown only for oe21 cell line) and 48 h (*Section* 2.2.27b). Irinotecan (25 µM), H_2O_2 (2 mM) and vehicle control were included in the experiment for comparison.

In all the cell lines, irinotecan treatment induced largely apoptosis (blue stained cytoplasm only) and H_2O_2 treatment induced largely necrosis (blue stained cytoplasm with red stained nuclei) **(Fig. 5.4.3a)**. Images of oe21 cells, at both 24 h and 48 h, suggest that most of the analogues exert their toxicity through induction of apoptosis. However, necrosis was observed with PN528 and significantly more with PN529 treatment **[Fig. 5.4.3a(i)** and **Fig. 5.4.3a(ii)]**. Oe33 and flo-1 cells treated with the compounds for 24 h showed mostly healthy cells with very few apoptotic cells (visual observation). However, large numbers of non-viable dead cells were seen floating within 24 h of treatment with PN529 suggesting it causes, at least in part, necrosis (visual observation). Images of oe33 **[Fig. 5.4.3a(iii)]** and flo-1 **[Fig. 5.4.3a(iv)]** cells at 48 h suggest that most of the analogues largely exert their toxicity via induction of apoptosis, although necrosis was quite evident with PN529 treatment. PN528 appeared to induce apoptosis in both oe33 and flo-1 cells **[Fig. 5.4.3a(iii)** and **Fig. 5.4.3a(iv)]**.

In general, PN517 treated cells were found to contain a mixture of apoptotic and necrotic cells (more apoptotic than necrotic) at 48 h **[Fig. 5.4.3a(ii), (iii) and (iv)]**. Apo-TRACE

was observed to accumulate more (both in terms of concentration/stain intensity inside cells and number of cells) in cells treated with PN524 and PN528 indicating that these analogues are more apoptotic **(Fig. 5.4.3a)**. Compared to oe21 and flo-1 cell lines, the number of cells undergoing apoptosis/necrosis (stained cells) was found to be very few in oe33 cell line. Also, Apo-TRACE was observed to irregularly accumulate/stain cytoplasm of irinotecan-treated oe33 cells **[Fig. 5.4.3a(iii)]**. Both, PN512 and PN514 induced apoptosis in all the three cell lines. However, number of cells undergoing apoptosis was more with oe21 cells **[Fig. 5.4.3a(ii)]** compared to the oe33 and flo-1 cells.

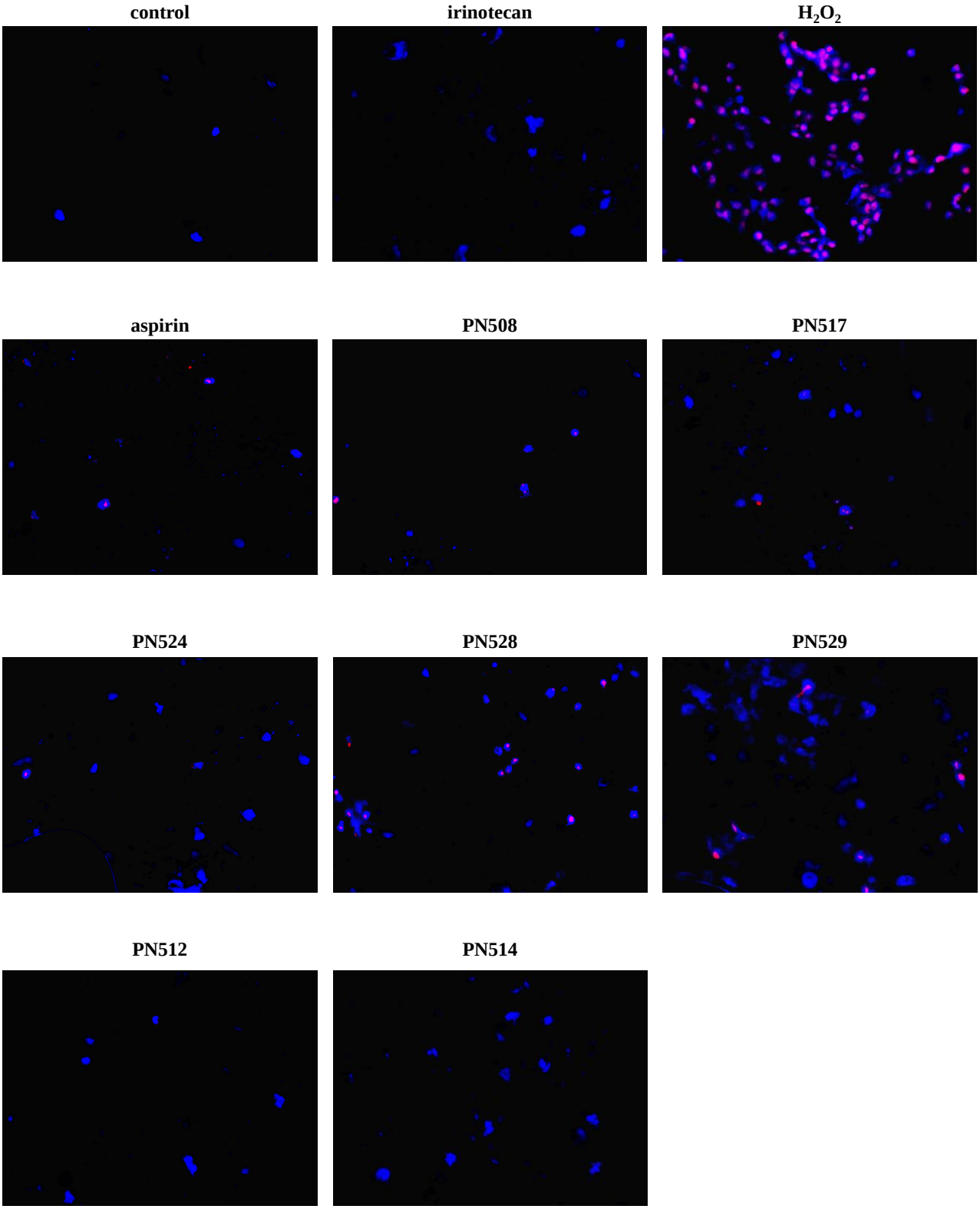

Figure 5.4.3a(i) Fluorescence imaging of oe21 cells (24 h)

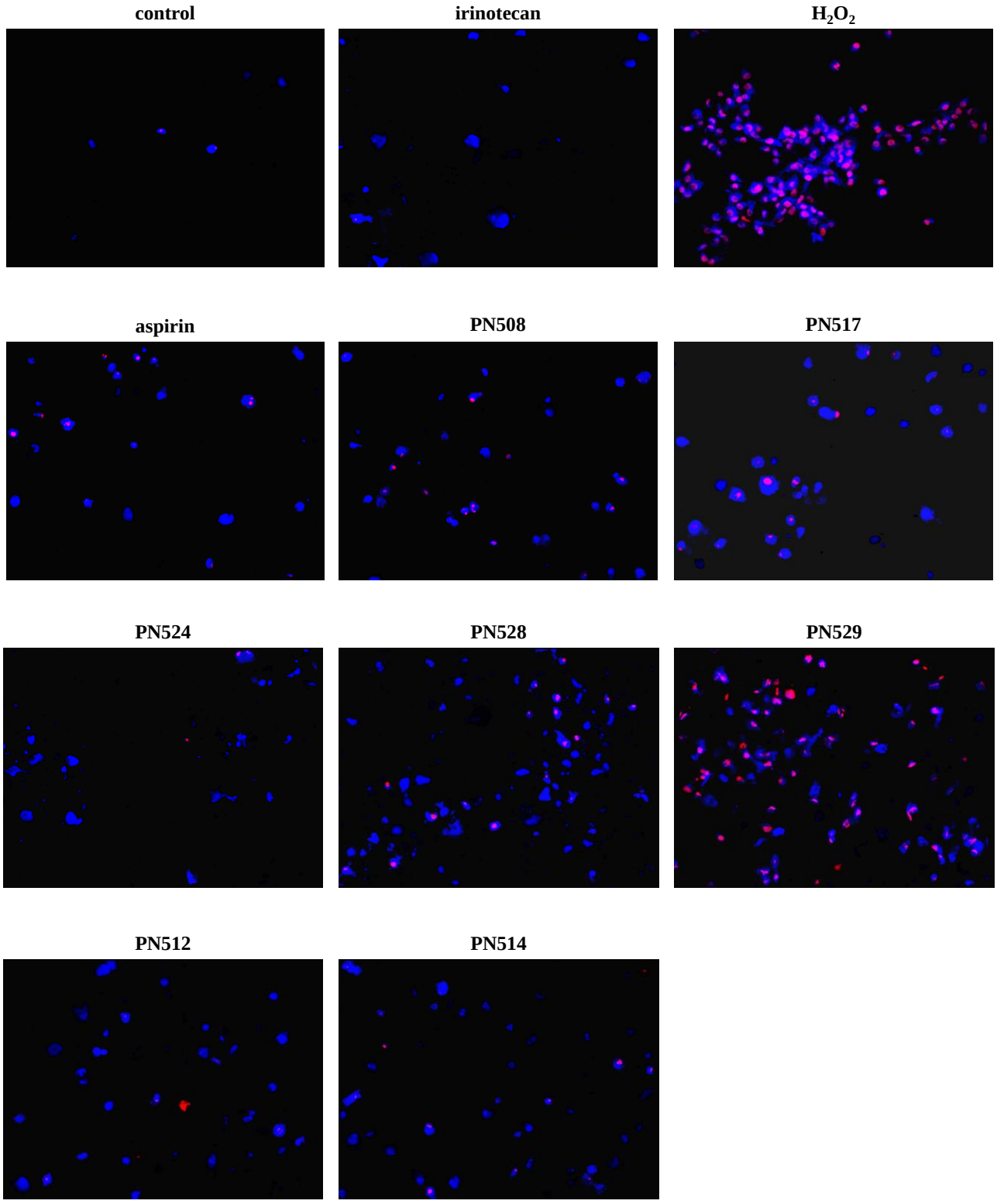

Figure 5.4.3a(ii) Fluorescence imaging of oe21 cells (48 h)

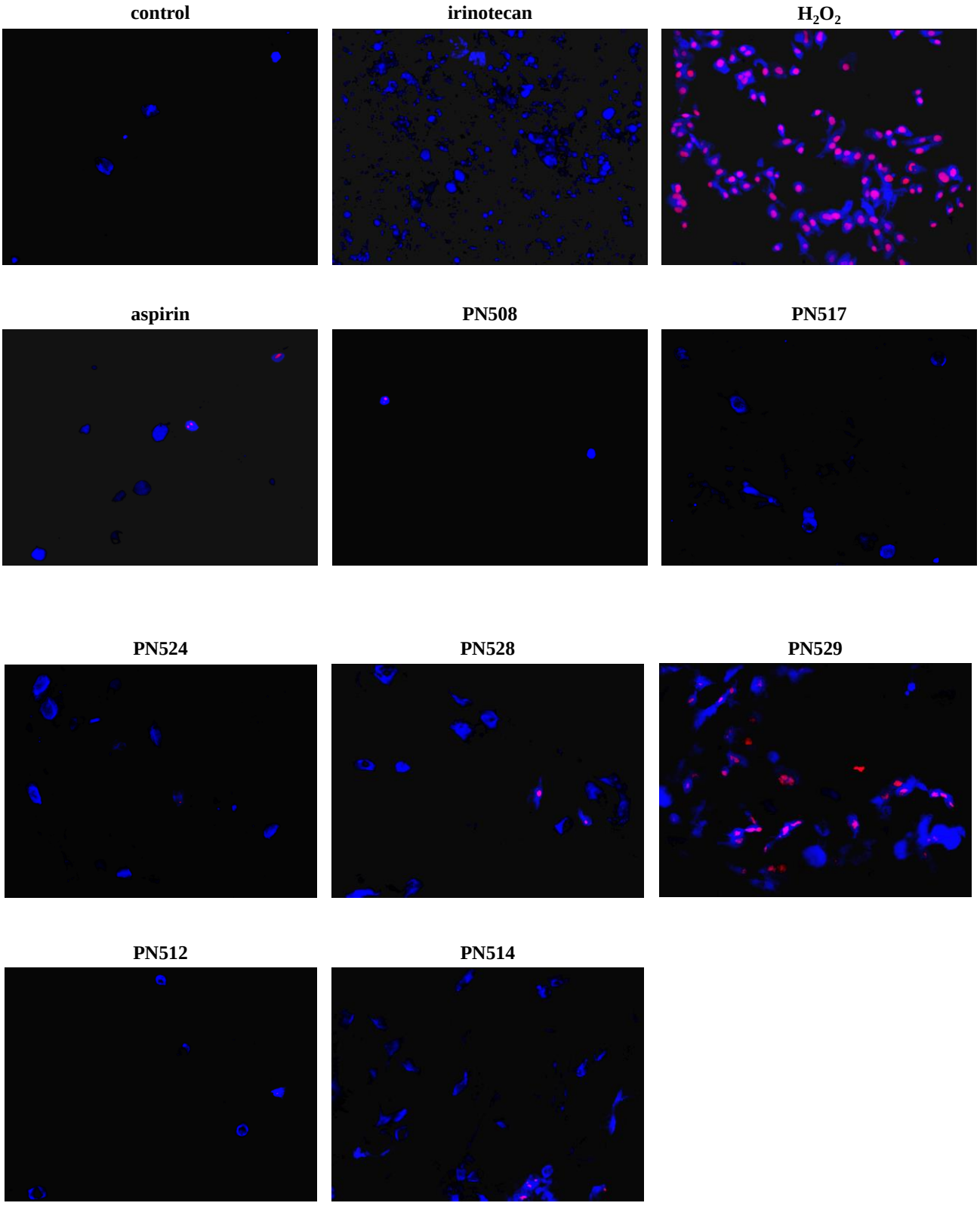

Figure 5.4.3a(iii) Fluorescence imaging of oe33 cells (48 h)

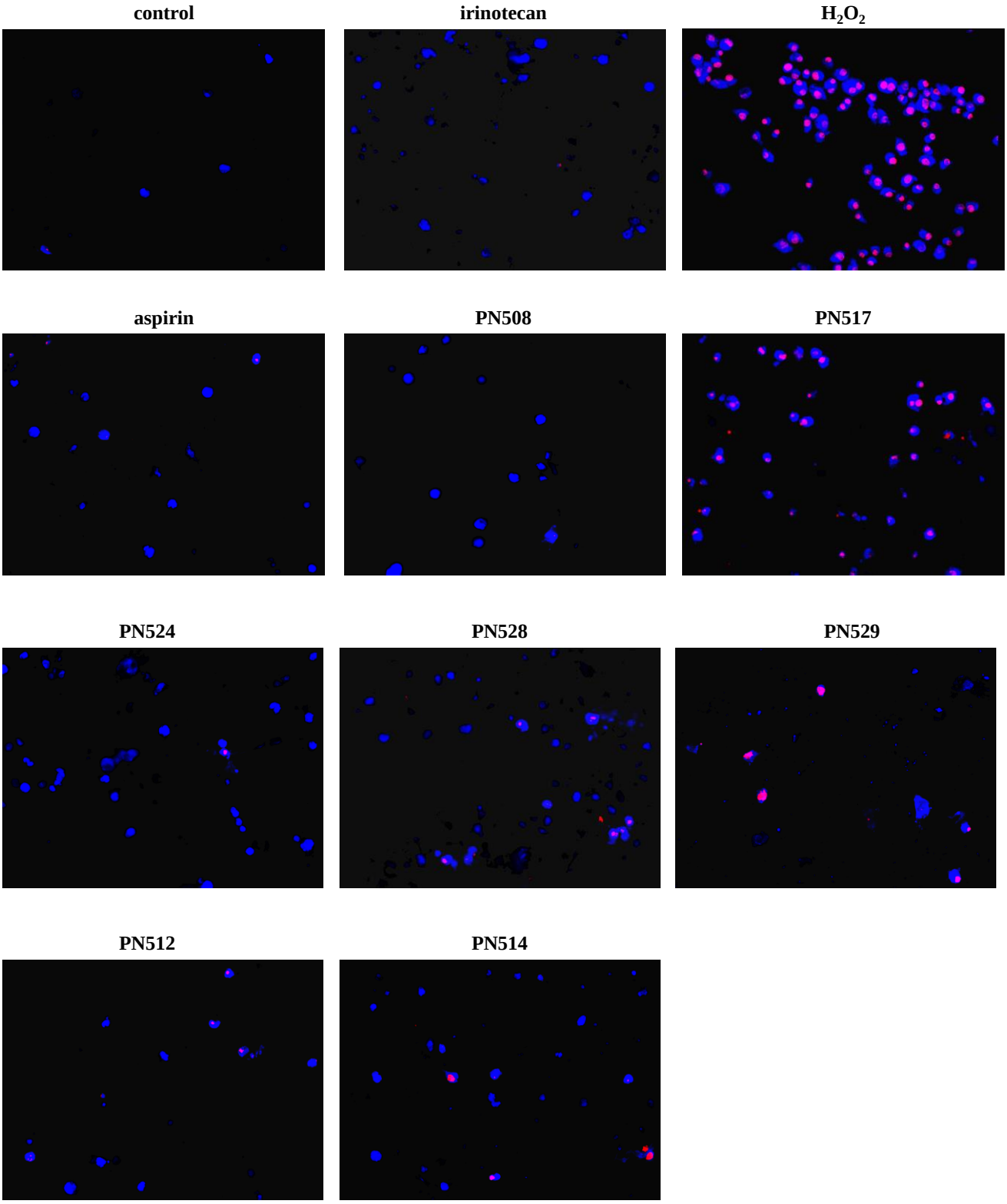

Fig.5.4.3a(iv) Fluorescence imaging of flo-1 cells (48 h)

Figure 5.4.3a Fluorescence imaging of cells treated with aspirin compounds and stained with the Apo-TRACE cell staining kit. Oe21 cells exposed to compounds for **(i)** 24 h and **(ii)** 48 h. Oe33 cells exposed to compounds for **(iii)** 48 h. Flo-1 cells exposed to compounds for **(iv)** 48 h. Oesophageal cancer cell lines at 50% confluency were treated with compound-containing culture medium for a further 24 h and 48 h. After treatment, cells were stained using Apo-TRACE cell staining kit (*Section* 2.2.27b) and observed by fluorescence microscopy. All compounds were prepared as stock solutions in DMSO and further diluted to a final concentration of 1mM in culture medium. Cells stained blue-only are apoptotic and cells stained both blue and red are late apoptotic/necrotic. Irinotecan and H_2O_2 were used as positive control for apoptosis and necrosis, respectively. Aspirin and vehicle control were included in the experiment for comparison. Images herein are representation of two individual experiments. The images were taken at 100x magnification (Olympus Bx60).

5.5 Do aspirin analogues act as cytostatic drugs?

During the exposure of some aspirin analogues to oesophageal cancer cells, a delay or inhibition in the cell growth was observed. To examine whether treatment with analogues induced the cells to undergo cytostasis, recovery experiments were performed (*Section* 2.2.28). Oesophageal cancer cells were treated with aspirin and aspirin compounds at a concentration of 1 mM for 72 h. The cells were removed from the medium containing drug and were further allowed to recover for 72 h to see if the cells continued to proliferate. Number of cells at the end of the experiment was counted and compared with the initial seeding number to decide if the drug was cytotoxic or cytostatic. Aspirin, irinotecan and H_2O_2 were included in this experiment for comparison

Oesophageal cancer cells treated with PN508 and especially aspirin, showed cell recovery equal to or more than that of untreated control cells, following withdrawal of the drug. In general, treatment with irinotecan and H_2O_2 affected the cancer cells irreversibly and thus cells struggled to grow during recovery period. Oe21 cells following treatment with the analogues PN517, PN524, PN528 and PN529 failed to recover as well as untreated control cells, suggesting that these analogues are more cytotoxic with oe21 cell line **(Fig. 5.5.1)**. Recovering ability of oe33 cells following treatment with these analogues was found to be affected, although not as severe as with oe21 cells **(Fig. 5.5.1)**. Conversely, recovery of flo-1 cells after treatment with PN517 and PN524 analogues showed signs of regained proliferation ability. However, flo-1 cells treated with PN528 and PN529 showed poor cell recovery, following withdrawal of the drug **(Fig. 5.5.1)**. Thus, in general, compounds PN528 and more significantly PN529 were cytotoxic to all three cancer cell lines tested. PN517 and PN524 appeared to be more cytotoxic to oe21cells but were more cytostatic to flo-1 cells.

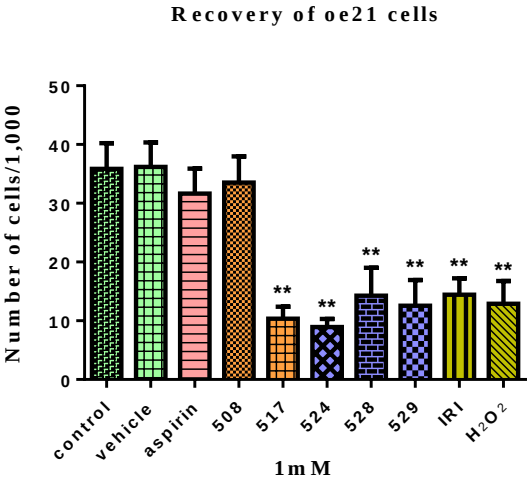
Recovery of oe21 cells
Number of cells/1,000
50
40
30
20
10
0
**
**
**
**
**
control
vehicle
aspirin
508
517
524
528
529
IRI
H2O2
1mM

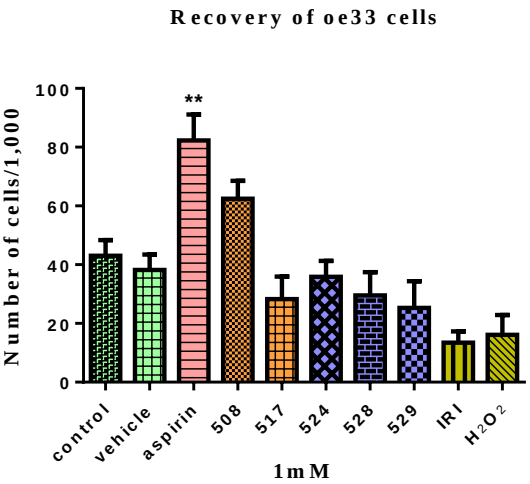
Recovery of oe33 cells
Number of cells/1,000
100
80
60
40
20
0
**
control
vehicle
aspirin
508
517
524
528
529
IRI
H2O2
1mM

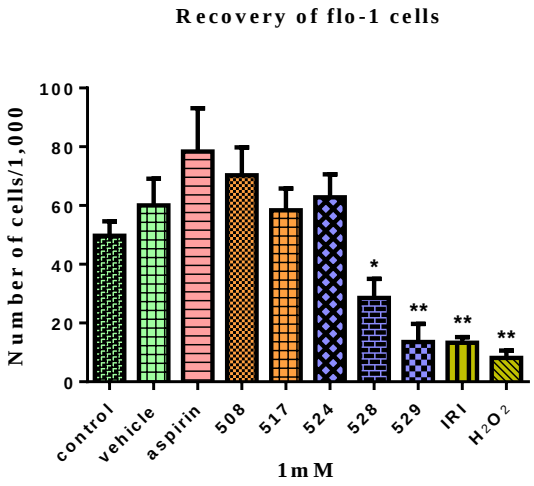

Figure 5.5.1 Recovery of oesophageal cancer cells following withdrawal of aspirin and aspirin compounds. Oe21, oe33 and flo-1 cells were seeded at a density of 5×10^3, 2×10^4 and, 2×10^4 cells/ml, respectively, in 6-well plates in their respective basal medium. 24 h after seeding, the cells were treated with drug-containing culture medium (1mM final concentration) for a further 72 h. After treatment time, viable/adherent cells were harvested, counted and re-seeded (same as initial density) in fresh 6-well plates with drug-free-medium (*Section* 2.2.28). After 72 h of recovery, cell counts were determined. Data plotted as mean ± SEM (N=3, performed in duplicates). The effect of aspirin, DMSO (vehicle control), irinotecan (IRI) and H_2O_2 is included for comparison. * $p \leq 0.05$ and ** $p \leq 0.01$ (*Section* 2.2.30).

5.6 COX inhibitor screening

Inhibitory activity of aspirin analogues against COX-1 and COX-2 enzymes was investigated with a COX inhibitor screening assay kit (*Section* 2.2.29). Values for IC_{50} were obtained by non-linear regression analysis (*Section* 2.2.30). The results showed aspirin to be the only potent inhibitor of COX-1 activity, with IC_{50} value of 0.6 mM. Other than PN526 and PN527 none of the aspirin analogues inhibited COX-1 **(Fig. 5.6.1)**. In all the experiments performed, aspirin failed to inhibit COX-2 enzyme even at a high concentration of 10 mM. Similarly, most of the analogues appeared to not inhibit COX-2 enzyme **(Fig. 5.6.1)**. The high absorbance recorded in case of PN528 and PN529 appeared to be due to the drug coming out of the solution. These results therefore need to be treated with caution.

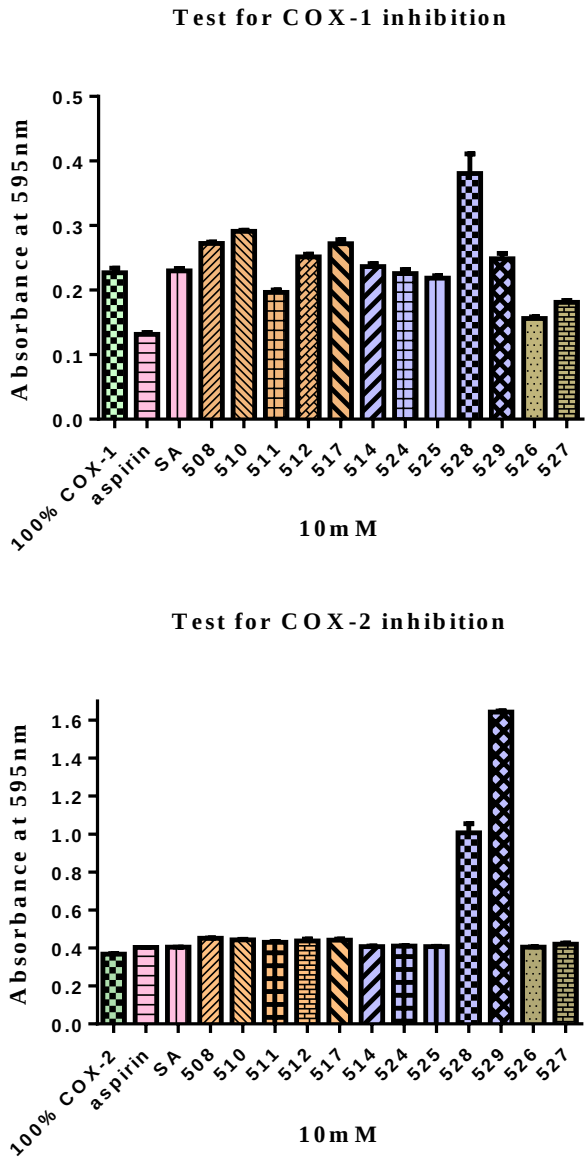

Figure 5.6.1 The inhibitory effect of aspirin analogues on COX-1 and COX-2. Aspirin compounds were prepared as stock solutions in DMSO. All the drug samples were added at a final concentration of 10 mM as DMSO solutions (10 µl final volume) to the assay mixture. The COX inhibition assay was performed at 37 ºC as described in the *Section* 2.2.29 and the absorbance of the samples were measure at 590 nm using a plate reader. Data plotted as mean ± SEM (N=3). Aspirin and SA was included in the experiment for comparison.

5.7 Discussion

Oesophageal cancer is a major cause of cancer-related mortality worldwide [CRUK(b)]. Present treatments are associated with significant morbidity and generally provide marginal benefit. Aspirin, though reported to provide only marginal anticancer benefit against several cancers, is one of the very few drugs that offer protection against GI cancers (NCI). Unlike most of the cancer drugs which have a single target, aspirin affects multiple pathways and influence physiological process including apoptosis and angiogenesis that are crucial for cancer progression (Langley *et al.*, 2011). Despite the benefits, use of aspirin for chemopreventative purposes universally is restricted because of (a) the potential gastropathy involved with long-term use (Laine, 2002) and (b) the unconfirmed dose regimen for safe and efficient use (NCI). Even the use of proton-pump inhibitors (long-term) to overcome aspirin-induced side effects are reported to involve side effects of its own (Sheen and Triadafilopoulos, 2011). Hence, there is an overwhelming rationale for novel developments that would lead to a reduction and/or in cancer-related morbidity and fatality.

Herein, the aspirin analogues with greater anti-proliferative effect against oesophageal cancer cells *in vitro* than aspirin and SA have been demonstrated. Diaspirin and benzoylsalicylate group of compounds were found to be highly potent against all three oesophageal cancer cell lines (i.e., flo-1, oe33 and oe21) compared to carbonates, aspirin and SA **(Fig. 5.2.1)**. Based on the IC_{50} data, the potency of the compounds were found to be in the order as follows: in case of flo-1 cell line-PN529>PN528>PN524>PN517>PN508>PN512>PN514>aspirin; in case of oe21 cells-PN529>PN528>PN524>PN517>PN514>PN512>PN508>aspirin; in case of oe33 cells-PN529>PN517>PN524>PN512>PN508>PN514>PN528>aspirin **(Fig. 5.3.1; Table 5.3.1)**.

PN529 was the most potent drug (IC_{50}<0.5mM) amongst all the analogues tested and across all the cell lines used. However, it appeared to lack specificity as it killed all the three cell lines efficiently at a lower concentration and at a short treatment time **(Fig. 5.3.1; Table 5.3.1)**. In support of this finding, lack of specificity of PN529 was also observed in colorectal (SW480, HCT116, LoVo) and non-colorectal (A549, MCF7, EA.hy926) cancer cell lines (Claudius *et al.*, 2014). PN528 was the second most potent drug in case of flo-1 and oe21 cell lines but showed less killing ability towards oe33 cell line. Poor potency of PN528 to oe33 cells could be due to resistance of the cell line or poor drug-uptake by cells due to precipitation of the drug. PN528, a methyl ester of benzoyl-salicylic acid (also known as, benzosalin), is a highly hydrophobic drug which although prepared as stock solution in a strong solvent such as DMSO, precipitated easily when introduced into growth medium (RPMI and DMEM). Precipitation and crystal-like formation was quite evident when observed under the microscope. Use of diluted stock solution of PN528 in DMSO (0.250 M) for experiments was of only little use. A similar precipitation concern was also observed with PN529 analogue. Whether such precipitation of compounds has an effect on pharmacodynamics of the drug on the cells is unclear. However, a historic study found benzosalin to be a useful drug for rheumatism and neuralgia (Bodenstein, 1907). The study also found benzosalin to have no unpleasant gastric-related side effects in patients as it dissociates to its constituents only in the intestine.

The most interesting and promising drugs in this study include PN517 and PN524. IC_{50} data from cytotoxicity assays demonstrated PN524 to be a more potent drug than PN517 in oesophageal cancer cell lines, except for oe33 cell line (PN517 was slightly more potent than PN524) **(Fig. 5.3.1; Table 5.3.1)**. However, PN517 and PN508 were shown to have profound antitumour effect than PN524 in SW480 CRC cells (Claudius *et al.*, 2014). Further investigation of cytotoxic effects of these aspirin analogues on other oesophageal cancer cell lines and more importantly non-cancerous/normal human oesophageal

epithelial cells would prove to be of great use in confirming the specificity of these compounds to oesophageal cancer cells.

Based on the cytotoxicity profile of PN517 from this study and study by Claudius *et al.* (2014) it is evident that PN517 exhibits modicum of specificity for not only CRC cell lines but also to oesophageal cancer cell lines *in vitro*. Furthermore, the study also demonstrated that PN517 and PN508 had potent antitumour action *in vivo*, in an implantable mouse model of CRC and also confirmed no drug-related side effects when introduced to mice intravenously over a 10-day period.

In this study, oe21 SCC cells were found to be the most sensitive to aspirin analogues compared to oe33 and flo-1 ADC cells. A difference in response to anticancer treatment has been previously observed between SCC and ADC. SCC cells are reported to be more sensitive to anticancer agents than ADC according to a study (Darnton *et al.*, 1995). Considerable resistance of flo-1 cells to compounds was evident with the increased cell-viability and higher IC_{50} values for the compounds **(Fig. 5.3.1; Table 5.3.1)**. Flo-1 (compared to oe33) cells have been reported to exhibit resistance to chemotherapy due to increased expression of insulin-like growth factor binding protein-2 both at mRNA and protein level (Silvers *et al.*, 2012). In this study, the observed variations in drug-sensitivity (IC_{50}s) across the different oesophageal cancer cell lines could be associated with proliferative rate of the cells. Cytotoxic cancer drugs are known to work by interrupting DNA synthesis or function and are believed to selectively affect the rapidly proliferating cells (Mitchison, 2012). This could be a possible explanation as to why the fast-growing oe21 cells are more sensitive to aspirin compounds, whereas slow-growing flo-1 cells are more resistant.

It has been stated in Claudius *et al.* (2014) study that cells cultured in DMEM show reduced sensitivity to aspirin compounds. Since flo-1 cells cultured in DMEM medium

were used for the experiments in this study, it is possible that the observed resistance to compounds was partly due to growth medium. Studies have reported that components of applied media (DMEM, MEM and RPMI) can influence cell proliferation and viability of cells (Lopez-Cazaux *et al.*, 2006; Wu *et al.*, 2009). DMEM is a nutrient-rich medium consisting of higher concentration of calcium (1.8 mM) and glucose (4.5 g/L) and lower concentration of phosphate (1 mM). In contrast RPMI, amino-acids-rich medium, contains higher levels of phosphate (5 mM), but carries low concentrations of calcium (0.8 mM) and glucose (2 g/L). Studies have shown that calcium rich medium can induce cell proliferation (Lopez-Cazaux *et al.*, 2006; Maeno *et al.*, 2005). Several studies have also shown reduced glucose level to enhance proliferation and higher glucose level to induce senescence in cells (Kim *et al.*, 2006; Stolzing *et al.*, 2006). Perhaps growing all the oesophageal cancer cell lines in either DMEM or RPMI basal medium for experiments could avoid such variability due to culture conditions. However, introducing the cell lines to a non-native culture medium for experimental purpose might affect the normal growth and vitality of the cells.

In this study, aspirin and most of the aspirin analogues tested other than PN529 **(Fig. 5.4.2a)** (induced necrosis in the tested cell lines within 24 h) largely exerted their toxicity via inducing apoptosis **(Fig. 5.4.1b and Fig. 5.4.3a)**. PN529 has been previously shown to induce necrosis in CRC cell lines (Deb *et al.*, 2011). Both qualitative and quantitative apoptosis assays confirmed PN517, PN524, PN528 and PN529 to be the most potent analogues to oesophageal cancer cell lines. PN524 was the only compound which consistently showed more apoptosis in all the three tested cell lines **(Fig. 5.4.1b and Fig. 5.4.3a)**. In contrast, compounds PN517 and PN528 appeared to induce both apoptosis and necrosis in the cell lines **(Fig. 5.4.3a)**. Since such mixture of cells were observed mostly after 48 h of drug treatment, it is possible that the cells were in late-apoptosis/secondary necrosis stage and thus have taken up both PI and Apo-TRACE staining. Studies have

stated that features of both apoptosis and necrosis can coexist in the same cell as a response to certain dose of death-inducing drugs (Zong and Thompson, 2006). In addition, process known as secondary necrosis, where the dead cells in their late apoptotic stage (not engulfed by means of phagocytosis), may present necrotic features due to loss of cellular energy and plasma membrane integrity has also been reported (Majno and Joris, 1995). NSAIDs such as indomethacin have been reported to induce both necrosis and apoptosis in gastric mucosal cells of guinea pig (Tomisato *et al.*, 2001). Although PN517 was initially shown to exert their toxicity in SW480 colon cancer cells via the necrotic pathway (Deb *et al.*, 2011), later it was reported to largely induce apoptosis (Claudius *et al.*, 2014).

In apoptosis experiments, use of H_2O_2 at a necrosis-inducing-dose proved beneficial to compare and judge whether the aspirin compounds induced necrosis or not. Use of irinotecan as positive control for apoptosis was beneficial; however, it induced low levels of apoptosis at the chosen concentration (25 µM) **(Fig. 5.4.3a)**. Also, fluorescent imaging of drug-treated oe33 cells showed poor uptake of apoptosis-cell stain and in particular cells treated with irinotecan showed an aberrant uneven uptake of Apo-TRACE stain **[Fig. 5.4.3a(iii)]**. However, flow cytometric analysis (used Annexin-V-fluos staining) of drug-treated oe33 cells showed increased number of necrotic cells/noisy debris **[Fig. 5.4.1b(ii) and Fig. 5.4.2a]**. One explanation for this could be that the cell debris generated by oe33 cells is rather auto-fluorescent. Although there is no experimental evidence from this study, one possibility is that the so called 'noisy debris/auto-fluorescent population' may as well be a side population (SP) containing stem-like cells (Donnenberg and Donnenberg, 2007). Dye-effluxing SP cells that are resistant to chemotherapy and resemble cancer stem cells were found in oesophageal cancer cell lines (Zhao *et al.*, 2014). In their study, oe33 cells (8.8% ± 2.7) were shown to have more SP cells than oe21 cells (0.6% ± 0.3).

From the apoptosis data, oe21 can again be concluded as the most sensitive cell line with PN524 being the most potent apoptosis-inducing agent **[Fig. 5.4.1b(i) and Fig. 5.4.3a(ii)]**. PN517 was the most potent in the case of oe33 **[Fig. 5.4.1b(ii)]**. Flow cytometric analysis confirmed flo-1 cells to be the most resistant with the least number of apoptotic cells at 72 h for most of the compounds **[Fig. 5.4.1b(iii)]**.

Although, the MTT assay showed decreased viability of cells in response to treatment with certain aspirin compounds, the number of cells that actually underwent apoptosis appeared to be relatively low in the apoptosis experiments. Also, a delay or inhibition in the cell growth was observed with exposure of oesophageal cancer cells to some of the most potent compounds. Recovery experiment conducted in this study revealed that the cytostatic and/or cytotoxic status of PN517 and PN524 compounds are hugely dependent on the cell line under investigation **(Fig. 5.5.1)**. However, PN528 and PN529 compounds were found to be more cytotoxic in all the three cell lines. Failure to recover after PN517 and PN524 treatment confirmed oe21 to be the most sensitive cell line whereas quick recovery of cells after drug removal proved flo-1 to be a more resistant cell line **(Fig. 5.5.1)**. Earlier studies have shown oe21 and oe33 cell lines to be sensitive and lack ability to recover following 5FU or cisplatin insult (O'Donovan *et al.*, 2011). Their report is in support with the observation from this study that oe21 cells and oe33 cells (not as sensitive as oe21) are sensitive to cytotoxic drugs. Such loss of cell viability during recovery from cytotoxic drug could be attributed to a defect in DNA repair.

In comparison to aspirin analogues, aspirin treated cells were found to recover as well as or even better than the untreated cells **(Fig. 5.5.1)**. Provided that aspirin has a short half-life in human circulation (Dovizio *et al.*, 2012), administering it in low doses for a longer time (~5 years) (Rothwell, Price, *et al.*, 2012) becomes necessary to reap the preventative anticancer benefits. A study observed aspirin to be ineffective in reducing the risk of CRC,

if its use was discontinued within 4 years (Chan *et al.*, 2008). Furthermore, discontinuation of aspirin therapy within 2 years prior to the study was attributed to threefold increase in risk for pancreatic cancer (Streicher *et al.*, 2014). It is possible that a similar repetitive dosing regimen is required to witness aspirin's therapeutic effects. However, this was not employed in this study and hence the observed ineffectiveness. A recent study also found aspirin to be weak in inhibiting intestinal adenomatous polyposis compared to a promising anticancer agent acetyl-11-keto-β-boswellic acid (Wang *et al.*, 2014). Moreover, the study proposed that unlike the latter, aspirin does not exhibit anticancer effect by modulating the Wnt/β-catenin pathway.

Finding the COX-inhibition status of aspirin analogues was important to have an insight into the potential mechanism behind analogues-mediated-anticancer effect and also to predict the possible COX-related side effects. For this purpose, Cayman Chemical's COX inhibitor screening assay kit (ovine) was employed. From the analysis, aspirin was found to inhibit COX-1with an IC_{50} of 600 µM **(Fig. 5.6.1)** which is much higher than the stated range (< 4 µM) in the literature. Such variations in the inhibitory concentration might be due to the difference in assays and in COX proteins (i.e., ovine, bovine, recombinant human). However, almost all the aspirin analogues tested in this study (other than carbonates) failed to inhibit COX-1 enzyme even at a very high concentration (10 mM). In case of COX-2, no inhibition was observed with aspirin or any other aspirin analogues at 10 mM concentration **(Fig. 5.6.1)**. A higher concentration of the compounds could not be used for these experiments due to the limitation in solubility. However, it is clear that the aspirin analogues tested are genuinely poor inhibitors of COX enzymes and their cytotoxicity effects are not mediated by COX inhibition. Since the aspirin analogues lack an acetyl group that could readily acetylate serine molecule of COX enzymes, it is possible that these compounds inhibit the COX isoforms at a very minimal level or do not inhibit at all. In the tested assay system, salicylic acid failed to inhibit the COX isoforms. Several

studies have shown salicylic acid to be a poor inhibitor of COX *in vitro* (Mitchell *et al.*, 1993) but an active inhibitor of COX at the site of inflammation *in vivo* (Mitchell *et al.*, 1997).

5.8 Conclusion

To sum up, novel aspirin compounds synthesised in-house were identified to be more potent against oesophageal cancer cell lines than aspirin itself. The aspirin compounds that showed strong killing ability include fumaryldiaspirin (PN517) and benzoylsalicylates (PN524, PN528 and PN529). Both, quantitative and qualitative apoptosis experiments conducted revealed that these compounds largely induce apoptosis, although some necrosis was noted with PN528 and PN529. Failure to recover following the treatment with these analogues emphasized that these drugs are largely cytotoxic in nature. Low IC_{50} values for the compounds, increased induction of cell death and poor recovery following treatment indicated oe21 (SSC) to be the most sensitive cell line, whereas flo-1 (ADC) cells were found to be more resistant. The anticancer properties of these novel aspirin compounds appear to not involve the COX-enzymes at the tested concentrations. These initial findings support further studies into the potential of these aspirin analogues as chemotherapeutic agents against oesophageal cancer. Future studies on the mechanisms of action that contributes to the anti-proliferative effect of these agents would prove valuable. Further, testing these agents in genetically defined mouse models of oesophageal cancer would help in understanding the toxicity profile, if any, of these compounds *in vivo*.

Concluding Remarks

The following conclusions can be made from this thesis:

1. IDPs are crucial for DNA repair following bleomycin or 5FU insult.

2. Yeast mutants- *arg82Δ* and *kcs1Δ,* both lacking IDPs are hypersensitive to bleomycin and 5FU.

3. Mutant *ipk1Δ and vip1Δ* show sensitivity similar to that of wild-type yeast, suggesting that neither $InsP_6$ nor $InsP_8$ play a crucial role in DNA repair.

4. The *kcs1Δ* yeast contains both UDG-like and APE1-like protein that is required to perform BER repair of damaged DNA. However, extreme extraction methods are required to access these proteins. APE1-like protein extracted from yeast was not efficient in removing the PG group.

5. Ung1, Apn1, Rad52 in both wild-type and *kcs1Δ* yeast and Rad51 in wild-type were successfully GFP-tagged for localisation studies. Due to poor GFP signal, confocal microscopy study was unable to reveal the exact localisation or movement of these GFP tagged proteins post bleomycin insult.

6. Ddp1, the yeast DIPP, was capable of hydrolysing not only 5-$InsP_7$ but also 1-$InsP_7$ and $InsP_8$ to a single product, $InsP_6$.

7. $InsP_7$ accumulation was observed to be relatively little during $InsP_8$ breakdown by DIPPs. Such low build-up was found to be due to rapid conversion of $InsP_7$ to $InsP_6$.

8. DIPP-1 is the most active enzyme amongst the five human DIPPs, irrespective of the substrate.

9. $InsP_8$ prefers to dephosphorylate through 1-$InsP_7$. In contrary, metabolically and functionally significant steady-state route of $InsP_8$ synthesis was observed to be via 5-$InsP_7$.

10. The pathway that $InsP_8$ chose to degrade (via 1-$InsP_7$) is metabolically distinct from the main pathway for $InsP_8$ synthesis (via 5-$InsP_7$).

11. Novel aspirin analogues synthesised in-house were identified to be more potent against oesophageal cancer cell lines than aspirin itself. Particularly, PN517, PN524, PN528 and PN529 analogues showed high killing ability.

12. Both quantitative and qualitative apoptosis experiments conducted revealed that these compounds largely induced apoptosis.

13. Inability of the cancer cells to recover following treatment with these analogues suggests that these drugs are cytotoxic and not cytostatic in nature.

14. Oe21 was found to be the most sensitive cell line, whereas flo-1 cells were found to be more resistant.

Future Studies

1. Tagging GFP at N-terminus of DNA-repair proteins to better the chances of visualising the signal much more efficiently

2. Use relevant antibodies to confirm the presence of Kcs1 and DNA repair proteins, check their functionality, and phosphorylation status.

3. Pursue Rad52, to determine whether Kcs1 is part of the epistasis group.

4. Determine whether IDPs act as cofactors acutely or are required for activation of enzymes prior to extraction.

5. Confirm that aspirin analogues induce apoptosis by checking the apoptotic protein levels (caspase activation, Bcl-2, Bax).

5. Determine levels of inositol lipids (particularly PIP_3) in order to determine whether the PI3K pathway is involved in aspirin analogues mediated killing of oesophageal cancer cells. Subsequent analysis of downstream proteins (e.g. PDK1, Akt).

6. Test the key aspirin analogues in an implantable mouse model of oesophageal cancer to confirm that there are no drug-related side effects when introduced.

Scientific Poster Presentations at Conferences

Signalling 2013	-	Effect of aspirin analogues on oesophageal cancer. *RS Kilari, CJ Perry, ST Safrany, ID Nicholl*
	-	First complete kinetic characterisation of the yeast and human diphosphoinositol polyphosphate hydrolases (DIPPs). *RS Kilari, JD Weaver, SB Shears, ST Safrany*
NCRI Conference 2013	-	Effect of aspirin analogues on oesophageal cancer. *RS Kilari, CJ Perry, ST Safrany, ID Nicholl*
AACR conference 2014	-	Effect of aspirin analogs on esophageal cancer. *RS Kilari, CJ Perry, A Devitt, ST Safrany, ID Nicholl*

Publications

- Kilari, R.S., Weaver, J.D., Shears, S.B. and Safrany, S.T. (2013) Understanding inositol pyrophosphate metabolism and function: kinetic characterization of the DIPPs. *FEBS Lett*, **587**(21), pp.3464-3470.
- Claudius, A., Kankipati, C.S., Kilari, R.S., Hassan, S., Guest, K., Russell, S.T., Perry, C.J., Stark, L.A. and Nicholl, I.D. (2014) Identification of aspirin analogues that repress NF-kB signalling and show anti-proliferative activity towards colorectal cancer *in vitro* and *in vivo*. *Oncol Rep*, **32**(4), pp.1670-1680.

REFERENCES

Abbaszadegan, M.R., Raziee, H.R., Ghafarzadegan, K., Shakeri, M.T., Afsharnezhad, S. and Ghavamnasiry, M.R. (2005) Aberrant p16 methylation, a possible epigenetic risk factor in familial esophageal squamous cell carcinoma. *Int J Gastrointest Cancer*, **36**(1), pp.47-54.

Abdalla, S.I., Sanderson, I.R. and Fitzgerald, R.C. (2005) Effect of inflammation on cyclooxygenase (COX)-2 expression in benign and malignant oesophageal cells. *Carcinogenesis*, **26**(9), pp.1627-1633.

Abnet, C.C., Freedman, N.D., Kamangar, F., Leitzmann, M.F., Hollenbeck, A.R. and Schatzkin, A. (2009) Non-steroidal anti-inflammatory drugs and risk of gastric and oesophageal adenocarcinomas: results from a cohort study and a meta-analysis. *Br J Cancer*, **100**(3), pp.551-557.

Aggarwal, S., Taneja, N., Lin, L., Orringer, M.B., Rehemtulla, A. and Beer, D.G. (2000) Indomethacin-induced apoptosis in esophageal adenocarcinoma cells involves upregulation of Bax and translocation of mitochondrial cytochrome C independent of COX-2 expression. *Neoplasia*, **2**(4), pp.346-356.

Ahmadi, N., Goldman, R., Seillier-Moiseiwitsch, F., Noone, A.M., Kosti, O. and Davidson, B.J. (2010) Decreased risk of squamous cell carcinoma of the head and neck in users of nonsteroidal anti-inflammatory drugs. *Int J Otolaryngol*, **2010**, pp.424161.

Albert, C., Safrany, S.T., Bembenek, M.E., Reddy, K.M., Reddy, K., Falck, J., Brocker, M., Shears, S.B. and Mayr, G.W. (1997) Biological variability in the structures of diphosphoinositol polyphosphates in Dictyostelium discoideum and mammalian cells. *Biochem J*, **327 (Pt 2)**, pp.553-560.

Alfonso, L.F., Srivenugopal, K.S., Arumugam, T.V., Abbruscato, T.J., Weidanz, J.A. and Bhat, G.J. (2009) Aspirin inhibits camptothecin-induced p21CIP1 levels and potentiates apoptosis in human breast cancer cells. *Int J Oncol*, **34**(3), pp.597-608.

Algra, A.M. and Rothwell, P.M. (2012) Effects of regular aspirin on long-term cancer incidence and metastasis: a systematic comparison of evidence from observational studies versus randomised trials. *Lancet Oncol*, **13**(5), pp.518-527.

Aminian, A., Karimian, F., Mirsharifi, R., Alibakhshi, A., Dashti, H., Jahangiri, Y., Safari, S., Ghaderi, H., Noaparast, M., Hasani, S.M. and Mirsharifi, A. (2011) Significance of platelet count in esophageal carcinomas. *Saudi J Gastroenterol*, **17**(2), pp.134-137.

Arber, N., Lightdale, C., Rotterdam, H., Han, K.H., Sgambato, A., Yap, E., Ahsan, H., Finegold, J., Stevens, P.D., Green, P.H., Hibshoosh, H., Neugut, A.I., Holt, P.R. and Weinstein, I.B. (1996) Increased expression of the cyclin D1 gene in Barrett's esophagus. *Cancer Epidemiol Biomarkers Prev*, **5**(6), pp.457-459.

Arico, S., Pattingre, S., Bauvy, C., Gane, P., Barbat, A., Codogno, P. and Ogier-Denis, E. (2002) Celecoxib induces apoptosis by inhibiting 3-phosphoinositide-dependent protein kinase-1 activity in the human colon cancer HT-29 cell line. *J Biol Chem*, **277**(31), pp.27613-27621.

Arthur, G., Tam, S.W. and Choy, P.C. (1984) The effects of detergents on CDP-choline:1,2-diacylglycerol phosphocholine transferase from hamster heart. *Can J Biochem Cell Biol*, **62**(11), pp.1059-1063.

Ason, B. and Reznikoff, W.S. (2004) A high-throughput assay for Tn5 Tnp-induced DNA cleavage. *Nucleic Acids Res*, **32**(10), pp.e83.

Auesukaree, C., Tochio, H., Shirakawa, M., Kaneko, Y. and Harashima, S. (2005) Plc1p, Arg82p, and Kcs1p, enzymes involved in inositol pyrophosphate synthesis, are essential for phosphate regulation and polyphosphate accumulation in *Saccharomyces cerevisiae*. *J Biol Chem*, **280**(26), pp.25127-25133.

Azevedo, C., Burton, A., Ruiz-Mateos, E., Marsh, M. and Saiardi, A. (2009) Inositol pyrophosphate mediated pyrophosphorylation of AP3B1 regulates HIV-1 Gag release. *Proc Natl Acad Sci U S A*, **106**(50), pp.21161-21166.

Bai, Y. and Symington, L.S. (1996) A Rad52 homolog is required for RAD51-independent mitotic recombination in *Saccharomyces cerevisiae*. *Genes Dev*, **10**(16), pp.2025-2037.

Baker, N., O'Meara, S.J., Scannell, M., Maderna, P. and Godson, C. (2009) Lipoxin A4: anti-inflammatory and anti-angiogenic impact on endothelial cells. *J Immunol*, **182**(6), pp.3819-3826.

Bambace, N.M. and Holmes, C.E. (2011) The platelet contribution to cancer progression. *J Thromb Haemost*, **9**(2), pp.237-249.

Barrett, M.T., Sanchez, C.A., Galipeau, P.C., Neshat, K., Emond, M. and Reid, B.J. (1996) Allelic loss of 9p21 and mutation of the CDKN2/p16 gene develop as early lesions during neoplastic progression in Barrett's esophagus. *Oncogene*, **13**(9), pp.1867-1873.

Berridge, M.J. (1983) Rapid accumulation of inositol trisphosphate reveals that agonists hydrolyse polyphosphoinositides instead of phosphatidylinositol. *Biochem J*, **212**(3), pp.849-858.

Bhandari, R., Juluri, K.R., Resnick, A.C. and Snyder, S.H. (2008) Gene deletion of inositol hexakisphosphate kinase 1 reveals inositol pyrophosphate regulation of insulin secretion, growth, and spermiogenesis. *Proc Natl Acad Sci U S A*, **105**(7), pp.2349-2353.

Bhandari, R., Saiardi, A., Ahmadibeni, Y., Snowman, A.M., Resnick, A.C., Kristiansen, T.Z., Molina, H., Pandey, A., Werner, J.K., Jr., Juluri, K.R., Xu, Y., Prestwich, G.D., Parang, K. and Snyder, S.H. (2007) Protein pyrophosphorylation by inositol pyrophosphates is a posttranslational event. *Proc Natl Acad Sci U S A*, **104**(39), pp.15305-15310.

Blake, R.D. and Delcourt, S.G. (1996) Thermodynamic effects of formamide on DNA stability. *Nucleic Acids Res*, **24**(11), pp.2095-2103.

Blanco, F.J., Guitian, R., Moreno, J., de Toro, F.J. and Galdo, F. (1999) Effect of antiinflammatory drugs on COX-1 and COX-2 activity in human articular chondrocytes. *J Rheumatol*, **26**(6), pp.1366-1373.

Bodenstein, J. (1907) Benzosalin. *An epitome of current medical literature (The British Medical Journal)*.

Boorstein, R.J., Cummings, A., Jr., Marenstein, D.R., Chan, M.K., Ma, Y., Neubert, T.A., Brown, S.M. and Teebor, G.W. (2001) Definitive identification of mammalian 5-hydroxymethyluracil DNA N-glycosylase activity as SMUG1. *J Biol Chem*, **276**(45), pp.41991-41997.

Bos, C.L., Kodach, L.L., van den Brink, G.R., Diks, S.H., van Santen, M.M., Richel, D.J., Peppelenbosch, M.P. and Hardwick, J.C. (2006) Effect of aspirin on the Wnt/beta-catenin pathway is mediated via protein phosphatase 2A. *Oncogene*, **25**(49), pp.6447-6456.

Botting, R.M. (2006) Inhibitors of cyclooxygenases: mechanisms, selectivity and uses. *J Physiol Pharmacol*, **57 Suppl 5**, pp.113-124.

Brachmann, C.B., Davies, A., Cost, G.J., Caputo, E., Li, J., Hieter, P. and Boeke, J.D. (1998) Designer deletion strains derived from Saccharomyces cerevisiae S288C: a useful

set of strains and plasmids for PCR-mediated gene disruption and other applications. *Yeast*, **14**(2), pp.115-132.

Bradford, M.M. (1976) A rapid and sensitive method for the quantitation of microgram quantities of protein utilizing the principle of protein-dye binding. *Anal Biochem*, **72**, pp.248-254.

Brown, K., Gerstberger, S., Carlson, L., Franzoso, G. and Siebenlist, U. (1995) Control of I kappa B-alpha proteolysis by site-specific, signal-induced phosphorylation. *Science*, **267**(5203), pp.1485-1488.

Bruno, A., Dovizio, M., Tacconelli, S. and Patrignani, P. (2012) Mechanisms of the antitumoural effects of aspirin in the gastrointestinal tract. *Best Pract Res Clin Gastroenterol*, **26**(4), pp.e1-e13.

Burkovics, P., Szukacsov, V., Unk, I. and Haracska, L. (2006) Human Ape2 protein has a 3'-5' exonuclease activity that acts preferentially on mismatched base pairs. *Nucleic Acids Res*, **34**(9), pp.2508-2515.

Burn, J., Gerdes, A.M., Macrae, F., Mecklin, J.P., Moeslein, G., Olschwang, S., Eccles, D., Evans, D.G., Maher, E.R., Bertario, L., Bisgaard, M.L., Dunlop, M.G., Ho, J.W., Hodgson, S.V., Lindblom, A., *et al.* (2011) Long-term effect of aspirin on cancer risk in carriers of hereditary colorectal cancer: an analysis from the CAPP2 randomised controlled trial. *Lancet*, **378**(9809), pp.2081-2087.

Caffrey, J.J., Safrany, S.T., Yang, X. and Shears, S.B. (2000) Discovery of molecular and catalytic diversity among human diphosphoinositol-polyphosphate phosphohydrolases. An expanding Nudt family. *J Biol Chem*, **275**(17), pp.12730-12736.

Caffrey, J.J. and Shears, S.B. (2001) Genetic rationale for microheterogeneity of human diphosphoinositol polyphosphate phosphohydrolase type 2. *Gene*, **269**(1-2), pp.53-60.

Campbell, N.P. and Villaflor, V.M. (2010) Neoadjuvant treatment of esophageal cancer. *World J Gastroenterol*, **16**(30), pp.3793-3803.

Capolicchio, S., Thakor, D.T., Linden, A. and Jessen, H.J. (2013) Synthesis of unsymmetric diphospho-inositol polyphosphates. *Angew Chem Int Ed Engl*, **52**(27), pp.6912-6916.

Cartwright, J.L. and McLennan, A.G. (1999) The *Saccharomyces cerevisiae* YOR163w gene encodes a diadenosine 5', 5'"-P1,P6-hexaphosphate (Ap_6A) hydrolase member of the MutT motif (Nudix hydrolase) family. *J Biol Chem*, **274**(13), pp.8604-8610.

Chak, A., Lee, T., Kinnard, M.F., Brock, W., Faulx, A., Willis, J., Cooper, G.S., Sivak, M.V., Jr. and Goddard, K.A. (2002) Familial aggregation of Barrett's oesophagus, oesophageal adenocarcinoma, and oesophagogastric junctional adenocarcinoma in Caucasian adults. *Gut*, **51**(3), pp.323-328.

Chakraborty, A., Koldobskiy, M.A., Bello, N.T., Maxwell, M., Potter, J.J., Juluri, K.R., Maag, D., Kim, S., Huang, A.S., Dailey, M.J., Saleh, M., Snowman, A.M., Moran, T.H., Mezey, E. and Snyder, S.H. (2010) Inositol pyrophosphates inhibit Akt signaling, thereby regulating insulin sensitivity and weight gain. *Cell*, **143**(6), pp.897-910.

Chalfie, M., Tu, Y., Euskirchen, G., Ward, W.W. and Prasher, D.C. (1994) Green fluorescent protein as a marker for gene expression. *Science*, **263**(5148), pp.802-805.

Chan, A.T. and Detering, E. (2013) An emerging role for anti-inflammatory agents for chemoprevention. *Recent Results Cancer Res*, **191**, pp.1-5.

Chan, A.T., Giovannucci, E.L., Meyerhardt, J.A., Schernhammer, E.S., Wu, K. and Fuchs, C.S. (2008) Aspirin dose and duration of use and risk of colorectal cancer in men. *Gastroenterology*, **134**(1), pp.21-28.

Chan, A.T., Ogino, S. and Fuchs, C.S. (2009) Aspirin use and survival after diagnosis of colorectal cancer. *Jama*, **302**(6), pp.649-658.

Chan, T.A. (2002) Nonsteroidal anti-inflammatory drugs, apoptosis, and colon-cancer chemoprevention. *Lancet Oncol*, **3**(3), pp.166-174.

Chang, M.S., Lee, H.S., Lee, B.L., Kim, Y.T., Lee, J.S. and Kim, W.H. (2005) Differential protein expression between esophageal squamous cell carcinoma and dysplasia, and prognostic significance of protein markers. *Pathol Res Pract*, **201**(6), pp.417-425.

Chattopadhyay, I., Phukan, R., Singh, A., Vasudevan, M., Purkayastha, J., Hewitt, S., Kataki, A., Mahanta, J., Kapur, S. and Saxena, S. (2009) Molecular profiling to identify molecular mechanism in esophageal cancer with familial clustering. *Oncol Rep*, **21**(5), pp.1135-1146.

Chen, J. and Stubbe, J. (2005) Bleomycins: towards better therapeutics. *Nat Rev Cancer*, **5**(2), pp.102-112.

Choi, J.H., Williams, J., Cho, J., Falck, J.R. and Shears, S.B. (2007) Purification, sequencing, and molecular identification of a mammalian PP-InsP_5 kinase that is activated when cells are exposed to hyperosmotic stress. *J Biol Chem*, **282**(42), pp.30763-30775.

Choi, Y.J., Li, H., Son, M.Y., Wang, X.H., Fornsaglio, J.L., Sobol, R.W., Lee, M., Vijg, J., Imholz, S., Dolle, M.E., van Steeg, H., Reiling, E. and Hasty, P. (2014) Deletion of individual Ku subunits in mice causes an NHEJ-independent phenotype potentially by altering apurinic/apyrimidinic site repair. *PLoS One*, **9**(1), pp.e86358.

Chou, W.Y., Marky, L.A., Zaunczkowski, D. and Breslauer, K.J. (1987) The thermodynamics of drug-DNA interactions: ethidium bromide and propidium iodide. *J Biomol Struct Dyn*, **5**(2), pp.345-359.

Clarke, R.J., Mayo, G., Price, P. and FitzGerald, G.A. (1991) Suppression of thromboxane A2 but not of systemic prostacyclin by controlled-release aspirin. *N Engl J Med*, **325**(16), pp.1137-1141.

Claudius, A.K., Kankipati, C.S., Kilari, R.S., Hassan, S., Guest, K., Russell, S.T., Perry, C.J., Stark, L.A. and Nicholl, I.D. (2014) Identification of aspirin analogues that repress NF-kappaB signalling and demonstrate anti-proliferative activity towards colorectal cancer in vitro and in vivo. *Oncol Rep*, **32**(4), pp.1670-1680.

Conteduca, V., Sansonno, D., Ingravallo, G., Marangi, S., Russi, S., Lauletta, G. and Dammacco, F. (2012) Barrett's esophagus and esophageal cancer: an overview. *Int J Oncol*, **41**(2), pp.414-424.

Cook, M.B., Chow, W.H. and Devesa, S.S. (2009) Oesophageal cancer incidence in the United States by race, sex, and histologic type, 1977-2005. *Br J Cancer*, **101**(5), pp.855-859.

Corley, D.A., Kerlikowske, K., Verma, R. and Buffler, P. (2003) Protective association of aspirin/NSAIDs and esophageal cancer: a systematic review and meta-analysis. *Gastroenterology*, **124**(1), pp.47-56.

Cramer, D.W., Harlow, B.L., Titus-Ernstoff, L., Bohlke, K., Welch, W.R. and Greenberg, E.R. (1998) Over-the-counter analgesics and risk of ovarian cancer. *Lancet*, **351**(9096), pp.104-107.

Craven, R.J., Greenwell, P.W., Dominska, M. and Petes, T.D. (2002) Regulation of genome stability by TEL1 and MEC1, yeast homologs of the mammalian ATM and ATR genes. *Genetics*, **161**(2), pp.493-507.

Craxton, A., Caffrey, J.J., Burkhart, W., Safrany, S.T. and Shears, S.B. (1997) Molecular cloning and expression of a rat hepatic multiple inositol polyphosphate phosphatase. *Biochem J*, **328 (Pt 1)**, pp.75-81.

CRUK(a). http://www.cancerresearchuk.org/about-cancer/cancers-in-general/cancer-questions/how-is-gastro-oesophageal-junction-cancer-treated.

CRUK(b). www.cancerresearchuk.org/cancer-info/cancerstats/types/oesophagus/incidence/#source1

Cubitt, A.B., Heim, R., Adams, S.R., Boyd, A.E., Gross, L.A. and Tsien, R.Y. (1995) Understanding, improving and using green fluorescent proteins. *Trends Biochem Sci*, **20**(11), pp.448-455.

Cui, R., Kamatani, Y., Takahashi, A., Usami, M., Hosono, N., Kawaguchi, T., Tsunoda, T., Kamatani, N., Kubo, M., Nakamura, Y. and Matsuda, K. (2009) Functional variants in ADH1B and ALDH2 coupled with alcohol and smoking synergistically enhance esophageal cancer risk. *Gastroenterology*, **137**(5), pp.1768-1775.

Daikoku, T., Wang, D., Tranguch, S., Morrow, J.D., Orsulic, S., DuBois, R.N. and Dey, S.K. (2005) Cyclooxygenase-1 is a potential target for prevention and treatment of ovarian epithelial cancer. *Cancer Res*, **65**(9), pp.3735-3744.

Daley, J.M., Zakaria, C. and Ramotar, D. (2010) The endonuclease IV family of apurinic/apyrimidinic endonucleases. *Mutat Res*, **705**(3), pp.217-227.

Damianovich, M., Ziv, I., Heyman, S.N., Rosen, S., Shina, A., Kidron, D., Aloya, T., Grimberg, H., Levin, G., Reshef, A., Bentolila, A., Cohen, A. and Shirvan, A. (2006) ApoSense: a novel technology for functional molecular imaging of cell death in models of acute renal tubular necrosis. *Eur J Nucl Med Mol Imaging*, **33**(3), pp.281-291.

Darnton, S.J., Jenner, K., Steyn, R.S., Ferry, D.R. and Matthews, H.R. (1995) Lack of correlation of P-glycoprotein expression with response to MIC chemotherapy in oesophageal cancer. *J Clin Pathol*, **48**(11), pp.1064-1066.

Das, D., Chilton, A.P. and Jankowski, J.A. (2009) Chemoprevention of oesophageal cancer and the AspECT trial. *Recent Results Cancer Res*, **181**, pp.161-169.

Deb, J., Dibra, H., Shan, S., Rajan, S., Manneh, J., Kankipati, C.S., Perry, C.J. and Nicholl, I.D. (2011) Activity of aspirin analogues and vanillin in a human colorectal cancer cell line. *Oncol Rep*, **26**(3), pp.557-565.

Din, F.V., Theodoratou, E., Farrington, S.M., Tenesa, A., Barnetson, R.A., Cetnarskyj, R., Stark, L., Porteous, M.E., Campbell, H. and Dunlop, M.G. (2010) Effect of aspirin and NSAIDs on risk and survival from colorectal cancer. *Gut*, **59**(12), pp.1670-1679.

Din, F.V., Valanciute, A., Houde, V.P., Zibrova, D., Green, K.A., Sakamoto, K., Alessi, D.R. and Dunlop, M.G. (2012) Aspirin inhibits mTOR signaling, activates AMP-activated protein kinase, and induces autophagy in colorectal cancer cells. *Gastroenterology*, **142**(7), pp.1504-1515 e1503.

Donnenberg, A.D. and Donnenberg, V.S. (2007) Rare-event analysis in flow cytometry. *Clin Lab Med*, **27**(3), pp.627-652, viii.

Dou, H., Mitra, S. and Hazra, T.K. (2003) Repair of oxidized bases in DNA bubble structures by human DNA glycosylases NEIL1 and NEIL2. *J Biol Chem*, **278**(50), pp.49679-49684.

Dovizio, M., Tacconelli, S., Sostres, C., Ricciotti, E. and Patrignani, P. (2012) Mechanistic and pharmacological issues of aspirin as an anticancer agent. *Pharmaceuticals (Basel)*, **5**(12), pp.1346-1371.

Downs, J.A., Lowndes, N.F. and Jackson, S.P. (2000) A role for *Saccharomyces cerevisiae* histone H2A in DNA repair. *Nature*, **408**(6815), pp.1001-1004.

Dubois, E., Scherens, B., Vierendeels, F., Ho, M.M., Messenguy, F. and Shears, S.B. (2002) In *Saccharomyces cerevisiae*, the inositol polyphosphate kinase activity of Kcs1p is required for resistance to salt stress, cell wall integrity, and vacuolar morphogenesis. *J Biol Chem*, **277**(26), pp.23755-23763.

Dulak, A.M., Stojanov, P., Peng, S., Lawrence, M.S., Fox, C., Stewart, C., Bandla, S., Imamura, Y., Schumacher, S.E., Shefler, E., McKenna, A., Carter, S.L., Cibulskis, K., Sivachenko, A., Saksena, G., *et al*. (2013) Exome and whole-genome sequencing of esophageal adenocarcinoma identifies recurrent driver events and mutational complexity. *Nat Genet*, **45**(5), pp.478-486.

Dyakonova, E.S., Koval, V.V., Ishchenko, A.A., Saparbaev, M.K., Kaptein, R. and Fedorova, O.S. (2012) Kinetic mechanism of the interaction of *Saccharomyces cerevisiae* AP-endonuclease 1 with DNA substrates. *Biochemistry (Mosc)*, **77**(10), pp.1162-1171.

Edwalds-Gilbert, G., Veraldi, K.L. and Milcarek, C. (1997) Alternative poly(A) site selection in complex transcription units: means to an end? *Nucleic Acids Res*, **25**(13), pp.2547-2561.

El-Serag, H.B., Mason, A.C., Petersen, N. and Key, C.R. (2002) Epidemiological differences between adenocarcinoma of the oesophagus and adenocarcinoma of the gastric cardia in the USA. *Gut*, **50**(3), pp.368-372.

Enzinger, P.C. and Mayer, R.J. (2003) Esophageal cancer. *N Engl J Med*, **349**(23), pp.2241-2252.

Eskandani, M., Hamishehkar, H. and Ezzati Nazhad Dolatabadi, J. (2013) Cyto/Genotoxicity study of polyoxyethylene (20) sorbitan monolaurate (tween 20). *DNA Cell Biol*, **32**(9), pp.498-503.

Esquivias, P., Cebrian, C., Morandeira, A., Santander, S., Ortego, J., Garcia-Gonzalez, M.A., Lanas, A. and Piazuelo, E. (2014) Effect of aspirin treatment on the prevention of esophageal adenocarcinoma in a rat experimental model. *Oncol Rep*, **31**(6), pp.2785-2791.

Folch, J. (1949) Brain diphosphoinositide, a new phosphatide having inositol metadiphosphate as a constituent. *J Biol Chem*, **177**(2), pp.505-519.

Forde, P.M. and Kelly, R.J. (2013) Genomic alterations in advanced esophageal cancer may lead to subtype-specific therapies. *Oncologist*, **18**(7), pp.823-832.

Fung, H. and Demple, B. (2005) A vital role for Ape1/Ref1 protein in repairing spontaneous DNA damage in human cells. *Mol Cell*, **17**(3), pp.463-470.

Fung, H. and Demple, B. (2011) Distinct roles of Ape1 protein in the repair of DNA damage induced by ionizing radiation or bleomycin. *J Biol Chem*, **286**(7), pp.4968-4977.

Galipeau, P.C., Cowan, D.S., Sanchez, C.A., Barrett, M.T., Emond, M.J., Levine, D.S., Rabinovitch, P.S. and Reid, B.J. (1996) 17p (p53) allelic losses, 4N (G2/tetraploid)

populations, and progression to aneuploidy in Barrett's esophagus. *Proc Natl Acad Sci U S A*, **93**(14), pp.7081-7084.

Game, J.C. (2002) New genome-wide methods bring more power to yeast as a model organism. *Trends Pharmacol Sci*, **23**(10), pp.445-447.

Gao, H., Wang, L.D., Zhou, Q., Hong, J.Y., Huang, T.Y. and Yang, C.S. (1994) p53 tumor suppressor gene mutation in early esophageal precancerous lesions and carcinoma among high-risk populations in Henan, China. *Cancer Res*, **54**(16), pp.4342-4346.

Gasic, G.J., Gasic, T.B. and Murphy, S. (1972) Anti-metastatic effect of aspirin. *Lancet*, **2**(7783), pp.932-933.

Gensini, G.F. and Conti, A.A. (2009) The preventive and therapeutic impact of antiplatelet agents: past and present. *Minerva Med*, **100**(2), pp.133-136.

Giardiello, F.M., Hamilton, S.R., Krush, A.J., Piantadosi, S., Hylind, L.M., Celano, P., Booker, S.V., Robinson, C.R. and Offerhaus, G.J. (1993) Treatment of colonic and rectal adenomas with sulindac in familial adenomatous polyposis. *N Engl J Med*, **328**(18), pp.1313-1316.

Giardiello, F.M., Offerhaus, G.J. and DuBois, R.N. (1995) The role of nonsteroidal anti-inflammatory drugs in colorectal cancer prevention. *Eur J Cancer*, **31A**(7-8), pp.1071-1076.

Gilroy, D.W. (2005) The role of aspirin-triggered lipoxins in the mechanism of action of aspirin. *Prostaglandins Leukot Essent Fatty Acids*, **73**(3-4), pp.203-210.

Glennon, M.C. and Shears, S.B. (1993) Turnover of inositol pentakisphosphates, inositol hexakisphosphate and diphosphoinositol polyphosphates in primary cultured hepatocytes. *Biochem J*, **293 (Pt 2)**, pp.583-590.

Gorecki, P. (2001). Gastro-esophageal reflux disease (GERD). In R. G. Holzheimer and J. A. Mannick (Eds.), Surgical Treatment: Evidence-Based and Problem-Oriented. Munich: Zuckschwerdt.

Greenhough, A., Smartt, H.J., Moore, A.E., Roberts, H.R., Williams, A.C., Paraskeva, C. and Kaidi, A. (2009) The COX-2/PGE2 pathway: key roles in the hallmarks of cancer and adaptation to the tumour microenvironment. *Carcinogenesis*, **30**(3), pp.377-386.

Gurpinar, E., Grizzle, W.E. and Piazza, G.A. (2013) COX-Independent Mechanisms of Cancer Chemoprevention by Anti-Inflammatory Drugs. *Front Oncol*, **3**, pp.181.

Guzder, S.N., Torres-Ramos, C., Johnson, R.E., Haracska, L., Prakash, L. and Prakash, S. (2004) Requirement of yeast Rad1-Rad10 nuclease for the removal of 3'-blocked termini from DNA strand breaks induced by reactive oxygen species. *Genes Dev*, **18**(18), pp.2283-2291.

Hagen, L., Kavli, B., Sousa, M.M., Torseth, K., Liabakk, N.B., Sundheim, O., Pena-Diaz, J., Otterlei, M., Horning, O., Jensen, O.N., Krokan, H.E. and Slupphaug, G. (2008) Cell cycle-specific UNG2 phosphorylations regulate protein turnover, activity and association with RPA. *Embo j*, **27**(1), pp.51-61.

Hamberg, M. and Samuelsson, B. (1973) Detection and isolation of an endoperoxide intermediate in prostaglandin biosynthesis. *Proc Natl Acad Sci U S A*, **70**(3), pp.899-903.

Hanada, M., Feng, J. and Hemmings, B.A. (2004) Structure, regulation and function of PKB/AKT--a major therapeutic target. *Biochim Biophys Acta*, **1697**(1-2), pp.3-16.

Hanakahi, L.A., Bartlet-Jones, M., Chappell, C., Pappin, D. and West, S.C. (2000) Binding of inositol phosphate to DNA-PK and stimulation of double-strand break repair. *Cell*, **102**(6), pp.721-729.

Hanakahi, L.A. and West, S.C. (2002) Specific interaction of IP_6 with human Ku70/80, the DNA-binding subunit of DNA-PK. *Embo j*, **21**(8), pp.2038-2044.

Hardie, D.G. (2011) AMP-activated protein kinase: an energy sensor that regulates all aspects of cell function. *Genes Dev*, **25**(18), pp.1895-1908.

Harris, R.E., Kasbari, S. and Farrar, W.B. (1999) Prospective study of nonsteroidal anti-inflammatory drugs and breast cancer. *Oncol Rep*, **6**(1), pp.71-73.

He, Y.H., Wu, M., Kobune, M., Xu, Y., Kelley, M.R. and Martin, W.J., 2nd. (2001) Expression of yeast apurinic/apyrimidinic endonuclease (APN1) protects lung epithelial cells from bleomycin toxicity. *Am J Respir Cell Mol Biol*, **25**(6), pp.692-698.

Hennan, J.K., Huang, J., Barrett, T.D., Driscoll, E.M., Willens, D.E., Park, A.M., Crofford, L.J. and Lucchesi, B.R. (2001) Effects of selective cyclooxygenase-2 inhibition on vascular responses and thrombosis in canine coronary arteries. *Circulation*, **104**(7), pp.820-825.

Hidaka, K., Caffrey, J.J., Hua, L., Zhang, T., Falck, J.R., Nickel, G.C., Carrel, L., Barnes, L.D. and Shears, S.B. (2002) An adjacent pair of human NUDT genes on chromosome X are preferentially expressed in testis and encode two new isoforms of diphosphoinositol polyphosphate phosphohydrolase. *J Biol Chem*, **277**(36), pp.32730-32738.

Hill, J.W., Hazra, T.K., Izumi, T. and Mitra, S. (2001) Stimulation of human 8-oxoguanine-DNA glycosylase by AP-endonuclease: potential coordination of the initial steps in base excision repair. *Nucleic Acids Res*, **29**(2), pp.430-438.

Hokin, M.R. and Hokin, L.E. (1953) Enzyme secretion and the incorporation of P32 into phospholipides of pancreas slices. *J Biol Chem*, **203**(2), pp.967-977.

Honda, S. and Selker, E.U. (2009) Tools for fungal proteomics: multifunctional neurospora vectors for gene replacement, protein expression and protein purification. *Genetics*, **182**(1), pp.11-23.

Hoskins, J. and Scott Butler, J. (2007) Evidence for distinct DNA- and RNA-based mechanisms of 5-fluorouracil cytotoxicity in *Saccharomyces cerevisiae*. *Yeast*, **24**(10), pp.861-870.

Houghton, J.A., Tillman, D.M. and Harwood, F.G. (1995) Ratio of 2'-deoxyadenosine-5'-triphosphate/thymidine-5'-triphosphate influences the commitment of human colon carcinoma cells to thymineless death. *Clin Cancer Res*, **1**(7), pp.723-730.

Houslay, M.D. (1998) Adaptation in cyclic AMP signalling processes: a central role for cyclic AMP phosphodiesterases. *Semin Cell Dev Biol*, **9**(2), pp.161-167.

Hu, N., Goldstein, A.M., Albert, P.S., Giffen, C., Tang, Z.Z., Ding, T., Taylor, P.R. and Emmert-Buck, M.R. (2003) Evidence for a familial esophageal cancer susceptibility gene on chromosome 13. *Cancer Epidemiol Biomarkers Prev*, **12**(10), pp.1112-1115.

Hua, L.V., Hidaka, K., Pesesse, X., Barnes, L.D. and Shears, S.B. (2003) Paralogous murine Nudt10 and Nudt11 genes have differential expression patterns but encode identical proteins that are physiologically competent diphosphoinositol polyphosphate phosphohydrolases. *Biochem J*, **373**(Pt 1), pp.81-89.

Huang, K.N. and Symington, L.S. (1995) Suppressors of a *Saccharomyces cerevisiae* pkc1 mutation identify alleles of the phosphatase gene PTC1 and of a novel gene encoding a putative basic leucine zipper protein. *Genetics*, **141**(4), pp.1275-1285.

Huttenhofer, A., Hudson, S., Noller, H.F. and Mascharak, P.K. (1992) Cleavage of tRNA by Fe(II)-bleomycin. *J Biol Chem*, **267**(34), pp.24471-24475.

Hvid-Jensen, F., Pedersen, L., Drewes, A.M., Sorensen, H.T. and Funch-Jensen, P. (2011) Incidence of adenocarcinoma among patients with Barrett's esophagus. *N Engl J Med*, **365**(15), pp.1375-1383.

Ingram, S.W., Safrany, S.T. and Barnes, L.D. (2003) Disruption and overexpression of the *Schizosaccharomyces pombe* aps1 gene, and effects on growth rate, morphology and intracellular diadenosine 5',5'''-P1,P5-pentaphosphate and diphosphoinositol polyphosphate concentrations. *Biochem J*, **369**(Pt 3), pp.519-528.

Irvine, R.F. and Schell, M.J. (2001) Back in the water: the return of the inositol phosphates. *Nat Rev Mol Cell Biol*, **2**(5), pp.327-338.

Itakura, Y., Sasano, H., Shiga, C., Furukawa, Y., Shiga, K., Mori, S. and Nagura, H. (1994) Epidermal growth factor receptor overexpression in esophageal carcinoma. An immunohistochemical study correlated with clinicopathologic findings and DNA amplification. *Cancer*, **74**(3), pp.795-804.

Itoh, T., Koshiba, S., Kigawa, T., Kikuchi, A., Yokoyama, S. and Takenawa, T. (2001) Role of the ENTH domain in phosphatidylinositol-4,5-bisphosphate binding and endocytosis. *Science*, **291**(5506), pp.1047-1051.

Jacobs, A.L. and Schar, P. (2012) DNA glycosylases: in DNA repair and beyond. *Chromosoma*, **121**(1), pp.1-20.

Jacobs, E.J., Rodriguez, C., Mondul, A.M., Connell, C.J., Henley, S.J., Calle, E.E. and Thun, M.J. (2005) A large cohort study of aspirin and other nonsteroidal anti-inflammatory drugs and prostate cancer incidence. *J Natl Cancer Inst*, **97**(13), pp.975-980.

Jadav, R.S., Chanduri, M.V., Sengupta, S. and Bhandari, R. (2013) Inositol pyrophosphate synthesis by inositol hexakisphosphate kinase 1 is required for homologous recombination repair. *J Biol Chem*, **288**(5), pp.3312-3321.

Jette, L., Bissoon-Haqqani, S., Le Francois, B., Maroun, J.A. and Birnboim, H.C. (2008) Resistance of colorectal cancer cells to 5-FUdR and 5-FU caused by Mycoplasma infection. *Anticancer Res*, **28**(4b), pp.2175-2180.

Jiang, X., Tseng, C.C., Bernstein, L. and Wu, A.H. (2014) Family history of cancer and gastroesophageal disorders and risk of esophageal and gastric adenocarcinomas: a case-control study. *BMC Cancer*, **14**, pp.60.

Jimenez, P., Piazuelo, E., Cebrian, C., Ortego, J., Strunk, M., Garcia-Gonzalez, M.A., Santander, S., Alcedo, J. and Lanas, A. (2010) Prostaglandin EP2 receptor expression is increased in Barrett's oesophagus and oesophageal adenocarcinoma. *Aliment Pharmacol Ther*, **31**(3), pp.440-451.

Jones, D.R. and Divecha, N. (2004) Linking lipids to chromatin. *Curr Opin Genet Dev*, **14**(2), pp.196-202.

Kala, Z., Dolina, J., Marek, F. and Izakovicova Holla, L. (2007) Polymorphisms of glutathione S-transferase M1, T1 and P1 in patients with reflux esophagitis and Barrett's esophagus. *J Hum Genet*, **52**(6), pp.527-534.

Kamangar, F., Chow, W.H., Abnet, C.C. and Dawsey, S.M. (2009) Environmental causes of esophageal cancer. *Gastroenterol Clin North Am*, **38**(1), pp.27-57, vii.

Kastelein, F., Spaander, M.C., Biermann, K., Steyerberg, E.W., Kuipers, E.J. and Bruno, M.J. (2011) Nonsteroidal anti-inflammatory drugs and statins have chemopreventative

effects in patients with Barrett's esophagus. *Gastroenterology*, **141**(6), pp.2000-2008; quiz e2013-2004.

Kato, H., Arao, T., Matsumoto, K., Fujita, Y., Kimura, H., Hayashi, H., Nishiki, K., Iwama, M., Shiraishi, O., Yasuda, A., Shinkai, M., Imano, M., Imamoto, H., Yasuda, T., Okuno, K., *et al.* (2013) Gene amplification of EGFR, HER2, FGFR2 and MET in esophageal squamous cell carcinoma. *Int J Oncol*, **42**(4), pp.1151-1158.

Kawamori, T., Kaneshiro, T., Okumura, M., Maalouf, S., Uflacker, A., Bielawski, J., Hannun, Y.A. and Obeid, L.M. (2009) Role for sphingosine kinase 1 in colon carcinogenesis. *Faseb j*, **23**(2), pp.405-414.

Khodyreva, S.N., Prasad, R., Ilina, E.S., Sukhanova, M.V., Kutuzov, M.M., Liu, Y., Hou, E.W., Wilson, S.H. and Lavrik, O.I. (2010) Apurinic/apyrimidinic (AP) site recognition by the 5'-dRP/AP lyase in poly(ADP-ribose) polymerase-1 (PARP-1). *Proc Natl Acad Sci U S A*, **107**(51), pp.22090-22095.

Kim, H.S., Park, J.W., Yeo, S.I., Choi, B.J. and Suh, J.Y. (2006) Effects of high glucose on cellular activity of periodontal ligament cells in vitro. *Diabetes Res Clin Pract*, **74**(1), pp.41-47.

Kim, Y.J. and Wilson, D.M., 3rd. (2012) Overview of base excision repair biochemistry. *Curr Mol Pharmacol*, **5**(1), pp.3-13.

Kimura, Y., Shiozaki, H., Doki, Y., Yamamoto, M., Utsunomiya, T., Kawanishi, K., Fukuchi, N., Inoue, M., Tsujinaka, T. and Monden, M. (1999) Cytoplasmic beta-catenin in esophageal cancers. *Int J Cancer*, **84**(2), pp.174-178.

Klump, B., Hsieh, C.J., Holzmann, K., Gregor, M. and Porschen, R. (1998) Hypermethylation of the CDKN2/p16 promoter during neoplastic progression in Barrett's esophagus. *Gastroenterology*, **115**(6), pp.1381-1386.

Koldobskiy, M.A., Chakraborty, A., Werner, J.K., Jr., Snowman, A.M., Juluri, K.R., Vandiver, M.S., Kim, S., Heletz, S. and Snyder, S.H. (2010) p53-mediated apoptosis requires inositol hexakisphosphate kinase-2. *Proc Natl Acad Sci U S A*, **107**(49), pp.20947-20951.

Kostadinov, R.L., Kuhner, M.K., Li, X., Sanchez, C.A., Galipeau, P.C., Paulson, T.G., Sather, C.L., Srivastava, A., Odze, R.D., Blount, P.L., Vaughan, T.L., Reid, B.J. and Maley, C.C. (2013) NSAIDs modulate clonal evolution in Barrett's esophagus. *PLoS Genet*, **9**(6), pp.e1003553.

Krokan, H.E., Drablos, F. and Slupphaug, G. (2002) Uracil in DNA--occurrence, consequences and repair. *Oncogene*, **21**(58), pp.8935-8948.

Krokan, H.E., Standal, R. and Slupphaug, G. (1997) DNA glycosylases in the base excision repair of DNA. *Biochem J*, **325 (Pt 1)**, pp.1-16.

Kulke, M.H., Odze, R.D., Mueller, J.D., Wang, H., Redston, M. and Bertagnolli, M.M. (2004) Prognostic significance of vascular endothelial growth factor and cyclooxygenase 2 expression in patients receiving preoperative chemoradiation for esophageal cancer. *J Thorac Cardiovasc Surg*, **127**(6), pp.1579-1586.

Kuroki, T., Trapasso, F., Yendamuri, S., Matsuyama, A., Alder, H., Mori, M. and Croce, C.M. (2003) Allele loss and promoter hypermethylation of VHL, RAR-beta, RASSF1A, and FHIT tumor suppressor genes on chromosome 3p in esophageal squamous cell carcinoma. *Cancer Res*, **63**(13), pp.3724-3728.

Ladner, R.D. (2001) The role of dUTPase and uracil-DNA repair in cancer chemotherapy. *Curr Protein Pept Sci*, **2**(4), pp.361-370.

Lagger, G., Doetzlhofer, A., Schuettengruber, B., Haidweger, E., Simboeck, E., Tischler, J., Chiocca, S., Suske, G., Rotheneder, H., Wintersberger, E. and Seiser, C. (2003) The tumor suppressor p53 and histone deacetylase 1 are antagonistic regulators of the cyclin-dependent kinase inhibitor p21/WAF1/CIP1 gene. *Mol Cell Biol*, **23**(8), pp.2669-2679.

Laine, L. (2002) The gastrointestinal effects of nonselective NSAIDs and COX-2-selective inhibitors. *Semin Arthritis Rheum*, **32**(3 Suppl 1), pp.25-32.

Langley, R.E., Burdett, S., Tierney, J.F., Cafferty, F., Parmar, M.K. and Venning, G. (2011) Aspirin and cancer: has aspirin been overlooked as an adjuvant therapy? *Br J Cancer*, **105**(8), pp.1107-1113.

Lapetina, E.G. and Michell, R.H. (1973) A membrane-bound activity catalysing phosphatidylinositol breakdown to 1,2-diacylglycerol, D-myoinositol 1:2-cyclic phosphate an D-myoinositol 1-phosphate. Properties and subcellular distribution in rat cerebral cortex. *Biochem J*, **131**(3), pp.433-442.

Laussmann, T., Hansen, A., Reddy, K.M., Reddy, K.K., Falck, J.R. and Vogel, G. (1998) Diphospho-myo-inositol phosphates in Dictyostelium and Polysphondylium: identification of a new bisdiphospho-myo-inositol tetrakisphosphate. *FEBS Lett*, **426**(1), pp.145-150.

Lee, C.H., Lee, J.M., Wu, D.C., Hsu, H.K., Kao, E.L., Huang, H.L., Wang, T.N., Huang, M.C. and Wu, M.T. (2005) Independent and combined effects of alcohol intake, tobacco smoking and betel quid chewing on the risk of esophageal cancer in Taiwan. *Int J Cancer*, **113**(3), pp.475-482.

Lee, J.Y., Kim, Y.R., Park, J. and Kim, S. (2012) Inositol polyphosphate multikinase signaling in the regulation of metabolism. *Ann N Y Acad Sci*, **1271**, pp.68-74.

Lee, Y.S., Mulugu, S., York, J.D. and O'Shea, E.K. (2007) Regulation of a cyclin-CDK-CDK inhibitor complex by inositol pyrophosphates. *Science*, **316**(5821), pp.109-112.

Lennerz, J.K., Kwak, E.L., Ackerman, A., Michael, M., Fox, S.B., Bergethon, K., Lauwers, G.Y., Christensen, J.G., Wilner, K.D., Haber, D.A., Salgia, R., Bang, Y.J., Clark, J.W., Solomon, B.J. and Iafrate, A.J. (2011) MET amplification identifies a small and aggressive subgroup of esophagogastric adenocarcinoma with evidence of responsiveness to crizotinib. *J Clin Oncol*, **29**(36), pp.4803-4810.

Leslie, N.R., McLennan, A.G. and Safrany, S.T. (2002) Cloning and characterisation of hAps1 and hAps2, human diadenosine polyphosphate-metabolising Nudix hydrolases. *BMC Biochem*, **3**, pp.20.

Leung, A.C., Wong, V.C., Yang, L.C., Chan, P.L., Daigo, Y., Nakamura, Y., Qi, R.Z., Miller, L.D., Liu, E.T., Wang, L.D., Li, J.L., Law, S., Tsao, S.W. and Lung, M.L. (2008) Frequent decreased expression of candidate tumor suppressor gene, DEC1, and its anchorage-independent growth properties and impact on global gene expression in esophageal carcinoma. *Int J Cancer*, **122**(3), pp.587-594.

Li, H., Marple, T. and Hasty, P. (2013) Ku80-deleted cells are defective at base excision repair. *Mutat Res*, **745-746**, pp.16-25.

Li, M., Lotan, R., Levin, B., Tahara, E., Lippman, S.M. and Xu, X.C. (2000) Aspirin induction of apoptosis in esophageal cancer: a potential for chemoprevention. *Cancer Epidemiol Biomarkers Prev*, **9**(6), pp.545-549.

Lieber, M.R. (2010) The mechanism of double-strand DNA break repair by the nonhomologous DNA end-joining pathway. *Annu Rev Biochem*, **79**, pp.181-211.

Lieber, M.R., Ma, Y., Pannicke, U. and Schwarz, K. (2003) Mechanism and regulation of human non-homologous DNA end-joining. *Nat Rev Mol Cell Biol*, **4**(9), pp.712-720.

Lim, S.T., Jue, C.K., Moore, C.W. and Lipke, P.N. (1995) Oxidative cell wall damage mediated by bleomycin-Fe(II) in *Saccharomyces cerevisiae*. *J Bacteriol*, **177**(12), pp.3534-3539.

Lin, H., Fridy, P.C., Ribeiro, A.A., Choi, J.H., Barma, D.K., Vogel, G., Falck, J.R., Shears, S.B., York, J.D. and Mayr, G.W. (2009) Structural analysis and detection of biological inositol pyrophosphates reveal that the family of VIP/diphosphoinositol pentakisphosphate kinases are 1/3-kinases. *J Biol Chem*, **284**(3), pp.1863-1872.

Lin, Y.H., Chang, C.C., Wong, C.W. and Teng, S.C. (2009) Recruitment of Rad51 and Rad52 to short telomeres triggers a Mec1-mediated hypersensitivity to double-stranded DNA breaks in senescent budding yeast. *PLoS One*, **4**(12), pp.e8224.

Lindahl, T. (1974) An N-glycosidase from Escherichia coli that releases free uracil from DNA containing deaminated cytosine residues. *Proc Natl Acad Sci U S A*, **71**(9), pp.3649-3653.

Lisby, M., Rothstein, R. and Mortensen, U.H. (2001) Rad52 forms DNA repair and recombination centers during S phase. *Proc Natl Acad Sci U S A*, **98**(15), pp.8276-8282.

Liu, C., Pouliot, J.J. and Nash, H.A. (2004) The role of TDP1 from budding yeast in the repair of DNA damage. *DNA Repair (Amst)*, **3**(6), pp.593-601.

Liu, J.F., Jamieson, G.G., Drew, P.A., Zhu, G.J., Zhang, S.W., Zhu, T.N., Shan, B.E. and Wang, Q.Z. (2005) Aspirin induces apoptosis in oesophageal cancer cells by inhibiting the pathway of NF-kappaB downstream regulation of cyclooxygenase-2. *ANZ J Surg*, **75**(11), pp.1011-1016.

Liu, J.F., Jamieson, G.G., Wu, T.C., Zhu, G.J. and Drew, P.A. (2009) A preliminary study on the postoperative survival of patients given aspirin after resection for squamous cell carcinoma of the esophagus or adenocarcinoma of the cardia. *Ann Surg Oncol*, **16**(5), pp.1397-1402.

Liu, Y., Ju, J., Xiao, H., Simi, B., Hao, X., Reddy, B.S., Huang, M.T., Newmark, H. and Yang, C.S. (2008) Effects of combination of calcium and aspirin on azoxymethane-induced aberrant crypt foci formation in the colons of mice and rats. *Nutr Cancer*, **60**(5), pp.660-665.

Lonetti, A., Szijgyarto, Z., Bosch, D., Loss, O., Azevedo, C. and Saiardi, A. (2011) Identification of an evolutionarily conserved family of inorganic polyphosphate endopolyphosphatases. *J Biol Chem*, **286**(37), pp.31966-31974.

Longley, D.B., Harkin, D.P. and Johnston, P.G. (2003) 5-fluorouracil: mechanisms of action and clinical strategies. *Nat Rev Cancer*, **3**(5), pp.330-338.

Longtine, M.S., McKenzie, A., 3rd, Demarini, D.J., Shah, N.G., Wach, A., Brachat, A., Philippsen, P. and Pringle, J.R. (1998) Additional modules for versatile and economical PCR-based gene deletion and modification in *Saccharomyces cerevisiae*. *Yeast*, **14**(10), pp.953-961.

Lopez-Cazaux, S., Bluteau, G., Magne, D., Lieubeau, B., Guicheux, J. and Alliot-Licht, B. (2006) Culture medium modulates the behaviour of human dental pulp-derived cells: technical note. *Eur Cell Mater*, **11**, pp.35-42; discussion 42.

Loss, O., Azevedo, C., Szijgyarto, Z., Bosch, D. and Saiardi, A. (2011) Preparation of quality inositol pyrophosphates. *J Vis Exp*(55), pp.e3027.

Luo, H.R., Saiardi, A., Yu, H., Nagata, E., Ye, K. and Snyder, S.H. (2002) Inositol pyrophosphates are required for DNA hyperrecombination in protein kinase c1 mutant yeast. *Biochemistry*, **41**(8), pp.2509-2515.

Luo, Z., Zang, M. and Guo, W. (2010) AMPK as a metabolic tumor suppressor: control of metabolism and cell growth. *Future Oncol*, **6**(3), pp.457-470.

Luthra, R., Singh, R.R., Luthra, M.G., Li, Y.X., Hannah, C., Romans, A.M., Barkoh, B.A., Chen, S.S., Ensor, J., Maru, D.M., Broaddus, R.R., Rashid, A. and Albarracin, C.T. (2008) MicroRNA-196a targets annexin A1: a microRNA-mediated mechanism of annexin A1 downregulation in cancers. *Oncogene*, **27**(52), pp.6667-6678.

Ma, W., Resnick, M.A. and Gordenin, D.A. (2008) Apn1 and Apn2 endonucleases prevent accumulation of repair-associated DNA breaks in budding yeast as revealed by direct chromosomal analysis. *Nucleic Acids Res*, **36**(6), pp.1836-1846.

Ma, Y. and Lieber, M.R. (2002) Binding of inositol hexakisphosphate (IP6) to Ku but not to DNA-PKcs. *J Biol Chem*, **277**(13), pp.10756-10759.

Madden, M., Song, C., K., T. and Wong, A. (2004) The Inhibitory Effect of EDTA and Mg2+ on the Activity of NADH Dehydrogenase in Lysozyme Lysis *Journal of Experimental Microbiology and Immunology*, **5**, pp.8-15.

Maeno, S., Niki, Y., Matsumoto, H., Morioka, H., Yatabe, T., Funayama, A., Toyama, Y., Taguchi, T. and Tanaka, J. (2005) The effect of calcium ion concentration on osteoblast viability, proliferation and differentiation in monolayer and 3D culture. *Biomaterials*, **26**(23), pp.4847-4855.

Mahaney, B.L., Meek, K. and Lees-Miller, S.P. (2009) Repair of ionizing radiation-induced DNA double-strand breaks by non-homologous end-joining. *Biochem J*, **417**(3), pp.639-650.

Majno, G. and Joris, I. (1995) Apoptosis, oncosis, and necrosis. An overview of cell death. *Am J Pathol*, **146**(1), pp.3-15.

Marenstein, D.R., Wilson, D.M., 3rd and Teebor, G.W. (2004) Human AP endonuclease (APE1) demonstrates endonucleolytic activity against AP sites in single-stranded DNA. *DNA Repair (Amst)*, **3**(5), pp.527-533.

Mariette, C., Finzi, L., Piessen, G., Van Seuningen, I. and Triboulet, J.P. (2005) Esophageal carcinoma: prognostic differences between squamous cell carcinoma and adenocarcinoma. *World J Surg*, **29**(1), pp.39-45.

Martin, E., Sharina, I., Kots, A. and Murad, F. (2003) A constitutively activated mutant of human soluble guanylyl cyclase (sGC): implication for the mechanism of sGC activation. *Proc Natl Acad Sci U S A*, **100**(16), pp.9208-9213.

Mathe, E.A., Nguyen, G.H., Bowman, E.D., Zhao, Y., Budhu, A., Schetter, A.J., Braun, R., Reimers, M., Kumamoto, K., Hughes, D., Altorki, N.K., Casson, A.G., Liu, C.G., Wang, X.W., Yanaihara, N., *et al.* (2009) MicroRNA expression in squamous cell carcinoma and adenocarcinoma of the esophagus: associations with survival. *Clin Cancer Res*, **15**(19), pp.6192-6200.

Matsumoto, K., Arao, T., Hamaguchi, T., Shimada, Y., Kato, K., Oda, I., Taniguchi, H., Koizumi, F., Yanagihara, K., Sasaki, H., Nishio, K. and Yamada, Y. (2012) FGFR2 gene amplification and clinicopathological features in gastric cancer. *Br J Cancer*, **106**(4), pp.727-732.

McClelland, S., Gawaz, M., Kennerknecht, E., Konrad, C.S., Sauer, S., Schuerzinger, K., Massberg, S., Fitzgerald, D.J. and Belton, O. (2009) Contribution of cyclooxygenase-1 to thromboxane formation, platelet-vessel wall interactions and atherosclerosis in the ApoE null mouse. *Atherosclerosis*, **202**(1), pp.84-91.

McKeague, A.L., Wilson, D.J. and Nelson, J. (2003) Staurosporine-induced apoptosis and hydrogen peroxide-induced necrosis in two human breast cell lines. *Br J Cancer*, **88**(1), pp.125-131.

McNeill, D.R. and Wilson, D.M., 3rd. (2007) A dominant-negative form of the major human abasic endonuclease enhances cellular sensitivity to laboratory and clinical DNA-damaging agents. *Mol Cancer Res*, **5**(1), pp.61-70.

McQuaid, K.R. and Laine, L. (2006) Systematic review and meta-analysis of adverse events of low-dose aspirin and clopidogrel in randomized controlled trials. *Am J Med*, **119**(8), pp.624-638.

Melhado, R.E., Alderson, D. and Tucker, O. (2010) The changing face of esophageal cancer. *Cancers (Basel)*, **2**(3), pp.1379-1404.

Menniti, F.S., Miller, R.N., Putney, J.W., Jr. and Shears, S.B. (1993) Turnover of inositol polyphosphate pyrophosphates in pancreatoma cells. *J Biol Chem*, **268**(6), pp.3850-3856.

Mikulec, C.D., Rundhaug, J.E., Simper, M.S., Lubet, R.A. and Fischer, S.M. (2013) The chemopreventive efficacies of nonsteroidal anti-inflammatory drugs: the relationship of

short-term biomarkers to long-term skin tumor outcome. *Cancer Prev Res (Phila)*, **6**(7), pp.675-685.

Mitchell, J.A., Akarasereenont, P., Thiemermann, C., Flower, R.J. and Vane, J.R. (1993) Selectivity of nonsteroidal antiinflammatory drugs as inhibitors of constitutive and inducible cyclooxygenase. *Proc Natl Acad Sci U S A*, **90**(24), pp.11693-11697.

Mitchell, J.A., Saunders, M., Barnes, P.J., Newton, R. and Belvisi, M.G. (1997) Sodium salicylate inhibits cyclo-oxygenase-2 activity independently of transcription factor (nuclear factor kappaB) activation: role of arachidonic acid. *Mol Pharmacol*, **51**(6), pp.907-912.

Mitchison, T.J. (2012) The proliferation rate paradox in antimitotic chemotherapy. *Mol Biol Cell*, **23**(1), pp.1-6.

Mol, C.D., Izumi, T., Mitra, S. and Tainer, J.A. (2000) DNA-bound structures and mutants reveal abasic DNA binding by APE1 and DNA repair coordination [corrected]. *Nature*, **403**(6768), pp.451-456.

Moore, C.W. (1990) Degradation of DNA and structure-activity relationship between bleomycins A2 and B2 in the absence of DNA repair. *Biochemistry*, **29**(5), pp.1342-1347.

Moore, C.W., McKoy, J., Dardalhon, M., Davermann, D., Martinez, M. and Averbeck, D. (2000) DNA damage-inducible and RAD52-independent repair of DNA double-strand breaks in *Saccharomyces cerevisiae*. *Genetics*, **154**(3), pp.1085-1099.

Morrison, B.H., Bauer, J.A., Kalvakolanu, D.V. and Lindner, D.J. (2001) Inositol hexakisphosphate kinase 2 mediates growth suppressive and apoptotic effects of interferon-beta in ovarian carcinoma cells. *J Biol Chem*, **276**(27), pp.24965-24970.

Morrison, B.H., Haney, R., Lamarre, E., Drazba, J., Prestwich, G.D. and Lindner, D.J. (2009) Gene deletion of inositol hexakisphosphate kinase 2 predisposes to aerodigestive tract carcinoma. *Oncogene*, **28**(25), pp.2383-2392.

Mulugu, S., Bai, W., Fridy, P.C., Bastidas, R.J., Otto, J.C., Dollins, D.E., Haystead, T.A., Ribeiro, A.A. and York, J.D. (2007) A conserved family of enzymes that phosphorylate inositol hexakisphosphate. *Science*, **316**(5821), pp.106-109.

Munemitsu, S., Albert, I., Souza, B., Rubinfeld, B. and Polakis, P. (1995) Regulation of intracellular beta-catenin levels by the adenomatous polyposis coli (APC) tumor-suppressor protein. *Proc Natl Acad Sci U S A*, **92**(7), pp.3046-3050.

Muscat, J.E., Chen, S.Q., Richie, J.P., Jr., Altorki, N.K., Citron, M., Olson, S., Neugut, A.I. and Stellman, S.D. (2003) Risk of lung carcinoma among users of nonsteroidal antiinflammatory drugs. *Cancer*, **97**(7), pp.1732-1736.

Nagata, E., Luo, H.R., Saiardi, A., Bae, B.I., Suzuki, N. and Snyder, S.H. (2005) Inositol hexakisphosphate kinase-2, a physiologic mediator of cell death. *J Biol Chem*, **280**(2), pp.1634-1640.

NCI. http://www.cancer.gov/cancertopics/research-updates/2014/aspirin

Nilsen, H., Rosewell, I., Robins, P., Skjelbred, C.F., Andersen, S., Slupphaug, G., Daly, G., Krokan, H.E., Lindahl, T. and Barnes, D.E. (2000) Uracil-DNA glycosylase (UNG)-deficient mice reveal a primary role of the enzyme during DNA replication. *Mol Cell*, **5**(6), pp.1059-1065.

Norris, F.A., Ungewickell, E. and Majerus, P.W. (1995) Inositol hexakisphosphate binds to clathrin assembly protein 3 (AP-3/AP180) and inhibits clathrin cage assembly in vitro. *J Biol Chem*, **270**(1), pp.214-217.

O'Donovan, T.R., O'Sullivan, G.C. and McKenna, S.L. (2011) Induction of autophagy by drug-resistant esophageal cancer cells promotes their survival and recovery following treatment with chemotherapeutics. *Autophagy*, **7**(5), pp.509-524.

Ocker, M. and Schneider-Stock, R. (2007) Histone deacetylase inhibitors: signalling towards p21cip1/waf1. *Int J Biochem Cell Biol*, **39**(7-8), pp.1367-1374.

Olsen, L.C., Aasland, R., Wittwer, C.U., Krokan, H.E. and Helland, D.E. (1989) Molecular cloning of human uracil-DNA glycosylase, a highly conserved DNA repair enzyme. *Embo j*, **8**(10), pp.3121-3125.

Ongusaha, P.P., Hughes, P.J., Davey, J. and Michell, R.H. (1998) Inositol hexakisphosphate in *Schizosaccharomyces pombe*: synthesis from Ins(1,4,5)P_3 and osmotic regulation. *Biochem J*, **335 (Pt 3)**, pp.671-679.

Onnebo, S.M. and Saiardi, A. (2009) Inositol pyrophosphates modulate hydrogen peroxide signalling. *Biochem J*, **423**(1), pp.109-118.

Otterlei, M., Warbrick, E., Nagelhus, T.A., Haug, T., Slupphaug, G., Akbari, M., Aas, P.A., Steinsbekk, K., Bakke, O. and Krokan, H.E. (1999) Post-replicative base excision repair in replication foci. *Embo j*, **18**(13), pp.3834-3844.

Otto, S.P. and Yong, P. (2002) The evolution of gene duplicates. *Adv Genet*, **46**, pp.451-483.

Owen, R.M., Baker, R.D., Bader, S., Dunlop, M.G. and Nicholl, I.D. (2007) The identification of a novel alternatively spliced form of the MBD4 DNA glycosylase. *Oncol Rep*, **17**(1), pp.111-116.

Ozenberger, B.A. and Roeder, G.S. (1991) A unique pathway of double-strand break repair operates in tandemly repeated genes. *Mol Cell Biol*, **11**(3), pp.1222-1231.

Padmanabhan, U., Dollins, D.E., Fridy, P.C., York, J.D. and Downes, C.P. (2009) Characterization of a selective inhibitor of inositol hexakisphosphate kinases: use in defining biological roles and metabolic relationships of inositol pyrophosphates. *J Biol Chem*, **284**(16), pp.10571-10582.

Pan, M.R., Chang, H.C. and Hung, W.C. (2008) Non-steroidal anti-inflammatory drugs suppress the ERK signaling pathway via block of Ras/c-Raf interaction and activation of MAP kinase phosphatases. *Cell Signal*, **20**(6), pp.1134-1141.

Parsons, J.L., Dianova, II and Dianov, G.L. (2004) APE1 is the major 3'-phosphoglycolate activity in human cell extracts. *Nucleic Acids Res*, **32**(12), pp.3531-3536.

Pathi, S., Jutooru, I., Chadalapaka, G., Nair, V., Lee, S.O. and Safe, S. (2012) Aspirin inhibits colon cancer cell and tumor growth and downregulates specificity protein (Sp) transcription factors. *PLoS One*, **7**(10), pp.e48208.

Pathi, S.S., Jutooru, I., Chadalapaka, G., Sreevalsan, S., Anand, S., Thatcher, G.R. and Safe, S. (2011) GT-094, a NO-NSAID, inhibits colon cancer cell growth by activation of a reactive oxygen species-microRNA-27a: ZBTB10-specificity protein pathway. *Mol Cancer Res*, **9**(2), pp.195-202.

Pesesse, X., Choi, K., Zhang, T. and Shears, S.B. (2004) Signaling by higher inositol polyphosphates. Synthesis of bisdiphosphoinositol tetrakisphosphate ("$InsP_8$") is selectively activated by hyperosmotic stress. *J Biol Chem*, **279**(42), pp.43378-43381.

Petronzelli, F., Riccio, A., Markham, G.D., Seeholzer, S.H., Stoerker, J., Genuardi, M., Yeung, A.T., Matsumoto, Y. and Bellacosa, A. (2000) Biphasic kinetics of the human

DNA repair protein MED1 (MBD4), a mismatch-specific DNA N-glycosylase. *J Biol Chem*, **275**(42), pp.32422-32429.

Pfeiffer, P., Goedecke, W., Kuhfittig-Kulle, S. and Obe, G. (2004) Pathways of DNA double-strand break repair and their impact on the prevention and formation of chromosomal aberrations. *Cytogenet Genome Res*, **104**(1-4), pp.7-13.

Pinckard, R.N., Hawkins, D. and Farr, R.S. (1968) In vitro acetylation of plasma proteins, enzymes and DNA by aspirin. *Nature*, **219**(5149), pp.68-69.

Popoff, S.C., Spira, A.I., Johnson, A.W. and Demple, B. (1990) Yeast structural gene (APN1) for the major apurinic endonuclease: homology to Escherichia coli endonuclease IV. *Proc Natl Acad Sci U S A*, **87**(11), pp.4193-4197.

Povirk, L.F., Zhou, T., Zhou, R., Cowan, M.J. and Yannone, S.M. (2007) Processing of 3'-phosphoglycolate-terminated DNA double strand breaks by Artemis nuclease. *J Biol Chem*, **282**(6), pp.3547-3558.

Poyner, D.R., Cooke, F., Hanley, M.R., Reynolds, D.J. and Hawkins, P.T. (1993) Characterization of metal ion-induced [3H]inositol hexakisphosphate binding to rat cerebellar membranes. *J Biol Chem*, **268**(2), pp.1032-1038.

Ramotar, D. and Wang, H. (2003) Protective mechanisms against the antitumor agent bleomycin: lessons from *Saccharomyces cerevisiae*. *Curr Genet*, **43**(4), pp.213-224.

Rizvi, S., Demars, C.J., Comba, A., Gainullin, V.G., Rizvi, Z., Almada, L.L., Wang, K., Lomberk, G., Fernandez-Zapico, M.E. and Buttar, N.S. (2010) Combinatorial chemoprevention reveals a novel smoothened-independent role of GLI1 in esophageal carcinogenesis. *Cancer Res*, **70**(17), pp.6787-6796.

Rohwer, J.M. (2012) Kinetic modelling of plant metabolic pathways. *J Exp Bot*, **63**(6), pp.2275-2292.

Rothwell, P.M., Price, J.F., Fowkes, F.G., Zanchetti, A., Roncaglioni, M.C., Tognoni, G., Lee, R., Belch, J.F., Wilson, M., Mehta, Z. and Meade, T.W. (2012) Short-term effects of daily aspirin on cancer incidence, mortality, and non-vascular death: analysis of the time course of risks and benefits in 51 randomised controlled trials. *Lancet*, **379**(9826), pp.1602-1612.

Rothwell, P.M., Wilson, M., Price, J.F., Belch, J.F., Meade, T.W. and Mehta, Z. (2012) Effect of daily aspirin on risk of cancer metastasis: a study of incident cancers during randomised controlled trials. *Lancet*, **379**(9826), pp.1591-1601.

Rudiger Siewert, J., Feith, M., Werner, M. and Stein, H.J. (2000) Adenocarcinoma of the esophagogastric junction: results of surgical therapy based on anatomical/topographic classification in 1,002 consecutive patients. *Ann Surg*, **232**(3), pp.353-361.

Rudolf, E., John, S. and Cervinka, M. (2012) Irinotecan induces senescence and apoptosis in colonic cells in vitro. *Toxicol Lett*, **214**(1), pp.1-8.

Rudolph, R.E., Vaughan, T.L., Kristal, A.R., Blount, P.L., Levine, D.S., Galipeau, P.C., Prevo, L.J., Sanchez, C.A., Rabinovitch, P.S. and Reid, B.J. (2003) Serum selenium levels in relation to markers of neoplastic progression among persons with Barrett's esophagus. *J Natl Cancer Inst*, **95**(10), pp.750-757.

Safrany, S.T. (2004) Protocols for regulation and study of diphosphoinositol polyphosphates. *Mol Pharmacol*, **66**(6), pp.1585-1591.

Safrany, S.T., Caffrey, J.J., Yang, X., Bembenek, M.E., Moyer, M.B., Burkhart, W.A. and Shears, S.B. (1998) A novel context for the 'MutT' module, a guardian of cell integrity, in a diphosphoinositol polyphosphate phosphohydrolase. *Embo j*, **17**(22), pp.6599-6607.

Safrany, S.T., Caffrey, J.J., Yang, X. and Shears, S.B. (1999) Diphosphoinositol polyphosphates: the final frontier for inositide research? *Biol Chem*, **380**(7-8), pp.945-951.

Safrany, S.T., Ingram, S.W., Cartwright, J.L., Falck, J.R., McLennan, A.G., Barnes, L.D. and Shears, S.B. (1999) The diadenosine hexaphosphate hydrolases from *Schizosaccharomyces pombe* and *Saccharomyces cerevisiae* are homologues of the human diphosphoinositol polyphosphate phosphohydrolase. Overlapping substrate specificities in a MutT-type protein. *J Biol Chem*, **274**(31), pp.21735-21740.

Saiardi, A., Bhandari, R., Resnick, A.C., Snowman, A.M. and Snyder, S.H. (2004) Phosphorylation of proteins by inositol pyrophosphates. *Science*, **306**(5704), pp.2101-2105.

Saiardi, A., Caffrey, J.J., Snyder, S.H. and Shears, S.B. (2000) Inositol polyphosphate multikinase (ArgRIII) determines nuclear mRNA export in *Saccharomyces cerevisiae*. *FEBS Lett*, **468**(1), pp.28-32.

Saiardi, A., Sciambi, C., McCaffery, J.M., Wendland, B. and Snyder, S.H. (2002) Inositol pyrophosphates regulate endocytic trafficking. *Proc Natl Acad Sci U S A*, **99**(22), pp.14206-14211.

Sambrook, J., Fritsch, E.F. and Maniatis, T. (1989). *Molecuar Cloning: A Laboratory Manual* (2nd ed. ed.). Cold Spring Harbor, NY: Cold Spring Harbor Laboratory Press.

Santi, D.V., McHenry, C.S., Raines, R.T. and Ivanetich, K.M. (1987) Kinetics and thermodynamics of the interaction of 5-fluoro-2'-deoxyuridylate with thymidylate synthase. *Biochemistry*, **26**(26), pp.8606-8613.

Sartori, A.A., Schar, P., Fitz-Gibbon, S., Miller, J.H. and Jiricny, J. (2001) Biochemical characterization of uracil processing activities in the hyperthermophilic archaeon Pyrobaculum aerophilum. *J Biol Chem*, **276**(32), pp.29979-29986.

Sciulli, M.G., Filabozzi, P., Tacconelli, S., Padovano, R., Ricciotti, E., Capone, M.L., Grana, M., Carnevale, V. and Patrignani, P. (2005) Platelet activation in patients with colorectal cancer. *Prostaglandins Leukot Essent Fatty Acids*, **72**(2), pp.79-83.

Seger, R. and Krebs, E.G. (1995) The MAPK signaling cascade. *Faseb j*, **9**(9), pp.726-735.

Seibert, K., Zhang, Y., Leahy, K., Hauser, S., Masferrer, J. and Isakson, P. (1997) Distribution of COX-1 and COX-2 in normal and inflamed tissues. *Adv Exp Med Biol*, **400a**, pp.167-170.

Seiple, L., Jaruga, P., Dizdaroglu, M. and Stivers, J.T. (2006) Linking uracil base excision repair and 5-fluorouracil toxicity in yeast. *Nucleic Acids Res*, **34**(1), pp.140-151.

SGDatabase. UNG1 / YML021C location. Retrieved 05/12/2014 http://www.yeastgenome.org/locus/S000004483/overview

Shames, D.S. and Minna, J.D. (2008) IP6K2 is a client for HSP90 and a target for cancer therapeutics development. *Proc Natl Acad Sci U S A*, **105**(5), pp.1389-1390.

Sharma, N.P., Dong, L., Yuan, C., Noon, K.R. and Smith, W.L. (2010) Asymmetric acetylation of the cyclooxygenase-2 homodimer by aspirin and its effects on the

oxygenation of arachidonic, eicosapentaenoic, and docosahexaenoic acids. *Mol Pharmacol*, **77**(6), pp.979-986.

Shears, S.B. (1998) The versatility of inositol phosphates as cellular signals. *Biochim Biophys Acta*, **1436**(1-2), pp.49-67.

Shears, S.B. (2001) Assessing the omnipotence of inositol hexakisphosphate. *Cell Signal*, **13**(3), pp.151-158.

Shears, S.B. (2004) How versatile are inositol phosphate kinases? *Biochem J*, **377**(Pt 2), pp.265-280.

Shears, S.B., Weaver, J.D. and Wang, H. (2013) Structural insight into inositol pyrophosphate turnover. *Adv Biol Regul*, **53**(1), pp.19-27.

Sheen, E. and Triadafilopoulos, G. (2011) Adverse effects of long-term proton pump inhibitor therapy. *Dig Dis Sci*, **56**(4), pp.931-950.

Shen, X., Xiao, H., Ranallo, R., Wu, W.H. and Wu, C. (2003) Modulation of ATP-dependent chromatin-remodeling complexes by inositol polyphosphates. *Science*, **299**(5603), pp.112-114.

Shiff, S.J., Qiao, L., Tsai, L.L. and Rigas, B. (1995) Sulindac sulfide, an aspirin-like compound, inhibits proliferation, causes cell cycle quiescence, and induces apoptosis in HT-29 colon adenocarcinoma cells. *J Clin Invest*, **96**(1), pp.491-503.

Shimada, H., Oohira, G., Okazumi, S., Matsubara, H., Nabeya, Y., Hayashi, H., Takeda, A., Gunji, Y. and Ochiai, T. (2004) Thrombocytosis associated with poor prognosis in patients with esophageal carcinoma. *J Am Coll Surg*, **198**(5), pp.737-741.

Shimizu, Y., Uchimura, Y., Dohmae, N., Saitoh, H., Hanaoka, F. and Sugasawa, K. (2010) Stimulation of DNA Glycosylase Activities by XPC Protein Complex: Roles of Protein-Protein Interactions. *J Nucleic Acids*, **2010**.

Shirvani, V.N., Ouatu-Lascar, R., Kaur, B.S., Omary, M.B. and Triadafilopoulos, G. (2000) Cyclooxygenase 2 expression in Barrett's esophagus and adenocarcinoma: Ex vivo induction by bile salts and acid exposure. *Gastroenterology*, **118**(3), pp.487-496.

Shtutman, M., Zhurinsky, J., Simcha, I., Albanese, C., D'Amico, M., Pestell, R. and Ben-Ze'ev, A. (1999) The cyclin D1 gene is a target of the beta-catenin/LEF-1 pathway. *Proc Natl Acad Sci U S A*, **96**(10), pp.5522-5527.

Shureiqi, I., Xu, X., Chen, D., Lotan, R., Morris, J.S., Fischer, S.M. and Lippman, S.M. (2001) Nonsteroidal anti-inflammatory drugs induce apoptosis in esophageal cancer cells by restoring 15-lipoxygenase-1 expression. *Cancer Res*, **61**(12), pp.4879-4884.

Sierko, E. and Wojtukiewicz, M.Z. (2004) Platelets and angiogenesis in malignancy. *Semin Thromb Hemost*, **30**(1), pp.95-108.

Silvers, A.L., Lin, L., Beer, D.G. and Chang, A.C. (2012). *Insulin-like growth factor binding protein-2 and chemosensitivity in esophageal adenocarcinoma.* Paper presented at the AACR 103rd Annual Meeting, Chicago, IL.

Singh, S. and Singh, P.P. (2013) Statin a day keeps cancer at bay. *World J Clin Oncol*, **4**(2), pp.43-46.

Slupphaug, G., Eftedal, I., Kavli, B., Bharati, S., Helle, N.M., Haug, T., Levine, D.W. and Krokan, H.E. (1995) Properties of a recombinant human uracil-DNA glycosylase from the UNG gene and evidence that UNG encodes the major uracil-DNA glycosylase. *Biochemistry*, **34**(1), pp.128-138.

SnapGene. Retrieved 05/12/14, from http://www.snapgene.com/resources/plasmid_files/yeast_plasmids/pFA6a-GFP%28S65T%29-His3MX6/

Solomon, S.D., McMurray, J.J., Pfeffer, M.A., Wittes, J., Fowler, R., Finn, P., Anderson, W.F., Zauber, A., Hawk, E. and Bertagnolli, M. (2005) Cardiovascular risk associated with celecoxib in a clinical trial for colorectal adenoma prevention. *N Engl J Med*, **352**(11), pp.1071-1080.

Song, M.G., Bail, S. and Kiledjian, M. (2013) Multiple Nudix family proteins possess mRNA decapping activity. *Rna*, **19**(3), pp.390-399.

Spoozak, L.A., Girda, E., Van Arsdale, A., Einstein, M.H., Goldberg, G.L. and Nevadunsky, N. (2013) Statin use in uterine malignancies. *J Clin Oncol*, **31**.

Steger, D.J., Haswell, E.S., Miller, A.L., Wente, S.R. and O'Shea, E.K. (2003) Regulation of chromatin remodeling by inositol polyphosphates. *Science*, **299**(5603), pp.114-116.

Steinbach, G., Lynch, P.M., Phillips, R.K., Wallace, M.H., Hawk, E., Gordon, G.B., Wakabayashi, N., Saunders, B., Shen, Y., Fujimura, T., Su, L.K., Levin, B., Godio, L., Patterson, S., Rodriguez-Bigas, M.A., *et al.* (2000) The effect of celecoxib, a cyclooxygenase-2 inhibitor, in familial adenomatous polyposis. *N Engl J Med*, **342**(26), pp.1946-1952.

Stephens, L., Radenberg, T., Thiel, U., Vogel, G., Khoo, K.H., Dell, A., Jackson, T.R., Hawkins, P.T. and Mayr, G.W. (1993) The detection, purification, structural characterization, and metabolism of diphosphoinositol pentakisphosphate(s) and bisdiphosphoinositol tetrakisphosphate(s). *J Biol Chem*, **268**(6), pp.4009-4015.

Stephens, L.R. and Irvine, R.F. (1990) Stepwise phosphorylation of myo-inositol leading to myo-inositol hexakisphosphate in *Dictyostelium*. *Nature*, **346**(6284), pp.580-583.

Stolzing, A., Coleman, N. and Scutt, A. (2006) Glucose-induced replicative senescence in mesenchymal stem cells. *Rejuvenation Res*, **9**(1), pp.31-35.

Stoner, G.D., Budd, G.T., Ganapathi, R., DeYoung, B., Kresty, L.A., Nitert, M., Fryer, B., Church, J.M., Provencher, K., Pamukcu, R., Piazza, G., Hawk, E., Kelloff, G., Elson, P. and van Stolk, R.U. (1999) Sulindac sulfone induced regression of rectal polyps in patients with familial adenomatous polyposis. *Adv Exp Med Biol*, **470**, pp.45-53.

Stoner, G.D., Wang, L.S. and Chen, T. (2007) Chemoprevention of esophageal squamous cell carcinoma. *Toxicol Appl Pharmacol*, **224**(3), pp.337-349.

Strande, N., Roberts, S.A., Oh, S., Hendrickson, E.A. and Ramsden, D.A. (2012) Specificity of the dRP/AP lyase of Ku promotes nonhomologous end joining (NHEJ) fidelity at damaged ends. *J Biol Chem*, **287**(17), pp.13686-13693.

Streb, H., Irvine, R.F., Berridge, M.J. and Schulz, I. (1983) Release of Ca^{2+} from a nonmitochondrial intracellular store in pancreatic acinar cells by inositol-1,4,5-trisphosphate. *Nature*, **306**(5938), pp.67-69.

Streicher, S.A., Yu, H., Lu, L., Kidd, M.S. and Risch, H.A. (2014) Case-control study of aspirin use and risk of pancreatic cancer. *Cancer Epidemiol Biomarkers Prev*, **23**(7), pp.1254-1263.

Subbegowda, R. and Frommel, T.O. (1998) Aspirin toxicity for human colonic tumor cells results from necrosis and is accompanied by cell cycle arrest. *Cancer Res*, **58**(13), pp.2772-2776.

Sugasawa, K. and Hanaoka, F. (2007) Sensing of DNA damage by XPC/Rad4: one protein for many lesions. *Nat Struct Mol Biol*, **14**(10), pp.887-888.

Sugiyama, H., Fujiwara, T., Ura, A., Tashiro, T., Yamamoto, K., Kawanishi, S. and Saito, I. (1994) Chemistry of thermal degradation of abasic sites in DNA. Mechanistic investigation on thermal DNA strand cleavage of alkylated DNA. *Chem Res Toxicol*, **7**(5), pp.673-683.

Summer, H., Gramer, R. and Droge, P. (2009) Denaturing urea polyacrylamide gel electrophoresis (Urea PAGE). *J Vis Exp*(32).

Sung, P., Trujillo, K.M. and Van Komen, S. (2000) Recombination factors of *Saccharomyces cerevisiae*. *Mutat Res*, **451**(1-2), pp.257-275.

Sutcliffe, P., Connock, M., Gurung, T., Freeman, K., Johnson, S., Kandala, N.B., Grove, A., Gurung, B., Morrow, S. and Clarke, A. (2013) Aspirin for prophylactic use in the primary prevention of cardiovascular disease and cancer: a systematic review and overview of reviews. *Health Technol Assess*, **17**(43), pp.1-253.

Swift, L.H. and Golsteyn, R.M. (2014) Genotoxic anti-cancer agents and their relationship to DNA damage, mitosis, and checkpoint adaptation in proliferating cancer cells. *Int J Mol Sci*, **15**(3), pp.3403-3431.

Tabernero, J., Macarulla, T., Ramos, F.J. and Baselga, J. (2005) Novel targeted therapies in the treatment of gastric and esophageal cancer. *Ann Oncol*, **16**(11), pp.1740-1748.

Tam, A.T., Pike, B.L., Hammet, A. and Heierhorst, J. (2007) Telomere-related functions of yeast KU in the repair of bleomycin-induced DNA damage. *Biochem Biophys Res Commun*, **357**(3), pp.800-803.

Thomas, M.P. and Potter, B.V. (2014) The enzymes of human diphosphoinositol polyphosphate metabolism. *Febs j*, **281**(1), pp.14-33.

Thorsell, A.G., Persson, C., Graslund, S., Hammarstrom, M., Busam, R.D. and Hallberg, B.M. (2009) Crystal structure of human diphosphoinositol phosphatase 1. *Proteins*, **77**(1), pp.242-246.

Thun, M.J., Henley, S.J. and Patrono, C. (2002) Nonsteroidal anti-inflammatory drugs as anticancer agents: mechanistic, pharmacologic, and clinical issues. *J Natl Cancer Inst*, **94**(4), pp.252-266.

Thun, M.J., Namboodiri, M.M., Calle, E.E., Flanders, W.D. and Heath, C.W., Jr. (1993) Aspirin use and risk of fatal cancer. *Cancer Res*, **53**(6), pp.1322-1327.

Toker, A. (2012) Phosphoinositide 3-kinases-a historical perspective. *Subcell Biochem*, **58**, pp.95-110.

Tomisato, W., Tsutsumi, S., Rokutan, K., Tsuchiya, T. and Mizushima, T. (2001) NSAIDs induce both necrosis and apoptosis in guinea pig gastric mucosal cells in primary culture. *Am J Physiol Gastrointest Liver Physiol*, **281**(4), pp.G1092-1100.

Tugendreich, S., Bassett, D.E., Jr., McKusick, V.A., Boguski, M.S. and Hieter, P. (1994) Genes conserved in yeast and humans. *Hum Mol Genet*, **3 Spec No**, pp.1509-1517.

Ulrych, T., Bohm, A., Polzin, A., Daum, G., Nusing, R.M., Geisslinger, G., Hohlfeld, T., Schror, K. and Rauch, B.H. (2011) Release of sphingosine-1-phosphate from human platelets is dependent on thromboxane formation. *J Thromb Haemost*, **9**(4), pp.790-798.

Van Dijken, P., de Haas, J.R., Craxton, A., Erneux, C., Shears, S.B. and Van Haastert, P.J. (1995) A novel, phospholipase C-independent pathway of inositol 1,4,5-trisphosphate formation in *Dictyostelium* and rat liver. *J Biol Chem*, **270**(50), pp.29724-29731.

Vaughan, T.L., Dong, L.M., Blount, P.L., Ayub, K., Odze, R.D., Sanchez, C.A., Rabinovitch, P.S. and Reid, B.J. (2005) Non-steroidal anti-inflammatory drugs and risk of neoplastic progression in Barrett's oesophagus: a prospective study. *Lancet Oncol*, **6**(12), pp.945-952.

Vermes, I., Haanen, C., Steffens-Nakken, H. and Reutelingsperger, C. (1995) A novel assay for apoptosis. Flow cytometric detection of phosphatidylserine expression on early apoptotic cells using fluorescein labelled Annexin V. *J Immunol Methods*, **184**(1), pp.39-51.

Vivanco, I. and Sawyers, C.L. (2002) The phosphatidylinositol 3-Kinase AKT pathway in human cancer. *Nat Rev Cancer*, **2**(7), pp.489-501.

Waddell, W.R. and Loughry, R.W. (1983) Sulindac for polyposis of the colon. *J Surg Oncol*, **24**(1), pp.83-87.

Wang, C.Y., Kim, H.H., Hiroi, Y., Sawada, N., Salomone, S., Benjamin, L.E., Walsh, K., Moskowitz, M.A. and Liao, J.K. (2009) Obesity increases vascular senescence and susceptibility to ischemic injury through chronic activation of Akt and mTOR. *Sci Signal*, **2**(62), pp.ra11.

Wang, H., Falck, J.R., Hall, T.M. and Shears, S.B. (2012) Structural basis for an inositol pyrophosphate kinase surmounting phosphate crowding. *Nat Chem Biol*, **8**(1), pp.111-116.

Wang, K.L., Wu, T.T., Choi, I.S., Wang, H., Resetkova, E., Correa, A.M., Hofstetter, W.L., Swisher, S.G., Ajani, J.A., Rashid, A. and Albarracin, C.T. (2007) Expression of

epidermal growth factor receptor in esophageal and esophagogastric junction adenocarcinomas: association with poor outcome. *Cancer*, **109**(4), pp.658-667.

Wang, L.D., Zhou, F.Y., Li, X.M., Sun, L.D., Song, X., Jin, Y., Li, J.M., Kong, G.Q., Qi, H., Cui, J., Zhang, L.Q., Yang, J.Z., Li, J.L., Li, X.C., Ren, J.L., *et al.* (2010) Genome-wide association study of esophageal squamous cell carcinoma in Chinese subjects identifies susceptibility loci at PLCE1 and C20orf54. *Nat Genet*, **42**(9), pp.759-763.

Wang, R., Wang, Y., Gao, Z. and Qu, X. (2014) The comparative study of acetyl-11-keto-beta-boswellic acid (AKBA) and aspirin in the prevention of intestinal adenomatous polyposis in APC(Min/+) mice. *Drug Discov Ther*, **8**(1), pp.25-32.

Wang, Z., Ayoub, E., Mazouzi, A., Grin, I., Ishchenko, A.A., Fan, J., Yang, X., Harihar, T., Saparbaev, M. and Ramotar, D. (2014) Functional variants of human APE1 rescue the DNA repair defects of the yeast AP endonuclease/3'-diesterase-deficient strain. *DNA Repair (Amst)*, **22c**, pp.53-66.

Waters, T.R., Gallinari, P., Jiricny, J. and Swann, P.F. (1999) Human thymine DNA glycosylase binds to apurinic sites in DNA but is displaced by human apurinic endonuclease 1. *J Biol Chem*, **274**(1), pp.67-74.

Weaver, J.D., Wang, H. and Shears, S.B. (2013) The kinetic properties of a human PPIP5K reveal that its kinase activities are protected against the consequences of a deteriorating cellular bioenergetic environment. *Biosci Rep*, **33**(2), pp.e00022.

Williams, C.S., Mann, M. and DuBois, R.N. (1999) The role of cyclooxygenases in inflammation, cancer, and development. *Oncogene*, **18**(55), pp.7908-7916.

Willis, J., Patel, Y., Lentz, B.L. and Yan, S. (2013) APE2 is required for ATR-Chk1 checkpoint activation in response to oxidative stress. *Proc Natl Acad Sci U S A*, **110**(26), pp.10592-10597.

Wilson, M.S., Livermore, T.M. and Saiardi, A. (2013) Inositol pyrophosphates: between signalling and metabolism. *Biochem J*, **452**(3), pp.369-379.

Winde, G., Schmid, K.W., Schlegel, W., Fischer, R., Osswald, H. and Bunte, H. (1995) Complete reversion and prevention of rectal adenomas in colectomized patients with familial adenomatous polyposis by rectal low-dose sulindac maintenance treatment. Advantages of a low-dose nonsteroidal anti-inflammatory drug regimen in reversing adenomas exceeding 33 months. *Dis Colon Rectum*, **38**(8), pp.813-830.

Wong, V.C., Ko, J.M., Qi, R.Z., Li, P.J., Wang, L.D., Li, J.L., Chan, Y.P., Chan, K.W., Stanbridge, E.J. and Lung, M.L. (2011) Abrogated expression of DEC1 during oesophageal squamous cell carcinoma progression is age- and family history-related and significantly associated with lymph node metastasis. *Br J Cancer*, **104**(5), pp.841-849.

Worley, J., Luo, X. and Capaldi, A.P. (2013) Inositol pyrophosphates regulate cell growth and the environmental stress response by activating the HDAC Rpd3L. *Cell Rep*, **3**(5), pp.1476-1482.

Wu, M., Dul, B.E., Trevisan, A.J. and Fiedler, D. (2013) Synthesis and characterization of non-hydrolysable diphosphoinositol polyphosphate second messengers. *Chem Sci*, **4**(1), pp.405-410.

Wu, T.T., Watanabe, T., Heitmiller, R., Zahurak, M., Forastiere, A.A. and Hamilton, S.R. (1998) Genetic alterations in Barrett esophagus and adenocarcinomas of the esophagus and esophagogastric junction region. *Am J Pathol*, **153**(1), pp.287-294.

Wu, X., Lin, M., Li, Y., Zhao, X. and Yan, F. (2009) Effects of DMEM and RPMI 1640 on the biological behavior of dog periosteum-derived cells. *Cytotechnology*, **59**(2), pp.103-111.

Xie, F., Ye, L., Chen, J., Wu, N., Zhang, Z., Yang, Y., Zhang, L. and Jiang, W.G. (2011) The impact of Metastasis Suppressor-1, MTSS1, on oesophageal squamous cell carcinoma and its clinical significance. *J Transl Med*, **9**, pp.95.

Xu, Y.J., Kim, E.Y. and Demple, B. (1998) Excision of C-4'-oxidized deoxyribose lesions from double-stranded DNA by human apurinic/apyrimidinic endonuclease (Ape1 protein) and DNA polymerase beta. *J Biol Chem*, **273**(44), pp.28837-28844.

Yamaguchi-Iwai, Y., Sonoda, E., Buerstedde, J.M., Bezzubova, O., Morrison, C., Takata, M., Shinohara, A. and Takeda, S. (1998) Homologous recombination, but not DNA repair, is reduced in vertebrate cells deficient in RAD52. *Mol Cell Biol*, **18**(11), pp.6430-6435.

Yamamoto, Y., Yin, M.J., Lin, K.M. and Gaynor, R.B. (1999) Sulindac inhibits activation of the NF-kappaB pathway. *J Biol Chem*, **274**(38), pp.27307-27314.

Yang, G.Z., Li, L., Ding, H.Y. and Zhou, J.S. (2005) Cyclooxygenase-2 is over-expressed in Chinese esophageal squamous cell carcinoma, and correlated with NF-kappaB: an immunohistochemical study. *Exp Mol Pathol*, **79**(3), pp.214-218.

Yang, X., Safrany, S.T. and Shears, S.B. (1999) Site-directed mutagenesis of diphosphoinositol polyphosphate phosphohydrolase, a dual specificity NUDT enzyme that attacks diadenosine polyphosphates and diphosphoinositol polyphosphates. *J Biol Chem*, **274**(50), pp.35434-35440.

Yashiro, M., Shinto, O., Nakamura, K., Tendo, M., Matsuoka, T., Matsuzaki, T., Kaizaki, R., Miwa, A. and Hirakawa, K. (2010) Synergistic antitumor effects of FGFR2 inhibitor with 5-fluorouracil on scirrhous gastric carcinoma. *Int J Cancer*, **126**(4), pp.1004-1016.

Ye, C., Bandara, W.M. and Greenberg, M.L. (2013) Regulation of inositol metabolism is fine-tuned by inositol pyrophosphates in *Saccharomyces cerevisiae*. *J Biol Chem*, **288**(34), pp.24898-24908.

York, S.J., Armbruster, B.N., Greenwell, P., Petes, T.D. and York, J.D. (2005) Inositol diphosphate signaling regulates telomere length. *J Biol Chem*, **280**(6), pp.4264-4269.

Yu, H.G., Huang, J.A., Yang, Y.N., Huang, H., Luo, H.S., Yu, J.P., Meier, J.J., Schrader, H., Bastian, A., Schmidt, W.E. and Schmitz, F. (2002) The effects of acetylsalicylic acid on proliferation, apoptosis, and invasion of cyclooxygenase-2 negative colon cancer cells. *Eur J Clin Invest*, **32**(11), pp.838-846.

Yun, J.P., Zhang, M.F., Hou, J.H., Tian, Q.H., Fu, J., Liang, X.M., Wu, Q.L. and Rong, T.H. (2007) Primary small cell carcinoma of the esophagus: clinicopathological and immunohistochemical features of 21 cases. *BMC Cancer*, **7**, pp.38.

Zabarovsky, E.R., Lerman, M.I. and Minna, J.D. (2002) Tumor suppressor genes on chromosome 3p involved in the pathogenesis of lung and other cancers. *Oncogene*, **21**(45), pp.6915-6935.

Zhang, T., Caffrey, J.J. and Shears, S.B. (2001) The transcriptional regulator, Arg82, is a hybrid kinase with both monophosphoinositol and diphosphoinositol polyphosphate synthase activity. *FEBS Lett*, **494**(3), pp.208-212.

Zhang, Y. (2013) Epidemiology of esophageal cancer. *World J Gastroenterol*, **19**(34), pp.5598-5606.

Zhao, Y., Bao, Q., Schwarz, B., Zhao, L., Mysliwietz, J., Ellwart, J., Renner, A., Hirner, H., Niess, H., Camaj, P., Angele, M., Gros, S., Izbicki, J., Jauch, K.W., Nelson, P.J., *et al.* (2014) Stem cell-like side populations in esophageal cancer: a source of chemotherapy resistance and metastases. *Stem Cells Dev*, **23**(2), pp.180-192.

Zheng, S.T., Huo, Q., Tuerxun, A., Ma, W.J., Lv, G.D., Huang, C.G., Liu, Q., Wang, X., Lin, R.Y., Sheyhidin, I. and Lu, X.M. (2011) The expression and activation of ERK/MAPK pathway in human esophageal cancer cell line EC9706. *Mol Biol Rep*, **38**(2), pp.865-872.

Zhivotovsky, B. and Kroemer, G. (2004) Apoptosis and genomic instability. *Nat Rev Mol Cell Biol*, **5**(9), pp.752-762.

Zhou, T., Akopiants, K., Mohapatra, S., Lin, P.S., Valerie, K., Ramsden, D.A., Lees-Miller, S.P. and Povirk, L.F. (2009) Tyrosyl-DNA phosphodiesterase and the repair of 3'-phosphoglycolate-terminated DNA double-strand breaks. *DNA Repair (Amst)*, **8**(8), pp.901-911.

Zhuo, W.L., Zhang, Y.S., Wang, Y., Zhuo, X.L., Zhu, B., Cai, L. and Chen, Z.T. (2009) Association studies of CYP1A1 and GSTM1 polymorphisms with esophageal cancer risk: evidence-based meta-analyses. *Arch Med Res*, **40**(3), pp.169-179.

Zimmermann, K.C., Sarbia, M., Weber, A.A., Borchard, F., Gabbert, H.E. and Schror, K. (1999) Cyclooxygenase-2 expression in human esophageal carcinoma. *Cancer Res*, **59**(1), pp.198-204.

Zong, W.X. and Thompson, C.B. (2006) Necrotic death as a cell fate. *Genes Dev*, **20**(1), pp.1-15.